Chapter 3

Representation Formulas and Examples of Minimal Surfaces

In this chapter we present the elements of the classical theory of minimal surfaces developed during the nineteenth century. We begin by representing minimal surfaces as real parts of holomorphic curves in $\mathbb{C}^3$ which are isotropic. This leads to useful and handy formulas for the line element, the Gauss map, the second fundamental form and the Gauss curvature of minimal surfaces. Moreover we obtain a complete description of all interior singular points of two-dimensional minimal surfaces as branch points of $\mathbb{C}^3$-valued power series, and we derive a normal form of a minimal surface in the vicinity of a branch point. Close to a branch point of order m, a minimal surface behaves, roughly speaking, like an m-fold cover of a disk, a property which is also reflected in the form of lower bounds for its area. Other by-products of the representation of minimal surfaces as real parts of isotropic curves in $\mathbb{C}^3$ are results on *adjoint* and *associated minimal surfaces* that were discovered by Bonnet.

In Section 3.3 we turn to the representation formula of Enneper and Weierstrass which expresses a given minimal surface in terms of integrals involving a holomorphic function μ and a meromorphic function ν. Conversely, any pair of such functions μ, ν can be used to define minimal surfaces provided that $\mu\nu^2$ is holomorphic. In the older literature this representation was mostly used for a local discussion of minimal surfaces. Following the example of Osserman (see [10] and [24]), the representation formula has become very important for the treatment of global questions for minimal surfaces. As an example of this development we describe in Section 3.7 the results concerning the omissions of the Gauss map of a complete regular minimal surface. These results are the appropriate generalization of Picard's theorem in function theory to differential geometry and culminate in the remarkable theorem of Fujimoto that the Gauss map of a nonplanar complete and regular minimal surface cannot miss more than four points on the Riemann sphere. Important steps to the final version of this result which can also be viewed as a generalization of Bernstein's theorem were taken by Osserman and Xavier. The proof given in

U. Dierkes, S. Hildebrandt, F. Sauvigny, *Minimal Surfaces*,
Grundlehren der mathematischen Wissenschaften 339,
DOI 10.1007/978-3-642-11698-8_3,

Section 3.7 is very close to Osserman's original approach and is due to Mo and Osserman [1].

Moreover, most of the sophisticated examples of minimal surfaces and, in particular, of families of complete embedded minimal surfaces and also of periodic surfaces of zero mean curvature are best described via the Enneper-Weierstrass formula. We shall not attempt to present a complete picture of this part of the theory which in recent years has gathered new momentum, but we shall content ourselves with a few examples mentioned in Section 3.6 and with a very short survey given in the Scholia Section 3.8. Instead of a careful discussion we include various figures depicting old and new examples of these fascinating species.

A few of the known classical minimal surfaces are briefly described in Section 3.5, and these surfaces are illustrated by numerous figures so that the reader has sufficient visual examples for the investigations carried out in the following chapters. We do not aim at completeness but we refer the reader to Nitsche's encyclopaedic treatise [28] as well as to the literature cited in Subsection 1 of the Scholia, Section 3.8. A brief survey of some of the newer examples can be found in Subsections 4 and 5 of the Scholia. For a detailed presentation of recent results on complete minimal surfaces we in particular refer to work of H. Karcher [1–5], to the encyclopaedia article by Karcher and Hoffmann in EMS, and to the collection of papers in GTMS.

The Enneper–Weierstrass representation formula of a minimal surface $X : \Omega \to \mathbb{R}^3$ is still somewhat arbitrary since the composition $Y = X \circ \tau$ of X with a conformal mapping $\tau : \Omega^* \to \Omega$ describes the same geometric object as X. Thus one can use a suitable map τ to eliminate one of the two functions μ, ν in the Weierstrass formula; consequently every minimal surface viewed as a geometric object, i.e., as an equivalence class of conformally equal surfaces, corresponds to *one* holomorphic function $\mathfrak{F}(\omega)$. Weierstrass derived a representation of this kind where $\mathfrak{F}$ is defined on the stereographic projection of the spherical image of the considered minimal surface. The Gauss curvature and the second fundamental form of a minimal surface can be expressed in a very simple way in terms of the functions μ, ν, or $\mathfrak{F}$.

Finally in Section 3.4 we discuss several contributions by H.A. Schwarz to the theory of minimal surfaces, in particular his solution of Björling's problem. This is just the Cauchy problem for minimal surfaces and an arbitrarily prescribed real analytic initial strip, and it is known to possess a unique solution due to the theorem of Cauchy–Kovalevskaya. Schwarz found a beautiful integral representation of this solution which can be used to construct interesting minimal surfaces, such as surfaces containing given curves as geodesics or as lines of curvature. As an interesting application of Schwarz's solution we treat his reflection principles for minimal surfaces.

3.1 The Adjoint Surface. Minimal Surfaces as Isotropic Curves in $\mathbb{C}^3$. Associate Minimal Surfaces

Let us begin by recalling the general definition of a minimal surface, given in Section 2.6.

A nonconstant surface $X : \Omega \to \mathbb{R}^3$ of class C^2 is said to be a minimal surface if it satisfies the equations

$$\Delta X = 0 \tag{1}$$

$$|X_u|^2 = |X_v|^2, \quad \langle X_u, X_v \rangle = 0 \tag{2}$$

on Ω.

If a minimal surface

$$X(u, v) = (x(u, v), y(u, v), z(u, v))$$

is defined on a simply connected domain Ω of $\mathbb{R}^2 \mathrel{\hat{=}} \mathbb{C}$, then we define an *adjoint surface*

$$X^*(u, v) = (x^*(u, v), y^*(u, v), z^*(u, v))$$

to $X(u, v)$ on Ω as solution of the *Cauchy–Riemann equations*

$$X_u = X_v^*, \quad X_v = -X_u^* \tag{3}$$

in Ω.

Clearly, all adjoint surfaces to some given minimal surface X differ only by a constant vector; thus we may speak of *the adjoint surface* $X^*(u, v)$ of some minimal surface $X(u, v)$ which is defined on a simply connected domain Ω of $\mathbb{R}^2$.

The equations (1)–(3) immediately imply

$$\Delta X^* = 0, \quad |X_u^*|^2 = |X_v^*|^2, \quad \langle X_u^*, X_v^* \rangle = 0,$$

that is, the adjoint surface X^* to some minimal surface X is a minimal surface.

Consider an arbitrary harmonic mapping $X : \Omega \to \mathbb{R}^3$ of a simply connected domain Ω in $\mathbb{R}^2 \mathrel{\hat{=}} \mathbb{C}$, and let X^* be the adjoint harmonic mapping to X, defined as a solution of (3). Then

$$f(w) := X(u, v) + iX^*(u, v), \quad w = u + iv \in \Omega \tag{4}$$

is a holomorphic mapping of Ω into $\mathbb{C}^3$ with components

$$\begin{aligned} \varphi(w) &= x(u, v) + ix^*(u, v), \\ \psi(w) &= y(u, v) + iy^*(u, v), \\ \chi(w) &= z(u, v) + iz^*(u, v), \end{aligned} \tag{5}$$

which can be considered as a *holomorphic curve* in $\mathbb{C}^3$. Its complex derivative $f' = \frac{df}{dw}$ is given by

$$f' = X_u + iX_u^* = X_u - iX_v, \tag{6}$$

whence it follows that

$$\langle f', f' \rangle = |X_u|^2 - |X_v|^2 - 2i\langle X_u, X_v \rangle. \tag{7}$$

Consequently, the conformality relations (2) are satisfied if and only if the *isotropy relation*

$$\langle f', f' \rangle = 0 \tag{8}$$

is fulfilled.

A holomorphic curve satisfying relation (8) is said to be an *isotropic curve*.

Using this notation, we obtain the following result:

Proposition 1. *If $X : \Omega \to \mathbb{R}^3$ is a minimal surface on a simply connected parameter domain Ω in $\mathbb{R}^2$, then the holomorphic curve $f : \Omega \to \mathbb{C}^3$, defined by (3) and (4), is a nonconstant isotropic curve. Conversely, if $f : \Omega \to \mathbb{C}^3$ is a nonconstant isotropic curve in $\mathbb{C}^3$, then*

$$X(u, v) := \operatorname{Re} f(w), \quad X^*(u, v) := \operatorname{Im} f(w) \tag{9}$$

defines two minimal surfaces $X : \Omega \to \mathbb{R}^3$ and $X^* : \Omega \to \mathbb{R}^3$ on Ω, whether or not Ω is simply connected.

We say that $X^*(u, v)$, $w \in \Omega$, is an *adjoint surface* to some minimal surface $X(u, v)$, $w \in \Omega$, if there is an isotropic curve $f : \Omega \to \mathbb{C}^3$ such that (9) is satisfied.

If X^* is adjoint to X, then $-X$ is adjoint to X^*, i.e.,

$$X^{**} = -X. \tag{10}$$

The isotropy condition (8) for a curve $f(w) = (\varphi(w), \psi(w), \chi(w))$ means that the derivatives of the three holomorphic functions φ, ψ, χ are coupled by the relation

$$\varphi'^2 + \psi'^2 + \chi'^2 = 0. \tag{11}$$

Let us introduce the two Wirtinger operators

$$\frac{\partial}{\partial w} = \frac{1}{2}\left(\frac{\partial}{\partial u} - i\frac{\partial}{\partial v}\right), \quad \frac{\partial}{\partial \bar{w}} = \frac{1}{2}\left(\frac{\partial}{\partial u} + i\frac{\partial}{\partial v}\right). \tag{12}$$

Then the equations (1) and (2) can equivalently be written as

$$X_{w\bar{w}} = 0 \tag{13}$$

and

$$\langle X_w, X_w \rangle = 0, \tag{14}$$

respectively, and we also have

$$f' = 2X_w. \tag{14'}$$

Suppose now that $X : \Omega \to \mathbb{R}^3$ is a minimal surface on some domain Ω. Then we have

$$\mathcal{W} = \sqrt{\mathcal{E}\mathcal{G} - \mathcal{F}^2} = \mathcal{E} = \mathcal{G} = \tfrac{1}{2}(\mathcal{E} + \mathcal{G}).$$

By restricting ourselves to simply connected subdomains Ω' of Ω, we can assume that there is an isotropic curve f such that $X = \operatorname{Re} f$, $f = (\varphi, \psi, \chi)$. Since $|f'|^2 = |\nabla X|^2 = 4|X_w|^2$, we obtain

$$\mathcal{W} = |X_u|^2 = \tfrac{1}{2}|\nabla X|^2 = \tfrac{1}{2}|f'|^2 = 2|X_w|^2. \tag{15}$$

Thus the zeros of $\mathcal{W}$ are the common zeros of the three holomorphic functions φ', ψ', χ' and must, therefore, be isolated in Ω, except if $X(w) \equiv \text{const}$, which is excluded.

Proposition 2. *The singular points w of a minimal surface $X : \Omega \to \mathbb{R}^3$ on a domain Ω are isolated. They are exactly the zeros of the function $|X_u|$ in Ω.*

As we shall see, the behavior of a minimal surface in the neighborhood of one of its singular points resembles the behavior of a holomorphic function $\varphi(w)$ in the neighborhood of a zero of its derivative $\varphi'(w)$. Therefore the singular points of minimal surfaces are called *branch points*. We shall look at them more closely in the next section.

The following statements are an immediate consequence of the equations (1)–(3).

Proposition 3. *Let $X^* : \Omega \to \mathbb{R}^3$ be an adjoint surface to the minimal surface $X : \Omega \to \mathbb{R}^3$.*

(i) *We have $X^*(w) \not\equiv \text{const}$.*

(ii) *Some point $w_0 \in \Omega$ is a branch point of X if and only if it is a branch point of X^*.*

(iii) *Denote by $N(w)$ and $N^*(w)$ the Gauss maps of $X(w)$ and $X^*(w)$ respectively, which are defined on the set Ω' of regular points of X in Ω. Then we have*

$$N(w) \equiv N^*(w) \quad \text{on } \Omega'. \tag{16}$$

Moreover, the tangent spaces of X and X^* coincide:

$$T_w X = T_w X^* \quad \text{for all } w \in \Omega',$$

and also the first fundamental forms of X and X^* agree:

$$I_X(V,W) = I_{X^*}(V,W) \quad \textit{for all } V,W \in T_wX,\ w \in \Omega',$$

i.e., the surfaces X and X^* are isometric to each other. Therefore the Gauss curvatures K and K^* of X and X^* are the same:

$$K(w) = K^*(w) \quad \textit{for all } w \in \Omega'.$$

The Weingarten maps S and S^* of X and X^* respectively differ by a rotation of 90 degrees on all tangent spaces T_wX, with $w \in \Omega'$.

Later on, we shall exhibit other relations between X, X^*, and their Gauss map N. Presently, we want to formulate a consequence of the Propositions 1 and 2.

Proposition 4. *Let Ω be a simply connected domain in $\mathbb{C}$, $X_0 \in \mathbb{R}^3$, $w_0 \in \Omega$, and suppose that $\Phi(w) = (\Phi_1(w), \Phi_2(w), \Phi_3(w)) \not\equiv 0$ is a holomorphic mapping of Ω into $\mathbb{C}^3$ which satisfies*

$$\Phi_1^2 + \Phi_2^2 + \Phi_3^2 = 0 \tag{17}$$

on Ω. Then the formula

$$X(w) = X_0 + \operatorname{Re} \int_{w_0}^{w} \Phi(\omega)\, d\omega, \quad w \in \Omega, \tag{18}$$

defines a minimal surface $X : \Omega \to \mathbb{R}^3$, and, for every $X_0^* \in \mathbb{R}^3$, the formula

$$X^*(w) = X_0^* + \operatorname{Im} \int_{w_0}^{w} \Phi(\omega)\, d\omega, \quad w \in \Omega, \tag{19}$$

yields an adjoint surface to X. The branch points of X are exactly the zeros of Φ.

Conversely, if $X : \Omega \to \mathbb{R}^3$ is a minimal surface defined on a simply connected domain Ω, then there is a holomorphic mapping $\Phi : \Omega \to \mathbb{C}^3$ satisfying (17) such that

$$X(w) = X(w_0) + \operatorname{Re} \int_{w_0}^{w} \Phi(\omega)\, d\omega$$

holds for arbitrary $w, w_0 \in \Omega$.

Remark. If Ω is not simply connected, then the integral (18) still defines a minimal surface on Ω provided that the differential form $\Phi\, d\omega$ only has purely imaginary periods, i.e., that $\int_\gamma \Phi(\omega)\, d\omega$ is a purely imaginary number for every closed path γ contained in Ω.

Formula (18) yields

$$X_w = \tfrac{1}{2}\Phi.$$

More generally, if $X : \Omega \to \mathbb{R}^3$ is a minimal surface given in the form

$$X(w) = \operatorname{Re} f(w),$$

where $f : \Omega \to \mathbb{C}^3$ denotes an isotropic curve with the derivative

$$f' = \Phi = (\Phi_1, \Phi_2, \Phi_3),$$

then we infer from

$$f' = X_u - iX_v$$

that

$$X_u = \operatorname{Re} \Phi, \quad X_v = -\operatorname{Im} \Phi.$$

Consequently, we obtain

$$X_u \wedge X_v = \operatorname{Im}(\Phi_2 \bar{\Phi}_3, \Phi_3 \bar{\Phi}_1, \Phi_1 \bar{\Phi}_2). \tag{20}$$

The line element $ds = |dX|$ takes the form

$$ds^2 = \lambda\{du^2 + dv^2\}$$

where

$$\Lambda := |X_u|^2 = \tfrac{1}{2}|\nabla X|^2 = \tfrac{1}{2}|f'|^2 = \tfrac{1}{2}|\Phi|^2 = \mathcal{W}. \tag{21}$$

Thus the spherical image $N : \Omega' \to S^2$, $N = \Lambda^{-1} X_u \wedge X_v$, $\Omega' := \{w \in \Omega : \Lambda(w) \neq 0\}$, is given by

$$N = 2|\Phi|^{-2} \operatorname{Im}(\Phi_2 \bar{\Phi}_3, \Phi_3 \bar{\Phi}_1, \Phi_1 \bar{\Phi}_2). \tag{22}$$

Moreover, the equation $f' = X_u - iX_v$ implies

$$f'' = X_{uu} - iX_{uv} = -X_{vv} - iX_{uv}$$

whence

$$\langle f'', N \rangle = \mathcal{L} - i\mathcal{M} = -\mathcal{N} - i\mathcal{M}$$

on Ω'. Therefore we obtain the well-known relation

$$\mathcal{L} = -\mathcal{N}, \tag{23}$$

expressing the fact that X has zero mean curvature, and also

$$|\langle f'', N \rangle|^2 = \mathcal{L}^2 + \mathcal{M}^2. \tag{24}$$

By the observation of H. Hopf (cf. Section 1.3), the function $\frac{1}{2}(\mathcal{L} - \mathcal{N}) - i\mathcal{M}$ is holomorphic on Ω'. Thus we obtain that *the function*

$$l(w) := \mathcal{L}(w) - i\mathcal{M}(w) = \langle f''(w), N(w) \rangle \tag{25}$$

is holomorphic on Ω'.

We infer from (23) and (24) that the Gauss curvature K of X on Ω' is given by

$$K = \frac{\mathcal{L}\mathcal{N} - \mathcal{M}^2}{\mathcal{W}^2} = -\frac{\mathcal{L}^2 + \mathcal{M}^2}{\mathcal{W}^2} = -\frac{|l|^2}{\Lambda^2} \tag{26}$$

or

$$K = -4|\Phi|^{-4}|\langle \Phi', N\rangle|^2, \quad \Phi = f'. \tag{26'}$$

We conclude that $K(w) \leq 0$ *on* Ω', *and that* $K(w) = 0$ *if and only if* $l(w) = 0$ *holds.*

Note that $K \leq 0$ also follows from $H = 0$ because of $2H = \kappa_1 + \kappa_2$ and $K = \kappa_1\kappa_2$.

Umbilical points w of a surface $X(w)$ are regular points where both principal curvatures κ_1 and κ_2 are equal. Since $H = \frac{1}{2}(\kappa_1 + \kappa_2) = 0$ and $K = \kappa_1\kappa_2 \leq 0$, the umbilical points $w \in \Omega'$ of a minimal surface $X : \Omega \to \mathbb{R}^3$ are characterized by the condition

$$K(w) = 0,$$

or equivalently, by

$$\mathcal{L}(w) = 0, \quad \mathcal{M}(w) = 0, \quad \mathcal{N}(w) = 0.$$

Since umbilical points of X are precisely the zeros of the holomorphic function $l : \Omega' \to \mathbb{C}$, they must either be isolated, or else $\mathcal{L}(w) \equiv 0$, $\mathcal{M}(w) \equiv 0$, and $\mathcal{N}(w) \equiv 0$ on Ω' which implies that $X(w)$, $w \in \Omega$, is a planar surface, taking the Weingarten equations (48) of Section 1.2 into account.

In the next section, we shall prove that $N(w)$ approaches a limit N_0 as w tends to some branch point $w_0 \in \Omega$. This implies that $l(w) = \mathcal{L}(w) - i\mathcal{M}(w)$ is actually holomorphic on Ω, since isolated singularities of holomorphic functions are removable if they are continuity points.

By means of the function $l(w), w \in \Omega$, it is easy to characterize the asymptotic lines and the curvature lines of a nonconstant minimal surface $X(w)$, $w \in \Omega$.

Let $\omega(t) = (\alpha(t), \beta(t))$, $t \in \mathcal{I}$, be a C^1-curve in Ω, i.e., $\omega(\mathcal{I}) \subset \Omega$. On account of Section 1.2, (48), this curve is an *asymptotic line* of X if and only if

$$\mathcal{L}\dot{\alpha}^2 + 2\mathcal{M}\dot{\alpha}\dot{\beta} + \mathcal{N}\dot{\beta}^2 = 0,$$

and, by 1.2, (53), it is a *line of curvature* if and only if

$$(\mathcal{E}\mathcal{M} - \mathcal{F}\mathcal{L})\dot{\alpha}^2 + (\mathcal{E}\mathcal{N} - \mathcal{G}\mathcal{L})\dot{\alpha}\dot{\beta} + (\mathcal{F}\mathcal{N} - \mathcal{G}\mathcal{M})\dot{\beta}^2 = 0.$$

Here $\mathcal{E}, \ldots, \mathcal{L}, \ldots$ have to be understood as $\mathcal{E}(\omega), \ldots, \mathcal{L}(\omega), \ldots$. Since $\mathcal{E} = \mathcal{G}$, $\mathcal{F} = 0$, $\mathcal{E} = -\mathcal{N}$, we obtain:

The asymptotic lines are described by

$$\mathfrak{L}(\dot{\alpha}^2 - \dot{\beta}^2) + 2\mathfrak{M}\dot{\alpha}\dot{\beta} = 0, \tag{27}$$

and the lines of curvature are characterized by

$$\mathfrak{M}(\dot{\alpha}^2 - \dot{\beta}^2) - 2\mathfrak{L}\dot{\alpha}\dot{\beta} = 0. \tag{28}$$

Let us introduce the complex valued quadratic form $\Xi(\dot{\omega})$, depending on $\dot{\omega} = (\dot{\alpha}, \dot{\beta})$, by

$$\Xi(\dot{\omega}) := l(\omega)(\dot{\alpha}^2 + i\dot{\beta}^2), \quad l = \mathfrak{L} - i\mathfrak{M}. \tag{29}$$

Then the asymptotic lines and the curvature lines are given by

$$\operatorname{Re}\Xi(\dot{\omega}) = 0 \quad \text{and} \quad \operatorname{Im}\Xi(\dot{\omega}) = 0 \tag{30}$$

respectively, or, in other words, by

$$\operatorname{Re} l(w)(dw)^2 = 0 \quad \text{and} \quad \operatorname{Im} l(w)(dw)^2 = 0, \tag{30'}$$

using the holomorphic quadratic differential $l(w)(dw)^2$.

Collecting these results, we obtain:

Proposition 5. *Let $X : \Omega \to \mathbb{R}^3$ be a minimal surface given by $X = \operatorname{Re} f$, where $f : \Omega \to \mathbb{C}^3$ is an isotropic curve with $f' = \Phi = (\Phi_1, \Phi_2, \Phi_3)$. Then its spherical image $N(w)$, $w \in \Omega'$, on the set of regular points $\Omega' := \{w \in \Omega\colon \Lambda(w) \neq 0\}$, $\Lambda := |X_u|$, is given by (22), and its Gauss curvature K on Ω' can be computed from (26) or (26'). On Ω', the curvature $K(w)$ is strictly negative, except for umbilical points, where $K(w)$ is vanishing. The umbilical points of X are exactly the zeros of the holomorphic function $l(w) = \mathfrak{L}(w) - i\mathfrak{M}(w)$, $w \in \Omega$. If X is a nonplanar surface, then its umbilical points are isolated. Moreover, the asymptotic lines of X are described by*

$$\operatorname{Re} l(w)(dw)^2 = 0,$$

and the curvature lines by

$$\operatorname{Im} l(w)(dw)^2 = 0.$$

Now we want to define the family of *associate minimal surfaces* to a given minimal surface $X : \Omega \to \mathbb{R}^3$ which is given as the real part of some isotropic curve $f : \Omega \to \mathbb{C}^3$. That is,

$$f(w) = X(w) + iX^*(w), \quad w = u + iv \in \Omega,$$

where

$$\langle f'(w), f'(w)\rangle \equiv 0 \quad \text{on } \Omega.$$

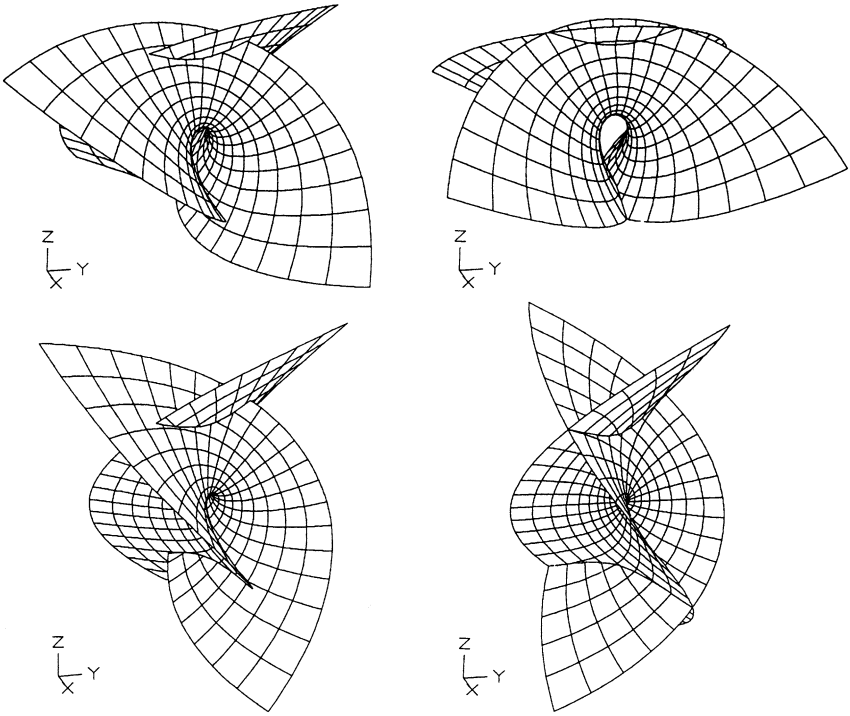

Fig. 1. The bending process leading to the associate surfaces of Enneper's surface corresponding to the square $[-2,2]^2$, counter-clockwise from top right: $\theta = 0$, $\pi/6$, $\pi/3$, and $\pi/2$

Then, for every $\theta \in \mathbb{R}$, also

$$g(w,\theta) := e^{-i\theta} f(w), \quad w \in \Omega \tag{31}$$

describes an isotropic curve, and

$$Z(w,\theta) := \mathrm{Re}\{e^{-i\theta} f(w)\} = X(w)\cos\theta + X^*(w)\sin\theta \tag{32}$$

defines a one-parameter family of minimal surfaces with the property that

$$Z(w,0) = X(w), \quad Z\left(w, \frac{\pi}{2}\right) = X^*(w). \tag{33}$$

The surfaces $Z(w,\theta)$, $w \in \Omega$, are called *associate minimal surfaces* to the surface $X(w)$, $w \in \Omega$. Relation (3) yields

$$\begin{aligned} Z_u &= X_u \cos\theta - X_v \sin\theta, \\ Z_v &= X_v \cos\theta + X_u \sin\theta, \end{aligned}$$

and therefore, by virtue of (2),

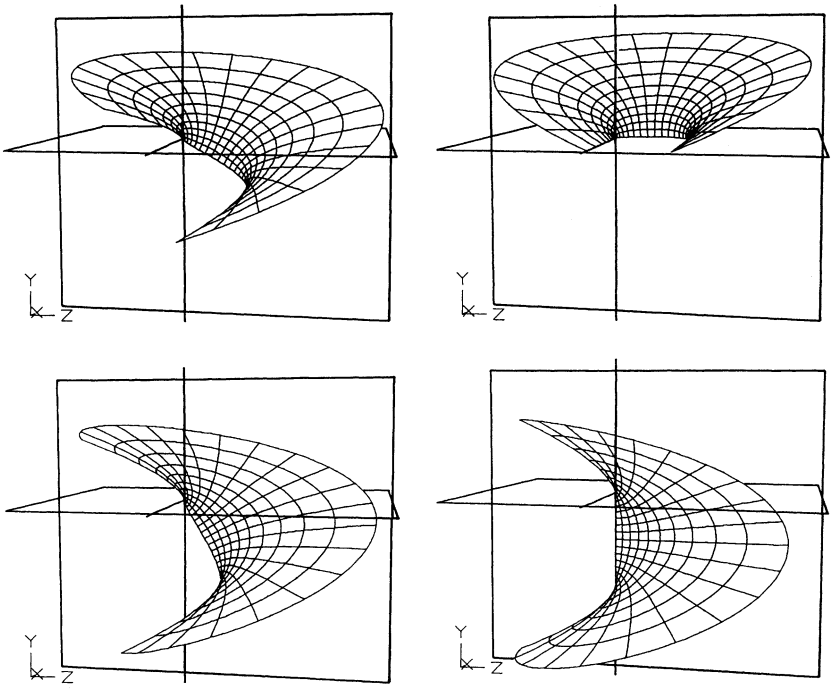

Fig. 2. The associates of Catalan's surface, counter-clockwise from top right ($\theta = 0, \pi/6, \pi/3, \pi/2$). The image of the curve $v = 0$ on Catalan's contained in the plane $y = 0$ is a geodesic. Its Gauss image on S^2 is an arc of a great circle

$$|Z_u|^2 = |Z_v|^2 = |X_u|^2 = |X_v|^2, \quad \langle Z_u, Z_v \rangle = 0.$$

As before, we denote by $\Omega' = \{w \in \Omega \colon \Lambda(w) \neq 0\}$, $\Lambda := |X_u|$, the domain of regular points of X in Ω. Then Ω' is also the domain of regular points for each of the associate surfaces $Z(\cdot, \theta)$, and also the tangent spaces $T_w X$ and $T_w Z(\cdot, \theta)$ of X and $Z(\cdot, \theta)$ coincide for all $w \in \Omega'$ and every $\theta \in \mathbb{R}$. Therefore the Gauss map $N : \Omega' \to S^2$ of X agrees with the spherical image of each of its associate surfaces. Moreover, we have

$$\langle dZ(\cdot, \theta), dZ(\cdot, \theta) \rangle = \langle dX, dX \rangle \tag{34}$$

for all $\theta \in \mathbb{R}$, that is, all associate minimal surfaces have the same first fundamental form and, therefore, all associate surfaces are isometric to each other.

Consider now, for every $\theta \in \mathbb{R}$, the holomorphic function

$$l(\theta) = \mathcal{L}(\theta) - i\mathcal{M}(\theta) := \langle g''(\cdot, \theta), N \rangle$$

which characterizes the asymptotic lines, the curvature lines, and the umbilical points of the associate minimal surface $Z(\cdot, \theta)$. Because of $g''(w, \theta) = e^{-i\theta} f''(w)$, we obtain

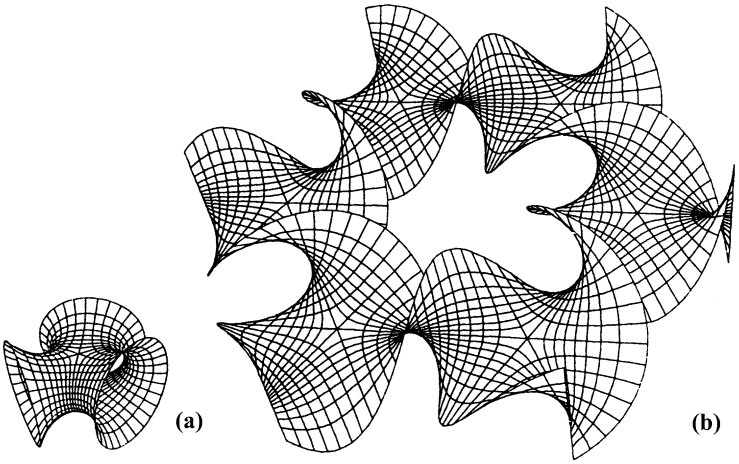

Fig. 3. (a) The Jorge–Meeks catenoid. With courtesy of J. Hahn and K. Polthier. **(b)** An associate minimal surface to the Jorge–Meeks catenoid. Courtesy of K. Polthier and M. Wohlgemuth

$$l(\theta) = e^{-i\theta} l(0) = [\mathcal{L}\cos\theta - \mathcal{M}\sin\theta] - i[\mathcal{L}\sin\theta + \mathcal{M}\cos\theta] \tag{35}$$

where $l(0) = l = \mathcal{L} - i\mathcal{M}$ is the characteristic function for $X = Z(\cdot, 0)$. It follows that $l(\frac{\pi}{2}) = -\mathcal{M} - i\mathcal{L}$. Set

$$\begin{aligned} \xi &:= \mathcal{L}(\dot\alpha^2 - \dot\beta^2) + 2\mathcal{M}\dot\alpha\dot\beta, \\ \eta &:= -\mathcal{M}(\dot\alpha^2 - \dot\beta^2) + 2\mathcal{L}\dot\alpha\dot\beta. \end{aligned}$$

Then we obtain

$$\begin{aligned} l(0)(\dot\alpha + i\dot\beta)^2 &= \xi + i\eta, \\ l\left(\frac{\pi}{2}\right)(\dot\alpha + i\dot\beta)^2 &= \eta - i\xi. \end{aligned} \tag{36}$$

Since $X = Z(\cdot, 0)$ and $X^* = Z(\cdot, \frac{\pi}{2})$, we infer from Proposition 5 that the asymptotic lines of X are the curvature lines of X^*, and conversely, the curvature lines of X are the asymptotic lines of X^*. Thus we have found:

Proposition 6. *All associate surfaces $Z(\cdot, \theta)$ are in isometric correspondence to each other. Each associate surface can be obtained from the original surface X by a bending procedure which, at every stage, passes through a minimal surface. For each $w \in \Omega$, all tangent spaces $T_w Z(\cdot, \theta)$ coincide as θ varies in $\mathbb{R}$. Finally if θ and θ' differ by $\frac{\pi}{2}$, then the asymptotic lines of $Z(\cdot, \theta)$ are the curvature lines of $Z(\cdot, \theta')$, and the curvature lines of $Z(\cdot, \theta)$ are the asymptotic lines of $Z(\cdot, \theta')$.*

One calls the bending procedure $X \mapsto Z(\cdot, \theta)$ *Bonnet's transformation.* For w fixed, the points $Z(w, \theta)$ describe an ellipse as θ varies between 0 and 2π.

To the first assertion of Proposition 6 one also can state a converse due to H.A. Schwarz [1], vol. I, p. 175.

Proposition 7. *Let $X : \Omega \to \mathbb{R}^3$ and $\hat{X} : \hat{\Omega} \to \mathbb{R}^3$ be two minimal surfaces defined on simply connected domains Ω and $\hat{\Omega}$ respectively. Suppose also that X and $\hat{X}$ are isometric to each other, and that $Z(\cdot, \theta)$, $\theta \in \mathbb{R}$, is a family of associate minimal surfaces to X. Then $\hat{X}$ is congruent to one of the surfaces $Z(\cdot, \theta)$. More precisely, there are a conformal mapping τ of Ω onto $\hat{\Omega}$, a motion T of $\mathbb{R}^3$, possibly followed by a reflection, and some $\theta_0 \in \mathbb{R}$ such that*

$$T \circ \hat{X} \circ \tau = Z(\cdot, \theta_0).$$

For a proof of this Proposition we refer to Nitsche [28], § 177, pp. 164–165, and to Calabi [1].

Let us return to the representation (18) in Proposition 4 which, in principle, yields all simply connected minimal surfaces. However, we have to satisfy the isotropy relation (17) which prevents us from inserting arbitrary holomorphic functions Φ_1, Φ_2, Φ_3. We can overcome this difficulty in the following way:

Let Ω be a sufficiently small neighborhood of w_0 and suppose that $\Phi_1(w) \neq 0$ on Ω. Then we can assume that the holomorphic function

$$\sigma(w) := \int_{w_0}^{w} \Phi_1(\underline{w})\, d\underline{w}$$

yields an invertible mapping of Ω onto $\Omega^* := \sigma(\Omega)$. Let $w = \tau(\zeta), \zeta \in \Omega^*$, be the inverse of $\zeta = \sigma(w), w \in \Omega$, and set

$$h(\zeta) := \int_0^{\zeta} \frac{\Phi_2 \circ \tau}{\Phi_1 \circ \tau}(\underline{\zeta})\, d\underline{\zeta}.$$

Then we obtain

$$\zeta = \int_{w_0}^{w} \Phi_1(\underline{w})\, d\underline{w}, \quad h(\zeta) = \int_{w_0}^{w} \Phi_2(\underline{w})\, d\underline{w},$$

and from

$$\Phi_3^2 = -\{\Phi_1^2 + \Phi_2^2\}$$

we infer that

$$\Phi_3(w)\, dw = i\sqrt{\Phi_1(w)^2 + \Phi_2(w)^2}\, dw = i\sqrt{1 + h'(\zeta)^2}\, d\zeta$$

if $\Phi_3(w) \neq 0$ on Ω. *Hence we see that $X|_\Omega$ is equivalent to the representation $Y := X \circ \tau$, which can be written as*

$$Y(\zeta) = X_0 + \mathrm{Re}\left(\zeta, h(\zeta), i\int_0^{\zeta} \sqrt{1 + h'(\underline{\zeta})^2}\, d\underline{\zeta}\right) \tag{37}$$

for $\zeta \in \Omega^*$.

Conversely, if $h(\zeta)$ *is holomorphic on* Ω^* and $1 + h'(\zeta)^2 \neq 0$ *for* $\zeta \in \Omega^*$, *then* (37) *defines a minimal surface* $Y(\zeta)$, $\zeta \in \Omega^*$, provided that Ω^* *is a simply connected domain in* $\mathbb{C}$.

This is the classical *representation formula of Monge*, stating that *every minimal surface is locally equivalent to some holomorphic function and, conversely, that essentially every holomorphic function* h *generates a minimal surface.* In Section 3.3 we shall derive global representation formulas for minimal surfaces.

3.2 Behavior of Minimal Surfaces Near Branch Points

Let $X : \Omega \to \mathbb{R}^3$ be a minimal surface on a domain Ω in $\mathbb{R}^2 \hat{=} \mathbb{C}$. For some $w_0 \in \Omega$, we choose a disk $B_R(w_0) \subset\subset \Omega$. Then, by virtue of Section 3.1, Proposition 1, there is an isotropic curve $f : B_R(w_0) \to \mathbb{C}^3$ such that

$$X(w) = \operatorname{Re} f(w) \tag{1}$$

holds for all $w \in B_R(w_0)$. As we have seen in Section 3.1, the point w_0 is a branch point of X if and only if

$$f'(w_0) = 0. \tag{2}$$

We now want to derive an asymptotic expansion for $X(w)$ in the neighborhood $B_R(w_0)$ of w_0, using the formula

$$f(w) = X(w) + iX^*(w), \quad w \in B_R(w_0). \tag{3}$$

Suppose that $f(w) \not\equiv \text{const}$, and that $f'(w_0) = 0$. Then there is an integer $m \geq 1$ such that

$$f^{(k)}(w_0) = 0 \quad \text{for } 1 \leq k \leq m, \quad f^{(m+1)}(w_0) \neq 0. \tag{4}$$

Thus we obtain the Taylor expansion

$$f(w) = f(w_0) + \frac{1}{(m+1)!} f^{(m+1)}(w_0)(w - w_0)^{m+1} + \cdots \tag{5}$$

on $B_R(w_0)$, and therefore also

$$f'(w) = \frac{1}{m!} f^{(m+1)}(w_0)(w - w_0)^m + \cdots.$$

Set $X_0 := X(w_0)$ and

$$A = \frac{1}{2}(\alpha - i\beta) := \frac{1}{2m!} f^{(m+1)}(w_0), \quad B := \frac{2}{m+1} A.$$

Then we conclude from

$$2X_w(w) = X_u(w) - iX_v(w) = f'(w)$$

that

$$X_w(w) = A(w - w_0)^m + O(|w - w_0|^{m+1}) \quad \text{as } w \to w_0,$$

and

$$X(w) = X_0 + \operatorname{Re}\{B(w - w_0)^{m+1} + O(|w - w_0|^{m+2})\}.$$

The conformality relation

$$\langle X_w, X_w \rangle = 0$$

implies that

$$\langle A, A \rangle = 0$$

holds, whence

$$|\alpha|^2 = |\beta|^2, \quad \langle \alpha, \beta \rangle = 0,$$

and $A \neq 0$ yields $|\alpha| = |\beta| > 0$. Moreover,

$$\begin{aligned} X_u(w) &= \operatorname{Re} f'(w) = \alpha \operatorname{Re}(w - w_0)^m + \beta \operatorname{Im}(w - w_0)^m + \cdots, \\ X_v(w) &= -\operatorname{Im} f'(w) = -\alpha \operatorname{Im}(w - w_0)^m + \beta \operatorname{Re}(w - w_0)^m + \cdots, \end{aligned}$$

where the remainder terms are of order $O(|w - w_0|^{m+1})$. Hence we conclude that

$$X_u(w) \wedge X_v(w) = (\alpha \wedge \beta)|w - w_0|^{2m} + O(|w - w_0|^{2m+1}) \quad \text{as } w \to w_0.$$

This implies that $N(w)$ tends to a limit vector N_0 as $w \to w_0$:

$$\lim_{w \to w_0} N(w) = N_0 = \frac{\alpha \wedge \beta}{|\alpha \wedge \beta|}.$$

Consequently, the Gauss map $N(w)$ of a minimal surface $X(w)$, $w \in \Omega$, is well-defined on all of Ω as a continuous mapping into S^2. In fact, $N : \Omega \to S^2$ is a harmonic mapping of Ω into the unit sphere S^2 (cf. Section 5.1) which satisfies

$$\Delta N + N|\nabla N|^2 = 0 \quad \text{in } \Omega.$$

Therefore N is real analytic (this also follows from the discussion in Section 3.2). From formula (6) in Section 1.4 we then infer

$$|N_u|^2 = |N_v|^2, \quad \langle N_u, N_v \rangle = 0$$

and

$$|\nabla N|^2 = -K|\nabla X|^2,$$

whence also

$$2|N_u \wedge N_v| = |\nabla N|^2,$$

and formula (44) in Section 1.2 yields

$$N_u \wedge N_v = K X_u \wedge X_v.$$

Since $K \leq 0$, one concludes

$$\Delta N = 2N_u \wedge N_v,$$

i.e. N is a surface of constant mean curvature one (cf. Chapter 5, and also Vol. 3, Section 2.3).

We now want to put X into some *normal form* which will explain the term *branch point*. Set

$$a := \frac{|\alpha|}{m+1} = \frac{|\beta|}{m+1}$$

and

$$e_1 := \frac{\alpha}{|\alpha|}, \quad e_2 := \frac{\beta}{|\beta|}, \quad e_3 := e_1 \wedge e_2 = N_0.$$

Then we can rewrite the formula

$$X(w) = X_0 + \operatorname{Re}\left\{ \frac{\alpha - i\beta}{m+1}(w - w_0)^{m+1} + O(|w - w_0|^{m+2}) \right\}$$

as

$$X(w) = X_0 + a e_1 \operatorname{Re}(w - w_0)^{m+1} + a e_2 \operatorname{Im}(w - w_0)^{m+1} + O(|w - w_0|^{m+2}).$$

If we rotate the axes of the given coordinate system in $\mathbb{R}^3$ such that e_1, e_2, and e_3 point in the directions of the new positive x, y, and z-axes respectively, we obtain

$$\begin{aligned} x(w) + iy(w) &= (x_0 + iy_0) + a(w - w_0)^{m+1} + O(|w - w_0|^{m+2}), \\ z(w) &= z_0 + O(|w - w_0|^{m+2}). \end{aligned} \tag{6}$$

This *normal form of a minimal surface* $X(w) = (x(w), y(w), z(w))$ shows that a minimal surface X behaves in a neighborhood of one of its branch points w_0 like a branch point of m-th order of a Riemann surface. Thus we shall denote the integer m, defined by (4), as the *order of the branch point* w_0 *of the minimal surface* X. *If we define* $m = 0$ *for regular points, we may consider regular points as branch points of order zero.*

Remark 1. In Vol. 2, Section 6, we denote the *order* of a branch point w_0 by n, while m is used for the *index* of w_0.

Let us collect some of the previous results in the following

Proposition 1. *If* $w_0 \in \Omega$ *is a branch point of a minimal surface* $X : \Omega \to \mathbb{R}^3$, *then there is a vector* $A \in \mathbb{C}^3$, $A \neq 0$, *and an integer* $m \geq 1$, *the so-called order of the branch point* w_0, *such that the following holds*:

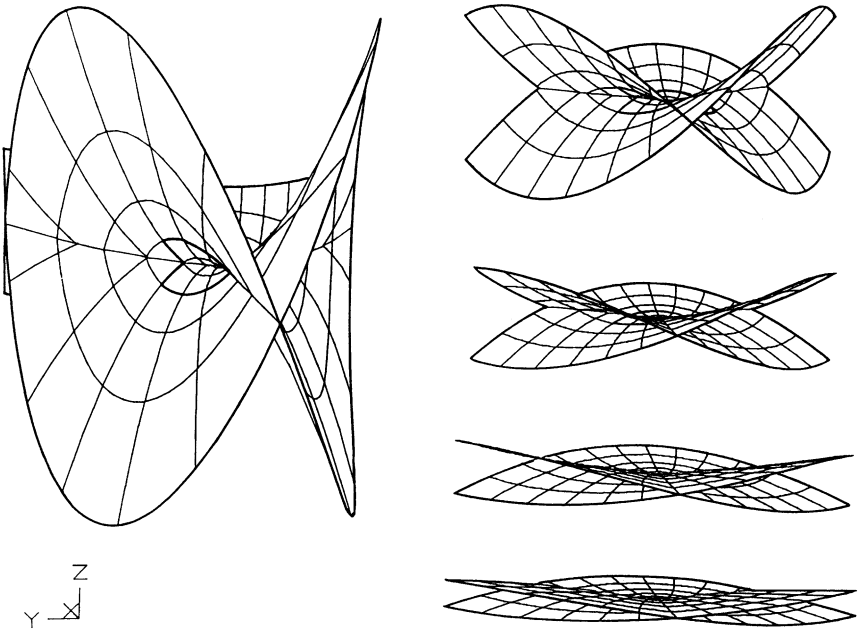

Fig. 1. $w = 0$ is a branch point of order one of Catalan's surface. The parts of the surface corresponding to the shrinking neighborhoods $[-2^n/10, 2^n/10]^2$ for $n = 5, 4, 3, 2, 1$ illustrate the convergence of the tangent planes in the vicinity of a branch point, a general property of all two-dimensional minimal surfaces. Note that the second picture shows an enlarged detail of the first one, the third one an enlarged detail of the second one, etc.

$$X_w(w) = A(w - w_0)^m + O(|w - w_0|^{m+1}) \quad \text{as } w \to w_0, \tag{7}$$

and N is a surface of constant mean curvature one;

$$X(w) = X_0 + \mathrm{Re}[B(w - w_0)^{m+1}] + O(|w - w_0|^{m+2}), \tag{8}$$

where $B = \frac{2}{m+1}A$, and $A = \frac{1}{2}(\alpha - i\beta)$ is an isotropic vector in $\mathbb{C}^3 \setminus \{0\}$:

$$\langle A, A\rangle = 0 \tag{9}$$

or

$$|\alpha|^2 = |\beta|^2 > 0, \quad \langle \alpha, \beta\rangle = 0, \quad \alpha, \beta \in \mathbb{R}^3. \tag{9'}$$

The normal $N(w)$ tends to the limit

$$N_0 = \frac{\alpha \wedge \beta}{|\alpha \wedge \beta|}, \tag{10}$$

and the tangent plane of X at w converges to a limiting position as $w \to w_0$.

Consequently, the function $l(w) = \mathfrak{L}(w) - i\mathfrak{M}(w)$ is holomorphic on Ω, and the spherical image map $N(w)$ is a continuous map from Ω into S^2.

Next we want to derive a *lower bound for the area of minimal surfaces.* Suppose that $B_R(P)$ is a ball in $\mathbb{R}^3$, the center P of which lies on the trace of some minimal surface $X : \Omega \to \mathbb{R}^3$ extending beyond $B_R(P)$, i.e., there are no boundary points of $X(\Omega)$ within $B_R(P)$. Let $w_0 \in \Omega$ be a branch point of X of order m, and suppose that $P = X(w_0)$. Then the normal form (6) suggests that the area of $X(\Omega) \cap B_R(P)$ is at least as large as the area of $m+1$ plane equatorial disks of $B_R(P)$, provided that the radius R is sufficiently small. In fact, we can prove:

Proposition 2. *Suppose that $X : \Omega \to \mathbb{R}^3$ is a minimal surface defined on a bounded simply connected domain Ω. Moreover, let $w_0 \in \Omega$ be a branch point of order $m \geq 0$, $X_0 = X(w_0)$, and let $R > 0$ be some number such that*

$$\liminf_{k\to\infty} |X(w_k)| \geq R \tag{11}$$

holds for every sequence $\{w_k\}$ of points $w_k \in \Omega$ with dist $(w_k, \partial\Omega) \to 0$ as $k \to \infty$. Then the area $A(X)$ of the surface X satisfies

$$A(X) \geq (m+1)\pi(R^2 - |X_0|^2). \tag{12}$$

Equality holds if and only if the image of X lies in a plane through the point X_0 which is perpendicular to the line from 0 to X_0.

Proof. Since Ω can be mapped conformally onto the unit disk such that w_0 is transformed into the origin, we may assume that $w_0 = 0, X_0 = X(0)$, and $\Omega = \{w\colon |w| < 1\}$.

Then we can find an isotropic curve $f : \Omega \to \mathbb{C}^3$ satisfying $f(0) = X_0 = X(0)$ and

$$f = X + iX^*,$$

where $X^* : \Omega \to \mathbb{R}^3$ is an adjoint surface to X with $X^*(0) = 0$. We can represent $f(w)$ by the Taylor series

$$f(w) = X_0 + \sum_{k=m+1}^{\infty} A_k w^k, \quad A_k \in \mathbb{C}^3,$$

which is convergent for $|w| < 1$. Applying Cauchy's integral formula to the holomorphic function $F(w) := \langle f(w), f(w)\rangle, |w| < 1$, it follows that

$$\int_0^{2\pi} F(re^{i\theta})\, d\theta = 2\pi F(0),$$

and therefore

$$\int_0^{2\pi} |X(re^{i\theta})|^2\, d\theta - \int_0^{2\pi} |X^*(re^{i\theta})|^2\, d\theta = 2\pi|X_0|^2,$$

for every $r \in (0, 1)$.

On the other hand, we obtain

$$\begin{aligned}\int_0^{2\pi} |f(re^{i\theta})|^2\,d\theta &= \int_0^{2\pi} |X(re^{i\theta})|^2\,d\theta + \int_0^{2\pi} |X^*(re^{i\theta})|^2\,d\theta \\ &= 2\pi\left\{|X_0|^2 + \sum_{k=m+1}^{\infty} |A_k|^2 r^{2k}\right\}.\end{aligned}$$

Combining the two identities, we arrive at

$$\int_0^{2\pi} |X(re^{i\theta})|^2\,d\theta = 2\pi|X_0|^2 + \pi \sum_{k=m+1}^{\infty} |A_k|^2 r^{2k}.$$

Setting

$$\mu(r) := \min_{|w|=r} |X(w)|^2,$$

we deduce the estimate

$$\mu(r) \le |X_0|^2 + \frac{1}{2} \sum_{k=m+1}^{\infty} |A_k|^2 r^{2k}.$$

Moreover, the area $A(r)$ of the image of $\{w\colon |w| < r\}$ under the mapping X is given by

$$\begin{aligned}A(r) &= \frac{1}{2}\int_{|w|<r} |\nabla X|^2\,du\,dv = \frac{1}{2}\int_0^r \int_0^{2\pi} |f'(te^{i\theta})|^2 t\,dt\,d\theta \\ &= \frac{\pi}{2} \sum_{k=m+1}^{\infty} k|A_k|^2 r^{2k}.\end{aligned}$$

Thus we infer that

$$(13)\quad \frac{\pi}{2} \sum_{k=m+2}^{\infty} [k-(m+1)]|A_k|^2 r^{2k} - (m+1)\pi|X_0|^2 \le A(r) - (m+1)\pi\mu(r).$$

By assumption (11), we have $\liminf_{r\to 1} \mu(r) \ge R^2$, whence

$$(14)\quad \frac{\pi}{2} \sum_{k=m+2}^{\infty} [k-(m+1)]|A_k|^2 + (m+1)\pi(R^2 - |X_0|^2) \le \lim_{r\to 1} A(r) = A(X),$$

and inequality (12) is proved.

Suppose now that equality holds in (12). Then we infer form (14) that $A_k = 0$ for $k \ge m+2$, whence

$$f(w) = X_0 + A_{m+1} w^{m+1}.$$

Let $A_{m+1} = a+ib$, $a, b \in \mathbb{R}^3$. Since f is isotropic, we obtain $\langle A_{m+1}, A_{m+1}\rangle = 0$, or $|a| = |b|, \langle a, b\rangle = 0$. Therefore, the vectors $e_1 := \frac{a}{|a|}$ and $e_2 := -\frac{b}{|b|}$ are orthonormal, and we have

$$X(w) = X_0 + |a| r^{m+1}\{e_1 \cos(m+1)\theta + e_2 \sin(m+1)\theta\}. \tag{15}$$

This yields

$$A(X) = (m+1)|a|^2\pi.$$

On the other hand, we have assumed that

$$A(X) = (m+1)\pi(R^2 - |X_0|^2)$$

holds. Then we conclude that

$$|a|^2 = R^2 - |X_0|^2. \tag{16}$$

Set $e_3 := e_1 \wedge e_2$. Then e_1, e_2, e_3 form an orthonormal frame in $\mathbb{R}^3$, and we can write

$$X_0 = \sum_{k=1}^{3} c_k e_k.$$

In conjunction with (15), it follows that

$$\begin{aligned} |X(e^{i\theta})|^2 &= (c_1 + |a|\cos(m+1)\theta)^2 + (c_2 + |a|\sin(m+1)\theta)^2 + c_3^2 \\ &= |X_0|^2 + |a|^2 + 2|a|\{c_1\cos(m+1)\theta + c_2\sin(m+1)\theta\}, \end{aligned}$$

and, on account of (16), we conclude that

$$|X(e^{i\theta})|^2 = R^2 + 2|a|\{c_1\cos(m+1)\theta + c_2\sin(m+1)\theta\}.$$

Therefore, unless $c_1 = c_2 = 0$, we can find an angle θ such that $|X(e^{i\theta})| < R$, which contradicts (11). Hence we see that

$$X_0 = c_3(e_1 \wedge e_2),$$

and formula (15) shows that $X(w)$ lies in an affine plane, perpendicular to the vector X_0, which contains the point with the position vector X_0.

Introducing suitable Cartesian coordinates x, y, z in $\mathbb{R}^3$, we obtain the normal form

$$\begin{aligned} x + iy &= \sqrt{R^2 - |X_0|^2}\, w^{m+1}, \quad |w| < 1, \\ z &= 0 \end{aligned}$$

for the minimal surface $X(w) = (x(w), y(w), z(w)), |w| < 1$, in the case that equality holds in (12).

This completes the proof of Proposition 2. □

3.3 Representation Formulas for Minimal Surfaces

In Proposition 4 of Section 3.1 we have stated that for every holomorphic map

$$\Phi(w) = (\Phi_1(w), \Phi_2(w), \Phi_3(w)), \quad w \in \Omega,$$

of a simply connected domain Ω in $\mathbb{C}$ with $\Phi(w) \not\equiv 0$ and

$$\langle \Phi, \Phi \rangle = \Phi_1^2 + \Phi_2^2 + \Phi_3^2 = 0, \tag{1}$$

the formula

$$X(w) = X_0 + \operatorname{Re} \int_{w_0}^{w} \Phi(\zeta)\, d\zeta, \quad w \in \Omega, \tag{2}$$

with $w_0 \in \Omega$ and $X_0 \in \mathbb{R}^3$, defines a minimal surface $X : \Omega \to \mathbb{R}^3$, and every such surface can be obtained in this way. At the end of Section 3.1 we have derived local solutions Φ of the isotropy equation (1). In this section we shall first determine all (global) holomorphic mappings $\Phi : \Omega \to \mathbb{C}^3$ satisfying (1). This in turn will lead us to the celebrated Enneper–Weierstrass representation formulas of minimal surfaces which, in particular, can be used to establish explicit expressions for the normal image, the Gauss curvature, and for the asymptotic and curvature lines of minimal surfaces.

Lemma 1. *If $\mu(w)$ is a holomorphic function and $\nu(w)$ is a meromorphic function in a domain Ω in $\mathbb{C}$ such that $\mu(w) \not\equiv 0$ and that μ has a zero of order at least $2n$ where ν has a pole of order n, then the functions*

$$\Phi_1 = \frac{1}{2}\mu(1 - \nu^2), \quad \Phi_2 = \frac{i}{2}\mu(1 + \nu^2), \quad \Phi_3 = \mu\nu \tag{3}$$

are holomorphic in Ω, and the triple $\Phi = (\Phi_1, \Phi_2, \Phi_3)$ satisfies (1) and $\Phi(w) \not\equiv 0$. Conversely, every triple $\Phi = (\Phi_1, \Phi_2, \Phi_3) \not\equiv 0$ of holomorphic functions on Ω satisfying (1) can be written in the form (3) if and only if $\Phi_1 - i\Phi_2 \not\equiv 0$.

Proof. The first part of the lemma follows by a straight-forward computation. In order to prove the converse, we note that the assumption $\Phi_1 - i\Phi_2 \not\equiv 0$ certainly is necessary for (3) to hold. In fact, (1) is equivalent to

$$(\Phi_1 - i\Phi_2)(\Phi_1 + i\Phi_2) + \Phi_3^2 = 0. \tag{4}$$

Hence $\Phi_1 - i\Phi_2 = 0$ yields $\Phi_3 = 0$, and $\Phi_3 = \mu\nu$ would imply $\mu = 0$ or $\nu = 0$. Since $\mu = 0$ would give $\Phi = 0$, we would have $\nu = 0$ and therefore $\Phi_1 = \mu/2, \Phi_2 = i\mu/2$; thus $\Phi_1 + i\Phi_2 = 0$. Consequently $\Phi_1 = \Phi_2 = \Phi_3 = 0$, which contradicts $\Phi \not\equiv 0$.

Suppose now that $\Phi_1 - i\Phi_2 \not\equiv 0$. Then the formulas

$$\mu := \Phi_1 - i\Phi_2, \quad \nu := \frac{\Phi_3}{\Phi_1 - i\Phi_2} \tag{5}$$

define a holomorphic function μ and a meromorphic function ν in Ω, satisfying $\mu\nu = \Phi_3$. Moreover, (4) implies

$$\Phi_1 + i\Phi_2 = -\frac{\Phi_3^2}{\Phi_1 - i\Phi_2} = -\mu\nu^2 \tag{6}$$

which, together with

$$\Phi_1 - i\Phi_2 = \mu,$$

yields

$$\Phi_1 = \frac{\mu}{2}(1 - \nu^2), \quad \Phi_2 = i\frac{\mu}{2}(1 + \nu^2).$$

Finally, the relation $\mu\nu^2 = -(\Phi_1 + i\Phi_2)$ shows that the function $\mu\nu^2$ is holomorphic. Therefore if $w_0 \in \Omega$ is a pole of order n of ν, then w_0 is a zero of order at least $2n$ for μ. □

In conjunction with (2), this lemma yields the following result:

Theorem 1 (Enneper–Weierstrass representation formula). *For every nonplanar minimal surface*

$$X(w) = (x(w), y(w), z(w)), \quad w \in \Omega,$$

defined on a simply connected domain Ω in $\mathbb{C}$, there are a holomorphic function μ and a meromorphic function ν in Ω with $\mu \not\equiv 0, \nu \not\equiv 0$ such that $\mu\nu^2$ is holomorphic in Ω, and that

$$\begin{aligned} x(w) &= x_0 + \operatorname{Re} \int_{w_0}^{w} \frac{1}{2}\mu(1 - \nu^2)\, d\zeta, \\ y(w) &= y_0 + \operatorname{Re} \int_{w_0}^{w} \frac{i}{2}\mu(1 + \nu^2)\, d\zeta, \\ z(w) &= z_0 + \operatorname{Re} \int_{w_0}^{w} \mu\nu\, d\zeta \end{aligned} \tag{7}$$

holds for $w, w_0 \in \Omega$ and $X_0 = (x_0, y_0, z_0) = X(w_0)$.

Conversely, two functions μ and ν as above define by means of (7) a minimal surface $X : \Omega \to \mathbb{R}^3$ provided that Ω is simply connected.

Remark. A point $w \in \Omega$ is a branch point of a minimal surface $X : \Omega \to \mathbb{R}^3$ represented by (1) and (2) if and only if $\Phi_1(w) = \Phi_2(w) = \Phi_3(w) = 0$. Thus, $w \in \Omega$ is a branch point of a minimal surface $X : \Omega \to \mathbb{R}^3$ represented by (7) if and only if both μ and $\mu\nu^2$ are vanishing at w. The set of regular points $\Omega' := \{w \in \Omega \colon \Lambda(w) \neq 0\}$ is therefore given by

$$\Omega' = \{w \in \Omega \colon |\mu(w)|(1 + |\nu(w)|^2) \neq 0\}.$$

The function ν has an important geometric meaning. It will turn out that ν is just the stereographic projection of the spherical image N of X onto the x, y-plane.

Before we prove this, we want to derive explicit expressions for the spherical image N and for the Gauss curvature of a minimal surface $X : \Omega \to \mathbb{R}^3$ given by

$$X(w) = \operatorname{Re} f(w), \tag{8}$$

with an isotropic curve $f : \Omega \to \mathbb{R}^3$ satisfying

$$\begin{aligned} f' &= X_u - iX_v = \Phi = (\Phi_1, \Phi_2, \Phi_3) \\ &= \left(\frac{1}{2}\mu(1-\nu^2), \frac{i}{2}\mu(1+\nu^2), \mu\nu\right), \end{aligned} \tag{9}$$

where μ and ν satisfy the assumptions stated in Theorem 1. Then the function

$$\Lambda := |X_u|^2 = \tfrac{1}{2}|\nabla X|^2 = \tfrac{1}{2}|f'|^2 = \tfrac{1}{2}|\Phi|^2$$

can be written as

$$\Lambda = \tfrac{1}{4}|\mu|^2(1+|\nu|^2)^2, \tag{10}$$

and the line element $ds = |dX|$ takes the form

$$ds^2 = \Lambda\{du^2 + dv^2\}.$$

By virtue of Section 3.1 (20), it follows that

$$X_u \wedge X_v = \tfrac{1}{4}|\mu|^2\{1+|\nu|^2\}(2\operatorname{Re}\nu, 2\operatorname{Im}\nu, |\nu|^2 - 1).$$

Taking (10) into account, we obtain the representation

$$N = \frac{1}{1+|\nu|^2}(2\operatorname{Re}\nu, 2\operatorname{Im}\nu, |\nu|^2 - 1) \tag{11}$$

for the spherical image $N : \Omega \to S^2$ of X.

In order to compute K, we first note that

$$f' = \mu\left(\frac{1}{2}(1-\nu^2), \frac{i}{2}(1+\nu^2), \nu\right)$$

implies

$$f'' = \frac{\mu'}{\mu}f' + \mu\nu' g, \quad g := (-\nu, i\nu, 1),$$

on $\{w \in \Omega\colon \mu(w) \neq 0\}$. From (11) we infer that

$$\langle N, g\rangle = -1.$$

Since the zeros of μ are isolated and $\langle N, f' \rangle = 0$, we obtain

$$\langle N, f'' \rangle = -\mu\nu',$$

and on account of (25) of Section 3.1, we arrive at

$$l = \mathfrak{L} - i\mathfrak{M} = -\mu\nu'. \tag{12}$$

The branch points of $X(w)$ are removable singularities of $l(w) = -\mu(w)\nu'(w)$ since $l(w)$ remains bounded if w approaches such a point. Hence $l(w)$ is holomorphic in Ω.

Recall that $\mu\nu^2$ is holomorphic in Ω, and that $w \in \Omega$ is a branch point of X if and only if both $\mu(w) = 0$ and $\mu(w)\nu^2(w) = 0$ are satisfied. If $\Lambda(w) \neq 0$, then $l(w) = 0$ if either $\nu'(w) = 0$, or w is a pole for ν and a zero of at least third order for μ.

Moreover, the formulas (10) and (12) together with (26) of Section 3.1 yield

$$K = -\left\{ \frac{4|\nu'|}{|\mu|(1 + |\nu|^2)^2} \right\}^2 \tag{13}$$

for the Gauss curvature of X on $\Omega' = \{w \in \Omega \colon \Lambda(w) \neq 0\}$. Then we infer for any $w \in \Omega'$ which is not a pole of ν that $K(w) \neq 0$ *holds if and only if* $\nu'(w) \neq 0$ *is satisfied.*

Moreover, Proposition 5 of Section 3.1 yields:

A curve $\gamma(t) = \alpha(t) + i\beta(t)$ *contained in* Ω *(with* $\alpha(t), \beta(t) \in \mathbb{R}$*) describes an asymptotic line of the minimal surface* X *if and only if*

$$\mathrm{Re}\{\mu(\gamma)\nu'(\gamma)\dot{\gamma}^2\} = 0, \tag{14}$$

and the lines of curvature are characterized by

$$\mathrm{Im}\{\mu(\gamma)\nu'(\gamma)\dot{\gamma}^2\} = 0. \tag{15}$$

Now we want to give *a geometric interpretation of the function* $\nu(w)$ that enters into the representation formula (7).

Let us identify the complex plane $\mathbb{C} = \{x + iy \colon x, y \in \mathbb{R}\}$ with the x, y-plane $\{(x, y, z) \colon z = 0\}$ in $\mathbb{R}^3$, and let $\bar{\mathbb{C}} = \mathbb{C} \cup \{\infty\}$ be the compactification of $\mathbb{C}$ with the point at infinity. As usual, we introduce the Riemann sphere $S^2 = \{(x, y, z) \colon x^2 + y^2 + z^2 = 1\}$, and denote by $P = (0, 0, 1)$ its north pole. Then the *stereographic projection*

$$\sigma : S^2 \to \bar{\mathbb{C}}$$

is the 1–1-mapping of S^2 onto the compactified complex plane $\bar{\mathbb{C}}$ which associates each point $Q \in S^2, Q \neq P$, with the intersection point ω of the x, y-plane

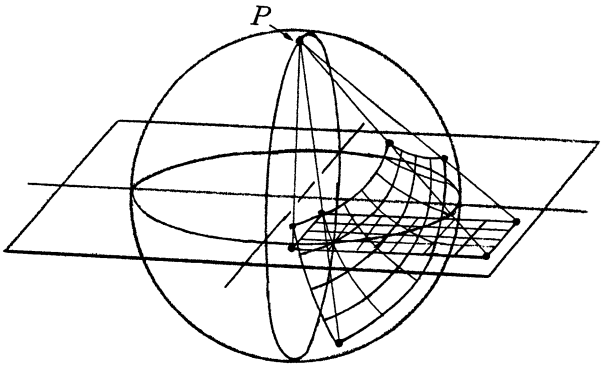

Fig. 1. The stereographic projection.

with the straight line through P and Q, whereas P is mapped to ∞ (cf. Fig. 1). Let $\rho : \bar{\mathbb{C}} \to S^2$ be the inverse of σ. Then the image $\rho(\omega) := (a, b, c) = Q$ of some point $\omega = \xi + i\eta \in \mathbb{C}$ is given by

$$a = \frac{2\xi}{1+\xi^2+\eta^2}, \quad b = \frac{2\eta}{1+\xi^2+\eta^2}, \quad c = \frac{\xi^2+\eta^2-1}{1+\xi^2+\eta^2} \tag{16}$$

and $\rho(\infty) = P$.

The formula (16) can be written as

$$\rho(\omega) = \frac{1}{1+|\omega|^2}(2\,\mathrm{Re}\,\omega, 2\,\mathrm{Im}\,\omega, |\omega|^2 - 1), \tag{17}$$

and we see that $\rho(\omega) \to (0, 0, 1) = P$ as $|\omega| \to \infty$. A straightforward computation yields for $\omega = \sigma(Q)$ the formula

$$\omega = \frac{a+ib}{1-c}. \tag{18}$$

If we now compare the formula (11) for the spherical image $N(w)$ of a minimal surface $X(w), w \in \Omega$, given by (8) and (9), with the expression (17) for $\rho = \sigma^{-1}$, then we see that

$$N(w) = \rho(\nu(w)), \tag{19}$$

whence

$$\nu(w) = \sigma(N(w)). \tag{20}$$

Thus *the meromorphic function $\nu : \Omega \to \bar{\mathbb{C}}$ is nothing but the stereographic projection of the normal image N of the given minimal surface X*:

$$\nu = \sigma \circ N, \quad N = \rho \circ \nu. \tag{21}$$

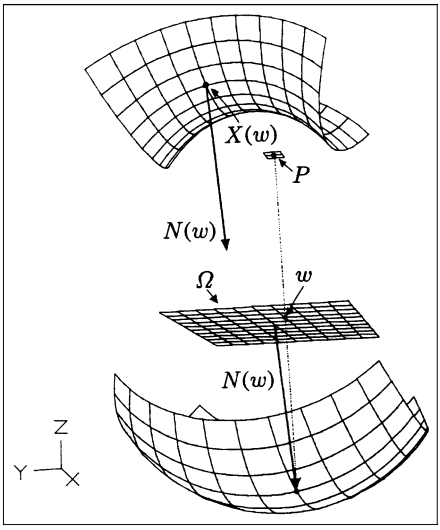

Fig. 2. The part of Enneper's surface corresponding to the rectangle $\Omega = [-1/2, 1/2]^2$ floats at the top of the picture; w is mapped to $X(w)$. The unit normal vector $N(w)$ of Enneper's surface at the point $X(w)$ is shown twice, one copy has its foot on the surface, the other one at the origin of space. The Gauss image, i.e. the set of all unit normals of this part of Enneper's surface is displayed at the bottom. For minimal surfaces the Gauss map corresponds to the meromorphic function $\nu(w)$ appearing in Weierstrass's representation formula (7) via the inverse of the stereographic projection from Ω to S^2. The latter is indicated by the dotted line starting at the north pole P, and for Enneper's surface $\nu(w) = w$

In particular, $w \in \Omega$ is a pole of ν if and only if the point $N(w) \in S^2$ is the north pole P.

Furthermore, the mapping

$$\omega = \nu(w), \quad w \in \Omega, \tag{22}$$

is a biholomorphic mapping of Ω onto $\Omega^* := \nu(\Omega)$ if the following two conditions are satisfied:

$$\begin{aligned} &\text{(i)} \quad N(w) \neq P \quad \text{for all } w \in \Omega; \\ &\text{(ii)} \quad \text{the mapping } N : \Omega \to S^2 \text{ is injective.} \end{aligned} \tag{23}$$

If $\nu : \Omega \to \Omega^*$ is biholomorphic, then we have $\nu'(w) \neq 0$ for all $w \in \Omega$, and this implies $K(w) < 0$ on Ω, i.e., X has no umbilical points.

Suppose now that $\nu : \Omega \to \Omega^*$ is a biholomorphic mapping, and let

$$w = \tau(\omega), \quad \omega \in \Omega^*, \tag{24}$$

be its inverse. Then the reparametrization $Y = X \circ \tau$ of the minimal surface X is again a minimal surface, and

$$Y(\omega) = X(\tau(\omega)), \quad \omega \in \Omega^*. \tag{25}$$

Let us introduce the function

$$\mathfrak{F}(\omega) := \frac{1}{2}\frac{\mu(\tau(\omega))}{\nu'(\tau(\omega))} = \frac{1}{2}\tau'(\omega)\mu(\tau(\omega)) \tag{26}$$

which is holomorphic in Ω^*. Then we infer from (7) the following *representation formula of Weierstrass*:

$$Y(\omega) = X_0 + \mathrm{Re}\begin{bmatrix} \int_{\omega_0}^{\omega}(1-\underline{\omega}^2)\mathfrak{F}(\underline{\omega})d\underline{\omega} \\ \int_{\omega_0}^{\omega} i(1+\underline{\omega}^2)\,\mathfrak{F}(\underline{\omega})d\underline{\omega} \\ \int_{\omega_0}^{\omega} 2\underline{\omega}\mathfrak{F}(\underline{\omega})\,d\underline{\omega} \end{bmatrix} \tag{27}$$

where $\omega, \omega_0 \in \Omega^*$, and $X_0 = X(w_0) = Y(\omega_0)$, $\omega_0 = \nu(w_0)$.

Instead of two (essentially) arbitrary functions μ and ν as in (7), the expression (27) only involves an arbitrary function $\mathfrak{F}(\omega)$. Conversely, for every holomorphic function $\mathfrak{F}(\omega) \not\equiv 0$ on a simply connected domain Ω^* in $\mathbb{C}$, the formula (27) defines a minimal surface $Y : \Omega^* \to \mathbb{R}^3$. In other words, *to each holomorphic function* $\mathfrak{F} \neq 0$ *corresponds some minimal surface, and vice versa.* Thus we have also recovered the result of Monge from the end of Section 3.1.

From (27), we can derive an *integral-free representation* formula by introducing a function $F(\omega)$ such that $F^{(3)}(\omega) = \mathfrak{F}(\omega)$, and performing some partial integrations. Let $Y = (Y^1, Y^2, Y^3)$. Then, for suitable constants c_1, c_2, c_3, we obtain

$$\begin{aligned} Y^1(\omega) &= \mathrm{Re}\{(1-\omega^2)F''(\omega) + 2\omega F'(\omega) - 2F(\omega)\} + c_1, \\ Y^2(\omega) &= \mathrm{Re}\{i(1+\omega^2)F''(\omega) - 2i\omega F'(\omega) + 2iF(\omega)\} + c_2, \\ Y^3(\omega) &= \mathrm{Re}\{2\omega F''(\omega) - 2F'(\omega)\} + c_3. \end{aligned} \tag{28}$$

Weierstrass ([1], pp. 48–50) has used this representation to prove the following theorem:

If $F(\omega)$ is an algebraic function of ω, then (28) defines an algebraic minimal surface, and conversely, every algebraic minimal surface possesses a parameter representation $Y(\omega)$ of type (28) with an algebraic function $F(\omega)$.

Let us now put together the main results for the representation formula (27). We first note that (27) goes over into (7) if we replace ω and ω_0 and w and $w_0, Y(\omega)$ and $X(w)$, and set $\mu(w) := 2\mathfrak{F}(w)$ and $\nu(w) := w$. Then we arrive at the following result:

Theorem 2. *Let $\mathfrak{F}(w)$ be a holomorphic function in a simply connected domain Ω of $\mathbb{C}, \mathfrak{F}(w) \not\equiv 0$, and set*

$$\Phi(w) = ((1-w^2)\mathfrak{F}(w), i(1+w^2)\mathfrak{F}(w), 2w\mathfrak{F}(w)). \tag{29}$$

Then

$$X(w) = X_0 + \operatorname{Re} \int_{w_0}^{w} \Phi(\underline{w})\, d\underline{w}, \quad w \in \Omega, \tag{30}$$

defines a minimal surface $X : \Omega \to \mathbb{R}^3$ *with the surface normal*

$$N(w) = \frac{1}{1+u^2+v^2}(2u, 2v, u^2+v^2-1), \quad w = u+iv. \tag{31}$$

If σ *denotes the stereographic projection from the north pole* $P = (0,0,1)$ *of* $S^2 = \{(x,y,z)\colon x^2+y^2+z^2 = 1\}$ *onto the* x,y*-plane, then we have*

$$\sigma(N(w)) = w.$$

The line element $ds = |dX|$ *on the surface* X *is given by*

$$ds^2 = \Lambda(w)\{du^2 + dv^2\} \tag{32}$$

where

$$\Lambda(w) = |\mathfrak{F}(w)|^2(1+u^2+v^2)^2, \quad w = u+iv. \tag{32'}$$

Thus the set $\Omega' := \{w \in \Omega\colon \Lambda(w) \neq 0\}$ *of regular points of the minimal surface* X *is described by*

$$\Omega' = \{w \in \Omega\colon \mathfrak{F}(w) \neq 0), \tag{33}$$

and its Gauss curvature $K(w)$ *on* Ω' *is given by*

$$K(w) = -\frac{4}{|\mathfrak{F}(w)|^2(1+u^2+v^2)^4}. \tag{34}$$

The coefficients $\mathcal{L}, \mathcal{M}, \mathcal{N}$ *of the second fundamental form satisfy* $\mathcal{L} + \mathcal{N} = 0$ *and can be obtained from the holomorphic function*

$$l(w) = \mathcal{L}(w) - i\mathcal{M}(w) = -2\mathfrak{F}(w), \quad w \in \Omega. \tag{35}$$

The branch points $w \in \Omega$ *of* X *are the zeros of the holomorphic function* $\mathfrak{F}(w), w \in \Omega$*. Thus* X *has no umbilical points since an umbilical point is a zero of* l *on the set of regular points* Ω'*. The directions* (du, dv) *of the asymptotic lines are characterized by the equation*

$$\operatorname{Re} \mathfrak{F}(w)(dw)^2 = 0, \tag{36}$$

and the lines of curvature are described by

$$\operatorname{Im} \mathfrak{F}(w)(dw)^2 = 0. \tag{37}$$

Finally, the associate minimal surfaces $Z(w,\theta)$ *to* $X(w)$ *are given by*

$$Z(w,\theta) = X_0 + \operatorname{Re}\int_{w_0}^{w} e^{-i\theta}\Phi(\underline{w})\,d\underline{w}; \tag{38}$$

their Weierstrass function $\tilde{\mathfrak{F}}(w,\theta)$ *is simply*

$$\tilde{\mathfrak{F}}(w,\theta) = e^{-i\theta}\mathfrak{F}(w). \tag{39}$$

Conversely, if $f : \tilde{\Omega} \to \mathbb{C}^3$ *is an isotropic map on a simply connected domain* $\tilde{\Omega} \subset \mathbb{C}$*, then the minimal surface*

$$\tilde{X}(w) = X_0 + \operatorname{Re}\int_{w_0}^{w} f'(\underline{w})\,d\underline{w}, \quad w \in \tilde{\Omega},$$

has an equivalent representation $X : \Omega \to \mathbb{R}^3$ *on* $\Omega := \sigma(\tilde{N}(\tilde{\Omega}))$*, given by* (29) *and* (30)*, provided that its normal* $\tilde{N}(w)$ *satisfies condition* (23)*:*

(i) $\tilde{N}(w) \neq$ *north pole of* S^2 *for all* $w \in \tilde{\Omega}$;

(ii) *the mapping* $\tilde{N} : \tilde{\Omega} \to S^2$ *is injective.*

Remark. In our computation of the Gauss curvature K we have used the theorema egregium. Yet for minimal surfaces we can obtain K in a much simpler way, basically by going back to the definition of K. First we note that the spherical image

$$N(w) = \frac{1}{1+u^2+v^2}(2u, 2v, u^2+v^2-1), \quad w = u+iv,$$

is given by conformal parameters u, v; in fact, a straightforward computation yields

$$\begin{aligned} |N_u(w)|^2 = |N_v(w)|^2 &= \frac{4}{(1+u^2+v^2)^2}, \\ \langle N_u(w), N_v(w)\rangle &= 0. \end{aligned} \tag{40}$$

(Note that N is just the inverse $\rho = \sigma^{-1}$ of the stereographic projection $\sigma : S^2 \to \bar{\mathbb{C}}$ restricted to Ω. The equations (40) express the fact that ρ and therefore also σ are conformal mappings.)

From (40) we obtain for the third fundamental form of X the expression

$$\mathrm{III}(du, dv) = \frac{4}{(1+u^2+v^2)^2}\{du^2 + dv^2\} \tag{41}$$

whereas (32) implies

$$\mathrm{I}(du, dv) = \Lambda(w)\{du^2 + dv^2\}.$$

On the other hand, it follows from Section 1.2, (26) that

$$\mathrm{III}(du, dv) = -KI(du, dv)$$

whence

$$K(w) = -\frac{4}{(1+u^2+v^2)^2 \Lambda(w)}. \tag{42}$$

On account of (32′), this relation is equal to (34).

Another possibility to compute K directly is to employ formula (44) (or (45)) of Section 1.2.

Goursat has found a procedure to generate from a given minimal surface $X : \Omega \to \mathbb{R}^3$ and its adjoint $X^* : \Omega \to \mathbb{R}^3$ a one-parameter family of minimal surfaces $Y(w, \kappa)$, $w \in \Omega$, where the parameter κ varies in $\mathbb{R}$, $\kappa \neq 0$. The *Goursat transformation* resembles Bonnet's transformation described in Section 3.1 but is less restrictive. It is defined by

$$Y(w, \kappa) = X_0 + \mathrm{Re} \int_{w_0}^{w} \Psi(\underline{w}, \kappa)\, d\underline{w} \tag{43}$$

where

$$\Psi(w, \kappa) = \left(\left(\frac{1}{\kappa} - \kappa w^2 \right) \mathfrak{F}(w), i \left(\frac{1}{\kappa} + \kappa w^2 \right) \mathfrak{F}(w), 2w\mathfrak{F}(w) \right), \tag{44}$$

and

$$\begin{aligned} X(w) + iX^*(w) &= X_0 + \int_{w_0}^{w} \Phi(\underline{w})\, d\underline{w}, \\ \Phi(w) &= ((1-w^2)\mathfrak{F}(w), i(1+w^2)\mathfrak{F}(w), 2w\mathfrak{F}(w)). \end{aligned}$$

If $X_0 = 0, Y = (\xi, \eta, \zeta), X = (x, y, z), X^* = (x^*, y^*, z^*)$, we can write

$$\begin{aligned} \xi &= \frac{1+\kappa^2}{2\kappa} x + \frac{1-\kappa^2}{2\kappa} y^*, \\ \eta &= \frac{1+\kappa^2}{2\kappa} y + \frac{\kappa^2-1}{2\kappa} x^*, \\ \zeta &= z. \end{aligned} \tag{45}$$

For fixed w and varying κ, the points $Y(w, \kappa)$ describe a branch of a parabola.

Goursat's transformation maps asymptotic lines into asymptotic lines and lines of curvature into lines of curvature. For further details, we refer to Goursat [1,2] (first and second mémoire).

Now we shall prove another representation formula, due to Weierstrass, which is often found in the literature:

Theorem 3 (Weierstrass representation formula). *For every regular minimal surface $X : \Omega \to \mathbb{R}^3$ on a simply connected domain Ω, there exist two holomorphic functions G and H without common zeros such that*

$$\begin{aligned} x(w) &= x_0 + \operatorname{Re} \int_{w_0}^{w} (G^2 - H^2)\, d\zeta, \\ y(w) &= y_0 + \operatorname{Re} \int_{w_0}^{w} i(G^2 + H^2)\, d\zeta, \\ z(w) &= z_0 + \operatorname{Re} \int_{w_0}^{w} 2GH\, d\zeta \end{aligned} \tag{46}$$

holds for $w, w_0 \in \Omega$ and $X_0 = X(w_0)$. Conversely, if G and H are two holomorphic functions on a simply connected domain Ω such that $|G(w)|^2 + |H(w)|^2 \not\equiv 0$, then (46) defines a nonconstant minimal surface which is regular if and only if G and H have no zeros in common.

Proof. The second part follows by a straightforward computation. In order to verify the first part, we consider an arbitrary minimal surface $X : \Omega \to \mathbb{R}^3$ given by

$$X(w) = X_0 + \operatorname{Re} \int_{w_0}^{w} \Phi(\zeta)\, d\zeta, \quad w \in \Omega,$$

where $\Phi = (\Phi_1, \Phi_2, \Phi_3) : \Omega \to \mathbb{C}^3$ is a holomorphic mapping satisfying

$$|\Phi_1|^2 + |\Phi_2|^2 + |\Phi_3|^2 > 0 \tag{47}$$

and

$$(\Phi_1 - i\Phi_2)(\Phi_1 + i\Phi_2) = -\Phi_3^2. \tag{48}$$

The last equation, which is equivalent to (1), implies that every zero of $\Phi_1 - i\Phi_2$ or of $\Phi_1 + i\Phi_2$ is also a zero of Φ_3. Then we infer that, because of (47), the two functions $\Phi_1 - i\Phi_2$ and $\Phi_1 + i\Phi_2$ cannot have common zeros. Since every zero of Φ_3^2 is of even order, it follows that the zeros of both $\Phi_1 - i\Phi_2$ and $\Phi_1 + i\Phi_2$ are of even order. Then the functions

$$G := \sqrt{\tfrac{1}{2}(\Phi_1 - i\Phi_2)}, \quad H := \sqrt{-\tfrac{1}{2}(\Phi_1 + i\Phi_2)}$$

are single-valued holomorphic functions which, for suitably chosen square roots, satisfy

$$2GH = \Phi_3,$$

and clearly

$$G^2 - H^2 = \Phi_1, \quad i(G^2 + H^2) = \Phi_2.$$

Moreover, the functions G and H have no common zeros. □

Remark. 1. If we omit the assumption (47), then not every minimal surface $X(w) = X_0 + \operatorname{Re}\int_{w_0}^{w} \Phi(\zeta)\,d\zeta$ can be written in the form (46). For instance, let

$$\Phi_1(w) = 3w, \quad \Phi_2(w) = 5iw, \quad \Phi_3(w) = 4w,$$

where Ω is a small disk centered at $w = 0$. If there were functions G and H such that

$$3w = G(w)^2 - H(w)^2, \quad 5iw = i\{G(w)^2 + H(w)^2\}, \quad 4w = 2G(w)H(w),$$

it would follow that $G^2(w) = 4w$. However, there is no (single-valued) holomorphic solution $G(w)$ of this equation in Ω.

2. Weierstrass has derived the representation (30) with Φ given by (29) from (46), by introducing a new variable

$$\omega = \frac{H(w)}{G(w)} = \frac{\Phi_1(w) + i\Phi_2(w)}{-\Phi_3(w)}$$

(arranging everything in such a way that the mapping $w \mapsto \omega$ is biholomorphic). Then

$$(\Phi_1 - i\Phi_2)(\Phi_1 + i\Phi_2) = -\Phi_3^2$$

implies that

$$\frac{1}{\omega} = \frac{\Phi_1(w) - i\Phi_2(w)}{\Phi_3(w)},$$

and it follows that

$$G^2(w)\frac{dw}{d\omega} = \frac{1}{2}(\Phi_1(w) - i\Phi_2(w))\frac{dw}{d\omega} = \mathfrak{F}(\omega).$$

Then one can pass from (46) to the desired equations.

As a remarkable application of the Enneper–Weierstrass representation formula we present the following[1]

Theorem of R. Krust. *If an embedded minimal surface $X : B \to \mathbb{R}^3$, $B = \{w \in \mathbb{C}\colon |w| < 1\}$, can be written as a graph over a convex domain in a plane, then the corresponding adjoint surface $X^* : B \to \mathbb{R}^3$ is a graph as well.*

First we write the representation formula (7) in a different way. Let us introduce the two meromorphic functions g and h by

$$g := \nu, \quad h' := \mu\nu.$$

Then we have

$$dh = \mu\nu\,d\zeta,$$

[1] Oral communication of R. Krust to H. Karcher. Our proof is borrowed from Karcher's note [3].

and we can write (7) in the form

$$X(w) = X(w_0) + \operatorname{Re} \int_{w_0}^{w} \psi'(\zeta)\, d\zeta, \tag{49}$$

where $d\psi(\zeta) = \psi'(\zeta)\, d\zeta$ is given by

$$d\psi = \left[\frac{1}{2}\left(\frac{1}{g} - g\right), \frac{i}{2}\left(\frac{1}{g} + g\right), 1\right] dh. \tag{50}$$

Note that the 1-forms $d\psi$ and dh are single-valued on B. The Gauss map $N : B \to S^2$ associated with X is given by

$$N = \frac{1}{1 + |g|^2}(2 \operatorname{Re} g, 2 \operatorname{Im} g, |g|^2 - 1). \tag{51}$$

Proof of Krust's Theorem. We can assume that X is nonplanar, that it can be represented as a graph above the x, y-plane, and that $N(w)$ always points into the lower hemisphere of S^2. Then we infer from (51) that the function g appearing in the Weierstrass representation (49), (50) of X satisfies

$$|g(w)| < 1 \quad \text{for all } w \in B. \tag{52}$$

Moreover, we can also suppose that $w_0 = 0$ and $X(w_0) = 0$. Introducing the functions $\sigma(w)$ and $\tau(w)$, $w \in B$, by

$$\sigma(w) := -\int_0^w \frac{g}{2}\, dh, \quad \tau(w) := \int_0^w \frac{1}{2g}\, dh, \tag{53}$$

we can write the first two coordinate functions $x(w)$ and $y(w)$ of $X(w)$ as

$$x(w) = \operatorname{Re}[\sigma(w) + \tau(w)], \quad y(w) = \operatorname{Re} i[\tau(w) - \sigma(w)]. \tag{54}$$

Then the orthogonal projections

$$\pi(w) := x(w) + iy(w), \quad \pi^*(w) := x^*(w) + iy^*(w) \tag{55}$$

of $X(w)$ and of its adjoint $X^*(w) = (x^*(w), y^*(w), z^*(w))$ onto the x, y-plane can be written as

$$\pi = \bar{\tau} + \sigma, \quad \pi^* = i(\bar{\tau} - \sigma). \tag{56}$$

Pick any two points w_1 and w_2 in B, $w_1 \neq w_2$ and set $p_1 := \pi(w_1)$, $p_2 := \pi(w_2)$. Since $D := \pi(B)$ is a convex domain in the x, y-plane, we can connect p_1 and p_2 within D by a line segment $\mathcal{L} : [0, 1] \to D$ such that $\mathcal{L}(0) = p_1$ and $\mathcal{L}(1) = p_2$. Then there is a piecewise smooth curve $\gamma : [0, 1] \to B$ such that $\mathcal{L} = \pi \circ \gamma$. We can assume that $|\dot{\mathcal{L}}(t)| = |p_2 - p_1|$ for all $t \in [0, 1]$ whence

$$p_2 - p_1 = \mathcal{L}\,(1) - \mathcal{L}(0) = \dot{\mathcal{L}}(t) \quad \text{for all } t \in [0, 1]$$

and therefore

$$p_2 - p_1 = \left[\overline{\frac{1}{2g(w)} h'(w)\dot{\gamma}(t)} - \frac{g(w)}{2} h'(w)\dot{\gamma}(t) \right] \Big|_{w=\gamma(t)}. \tag{57}$$

Consider the scalar product S of the two vectors $p_2 - p_1$ and $i[\pi^*(w_2) - \pi^*(w_1)]$ of $\mathbb{R}^2$:

$$\begin{aligned} S &:= \langle p_2 - p_1, i[\pi^*(w_2) - \pi^*(w_1)] \rangle \\ &= \left\langle p_2 - p_1, -\int_\gamma \left(\frac{g}{2} dh + \overline{\frac{1}{2g} dh} \right) \right\rangle. \end{aligned} \tag{58}$$

Since for any two vectors $w_1, w_2 \in \mathbb{R}^2 \hat{=} \mathbb{C}$ we have $\langle w_1, w_2 \rangle = \mathrm{Re}(w_1 \bar{w}_2)$, it follows from (57) that

$$\begin{aligned} S &= \int_0^1 \mathrm{Re} \left\{ \left[\left(\overline{\frac{g}{2} h'} + \frac{1}{2g} h' \right) \circ \gamma \right] \overline{\dot{\gamma}(t)} \left[\left(\frac{g}{2} h' - \overline{\frac{1}{2g} h'} \right) \circ \gamma \right] \dot{\gamma}(t) \right\} dt \\ &= \int_0^1 \frac{1}{4} |\dot{\gamma}(t)|^2 \left[|g(\gamma(t))|^2 - \frac{1}{|g(\gamma(t))|^2} \right] |h'((\gamma(t))|^2 \, dt. \end{aligned}$$

Then we infer from (52) that $S < 0$. Therefore we obtain from (58) that $\pi^*(w_2) - \pi^*(w_1) \neq 0$ for any pair of distinct points $w_1, w_2 \in B$, and we conclude that the adjoint surface X^* is a graph.

Remark. Similarly one proves that all associate surfaces $X : B \to \mathbb{R}^3$ of a minimal embedding $X : B \to \mathbb{R}^3$ are graphs if $X(B)$ can be written as a graph over a convex domain in a plane.

3.4 Björling's Problem. Straight Lines and Planar Lines of Curvature on Minimal Surfaces. Schwarzian Chains

Given a real analytic strip S in $\mathbb{R}^3$, Björling's problem is to find a minimal surface X containing this strip in its interior. This is but a special case of the general theorem by Cauchy–Kovalevskaya whence we will expect to find a uniquely determined solution. Following an idea by H.A. Schwarz, this solution can be given by an explicit formula in terms of the initial data, i.e., in terms of the prescribed strip S. Schwarz's solution of the Björling problem yields a beautiful method for generating minimal surfaces with interesting geometric properties.

Let us now describe the problem in detail. We consider a real-analytic strip

$$S = \{(c(t), n(t)) \colon t \in I\}$$

consisting of a real-analytic curve $c : I \to \mathbb{R}^3$ with $\dot{c}(t) \neq 0$ (or at least $\dot{c}(t) = 0$ only in isolated points $t \in I$), and of a real-analytic vector field $n : I \to \mathbb{R}^3$ along c, with $|n(t)| \equiv 1$ and $\langle \dot{c}(t), n(t) \rangle \equiv 0$.

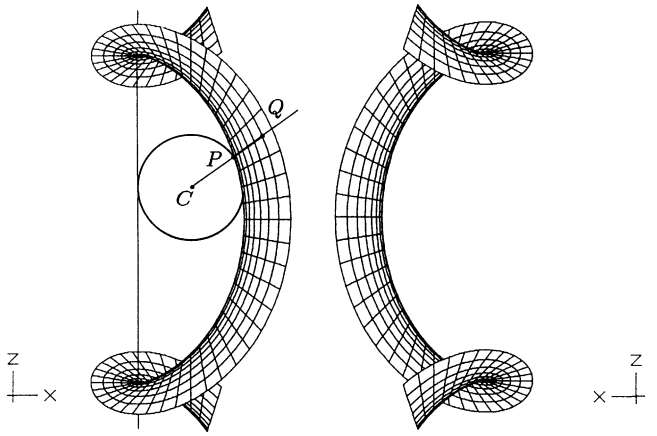

Fig. 1. A cycloid is the curve generated by a point P on the periphery of a *circle with center* C rolling along a *straight line*. Catalan's surface, whose part corresponding to $-3\pi/5 \le u \le 13\pi/5, -2\pi/5 \le v \le 0$ has been drawn here, solves Björling's problem to find a minimal surface passing through the cycloid in such a way that the surface normal coincides with the cycloid's principal normal vector. The two parallel projections onto the x, z-plane show that the curves $u =$ constant (e.g. the curve passing through the points P and Q) are planar and perpendicular to the x, z-plane. Each of them is, in fact, a parabola having its apex on the cycloid

We assume that I is an open interval in $\mathbb{R}$.

Björling's problem consists in finding a minimal surface $X : \Omega \to \mathbb{R}^3$ with $I \subset \Omega$ such that the following conditions are satisfied:

$$\begin{aligned} &\text{(i)} \quad X(u,0) = c(u) \quad \text{for } u \in I, \\ &\text{(ii)} \quad N(u,0) = n(u) \quad \text{for } u \in I, \end{aligned}$$

N being the normal of $X, N : \Omega \to \mathbb{R}^3$.

Theorem 1. *For any prescribed real-analytic strip* $S = \{(c(t), n(t)) : t \in I\}$, *the corresponding Björling problem has exactly one solution* $X(u,v)$, *given by*

$$X(u,v) = \operatorname{Re}\left\{ c(w) - i \int_{u_0}^{w} n(\underline{w}) \wedge dc(\underline{w}) \right\}, \tag{1}$$

$w = u + iv \in \Omega$, $u_0 \in I$, *where* Ω *is a simply connected domain with* $I \subset \Omega$ *in which the power-series expansions of both* c *and* n *are converging.*

Remark. 1. The uniqueness is to be understood in the following sense: If $\tilde{X}(u,v)$, $w = u + iv \in \tilde{\Omega}$, is another solution, then $X(u,v) = \tilde{X}(u,v)$ for $u + iv \in \Omega \cap \tilde{\Omega}$.

2. Formula (1) means the following: One determines holomorphic extensions $c(u + iv)$ and $n(u + iv)$ of the real-analytic functions $c(t)$ and $n(t)$,

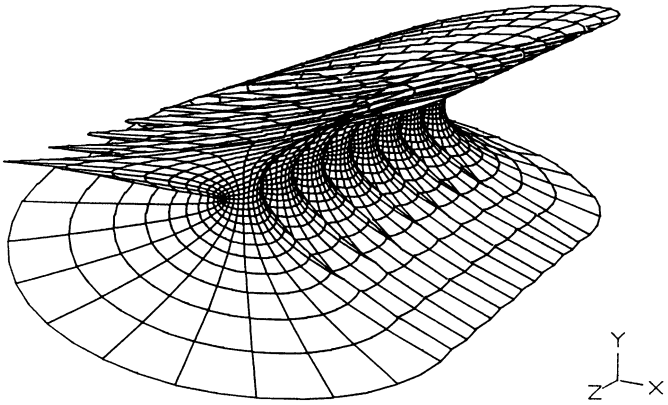

Fig. 2. A large piece of Catalan's surface generated by the cycloid via Björling's problem

$t \in I$, to a suitable simply-connected domain Ω with $I \subset \Omega$, and then one determines the line integral

$$\int_{u_0}^{w} n(\underline{w}) \wedge dc(\underline{w}) = \int_{u_0}^{w} n(\underline{w}) \wedge c'(\underline{w})\, d\underline{w}$$

where $c'(w)$ is the complex derivative of the holomorphic function $c(w)$.

Proof of Theorem 1. Suppose that $X(u, v)$ is a solution of Björling's problem, defined in the simply connected domain Ω, and let $X^* : \Omega \to \mathbb{R}^3$ be its adjoint surface with $X^*(u_0, 0) = 0$, $u_0 \in I$. Then

$$f(w) = X(u, v) + iX^*(u, v), \quad w = u + iv \in \Omega,$$

is an isotropic curve with $X = \operatorname{Re} f$ and

$$f' = X_u + iX_u^* = X_u - iX_v.$$

Since $X_v = N \wedge X_u$, it follows that

$$f' = X_u - iN \wedge X_u$$

whence

$$f'(u) = \dot{c}(u) - in(u) \wedge \dot{c}(u)$$

and therefore

$$f(u) = c(u) - i \int_{u_0}^{u} n(t) \wedge dc(t) \quad \text{for all } u \in I.$$

This implies

$$f(w) = c(w) - i\int_{u_0}^{w} n(\underline{w}) \wedge dc(\underline{w}), \quad w \in \Omega, \tag{2}$$

since both sides are holomorphic functions of w. Hence any possible solution X must be of the form (1), which yields the uniqueness.

Now we shall prove that (1), in fact, yields the solution to Björling's problem. To this end, we consider the holomorphic curve $f : \Omega \to \mathbb{C}^3$ defined by (2). For $w \in I$, we have

$$\operatorname{Re} f'(w) = \dot{c}(w), \quad \operatorname{Im} f'(w) = -n(w) \wedge \dot{c}(w).$$

Since the real vectors $\dot{c}(w)$ and $\dot{c}(w) \wedge n(w)$ are orthogonal to each other and have the same length, we infer that

$$\langle f'(w), f'(w)\rangle = 0 \quad \text{for all } w \in I,$$

and therefore also

$$\langle f'(w), f'(w)\rangle = 0 \quad \text{for all } w \in \Omega.$$

Hence $X(u, v) = \operatorname{Re} f(w), w = u + iv \in \Omega$, is a minimal surface. Since $c(w), n(w)$, and $c'(w)$ are real for $w \in I$, we infer that

$$X(u, 0) = \operatorname{Re} f(u) = c(u) \quad \text{for } u \in I, \tag{3}$$

and

$$X_u(u, 0) - iX_v(u, 0) = f'(u) = \dot{c}(u) - in(u) \wedge \dot{c}(u), \quad u \in I,$$

whence

$$X_u(u, 0) = \dot{c}(u), \quad X_v(u, 0) = n(u) \wedge \dot{c}(u). \tag{4}$$

Moreover, we have

$$X_v(u, 0) = N(u, 0) \wedge X_u(u, 0).$$

Because of

$$\langle X_u(u, 0), X_v(u, 0)\rangle = 0$$

and of

$$\langle n(u), \dot{c}(u)\rangle = 0, \quad |N(u, 0)| = |n(u)| = 1,$$

we infer that

$$N(u, 0) = n(u).$$

□

Corollary 1. *Let $X(u, v)$ be the solution of Björling's problem, given by (1). Then we have*

$$X(u, -v) = \operatorname{Re}\{c(w) + i\int_{u_0}^{w} n(\underline{w}) \wedge dc(\underline{w})\}, \quad w = u + iv. \tag{5}$$

Proof. The surface $\tilde{X}(u,v) := X(u,-v)$ is again a minimal surface with the normal $\tilde{N}(u,v) = -N(u,-v)$. Hence $\tilde{X}$ solves Björling's problem for the strip

$$\tilde{S} = \{(c(t), -n(t)) \colon t \in I\}$$

and is, therefore, given by

$$\tilde{X}(u,v) = \mathrm{Re}\left\{ c(w) + i \int_{u_0}^{w} n(\underline{w}) \wedge dc(\underline{w}) \right\}. \qquad \square$$

The formulae (1) and (5) imply the following two symmetry principles discovered by H.A. Schwarz:

Theorem 2. (i) *Every straight line contained in a minimal surface is an axis of symmetry of the surface.*

(ii) *If a minimal surface intersects some plane E perpendicularly, then E is a plane of symmetry of the surface.*

In fact, this theorem is an immediate consequence of the following

Lemma 1. *Let $X(u,v) = (x(u,v), y(u,v), z(u,v))$, $w = u + iv \in \Omega$, be a minimal surface whose domain of definition Ω contains some interval I that lies on the real axis.*

(i) *If, for all $u \in I$, the points $X(u,0)$ are contained in the x-axis, then we have for $w = u + iv \in \Omega$ with $u \in I$ and $\overline{w} = u - iv \in \Omega$ that*

$$\begin{aligned} x(u,-v) &= x(u,v), \\ y(u,-v) &= -y(u,v), \\ z(u,-v) &= -z(u,v). \end{aligned} \tag{6}$$

(ii) *If the curve $\Sigma = \{X(u,0) \colon u \in I\}$ is contained in the x,y-plane E, and if the surface X intersects orthogonally at Σ, then it follows*

$$\begin{aligned} x(u,-v) &= x(u,v), \\ y(u,-v) &= y(u,v), \\ z(u,-v) &= -z(u,v) \end{aligned} \tag{7}$$

for $u \in I$ and $w, \overline{w} \in \Omega$.

Proof. (i) Set $c(u) := X(u,0)$ and $n(u) := N(u,0)$. By assumption, we have

$$c(u) = (c^1(u), 0, 0), n(u) = (0, n^2(u), n^3(u)),$$

and therefore

$$n(u) \wedge \dot{c}(u) = (0, \dot{c}^1(u) n^3(u), -\dot{c}^1(u) n^2(u)).$$

On account of (1) and (5), we then arrive at the formulae (6).

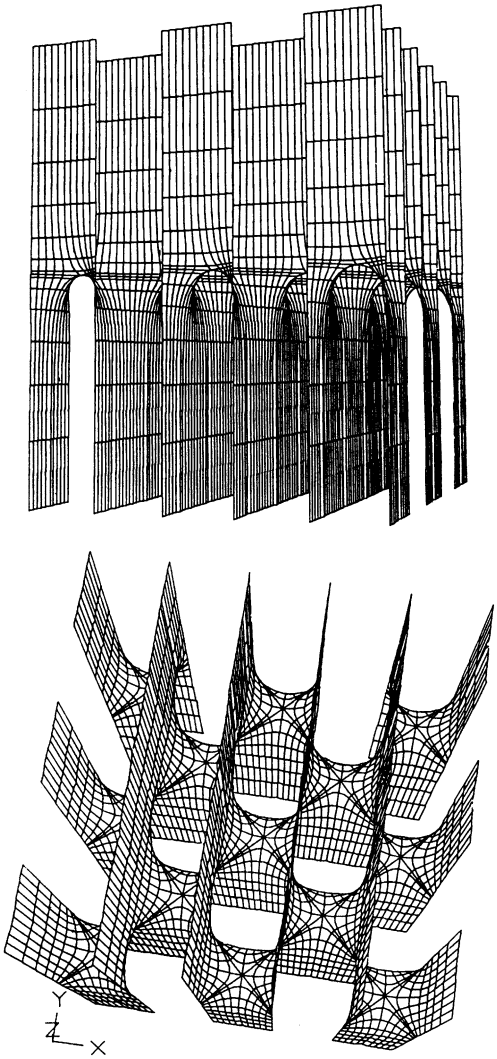

Fig. 3. Lines of symmetry of Scherk's surface demonstrate Schwarz's first reflection principle

(ii) If X intersects $E = \{z = 0\}$ at $c(u) := X(u, 0)$ orthogonally, and if $n(u) := N(u, 0)$, it follows that

$$c(u) = (c^1(u), c^2(u), 0), \quad n(u) = (n^1(u), n^2(u), 0),$$

whence

$$n(u) \wedge \dot{c}(u) = (0, 0, n^1(u)\dot{c}^2(u) - n^2(u)\dot{c}^1(u)).$$

In conjunction with (1) and (5), we then obtain the identities (7). □

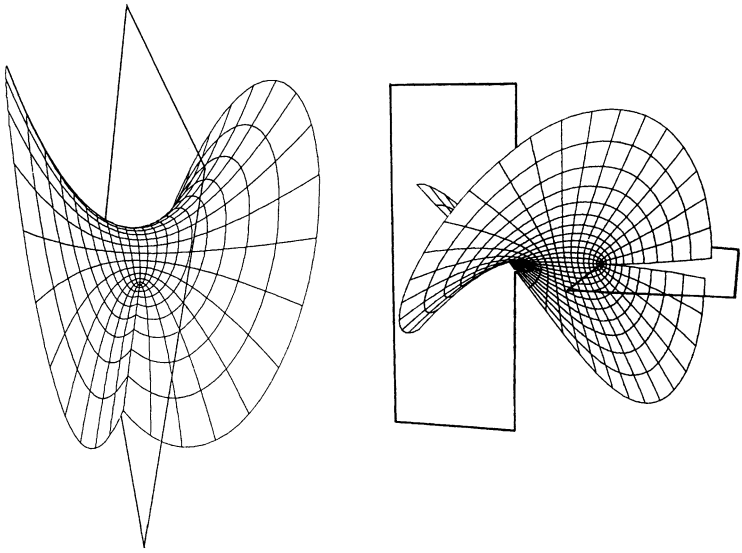

Fig. 4. Planes of symmetry in Catalan's and Henneberg's surfaces

Lemma 2. *Let $X(w)$, $w \in \Omega$, be a regular surface of class $C^3(\Omega, \mathbb{R}^3)$, and let $c(t) = X(\omega(t))$, $t \in I$, be a regular curve on X defined by some C^3-curve $\omega : I \to \Omega$. Then the following holds*:

(i) *The curve c is both a geodesic and an asymptotic line if and only if it is a straight line.*

(ii) *Let c be a geodesic on X. Then c is also a line of curvature if and only if it is a plane curve.*

(iii) *Suppose that c is contained in a plane E. Then c is a line of curvature on X if and only if X intersects E along c at a constant angle φ (if $\varphi = \frac{\pi}{2}$, then c is a geodesic).*

Proof. We may assume that t coincides with the parameter of arc length s. Let $\{\boldsymbol{t}(s), \boldsymbol{s}(s), \mathfrak{N}(s)\}$ be the moving frame along $c(s)$, consisting of the tangent vector $\boldsymbol{t}(s) = \dot{c}(s)$, the side normal $\boldsymbol{s}(s)$, and the surface normal $\mathfrak{N}(s) = N(\omega(s))$. Secondly, we consider the frame $\{\boldsymbol{t}(s), \boldsymbol{n}(s), \boldsymbol{b}(s)\}$, where $\boldsymbol{n}(s)$ is the principal normal, and $\boldsymbol{b}(s) = \boldsymbol{t}(s) \wedge \boldsymbol{n}(s)$ stands for the binormal vector of $c(s)$. Let us recall the formula (14) of Section 1.2:

$$\dot{\boldsymbol{t}} = \kappa_g \boldsymbol{s} + \kappa_n \mathfrak{N}, \tag{8}$$

where $\kappa_n = \kappa \cos\theta$ is the normal curvature of $c, \kappa_g = \pm\kappa \sin\theta$ the geodesic curvature of c, $\cos\theta = \langle \boldsymbol{n}, \mathfrak{N} \rangle$, and

$$\dot{\boldsymbol{t}} = \kappa \boldsymbol{n},$$

where κ denotes the curvature of c.

(i) Suppose now that $\kappa_n(s) \equiv 0$ and $\kappa_g(s) \equiv 0$. Then the relation (8) implies $\boldsymbol{t}\,(s) \equiv \text{const}$, whence $c(s)$ must be a straight line. Conversely, if $c(s)$ is a straight line, then $\dot{\boldsymbol{t}}(s) \equiv 0$, and therefore $\kappa_n(s) \equiv 0$ as well as $\kappa_g(s) \equiv 0$. Thus the first assertion is proved.

(ii) Suppose that $c(s)$ is a geodesic line, i.e., $\kappa_g(s) \equiv 0$, or $\boldsymbol{n}(s) \equiv \pm\mathfrak{N}(s)$. We may assume that $\boldsymbol{n}(s) = \mathfrak{N}(s)$. Then the identity

$$\dot{\boldsymbol{b}} = \dot{\boldsymbol{t}} \wedge \boldsymbol{n} + \boldsymbol{t} \wedge \dot{\boldsymbol{n}} = \kappa \boldsymbol{n} \wedge \boldsymbol{n} + \boldsymbol{t} \wedge \dot{\boldsymbol{n}} = \boldsymbol{t} \wedge \dot{\boldsymbol{n}}$$

yields

$$\dot{\boldsymbol{b}} = \boldsymbol{t} \wedge \dot{\mathfrak{N}}.$$

Since $\dot{\mathfrak{N}}(s) \in T_{\omega(s)}X$, we can write

$$\dot{\mathfrak{N}} = \gamma_1 \boldsymbol{t} + \gamma_2 \boldsymbol{s}, \tag{9}$$

whence

$$\dot{\boldsymbol{b}} = \gamma_2 \mathfrak{N}.$$

It follows that $\dot{\boldsymbol{b}}(s) \equiv 0$ if and only if $\gamma_2(s) \equiv 0$, that is, if and only if we have $\dot{\mathfrak{N}}(s) \equiv \gamma_1(s)\boldsymbol{t}(s)$. Thus we conclude that $c(s)$ is planar if and only if c is a line of curvature.

(iii) Introduce $\varphi(s)$ as the angle between the tangent plane of the surface at $w = \omega(s)$ and the osculating plane of the curve c for the parameter value s, i.e.,

$$\cos\varphi = \langle \mathfrak{N}, \boldsymbol{b} \rangle.$$

Then we obtain

$$\frac{d}{ds}\cos\varphi = \langle \dot{\mathfrak{N}}, \boldsymbol{b} \rangle + \langle \mathfrak{N}, \dot{\boldsymbol{b}} \rangle. \tag{10}$$

If c is a planar curve, we have $\dot{\boldsymbol{b}} = 0$, and it satisfies

$$-\dot{\mathfrak{N}} = k\boldsymbol{t}, \quad k = \kappa_1 \text{ or } \kappa_2,$$

if it is a line of curvature. Hence a planar line of curvature fulfills

$$\frac{d}{ds}\cos\varphi = -k\langle \boldsymbol{t}, \boldsymbol{b} \rangle = 0$$

or $\varphi(s) \equiv \text{const}$.

Conversely, suppose that c is a plane curve such that $\varphi(s) \equiv \text{const}$. Then we have $\dot{\boldsymbol{b}}(s) \equiv 0$, and (10) implies

$$\langle \dot{\mathfrak{N}}(s), \boldsymbol{b}(s) \rangle \equiv 0. \tag{11}$$

Moreover, we can use formula (9) from part (ii):

$$\dot{\mathfrak{N}}(s) \equiv \gamma_1(s)\boldsymbol{t}(s) + \gamma_2(s)\boldsymbol{s}(s), \tag{12}$$

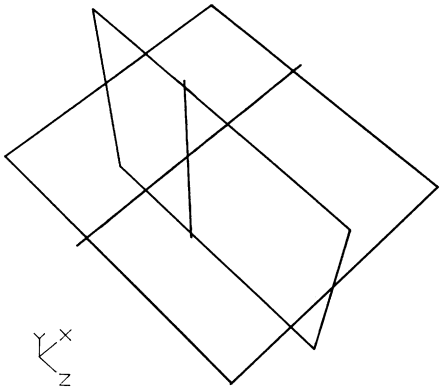

Fig. 5. The affine spaces shown here are the setting in which a part of Catalan's surface is deformed into its adjoint surface. It will be illustrated that if a minimal surface is perpendicular to a plane along a part of the boundary of its domain of definition, then its adjoint minimal surface maps that part of the boundary onto a straight line perpendicular to that plane, and vice versa (Section 3.4, Proposition 1)

and (11) yields

$$\dot{\mathfrak{N}}(s) \equiv \gamma_1(s)\boldsymbol{t}(s) + \gamma_3(s)\boldsymbol{n}(s) \tag{13}$$

for an appropriate function $\gamma_3(s)$. Thus, for every admissible value of the parameter s, at least one of the two relations

$$\gamma_2(s) = \gamma_3(s) = 0 \quad \text{or} \quad \boldsymbol{s}(s) = \boldsymbol{n}(s).$$

must be satisfied. Suppose that, for some admissible value s_0, the equation $\boldsymbol{s}(s_0) = \boldsymbol{n}(s_0)$ holds. Then we have $\boldsymbol{b}(s_0) = \pm\mathfrak{N}(s_0)$, i.e. $\varphi(s_0) = 0$. On the other hand, since $\varphi(s) \equiv$ const, we find $\varphi(s) \equiv 0$, i.e., $\boldsymbol{b}(s) \equiv \mathfrak{N}(s)$ or $\boldsymbol{b}(s) \equiv -\mathfrak{N}(s)$. Since $\dot{\boldsymbol{b}}(s) \equiv 0$, we infer that $\dot{\mathfrak{N}}(s) \equiv 0$ and therefore (12) and (13) yield $\gamma_2(s) \equiv 0$ and $\gamma_3(s) \equiv 0$. Hence in all cases our assumptions imply $\gamma_2(s) \equiv 0$ and $\gamma_3(s) \equiv 0$, whence $\dot{\mathfrak{N}}(s) \equiv \gamma_1(s)\boldsymbol{t}\,(s)$, which means that $c(s)$ is a line of curvature. □

Supplement. *It is easy to see that the assertions of Lemma 2 remain valid if X is assumed to be a minimal surface with branch points and if $c(t)$ is supposed to be regular except for isolated points $t \in I$.*

Now we can construct minimal surfaces with interesting special properties by combining Schwarz's formula (1) and Lemma 2. Before doing this, we want to state a few observations, following from Lemma 2, which are pertinent to the so-called *Schwarzian chain problem*.

Proposition 1. *Let $X : \Omega \to \mathbb{R}^3$ be a minimal surface with the normal mapping $N : \Omega \to S^2$, and assume that $X^* : \Omega \to \mathbb{R}^3$ is an adjoint minimal*

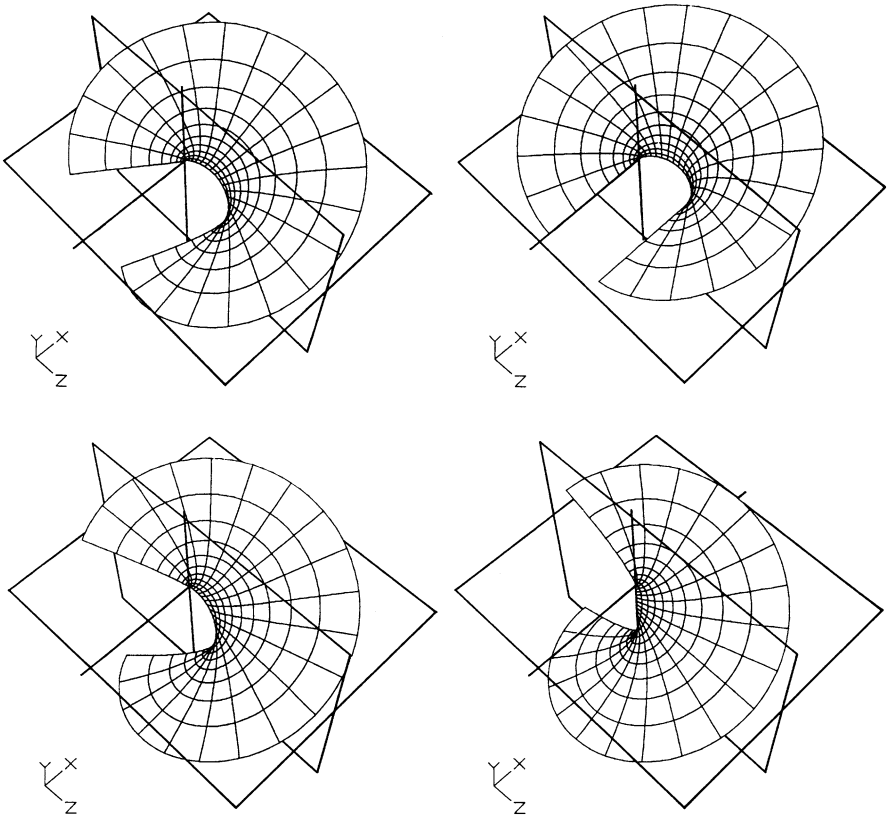

Fig. 6. The bending process for the fundamental part $0 \leq u \leq 2\pi$, $0 \leq v\ (\leq \pi) < \infty$ of Catalan's surface into its adjoint surface through the family of its associated surfaces (counter-clockwise from top right: $\theta = 0, \pi/6, \pi/3$, and $\pi/2$). Catalan's surface is perpendicular to $y = 0$ along $v = 0$ and maps $u = 0$ and $u = 2\pi$ onto straight lines orthogonal to $x = 0$. Proposition 1 describes the resulting properties of the adjoint and the Gauss map

surface of X (*hence,* X^* *has the same normal mapping as* X). *Choose some* C^3*-curve* $\omega : I \to \Omega$ *with* $\dot{\omega}(t) \neq 0$ *except for isolated points* t *in the interval* I, *and consider the curves* $c := X \circ \omega$ *and* $c^* := X^* \circ \omega$. *Both have the same spherical image* $\gamma := N \circ \omega$, *and the following holds*:

(i) *If* c *is a straight arc, i.e.* $c(I)$ *is contained in some straight line* L, *then* $\gamma(I)$ *is contained in the great circle* C *of* S^2 *that lies in the plane* E_0 *through the origin which is perpendicular to* L. *Moreover,* c *is both a geodesic and an asymptotic line of* X, *and* c^* *is a planar geodesic of* X^*. *The curve* c^* *lies in some plane* E *parallel to* E_0, *and* X^* *intersects* E *orthogonally along* c^*.

(ii) *If* c *is a planar geodesic on* X, *i.e. the orthogonal intersection of* X *with some plane* E, *then* $\gamma(I)$ *lies in the great circle* $C = E_0 \cap S^2$ *where* E_0 *is the plane parallel to* E *with* $0 \in E_0$, *and* c^* *is a straight arc* (*and hence a*

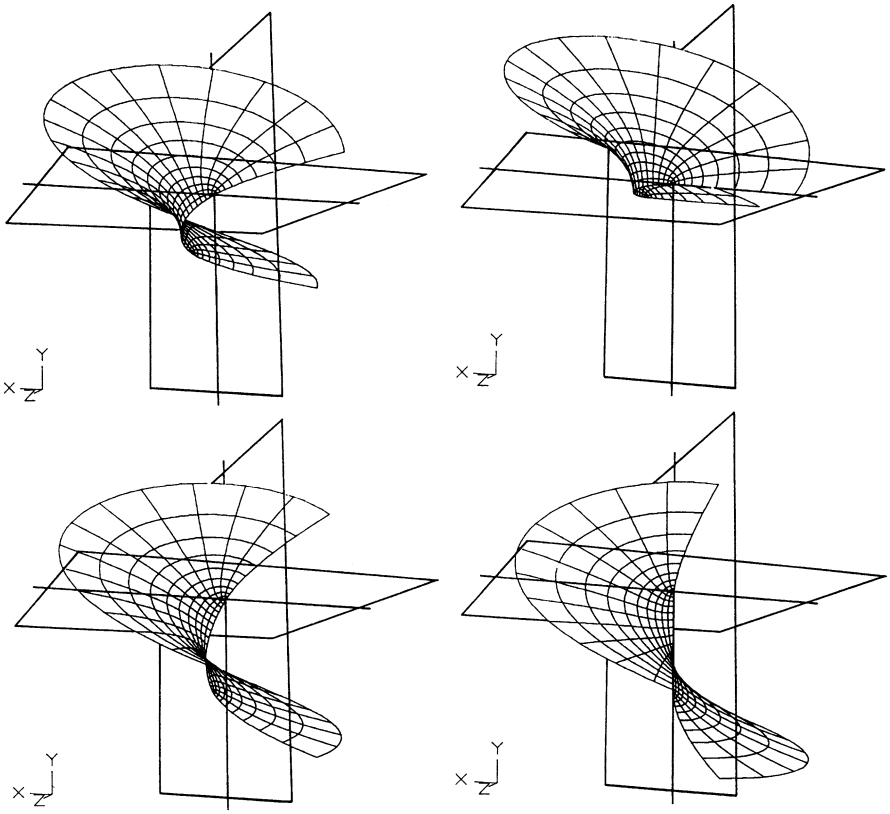

Fig. 7. Another view of the bending of Catalan's surface. The curve $v = 0$ is a geodesic, and the lines $u = 0$ and $u = 2\pi$ are asymptotic lines of the surface. The Gauss images of these lines lie on great circles of the sphere S^2

geodesic asymptotic line) *on* X^*. *Moreover,* $c^*(I)$ *is contained in some straight line* L *perpendicular to* E.

The *proof* of these very useful facts is either obvious or a direct consequence of Lemma 2 and of Proposition 6 in Section 3.1. In particular, we emphasize the following observation:

Straight arcs and planar geodesics on a minimal surface X *are mapped by the normal* N *of* X *into great circles on the Riemann sphere* S^2.

Similarly, one sees:

Planar lines of curvature on X *are mapped by* N *into circles on* S^2.

By virtue of Theorem 2, we also obtain:

Straight arcs and planar geodesics on a minimal surface X *are lines of rotational symmetry or of mirror symmetry respectively.*

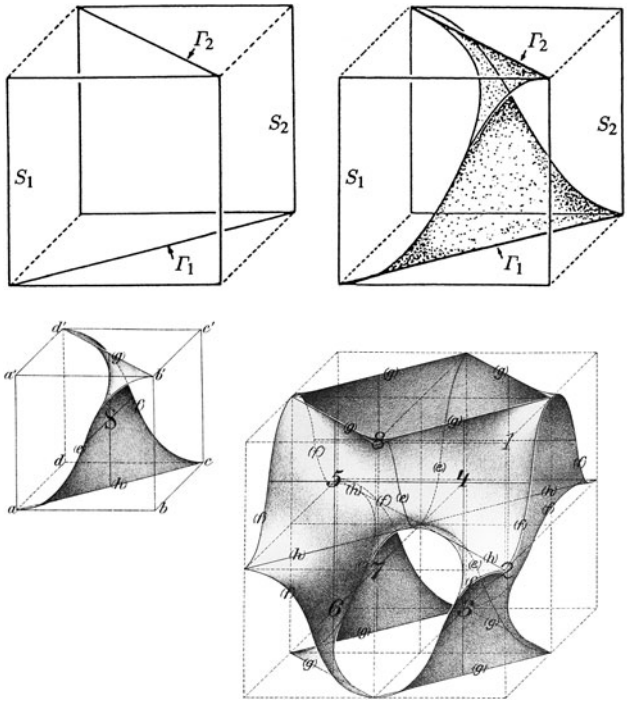

Fig. 8. A Schwarzian chain problem consisting of two plane faces of a cube and two straight lines. Its solution can be used to construct periodic minimal surfaces. Lithograph by H.A. Schwarz

Consider now a minimal surface $X : \Omega_0 \to \mathbb{R}^3$ without branch points, and a simply connected subdomain Ω of Ω_0 with $\bar{\Omega} \subset \Omega_0$. Suppose also that the normal N of X yields an injective mapping of Ω_0 into S^2, and that the boundary of $X(\bar{\Omega})$ consists of finitely many straight arcs and planar geodesics (i.e., of orthogonal intersections of X with planes). In other words, the minimal surface $X : \bar{\Omega} \to \mathbb{R}^3$ is spanned into a frame $\{L_1, \ldots, L_j, E_1, \ldots, E_k\}$ consisting of finitely many straight lines $L_1, \ldots, L_j$ and planes $E_1, \ldots, E_k$. Such a frame is usually called a *Schwarzian chain* $\mathfrak{C}$. The boundary $X : \partial\Omega \to \mathbb{R}^3$ of the minimal surface $X : \bar{\Omega} \to \mathbb{R}^3$ by assumption lies on a Schwarzian chain, and along its boundary, X is perpendicular to all planar parts of the chain $\mathfrak{C}$. *We say that* $X : \bar{\Omega} \to \mathbb{R}^3$ *is a minimal surface solving the Schwarzian chain problem for the chain* $\mathfrak{C}$.

By Proposition 1 the boundary $N : \partial\Omega \to S^2$ of the spherical image $N : \bar{\Omega} \to S^2$ of a solution $X : \bar{\Omega} \to \mathbb{R}^3$ of a Schwarzian chain problem consists of circular arcs, all of which belong to great circles on S^2. Moreover, the stereographic projection $\sigma : S^2 \to \bar{\mathbb{C}}$ maps circles on S^2 onto circles (or straight lines) in $\bar{\mathbb{C}}$. As described in Section 3.3, we can introduce new coordinates ω by some holomorphic mapping $w = \tau(\omega)$, $\omega \in \Omega^*$, such that

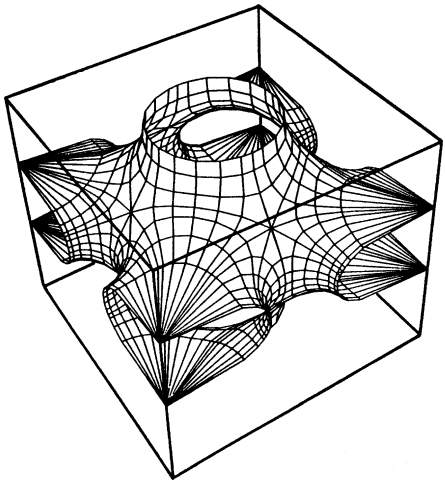

Fig. 9. A fundamental cell of A. Schoen's $S' - S''$ cell in a cuboid whose top and bottom faces are squares. The Schwarzian chain $\langle S_1, S_2, \ldots, S_6 \rangle$ consists of the six faces of the cuboid. It is spanned by a minimal surface which is clearly not of the type of the disk; it consists of sixteen congruent pieces. (Varying the surface normal in the branch points of the Gauss map up and down leads to a one-parameter family of minimal surfaces in cuboids of different height.) Courtesy of K. Polthier

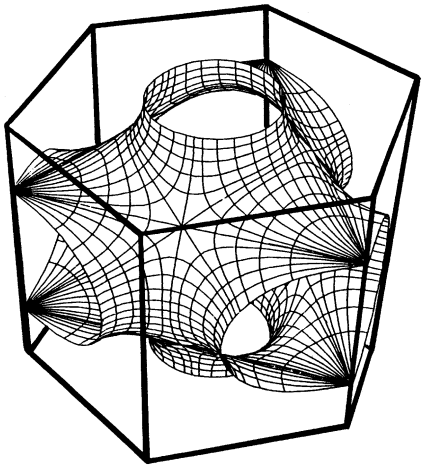

Fig. 10. A Schwarzian chain consisting of the faces of a hexagonal prism. Courtesy of K. Polthier

the equivalent representation

$$Y(\omega) := X(\tau(\omega)), \quad \omega \in \Omega^*,$$

is defined on a domain Ω^* bounded by circular arcs, if we assume that $N(w) \neq$ north pole for $w \in \Omega_0$. Moreover, there is a holomorphic function $\mathfrak{F}(\omega)$, $\omega \in$

Ω^*, with $\mathfrak{F}(\omega) \neq 0$, such that Y is given by

$$
\begin{aligned}
Y(\omega) &= X_0 + \operatorname{Re} \int_{\omega_0}^{\omega} \Phi(\underline{\omega})\, d\underline{\omega}, \quad X_0 \in \mathbb{R}^3, \\
\Phi(\omega) &= ((1-\omega^2)\mathfrak{F}(\omega), i(1+\omega^2)\mathfrak{F}(\omega), 2\omega\mathfrak{F}(\omega)).
\end{aligned} \tag{14}
$$

The functions $\nu(w) = \sigma(N(w))$ and $l(w) = \mathfrak{L}(w) - i\mathfrak{M}(w)$ are holomorphic on Ω_0, ν yields the inverse of τ, and we have $l(w) \neq 0$ for $w \in \Omega_0$.

Fix some $w_0 \in \Omega$ and set

$$
p(w) := \int_{w_0}^{w} \sqrt{l(\underline{w})}\, d\underline{w}, \quad w \in \bar{\Omega}. \tag{15}
$$

This defines a holomorphic function $p(w)$, $w \in \bar{\Omega}$. Since $p'(w) = \sqrt{l(w)} \neq 0$, we obtain by

$$
\zeta = p(w), \quad w \in \bar{\Omega},
$$

a conformal mapping of Ω onto some domain Ω^{**} in the ζ-plane. Note that

$$
d\zeta = p'(w)\, dw = \sqrt{l(w)(dw)^2}. \tag{16}
$$

Moreover, we know that the asymptotic lines on X are given by $\operatorname{Re} l(w)(dw)^2 = 0$, and the relation $\operatorname{Im} l(w)(dw)^2 = 0$ yields the lines of curvature (cf. Section 3.1, Proposition 5). Thus the ζ-images of the asymptotic lines $w = w(t)$ lie on straight lines which intersect the real axis at an angle of 45° or of 135°, whereas the lines of curvature $w = w(t)$ are mapped by $\zeta = p(w)$ into straight lines in the ζ-plane which are parallel either to the real axis or to the imaginary axis.

For the solution $X : \bar{\Omega} \to \mathbb{R}^3$ of the Schwarzian chain problem, the boundary $\partial\Omega$ consists of arcs corresponding to asymptotic lines and to lines of curvature. Hence the conformal mapping $\zeta = p(w)$ defined by (15) maps Ω onto some polygonal domain Ω^{**} in the ζ-plane. If we compose the two conformal mappings

$$
\tau : \Omega^* \to \Omega, \quad p : \Omega \to \Omega^{**},
$$

then $q = p \circ \tau : \Omega^* \to \Omega^{**}$ yields a conformal mapping of Ω^* onto Ω^{**}. By the arguments given in Section 3.3 (cf. in particular the formulae (12), (26) and (35)), we obtain from (15) the relation

$$
\begin{aligned}
q(\omega) = p(\tau(\omega)) &= \int_{\omega_0}^{\omega} \sqrt{l(\tau(\underline{\omega}))}\tau'(\omega)\, d\underline{\omega} \\
&= \int_{\omega_0}^{\omega} \sqrt{-\mu(\tau(\underline{\omega}))\nu'(\tau(\underline{\omega}))\tau'(\underline{\omega})^2}\, d\underline{\omega} \\
&= \int_{\omega_0}^{\omega} \sqrt{-2\mathfrak{F}(\underline{\omega})}\, d\underline{\omega},
\end{aligned}
$$

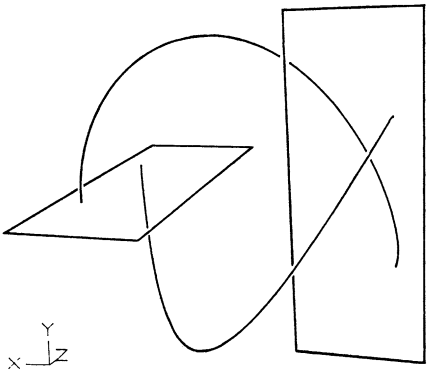

Fig. 11. A (generalized) Schwarzian chain made up of two analytic curves connecting two plane rectangles. The Schwarzian chain problem is to find a minimal surface spanning this configuration

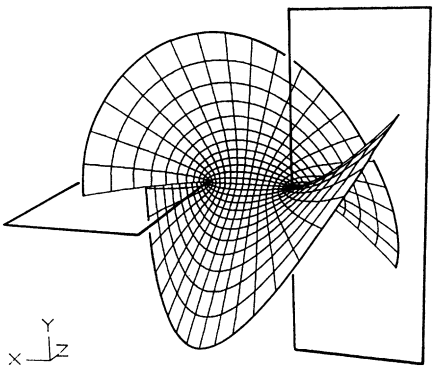

Fig. 12. This particular Schwarzian chain problem is solved by the part of Henneberg's surface corresponding to the rectangle $-0.3\pi \le u \le 0.3\pi$, $0 \le v \le \pi/4$. The surface maps the sides parallel to the v-axis onto the two analytic boundary curves of the chain whereas the two others correspond to Neil's parabolas along which the minimal surface is perpendicular to the two rectangles

that is,

$$q(\omega) = \int_{\omega_0}^{\omega} \sqrt{-2\mathfrak{F}(\underline{\omega})}\, d\underline{\omega}. \tag{17}$$

Hence the Weierstrass function $\mathfrak{F}(\omega)$ used in the representation (14) can be computed from the conformal mapping $q : \Omega^* \to \Omega^{**}$ by the formula

$$\mathfrak{F}(\omega) = -\frac{1}{2}\left(\frac{dq(\omega)}{d\omega}\right)^2. \tag{18}$$

By our assumptions, the mapping $\tau : \Omega^* \to \Omega$ is 1–1. If we also assume that $p : \Omega \to \Omega^{**}$ is 1–1, then $q = p \circ \tau$ provides a biholomorphic mapping of Ω^*

onto Ω^{**} whose extension to $\bar{\Omega}^*$ maps the vertices of the circular polygonal domain Ω^* into the vertices of the polygonal domain Ω^{**}. (Note that the vertices of Ω^* are well defined by the chain $\mathfrak{C}$ since we have assumed that the normal mapping is defined on $\bar{\Omega}^*$.)

This reasoning, using the mappings $\tau : \Omega^* \to \Omega$ and $p : \Omega \to \Omega^{**}$ together with symmetry arguments, yields a handy method to solve the Schwarzian chain problem in many interesting cases by explicit formulas. It can also be used to construct many specimen of complete and, in particular, of periodic minimal surfaces. For details, we refer to Karcher [1–3].

During the 19th century, function theoretic methods were the only known tools for proving existence of minimal surfaces spanning a given boundary configuration. These methods, however, limited the study of existence questions to frames consisting only of straight lines and planar parts. In the following chapters we shall develop another approach that is suitable for tackling more general boundary problems for minimal surfaces. Yet this approach will only yield the existence of minimal surfaces within a prescribed boundary configuration and does not give explicit formulas for solutions of a given boundary problem. One has to use numerical methods to obtain further information on the geometric shape of solutions. The classical methods of function theory, on the other hand, have the appeal that they furnish explicit representation formulas from which, in principle, one can read off all desired geometric properties of solutions. Surveys of and references to the classical results can be found in Riemann [1], Schwarz [2], Weierstrass [1–5], Enneper [1], Darboux [1], von Lilienthal [1], Blaschke [1], and Nitsche [28,37].

Now we are going to construct minimal surfaces with interesting special properties by combining Lemma 2 with Schwarz's solution (1) of the Björling problem.

Firstly, Lemma 2(i) yields:

Proposition 2. *Let $S = \{(c(t), n(t)) : t \in I\}$ be a real analytic strip whose supporting curve $c(t)$, $t \in I$, is a straight line. Then*

$$X(u,v) = \operatorname{Re}\left\{ c(w) - i \int_{u_0}^{w} n(\underline{w}) \wedge dc(\underline{w}) \right\}, \quad w = u + iv,$$

$u_0 \in I$, defines a minimal surface with $c(u) = X(u,0)$ as geodesic. Moreover, c is also an asymptotic line of X, and the surface normal $N(u,v)$ of X coincides on I with n, i.e., $N(u,0) = n(u)$.

Consider now a real analytic strip $S = \{(c(t), n(t)) : t \in I\}$ whose supporting curve c is contained in a plane E with a normal vector e which satisfies

$$\langle n(t), e \rangle \equiv \cos\varphi, \quad t \in I,$$

for some constant angle φ. Then (1) defines a minimal surface X for which c is a line of curvature contained in the plane E which intersects X at c under the constant angle φ.

Conversely, if $c(t)$, $t \in I$, is a real analytic regular curve contained in a plane E, and if $\varphi(t)$ is a real analytic function, then

$$S = \{(c(t), n(t)) : t \in I\} \quad \text{with} \tag{19}$$
$$n(t) := e\cos\varphi(t) + \dot{c}(t) \wedge e\frac{1}{|\dot{c}(t)|}\sin\varphi(t)$$

is a real analytic strip such that $n(t)$ intersects E at its point of support $c(t)$ under the angle $\varphi(t)$. By inserting (19) into (1), we obtain:

Proposition 3. *Let $c(t)$, $t \in I$, be some real analytic regular curve contained in a plane E with a normal vector e, and let φ be some constant angle. Then, for $w = u + iv$ and $u_0 \in I$,*

$$X(w) = \operatorname{Re}\Big\{c(w) - ie \wedge [c(w) - c(u_0)]\cos\varphi \tag{20}$$
$$- i\sin\varphi \int_{u_0}^{w} \langle c'(\underline{w}), c'(\underline{w})\rangle^{1/2}\, d\underline{w}\, e\Big\}$$

defines a minimal surface containing $c(u) = X(u, 0)$ as a planar line of curvature. Moreover, X intersects E along c at a constant angle φ. Finally, if $\varphi = \frac{\pi}{2}$, then c furnishes a planar geodesic on the surface X given by (20).

By choosing E as the x, z-plane, we in particular obtain:

Proposition 4. *If $c(t) = (\xi(t), 0, \zeta(t))$, $t \in \mathbb{R}$, is a real analytic regular curve contained in the x, z-plane E, then*

$$X(u, v) = \left(\operatorname{Re}\xi(w), \operatorname{Im}\int_0^w \{\xi'(\underline{w})^2 + \zeta'(\underline{w})^2\}^{1/2}\, d\underline{w}, \operatorname{Re}\zeta(w)\right) \tag{21}$$

defines a minimal surface X that intersects E perpendicularly along c. Moreover, the curve c is a planar line of curvature on X; in fact, c is a planar geodesic.

If c is a smooth regular curve with nonvanishing curvature, then the principal normal $\boldsymbol{n}$ and the binormal $\boldsymbol{b}$ of c are well defined. If c is a geodesic or an asymptotic line on a regular surface X, then the surface normal N of X can be identified along c with $\boldsymbol{n}$ or with $\pm\boldsymbol{b}$, respectively. Thus we infer from Theorem 1:

Proposition 5. *Let c be a regular real analytic curve of nonvanishing curvature. Then there exists a minimal surface X containing c as geodesic; X is the only such surface if we assume that the surface normal of X along c coincides with the principal normal $\mathcal{N}$ of c. Secondly, there is a minimal surface Y containing c as an asymptotic line, and there is no other such surface if we require that the surface normal of Y along c agrees with the binormal $\boldsymbol{b}$ of c.*

3.5 Examples of Minimal Surfaces

In this section we shall briefly discuss some of the classical minimal surfaces found in the nineteenth century, as well as some new examples. Detailed accounts and further information can be found in the treatises of Darboux [1] and Nitsche [28,37], in the lecture notes of Barbosa and Colares [1], and in the papers and reports of Hoffman [1–4], Hoffman and Meeks [1–10], Karcher [1–5], Hoffman and Karcher [1] and Karcher and Polthier [1].

3.5.1 Catenoid and Helicoid

Figure 1 shows a part of the *catenoid*. This minimal surface owes its name to the fact that it can be obtained by rotating a certain *catenary* (or *chain line*) about some axis. If we choose the z-axis as axis of rotation, all catenoids are generated by rotating the catenaries

$$x = \alpha \cosh\left(\frac{z - z_0}{\alpha}\right), \quad z \in \mathbb{R}, \tag{1}$$

where z_0 and α are arbitrary constants, $\alpha \neq 0$. It is one of the classical results of the calculus of variations that every nonplanar rotationally symmetric minimal surface is congruent to a piece of a catenoid. We leave the simple proof of this fact as an exercise to the reader.

Clearly, every catenoid is a doubly connected minimal surface which can be parametrized[2] by

$$\begin{aligned} x(u,v) &= \alpha \cosh u \cos v, \\ y(u,v) &= -\alpha \cosh u \sin v, \\ z(u,v) &= \alpha u \end{aligned} \tag{2}$$

with $-\infty < u < \infty$, $0 \leq v < 2\pi$, if we choose $z_0 = 0$.

Note that the representation (2) is defined for all $w = u + iv \in \mathbb{C}$. Hence the mapping $X : \mathbb{C} \to \mathbb{R}^3$, $X(w) := (x(w), y(w), z(w))$, represents the *universal covering surface* of the catenoid generated by the meridian (1). The mapping $X : \mathbb{C} \to \mathbb{R}^3$ is harmonic and conformal. In fact, by means of the formulas

$$\begin{aligned} \cosh(u + iv) &= \cosh u \cos v + i \sinh u \sin v, \\ \sinh(u + iv) &= \sinh u \cos v + i \cosh u \sin v \end{aligned} \tag{3}$$

we infer that

$$X(w) = \operatorname{Re} f(w) \tag{4}$$

where $f : \mathbb{C} \to \mathbb{C}^3$ denotes the isotropic curve given by

[2] We could as well define $y(u,v) = \alpha \cosh u \sin v$; this would amount to a change of the sense of rotation.

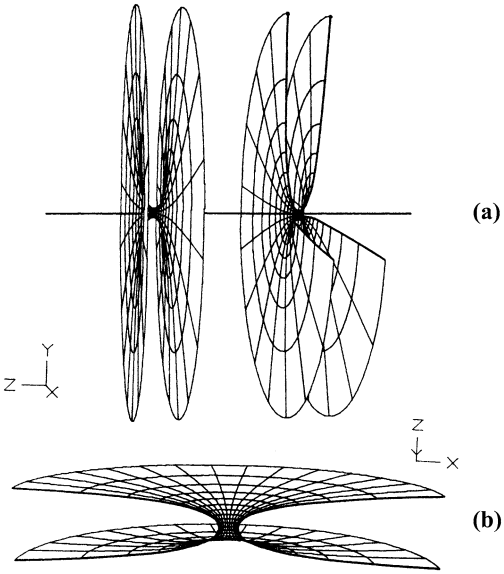

Fig. 1. (a) Three quarters and all of the subset $|z| \leq 1.4\pi$ of the catenoid. The *line* along which the model is cut open is a catenary, the curve described by a hanging chain. The parts contained in *large, origin-centered balls* indicate a global view of the catenoid. They look like two parallel plane disks connected by a thin funnel. **(b)** The part $|u| \leq 1.2\pi$, $0 \leq v \leq \pi$, of the catenoid

$$f(w) = (\alpha \cosh w, \alpha i \sinh w, \alpha w). \tag{5}$$

In order to find the Weierstrass function $\mathfrak{F}(\omega)$ and the representation $Y(\omega)$ of the catenoid given by Section 3.3, (27), or precisely by

$$\begin{aligned} x &= \alpha + \operatorname{Re} \int_1^\omega (1-\omega^2)\mathfrak{F}(\omega)\, d\omega, \\ y &= \operatorname{Re} \int_1^\omega i(1+\omega^2)\mathfrak{F}(\omega)\, d\omega, \\ z &= \operatorname{Re} \int_1^\omega 2\omega\mathfrak{F}(\omega)\, d\omega, \end{aligned} \tag{6}$$

we introduce the new variable $\omega = e^{-w}$ instead of $w = u + iv$. Set $r = |\omega|$ and $\theta = \arg \omega$, i.e. $\omega = re^{i\theta}$. Then $\log \omega = \log r + i\theta = -u - iv$, and we can write (2) in the new form

$$\begin{aligned} x &= \frac{\alpha}{2}\left(\frac{1}{r} + r\right)\cos\theta = \operatorname{Re}\frac{\alpha}{2}\left(\frac{1}{\omega} + \omega\right), \\ y &= \frac{\alpha}{2}\left(\frac{1}{r} + r\right)\sin\theta = \operatorname{Re}\frac{i\alpha}{2}\left(\frac{1}{\omega} - \omega\right), \\ z &= -\alpha \log r = -\operatorname{Re}\alpha \log \omega. \end{aligned} \tag{7}$$

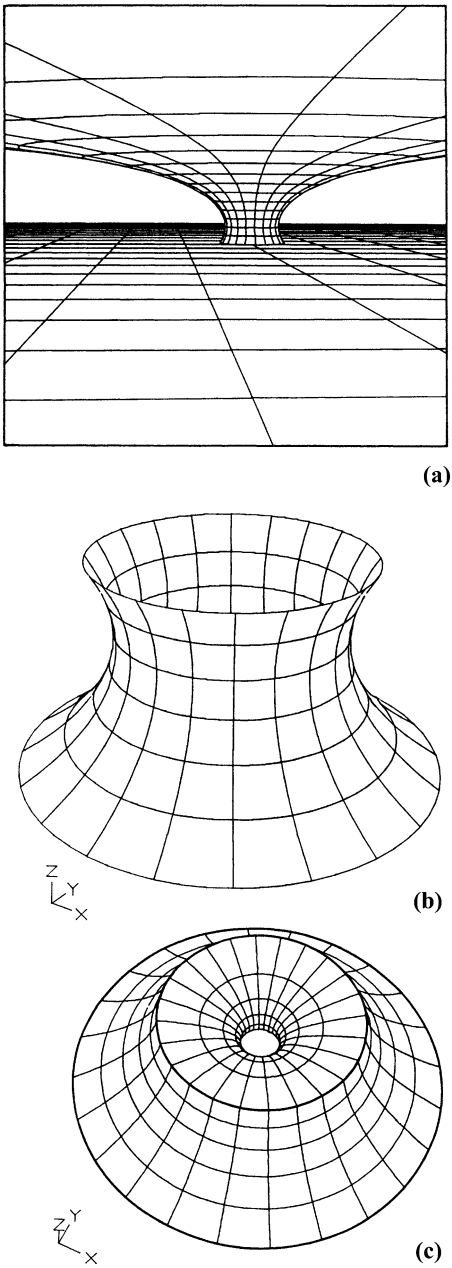

Fig. 2. (a) A view of the part $u \geq -\pi/5$ of the catenoid sitting on the plane $z = -\pi/5$. **(b)** The subset $-\pi/5 \leq z \leq \pi/10$ shows the behaviour of the catenoid close to its plane of symmetry $z = 0$. **(c)** Two catenoids sitting in the same boundary configuration

By a straight-forward computation we infer that these equations are identical with (6) if we choose

$$\mathfrak{F}(\omega) = -\frac{\alpha}{2\omega^2}, \quad \omega \in \mathbb{C} \setminus \{0\}. \tag{8}$$

The geometrical meaning of the parameter ω implies that *the normal map* $N(\omega)$ *of the representation* $Y(\omega)$ *of the catenary given by* (6) *or* (7)*, respectively, omits exactly two points on the Riemann sphere* S^2, the north pole $\rho(\infty)$ and the south pole $\rho(0)$. Cut the ω-plane along the positive part of the real axis and denote the resulting set $\{\omega = \xi + i\eta\colon |\omega| > 0,\ 0 < \arg\omega < 2\pi\}$ by $\mathbb{C}'$. Then N maps $\mathbb{C}'$ one-to-one onto S^2 minus a meridian connecting $\rho(0)$ and $\rho(\infty)$, and we infer that the area of the spherical image N is given by

$$\int dA_N = \int_{\mathbb{C}'} |N_\xi \wedge N_\eta|\, d\xi\, d\eta = 4\pi.$$

Since

$$dA_N = -K\, dA_Y \tag{9}$$

(cf. Section 1.2, (44)), we infer that the total curvature of the catenoid has the value -4π:

$$\int_Y K\, dA = -4\pi. \tag{10}$$

From (5), we read off that the adjoint surface

$$X^*(w) := \operatorname{Im} f(w) \tag{11}$$

of the catenoid (2) is given by

$$\begin{aligned} x^*(u,v) &= \alpha \sinh u \sin v, \\ y^*(u,v) &= \alpha \sinh u \cos v, \\ z^*(u,v) &= \alpha v \end{aligned} \tag{12}$$

or

$$X^* = \alpha Y(v) + \sinh u Z(v)$$

with

$$Y(v) = (0,0,v), \quad Z(v) = (\sin v, \cos v, 0).$$

Thus, for every $v \in \mathbb{R}$, the curve $X^*(\cdot, v)$ is a straight line which meets the z-axis perpendicularly. If we fix $u \neq 0$, then $X^*(u,\cdot)$ describes a *helix* of pitch $2\pi|\alpha|$. This helix is left-handed for $\alpha > 0$ and right-handed for $\alpha < 0$. We see that X^* is generated by a screw motion of some straight line $\mathfrak{L}$ meeting the z-axis perpendicularly, whence X^* is called *helicoid* or *screw surface*. *Thus*

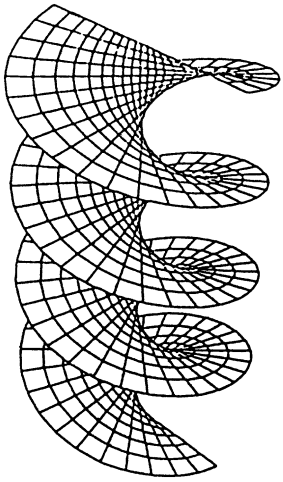

Fig. 3. A part of the helicoid, a ruled minimal surface

the helicoid X^*, the adjoint of the catenoid X, is a ruled surface with the z-axis as its directrix.

We claim that *the point set represented by some ruled surface*

$$X(u,v) = a(v) + ub(v)$$

with $a(v), b(v) \in \mathbb{R}^3$, which is regular, skew (i.e. $[a', b, b'] \neq 0$) and of zero mean curvature, must be congruent to a piece of the helicoid (E. Catalan [1]).

For the proof of this fact we can assume that $|b| = 1$ and $|b'| = 1$ whence

$$\langle b, b' \rangle = 0, \quad \langle b', b'' \rangle = 0.$$

Moreover, we can also assume that

$$\langle a'(v), b(v) \rangle = 0, \quad \langle a'(0), b'(0) \rangle = 0$$

as we can pass from $a(v)$ to a new directrix $\bar{a}(v)$ given by

$$\begin{aligned} \bar{a}(v) &= a(v) - \lambda(v) b(v), \\ \lambda(v) &= \langle a'(0), b'(0) \rangle + \int_0^v \langle a'(t), b(t) \rangle \, dt. \end{aligned}$$

This yields

$$\mathcal{F} = 0, \quad \mathcal{L} = 0,$$

and the equation $H = 0$ is equivalent to $\mathcal{N} = 0$ whence $\langle N, X_{vv} \rangle = 0$, and therefore

$$\det(X_u, X_v, X_{vv}) = 0;$$

see Section 1.2, (31) and (43). Collecting the powers of u, we obtain the three relations

$$\det(b, a', a'') = 0, \quad \det(b, b', b'') = 0,$$
$$\det(b, a', b'') + \det(b, b', a'') = 0.$$

Since b' is perpendicular to b and b'', the second relation yields $b'' = \langle b'', b\rangle b$. Hence $(b \wedge b')' = 0$, and we infer from $|b| = 1$ that the curve $b(v)$ describes a unit circle in a fixed plane E. Now, from the third relation, we obtain $\det(b, b', a'') = 0$, and therefore $a'' \in E$ as well as

$$a'' = \langle a'', b\rangle b + \langle a'', b'\rangle b'.$$

Inserting this expression for a'' into the equation $\det(b, a', a'') = 0$, we infer

$$\langle a'', b'\rangle \det(b, a', b') = 0.$$

The determinant does not vanish for v close to zero (since its columns are mutually orthogonal at $v = 0$ and $X(u, v)$ is a regular surface), and therefore $\langle a'', b'\rangle = 0$. Hence $\langle a', b'\rangle' = 0$ and $\langle a'(0), b'(0)\rangle = 0$ implies $\langle a', b'\rangle = 0$. Together with $\langle a', b\rangle = 0$ we obtain that a' is perpendicular to $\operatorname{span}\{b, b'\} = E$. Since E does not depend on v, we conclude that also a'' is orthogonal to E. On the other hand we know that $a'' \in E$. Thus we obtain $a'' = 0$, i.e., the directrix $a(v)$ is a straight line, and we have proved that $X(u, v)$ is a piece of a helicoid since $\langle a', b\rangle = 0$.

There are various other proofs of this characterization of the helicoid. We particularly mention the elegant approach of H.A. Schwarz by means of the solution of a suitable Björling problem (see Schwarz [2], vol. I, pp. 181–182).

The coordinates of the *associate surfaces*

$$Z(w, \theta) = \operatorname{Re}\{e^{-i\theta} f(w)\}, \quad \theta \in \mathbb{R}, \tag{13}$$

to the catenoid $X(w)$ as well as to the helicoid $X^*(w)$ are given by

$$\begin{aligned} x &= \alpha \cosh u \cos v \cos\theta + \alpha \sinh u \sin v \sin\theta, \\ y &= -\alpha \cosh u \sin v \cos\theta + \alpha \sinh u \cos v \sin\theta, \\ z &= \alpha u \cos\theta + \alpha u \sin\theta. \end{aligned} \tag{14}$$

The bending process of deforming the catenoid X into the helicoid X^* via the associate surfaces $Z(w, \theta)$, $0 \le \theta \le \frac{\pi}{2}$, is depicted in Fig. 4.

3.5.2 Scherk's Second Surface: The General Minimal Surface of Helicoidal Type

Consider the minimal surface $Y(\omega)$ defined by

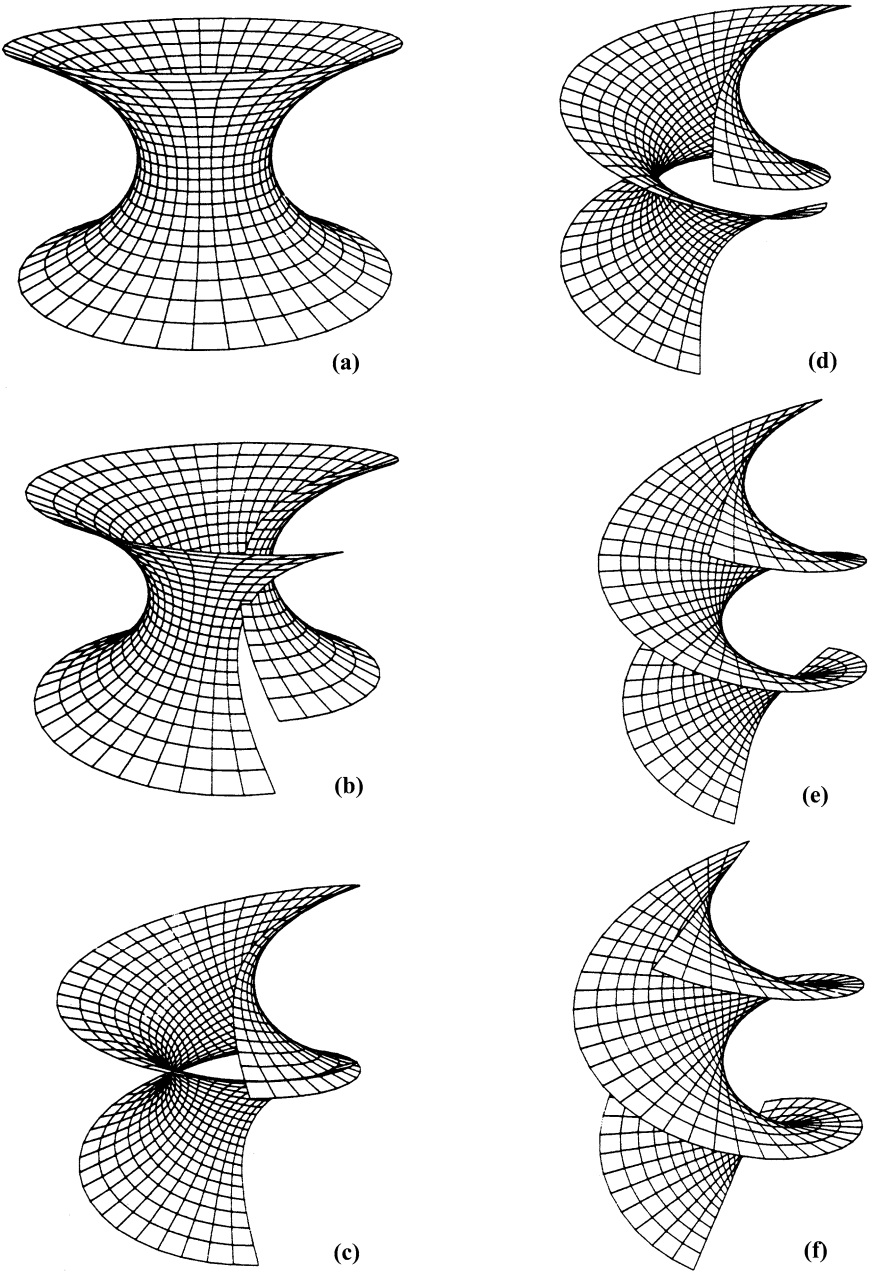

Fig. 4. The catenoid, a minimal surface of rotation, can be bent through its family of associate minimal surfaces into the helicoid, its adjoint surface, which is a ruled surface

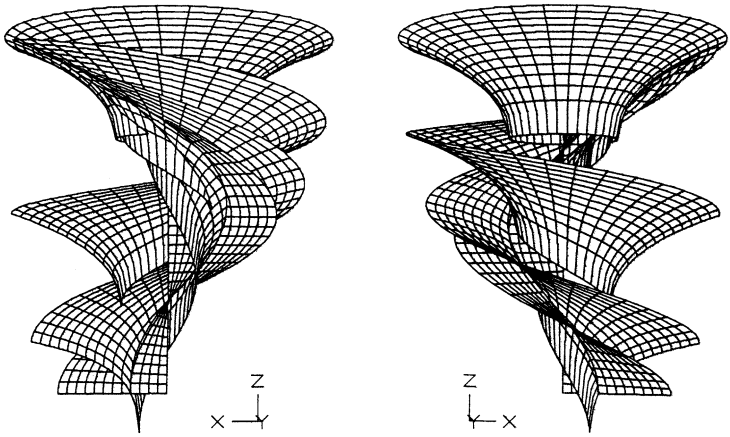

Fig. 5. Scherk's second surface is the family of associate surfaces of the catenoid viewed in a different way. Every member of this family is generated by a screw motion of a planar curve. The illustration shows the parts next to the z-axis of the associate surfaces with parameter values $\theta = k\pi/6$ for $k = 0, 1, 2, 3$

$$
\begin{aligned}
x &= \alpha + \operatorname{Re} \int_1^\omega (1-\omega^2)\mathfrak{F}(\omega)\, d\omega, \\
y &= \operatorname{Re} \int_1^\omega i(1+\omega^2)\mathfrak{F}(\omega)\, d\omega, \\
z &= \gamma + \operatorname{Re} \int_1^\omega 2\omega\mathfrak{F}(\omega)\, d\omega
\end{aligned}
\tag{15}
$$

with the Weierstrass function

$$
\mathfrak{F}(\omega) = \frac{-(\alpha - i\beta)}{2\omega^2}, \quad \alpha, \beta \in \mathbb{R},\ \alpha^2 + \beta^2 \neq 0. \tag{16}
$$

For $\alpha = 0$ or $\beta = 0$, we obtain a helicoid or a catenoid, respectively. If we switch by $\omega = e^{-w}$, $w = u + iv$, from ω to the new variable w, then (15) is transformed into

$$
\begin{aligned}
x &= \alpha \cosh u \cos v + \beta \sinh u \sin v, \\
y &= -\alpha \cosh u \sin v + \beta \sinh u \cos v, \\
z &= \alpha u + \beta v + \gamma.
\end{aligned}
\tag{17}
$$

This is a parameter representation of a family of minimal surfaces. For a fixed choice of α, β, γ, we want to denote a surface (17) as *Scherk's second surface.* This family comprises the catenoid ($\beta = 0$) and the helicoid ($\alpha = 0$). In fact, we can write $X(w)$ in the following way, using the formulae

$$
X^{\mathrm{cat}}(w) = (\cosh u \cos v, -\cosh u \sin v, u)
$$

for the catenoid and

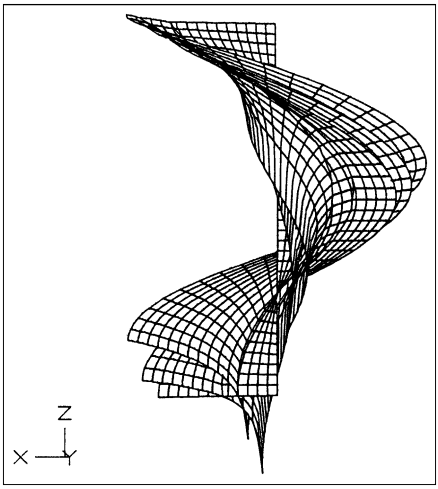

Fig. 6. Another view of parts of three members of the family of minimal surfaces called Scherk's second surface ($\theta = 60, 75, 90$ degrees)

$$X^{\mathrm{hel}}(w) = (\sinh u \sin v, \sinh u \cos v, v)$$

for the helicoid and choosing $\gamma = 0$:

$$X(w) = \alpha X^{\mathrm{cat}}(w) + \beta X^{\mathrm{hel}}(w). \tag{17′}$$

As we can write

$$\alpha = c\cos\theta, \quad \beta = c\sin\theta \quad \text{with } c = \sqrt{\alpha^2 + \beta^2},$$

it follows that

$$X(w) = c[\cos\theta X^{\mathrm{cat}}(w) + \sin\theta X^{\mathrm{hel}}(w)].$$

In other words, Scherk's second surface is nothing but an associate surface of the catenoid.

We want to show that (17) *provides a minimal surface of helicoid type generated by a screw motion of some planar curve $z = h(\rho)$ about the z-axis.* (One can easily prove that there exists no other nonplanar minimal surface of helicoidal type; cf. Nitsche [28], pp. 62–63). To this end, we introduce cylindrical coordinates ρ, φ, z instead of the Cartesian coordinates x, y, z by

$$x = \rho\cos\varphi, \quad y = \rho\sin\varphi, \quad z = z. \tag{18}$$

From the first two formulas of (17), we infer that

$$\begin{aligned}\tan(\varphi + v) &= \frac{\sin\varphi\cos v + \cos\varphi\sin v}{\cos\varphi\cos v - \sin\varphi\sin v} \\ &= \frac{y\cos v + x\sin v}{x\cos v - y\sin v} = \frac{\beta}{\alpha}\tanh u\end{aligned}$$

whence

$$v = -\varphi + \arctan\left(\frac{\beta}{\alpha}\tanh u\right). \tag{19}$$

Moreover, the formulas

$$\rho^2 - \alpha^2 = (\alpha^2 + \beta^2)\sinh^2 u, \quad \rho^2 + \beta^2 = (\alpha^2 + \beta^2)\cosh^2 u$$

yield

$$\frac{\rho^2 - \alpha^2}{\rho^2 + \beta^2} = \tanh^2 u < 1$$

and

$$\tanh u = \pm\sqrt{\frac{\rho^2 - \alpha^2}{\rho^2 + \beta^2}},$$

where the plus sign holds for $u \geq 0$, and the minus sign is to be taken if $u \leq 0$. Thus

$$u = \tanh^{-1}\left(\pm\sqrt{\frac{\rho^2 - \alpha^2}{\rho^2 + \beta^2}}\right),$$

and the identity

$$\tanh^{-1}\xi = \frac{1}{2}\log\frac{1+\xi}{1-\xi} \quad \text{for } |\xi| < 1$$

implies

$$u = \frac{1}{2}\log\frac{\sqrt{\rho^2+\beta^2} \pm \sqrt{\rho^2-\alpha^2}}{\sqrt{\rho^2+\beta^2} \mp \sqrt{\rho^2-\alpha^2}}.$$

A brief computation yields

$$u = -\log\sqrt{\alpha^2+\beta^2} + \log(\sqrt{\rho^2+\beta^2} \pm \sqrt{\rho^2-\alpha^2}). \tag{20}$$

Combining the relations (17)–(20), we arrive at

$$\begin{aligned} x &= \rho\cos\varphi, \quad y = \rho\sin\varphi, \quad z = -\beta\varphi + h(\rho), \\ h(\rho) &:= \alpha\log(\sqrt{\rho^2+\beta^2} \pm \sqrt{\rho^2-\alpha^2}) \\ &\quad + \beta\arctan\left(\pm\frac{\beta}{\alpha}\sqrt{\frac{\rho^2-\alpha^2}{\rho^2+\beta^2}}\right) + \gamma - \alpha\log\sqrt{\alpha^2+\beta^2}. \end{aligned} \tag{21}$$

This representation shows that Scherk's second surface is a helicoidal surface generated by a screw motion of a planar curve $z = h(\rho)$ about the z-axis.

3.5.3 The Enneper Surface

The minimal surface $X(w), w \in \mathbb{C}$, given by the Weierstrass representation (29), (30) of Section 3.3 with

$$\mathfrak{F}(w) \equiv 1$$

is the *Enneper surface*:

$$X(w) = \operatorname{Re}\left(\int_0^w (1-w^2)\mathfrak{F}(w)\,dw, \int_0^w i(1+w^2)\mathfrak{F}(w)\,dw, \int_0^w 2w\mathfrak{F}(w)\,dw \right),$$

that is,

$$X(w) = \operatorname{Re}\left(w - \frac{w^3}{3}, iw + \frac{iw^3}{3}, w^2 \right). \tag{22}$$

Thus the components of the Enneper surface are given by

$$\begin{aligned} x &= u - \tfrac{1}{3}u^3 + uv^2, \\ y &= -v - u^2 v + \tfrac{1}{3}v^3, \\ z &= u^2 - v^2 \end{aligned} \tag{23}$$

for $w = u + iv \in \mathbb{C}$.

The Gauss curvature $K(w)$ of $X(w)$ has the form

$$K(w) = -\frac{4}{(1+|w|^2)^4}, \tag{24}$$

and

$$N(w) = \frac{1}{1+|w|^2}(2\operatorname{Re} w, 2\operatorname{Im} w, |w|^2 - 1) \tag{25}$$

is *its spherical image*, which *omits exactly one point on the Riemann surface*, the north pole $\rho(\infty)$. Moreover, the mapping $N : \mathbb{C} \to S^2 \setminus \{\rho(\infty)\}$ is one-to-one whence $\int dA_N = 4\pi$, and by

$$dA_N = -K\,dA_X$$

we obtain

$$\int_X K\,dA = -4\pi \tag{26}$$

for the total curvature of the Enneper surface. This formula can also be verified by a direct computation using (24) as well as

$$|dX(w)|^2 = |\mathfrak{F}(w)|^2(1+|w|^2)^2|dw|^2.$$

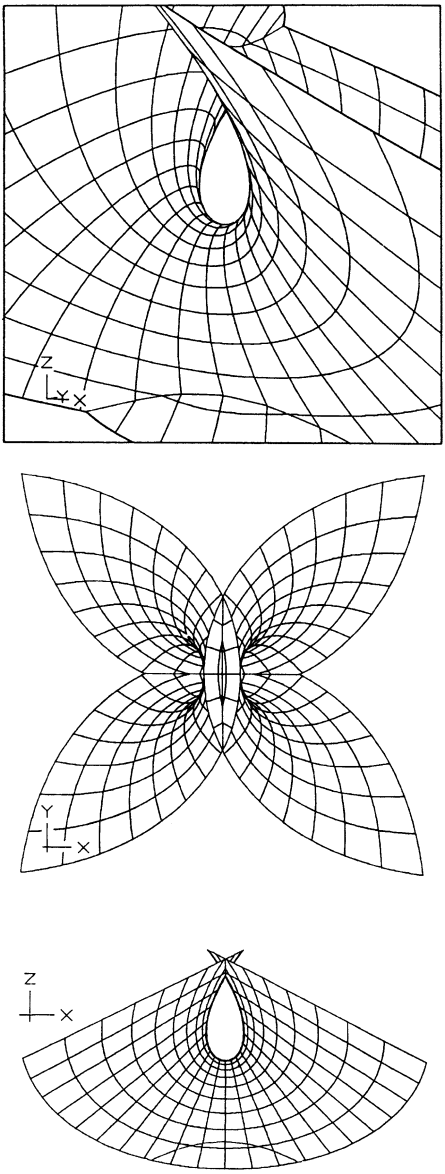

Fig. 7. These views of the subset of Enneper's surface corresponding to $|u| \leq 2$, $|v| \leq 2$ reveal the behavior of the surface close to the origin. The planes and lines of symmetry of the surface can be seen in the two projections onto the coordinate planes

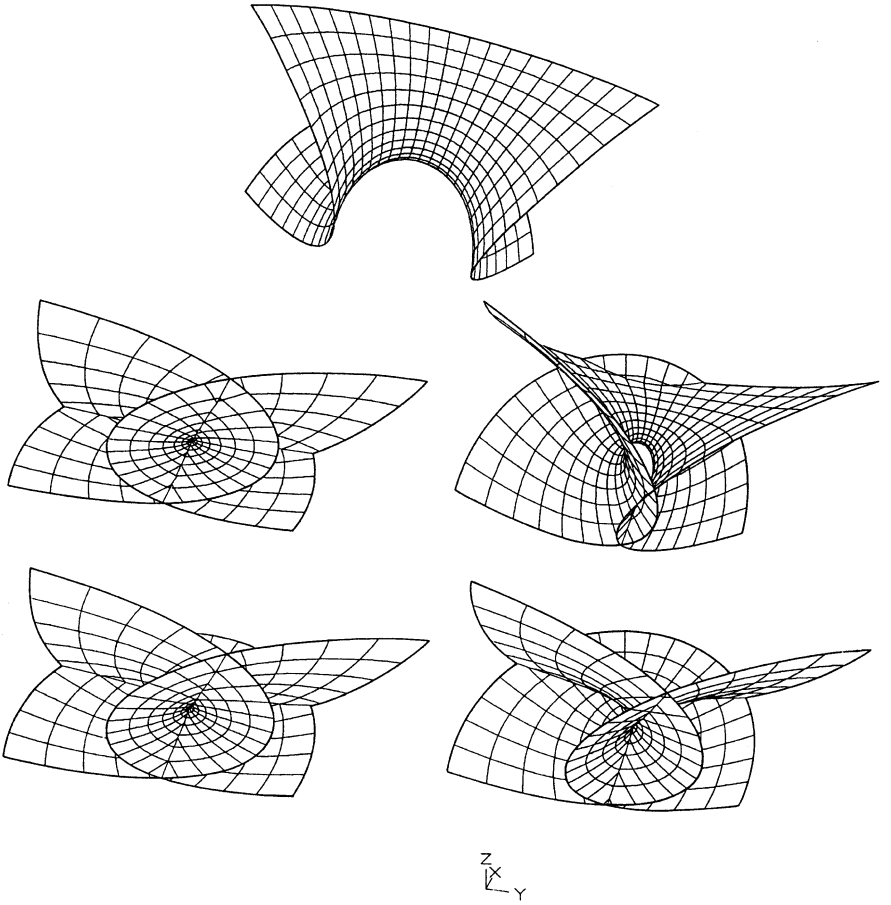

Fig. 8. Large parts of Enneper's surface: the parts shown correspond to the squares $[-R, R]^2, R = 1, 2, 4, 8, 16$, of the parameter plane (clockwise from the top). The shapes of the rescaled figures converge in view of the convergence of $X(Rw)/R^3$

The trace of the Enneper surface X is congruent to the traces of its associate surfaces

$$Z(w, \theta) = \mathrm{Re}\left\{ e^{-i\theta}\left(w - \frac{w^3}{3}\right), ie^{-i\theta}\left(w + \frac{w^3}{3}\right), e^{-i\theta}w^2 \right\}.$$

This can be seen as follows: First we introduce new Cartesian coordinates ξ, η, z instead of x, y, z by a rotation about the z-axis with the angle $-\frac{\theta}{2}$:

$$\xi + i\eta = e^{-i\theta/2}(x + iy).$$

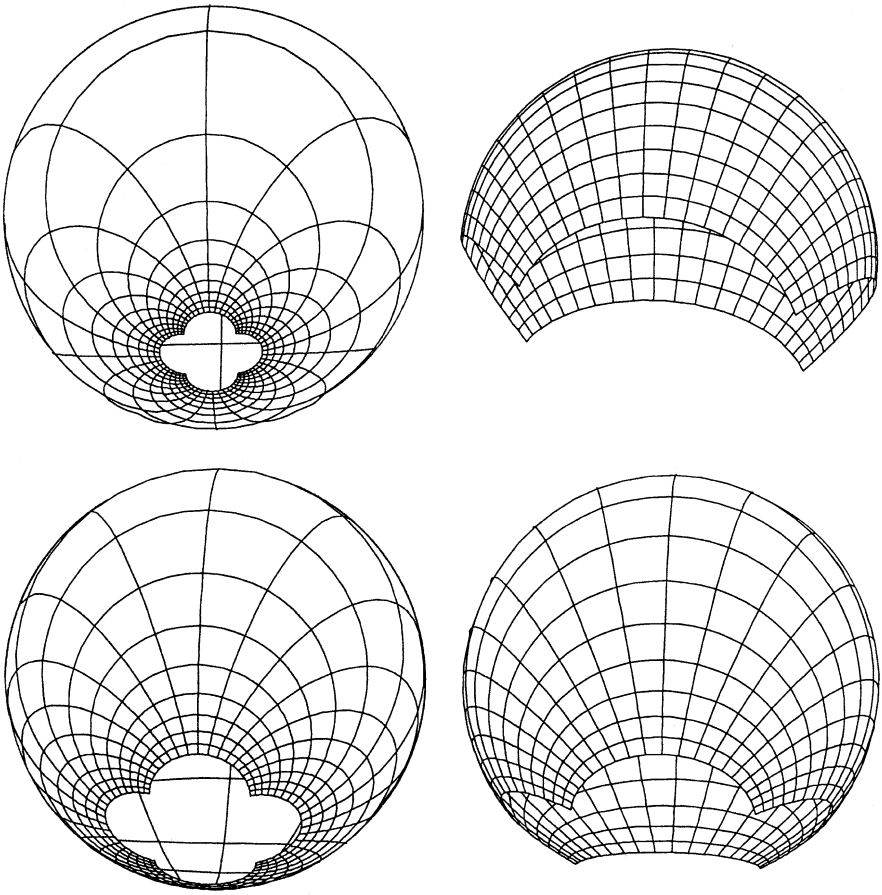

Fig. 9. The (negative of the) Gauss map of the first four parts of Enneper's surface shown before

Then the new coordinates $\xi(w)$, $\eta(w)$ of the associate surface will be obtained from

$$\begin{aligned}\xi + i\eta \;=\; & e^{-i\theta/2}[\mathrm{Re}(e^{-i\theta}w) + i\,\mathrm{Re}(ie^{-i\theta}w)] \\ & + e^{-i\theta/2}\left[\mathrm{Re}\left(-\frac{1}{3}\,e^{-i\theta}w^3\right) + i\,\mathrm{Re}\left(ie^{-i\theta}\frac{w^3}{3}\right)\right].\end{aligned}$$

Let us now introduce the new independent variable $\zeta = e^{-i\theta/2}w$. Using the identities

$$\mathrm{Re}\,c + i\,\mathrm{Re}\,ic = \bar{c}, \quad \mathrm{Re}\,c + i\,\mathrm{Re}(-ic) = c$$

for $c \in \mathbb{C}$, it follows that

$$\xi + i\eta = \mathrm{Re}(\zeta - \tfrac{1}{3}\zeta^3) + i\,\mathrm{Re}\,i(\zeta + \tfrac{1}{3}\zeta^3).$$

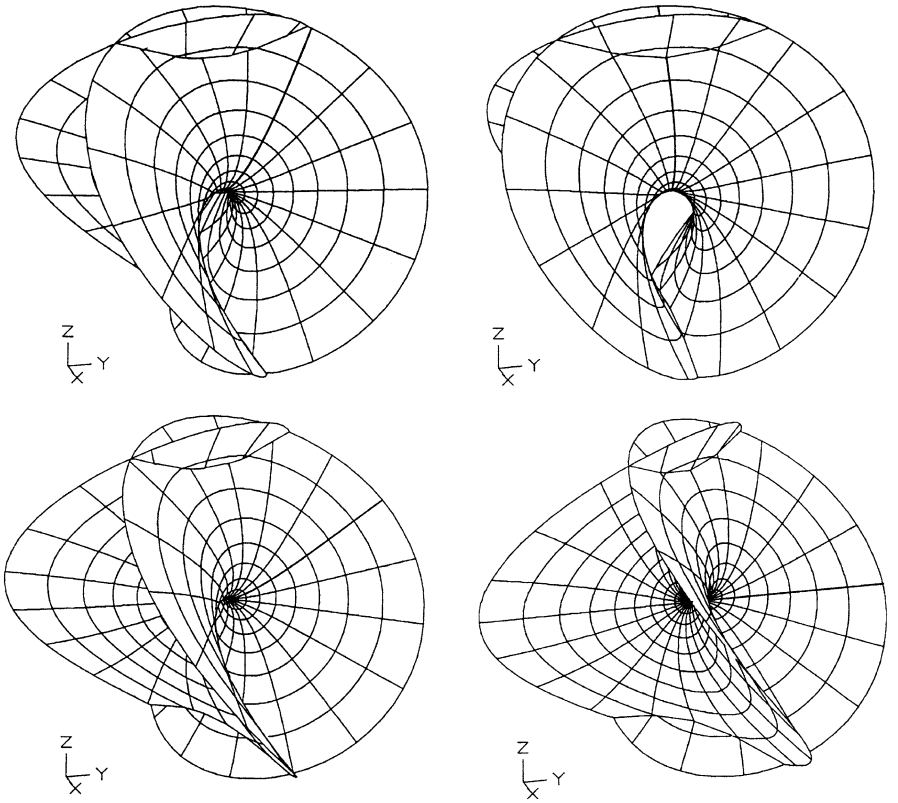

Fig. 10. For every parameter θ the subset of the associate surface corresponding to a disk B_R centered at $w = 0$ is obtained by rotating the same subset of Enneper's surface around the z-axis by an angle $\theta/2$ (counter-clockwise from top right $\theta = 0, \pi/6, \pi/3$, and $\pi/2$)

Thus we arrive at

$$\begin{aligned} \xi &= \operatorname{Re}(\zeta - \tfrac{1}{3}\zeta^3), \\ \eta &= \operatorname{Re} i(\zeta + \tfrac{1}{3}\zeta^3), \\ z &= \operatorname{Re} \zeta^2. \end{aligned}$$

Comparing these expressions with (22), we see that Enneper's surface and its associates are the same geometric objects.

3.5.4 Bour Surfaces

Bour's surfaces are given by

$$X(w) = X_0 + \operatorname{Re}\left(\int_1^w (1-w^2)\mathfrak{F}(w)\, dw, \int_1^w i(1+w^2)\mathfrak{F}(w)\, dw, \int_1^w 2w\mathfrak{F}(w)\, dw \right)$$

with the Weierstrass function

$$\mathfrak{F}(w) = cw^{m-2}, \quad w \in \mathbb{C} \text{ (or } \mathbb{C} \setminus \{0\}), \tag{27}$$

where $m \in \mathbb{R}$ and $c \in \mathbb{C}$, $c \neq 0$. This class of minimal surfaces clearly contains the previously considered examples where we had $m = 0$ or $m = 2$. It was proved by Bour that the surfaces with (27) are exactly those minimal surfaces which are developable onto some surface of revolution; cf. Schwarz [2], pp. 184–185, and Darboux [1], vol. 1, in particular pp. 392–395. Further references can be found in Nitsche [28], p. 57.

3.5.5 Thomsen Surfaces

Surfaces which are both minimal surfaces as well as affine minimal surfaces in the sense of Blaschke [1] have been discussed by Thomsen. A comprehensive discussion and a new derivation of all such surfaces can be found in Barthel, Volkmer, and Haubitz [1]. It turns out that, besides the Enneper surfaces, all other surfaces of this type belong to one of two families. The first family is given by

$$\begin{aligned} X(w) \;=\; & X_0 + \operatorname{Re}\alpha^{-2}(\alpha\beta w + \sqrt{1+\beta^2}\sinh\ \alpha w, \\ & -i\alpha\sqrt{1+\beta^2}w - i\beta\sinh\alpha w, -i\cosh\alpha w) \end{aligned} \tag{28}$$

or

$$\begin{aligned} x &= x_0 + \alpha^{-2}\{\alpha\beta u + \sqrt{1+\beta^2}\sinh\alpha u\cos\alpha v\}, \\ y &= y_0 + \alpha^{-2}\{\alpha\sqrt{1+\beta^2}v + \beta\cosh\alpha u\sin\alpha v\}, \\ z &= z_0 + \alpha^{-2}\{\sinh\alpha u\sin\alpha v\}, \end{aligned} \tag{29}$$

and the second family is obtained from the first by interchanging x and y as well as u and v; here we have assumed $\alpha > 0$.

For $\beta = 0$, the first family yields the left-handed helicoid, the second family the right-handed helicoid. One passes from one family to the other via the Enneper surface or some plane, respectively. Four views of a Thomsen surface are depicted in Fig. 11.

3.5.6 Scherk's First Surface

The nonparametric surface $z = \psi(x, y)$, defined by

$$e^z = \frac{\cos y}{\cos x} \tag{30}$$

or equivalently, by

$$z = \log\frac{\cos y}{\cos x} \tag{31}$$

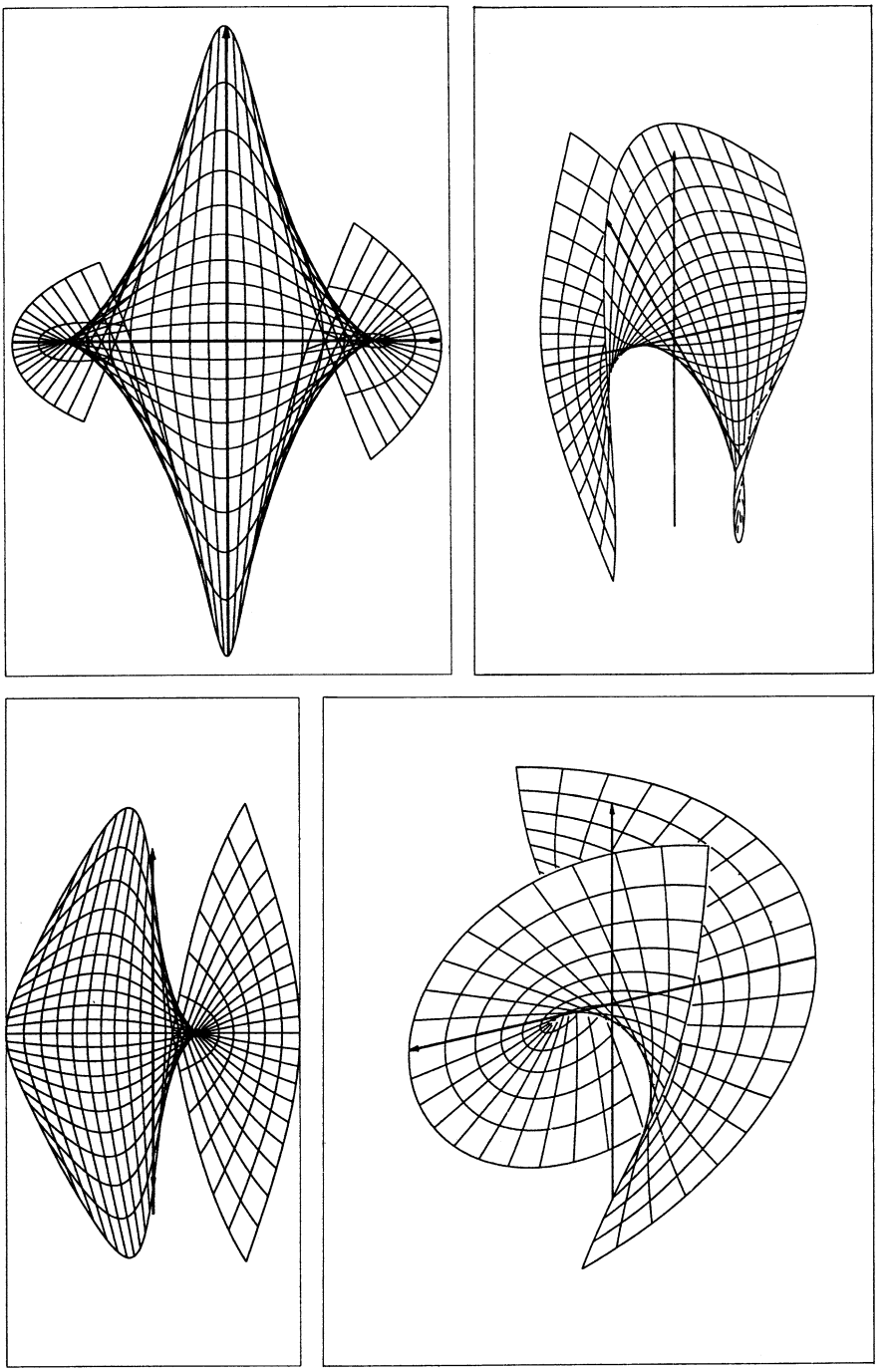

Fig. 11. Four different views of a piece of a Thomsen surface. Courtesy of I. Haubitz

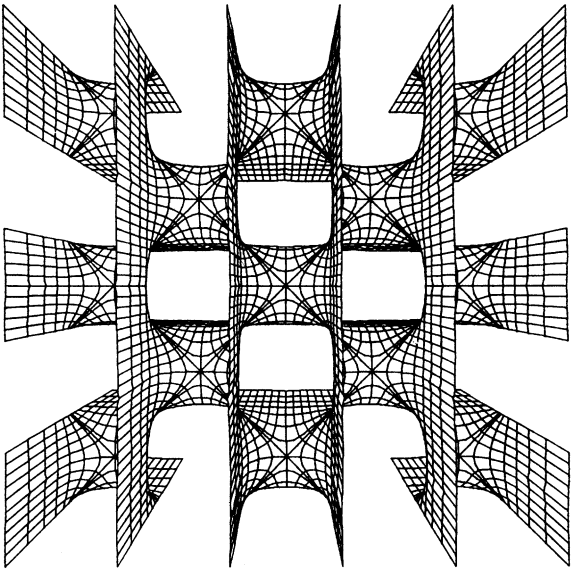

Fig. 12. The part $|z| < 10$, $|x|, |y| < 5\pi/2$, of Scherk's first surface seen from $z = +\infty$

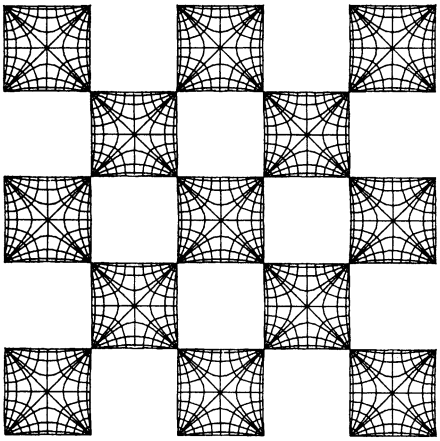

Fig. 13. Scherk's first surface is a non-parametric minimal surface defined on the set $0 < \cos(y)/\cos(x) < +\infty$, which is made up of the black squares of the infinite checker board shown in the figure

on the black squares

$$\Omega_{k,l} := \left\{(x, y)\colon |x - \pi k| < \frac{\pi}{2}, |y - \pi l| < \frac{\pi}{2}\right\},$$

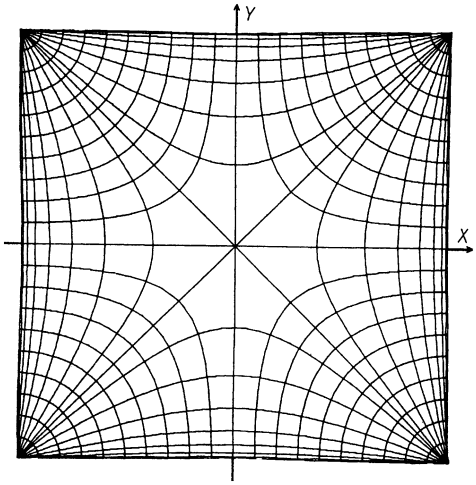

Fig. 14. A closer view of one of the black squares shows the level lines of the surface emanating from the corners. They satisfy $\cos(y)/\cos(x) = \text{constant}$, and the gradient lines perpendicular to them solve the equation $\sin(x)\sin(y) = \text{constant}$

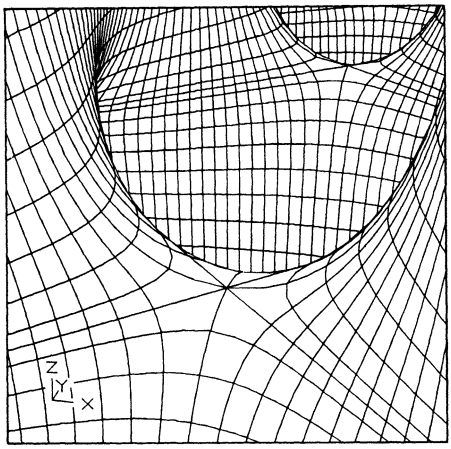

Fig. 15. A view of Scherk's first surface in the vicinity of the plane $z = 0$. The level curves $z = \text{constant}$ include the straight lines $x = \pm y$ as axes of symmetry

$k, l \in \mathbb{Z}$, $k + l =$ even, of the infinite checkerboard shown in Fig. 7, satisfies the nonparametric minimal surface equation

$$(1 + \psi_y^2)\psi_{xx} - 2\psi_x\psi_y\psi_{xy} + (1 + \psi_x^2)\psi_{yy} = 0.$$

This surface is *Scherk's doubly periodic surface* which we want to call *Scherk's first minimal surface*; clearly it is periodic both in the x- and in the y-direction. The graph is repeated on each black square $\Omega_{k,l}$.

The parameter lines shown in our illustrations of Scherk's surface all have the form

$$x = x(t), \quad y = y(t), \quad z = \psi(x(t), y(t))$$

with t varying in the interval $[0, 1]$, and $\psi(x, y) = \log \frac{\cos y}{\cos x}$. Any of the projected curves $(x(t), y(t))$ is either a level line or a gradient line of ψ, that is, we either have

$$\psi(x(t), y(t)) = \text{const},$$

or else

$$\begin{aligned} \frac{dx}{dt} &= \psi_x(x, y) = \tan x, \\ \frac{dy}{dt} &= \psi_y(x, y) = -\tan y. \end{aligned}$$

The gradient lines have the interesting property that they are just the solutions to the equation

$$\sin x \sin y = \text{const}.$$

Let us show that Scherk's surface has the Weierstrass representation

$$\begin{aligned} x &= -\pi + \operatorname{Re} \int_0^w (1 - w^2)\mathfrak{F}(w)\, dw \\ y &= \pi + \operatorname{Re} \int_0^w i(1 + w^2)\mathfrak{F}(w)\, dw, \\ z &= 0 + \operatorname{Re} \int_0^w 2w\mathfrak{F}(w)\, dw \end{aligned}$$

with

$$\mathfrak{F}(w) = \frac{2}{1 - w^4} = \frac{2}{(1 + w)(1 - w)(w + i)(w - i)} \tag{32}$$

on the parameter domain $\mathbb{C}\backslash\{\pm 1, \pm i\}$. This will show that the spherical image $N(w)$ of the Scherk surface $X(w)$ omits exactly four points on S^2, namely the points ± 1 and $\pm\, i$ on the equator. Since

$$\begin{aligned} (1 - w^2)\mathfrak{F}(w) &= \frac{2}{1 + w^2} = \frac{i}{w + i} - \frac{i}{w - i}, \\ i(1 + w^2)\mathfrak{F}(w) &= \frac{2i}{1 - w^2} = \frac{i}{w + 1} - \frac{i}{w - 1}, \\ 2w\mathfrak{F}(w) &= \frac{4w}{1 - w^4} = \frac{2w}{w^2 + 1} - \frac{2w}{w^2 - 1}, \end{aligned}$$

we infer that

$$X(w) = \operatorname{Re}\left(i \log \frac{w + i}{w - i}, i \log \frac{w + 1}{w - 1}, \log \frac{w^2 + 1}{w^2 - 1} \right) \tag{33}$$

(using the branch with $\log 1 = 0$), and therefore

$$X(w) = \left(-\arg \frac{w+i}{w-i}, -\arg \frac{w+1}{w-1}, \log \left| \frac{w^2+1}{w^2-1} \right| \right). \tag{34}$$

Let us first restrict our considerations to the set $\{w\colon |w| \le 1, w \ne \pm 1, \pm i\}$. From

$$\frac{w+i}{w-i} = \frac{|w|^2-1}{|w-i|^2} + i\frac{w+\bar{w}}{|w-i|^2}, \quad \frac{w+1}{w-1} = \frac{|w|^2-1}{|w-1|^2} + \frac{\bar{w}-w}{|w-1|^2}$$

we infer that

$$\operatorname{Re} \frac{w+i}{w-i} = \frac{|w|^2-1}{|w-i|^2} \le 0, \quad \operatorname{Re} \frac{w+1}{w-1} = \frac{|w|^2-1}{|w-1|^2} \le 0,$$

whence

$$\frac{\pi}{2} \le \arg \frac{w+i}{w-i}, \arg \frac{w+1}{w-1} \le \frac{3\pi}{2}$$

and therefore

$$-\frac{3\pi}{2} \le x, y \le -\frac{\pi}{2}.$$

We conclude that the mapping $(x(w), y(w))$, formed by the first two components of (34), maps the disk $\{w\colon |w| < 1\}$ one-to-one onto the square $\Omega_{-1,-1}$.

It follows that

$$\cos x = \frac{|w|^2-1}{|w-i|^2}\frac{|w-i|}{|w+i|} = \frac{|w|^2-1}{|w^2+1|},$$
$$\cos y = \frac{|w|^2-1}{|w-1|^2}\frac{|w-1|}{|w+1|} = \frac{|w|^2-1}{|w^2-1|},$$

and therefore

$$\frac{\cos y(w)}{\cos x(w)} = \left| \frac{w^2+1}{w^2-1} \right| = e^{z(w)}.$$

This proves that the representation $X(w)$, $|w| < 1$, defined by (34), parametrizes Scherk's surface (30). Moreover, the mapping $X(w) = (x(w), y(w), z(w))$ has the following properties:

(i) Let $|w| = 1$, $w \ne \pm 1, \pm i$. Setting $w = e^{i\varphi}$, we obtain

$$\left| \frac{w^2+1}{w^2-1} \right| = |\cot \varphi|$$

and therefore

$$z(w) = \log|\cot \varphi|.$$

Furthermore, we have $x(e^{i\varphi}) = -\frac{\pi}{2}$, $y(e^{i\varphi}) = -\frac{3\pi}{2}$ for all $\varphi \in (0, \frac{\pi}{2})$. Hence $X(w)$ maps the open arc $\{e^{i\varphi}\colon 0 < \varphi < \frac{\pi}{2}\}$ of the unit circle $\{|w| = 1\}$ onto the straight line through $(-\frac{\pi}{2}, -\frac{3\pi}{2}, 0)$ which is parallel to the z-axis.

More generally, if $C_1, \dots, C_4$ denote the four open quartercircles on $\{|w| = 1\}$ between the points $1, i, -1, -i$ and if $L_1, \dots, L_4$ are the parallels to the z-axis through the vertices $P_1, \dots, P_4$ of the square $\Omega_{-1,-1}$, then X provides a 1–1-mapping of C_j onto L_j (cf. Figs. 17, 18).

(ii) The rays $w = re^{i\theta}$, $r \geq 0$, $\theta = \frac{\pi}{4}, \frac{3\pi}{4}, \frac{5\pi}{4}, \frac{7\pi}{4}$ satisfy

$$\cos x(w) = \frac{r^2 - 1}{|\pm ir^2 + 1|} = \frac{r^2 - 1}{|\pm ir^2 - 1|} = \cos y(w),$$

whence $z(w) = 0$. Therefore X maps these rays onto straight halflines in the plane $\{z = 0\}$ emanating from the center $(-\pi, -\pi)$ of $\Omega_{-1,-1}$ and passing through $P_1, \dots, P_4$.

(iii) Similarly, the rays $w = re^{i\theta}$, $r \geq 0$, $\theta = 0, \frac{\pi}{2}, \pi, \frac{3\pi}{2}$ are mapped by $(x(w), y(w))$ onto the straight halflines emanating from $(-\pi, -\pi)$ which are parallel to the x-axis or to the y-axis respectively. (In this case, however, the curve $X(w)$ is no longer a straight line since $z(w)$ is nonlinear.)

Applying Schwarz's reflection principle for holomorphic functions and his symmetry principle for minimal surfaces (Section 3.4, Theorem 2(i)), we infer that a reflection of $\{w\colon |w| \leq 1,\ w \neq \pm 1, \pm i\}$ at one of the circular arcs $C_1, \dots, C_4$ corresponds to a reflection of the surface $X(w)$ at one of the straight lines $L_1, \dots, L_4$. More precisely, each of the four quarterdisks $B_1, \dots, B_4$ excised from $\{w\colon |w| < 1\}$ by the u- and v-axes corresponds to one of the four congruent subsquares $Q_1, \dots, Q_4$ of $\Omega_{-1,-1}$ having $(-\pi, -\pi)$ as one of their corner points (cf. Fig. 17), and the representation X maps the mirror image B_j^* of B_j onto the part of Scherk's surface obtained from the graph over the square Q_j by reflection in the straight line L_j.

This way it becomes clear which part of Scherk's surface (30) is parametrized by the representation $X : \mathbb{C} \setminus \{\pm 1, \pm i\} \to \mathbb{R}^3$. If we lift X from the 4-punctured plane to the corresponding universal covering surface, we obtain a parametrization of the full Scherk surface in $\mathbb{R}^3$ sitting as a graph over the black squares of the infinite checkerboard, except for the straight lines parallel to the z-axis through the vertices of the black squares. These lines are also contained in the complete Scherk surface. In addition to these lines of symmetry, we have two further families of parallel lines of symmetry which sit in the plane $\{z = 0\}$ and cross each other at an angle of 90 degrees. As we know, these straight lines are asymptotic lines of the Scherk surface given by $\arg w = \frac{\pi}{4}, \frac{3\pi}{4}, \frac{5\pi}{4}, \frac{7\pi}{4}$ in the representation X. This can also be seen by investigating the quadratic differential $\mathfrak{F}(w)(dw)^2$. Looking at the rays $\{w = re^{i\varphi},\ r \geq 0,\ \varphi = \text{fixed}\}$, we obtain $(dw)^2 = \frac{w^2}{r^2}\, dr^2$, and therefore

$$\mathfrak{F}(w)(dw)^2 = \frac{2w^2\, dr^2}{r^2(1 - w^4)} = \frac{-2\, dr^2}{r^2(w + \frac{1}{w})(w - \frac{1}{w})}.$$

Setting $w = e^{\omega}$, $\operatorname{Re}\omega = \log r, \operatorname{Im}\omega = \varphi$, it follows that

$$\mathfrak{F}(w)(dw)^2 = \frac{-(\frac{1}{2})\, dr^2}{r^2 \sinh\omega \cosh\omega} = \frac{-dr^2}{r^2 \sinh 2\omega}$$

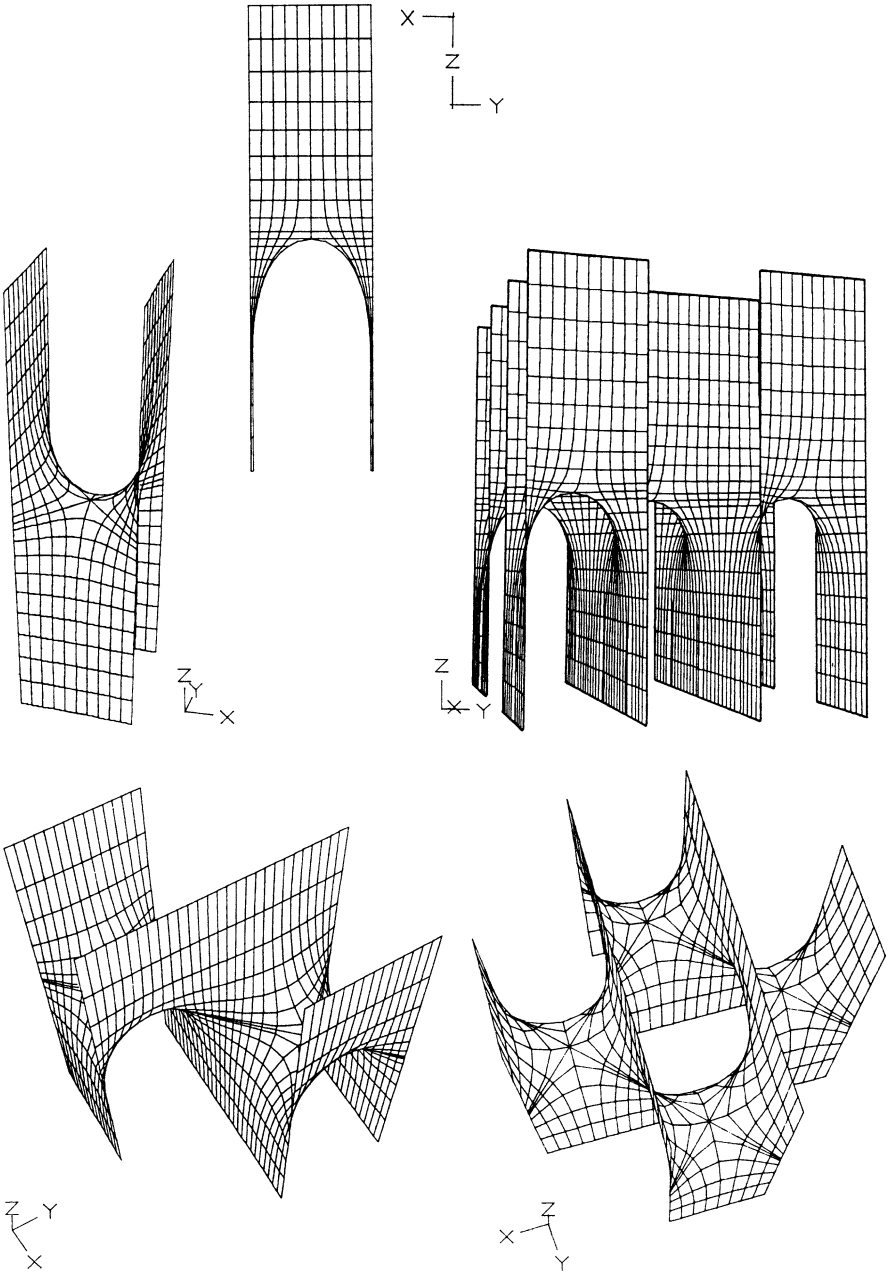

Fig. 16. Scherk's first surface is made up of infinitely many copies of its subset contained in the slab $-\pi/2 < x, y < \pi/2$ of which $|z| \leq 6$ is shown here. Each of the four straight edges of the slab parallel to the z-axis forms a part of the boundary of this fundamental saddle-shaped piece of the surface, and through repeated reflections in these edges Scherk's surface can be built (counter-clockwise from top left)

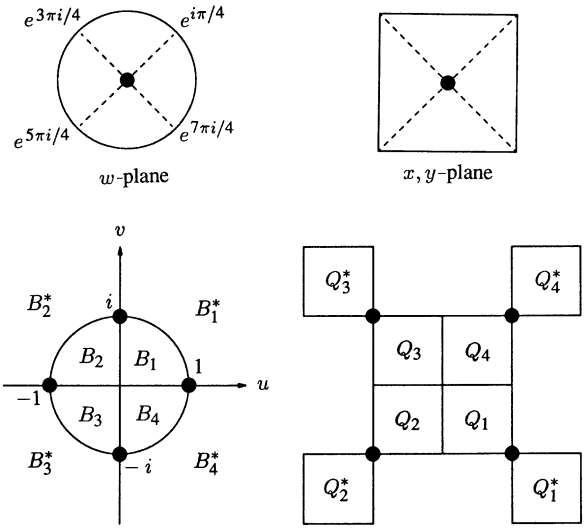

Fig. 17. Construction of Scherk's surface

and

$$\sinh 2\omega = \sinh(2\log r)\cos 2\varphi + i\cosh(2\log r)\sin 2\varphi.$$

Recall now that $\{w = re^{i\varphi}\colon rg \geq 0\}$ is an asymptotic line if $\mathfrak{F}(w)(dw)^2 \in i\mathbb{R}$, and that it is a line of curvature if $\mathfrak{F}(w)(dw)^2 \in \mathbb{R}$. Thus the formula $\varphi = (2k+1)\pi/4$, $k \in \mathbb{Z}$, yields asymptotic lines, and $\varphi = k\pi/2$, $k \in \mathbb{Z}$, provides lines of curvature. As we had already proved, the curves $X(re^{i\varphi}), \varphi = k\pi/2$, are planar curves contained in planes $x = \text{const}$ or $y = \text{const}$ respectively, which turn out to be planes of symmetry for Scherk's surface. This can either be verified by a direct computation or by applying formula (31) of Section 3.3.

If we restrict $X(w)$ to the quarter disk

$$\left\{w = re^{i\varphi}\colon 0 \leq r \leq 1,\ 0 \leq \varphi \leq \frac{\pi}{2},\ w \neq 1, i\right\},$$

we obtain a minimal surface within the Schwarzian chain formed by the straight line $L = \{x = -\frac{\pi}{2}, y = -\frac{3\pi}{2}\}$ and by the planes $E_1 = \{y = -\pi\}$ and $E_2 = \{x = -\pi\}$. Moreover, X meets the two planes perpendicularly in planar lines of curvature which are plane geodesics of X. In other words, this part of X solves the Schwarzian chain problem for the chain $\{L, E_1, E_2\}$. Then the adjoint surface X^* solves the chain problem for a chain $\{E, L_1, L_2\}$ consisting of a plane E and two straight lines L_1 and L_2 (cf. Fig. 19).

We infer that both X and X^* can be built, by reflection, from elementary pieces which are solutions of Schwarzian chain problems. This situation is typ-

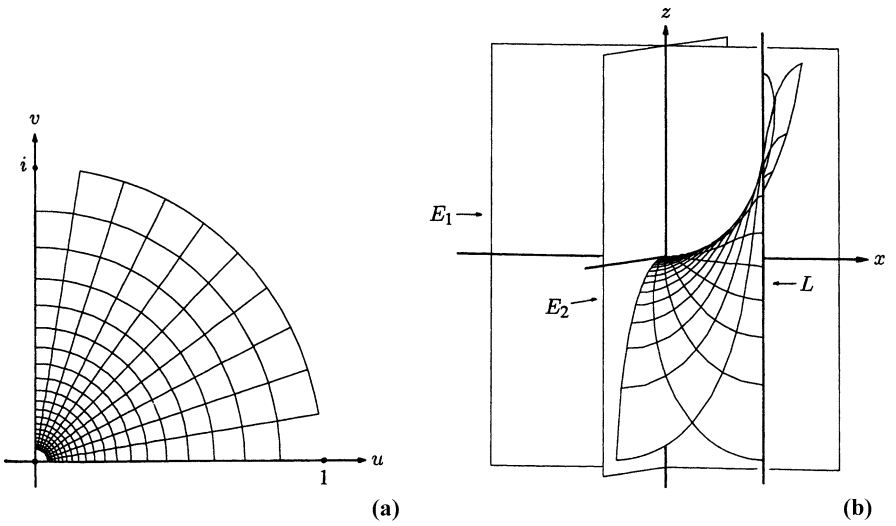

Fig. 18. A conformal representation of Scherk's surface. The part corresponding to a quarter of the unit disk **(a)** solves a Schwarzian chain problem for two perpendicular planes E_1, E_2 and a straight line L parallel to them **(b)**

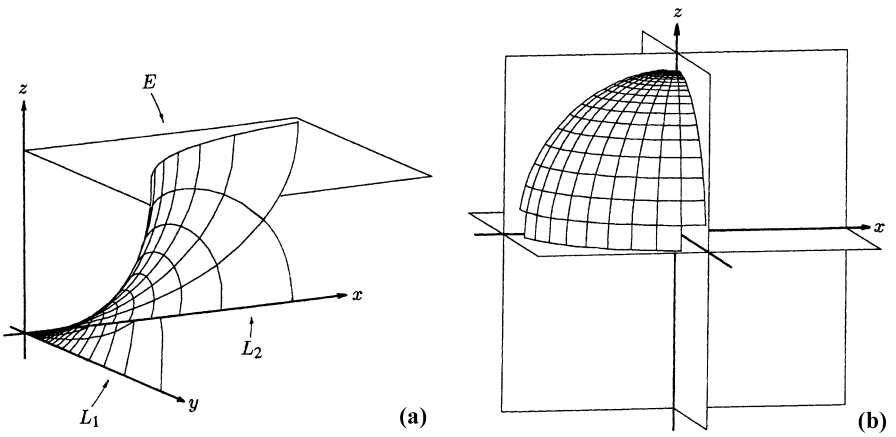

Fig. 19. (a) The corresponding part of the adjoint surface of Scherk's surface solves a Schwarzian chain problem for two straight lines L_1, L_2, and a plane E perpendicular to E_1, E_2, and L respectively; cf. Fig. 18. **(b)** The common (negative of the) Gauss map of these surfaces

ical of all cases where we have sufficiently many planes and lines of symmetry. In our present case, the two elementary pieces are mapped by their spherical image N bijectively onto some spherical triangle bounded by great-circular arcs (cf. Fig. 19).

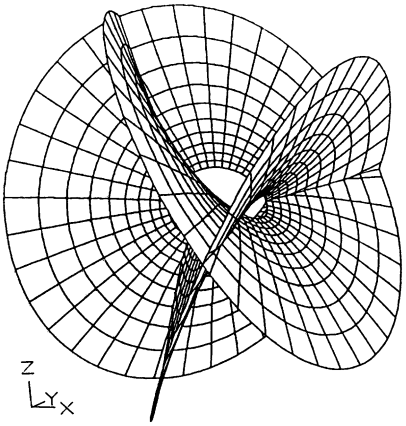

Fig. 20. Part of Henneberg's surface

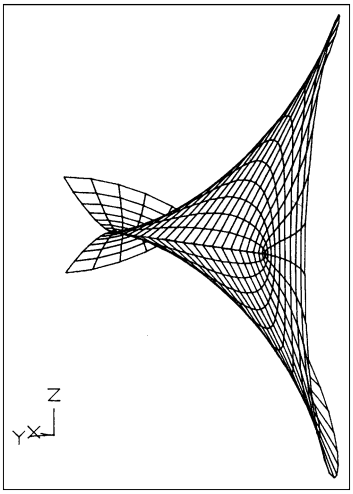

Fig. 21. Henneberg's surface maps the whole v-axis onto a straight line segment of length 2 on the x-axis. (Here we have depicted the part of the surface corresponding to $0 \leq u \leq \pi/5,\ 0 \leq v \leq \pi$.) The end points of these straight line segments are the two branch points on the surface; the limiting tangent plane in one of them is the x, y-plane, in the other one it is the x, z-plane

3.5.7 The Henneberg Surface

Many interesting minimal surfaces are obtained by solving Björling's problem for a given real analytic strip

$$\Sigma = \{(c(t), n(t)) \colon t \in I\}$$

where c is a given regular, real analytic curve and n its principal normal. If we in addition assume that c is contained in a plane E, then the solution X

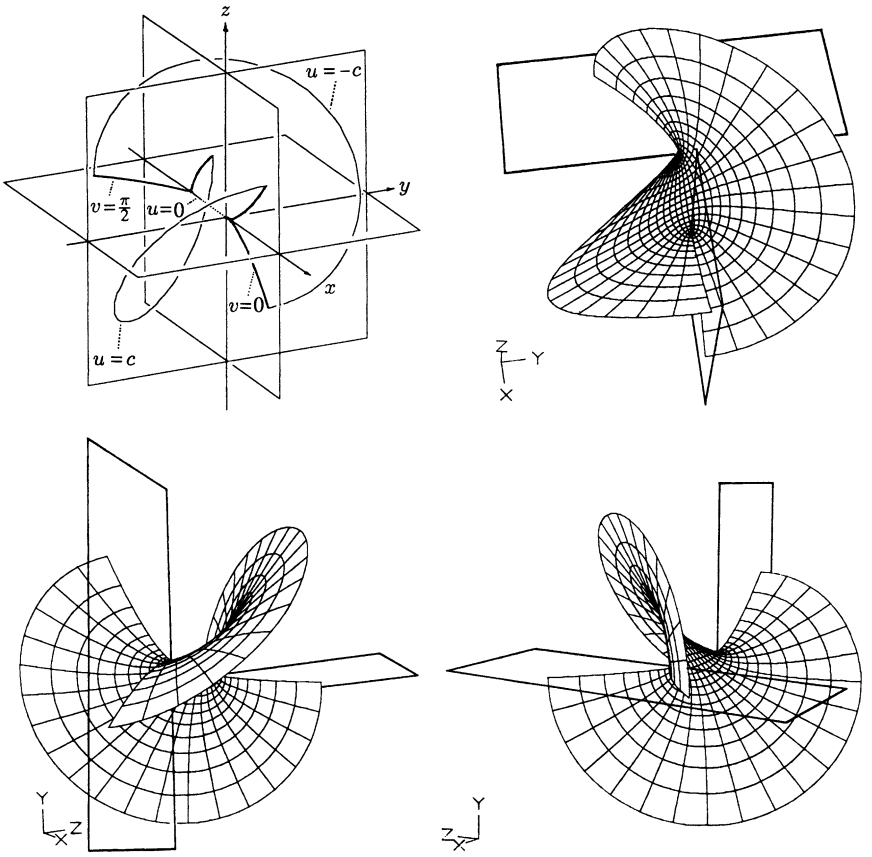

Fig. 22. The curves $v = 0$ and $v = \pi/2$ on Henneberg's surface are Neil parabolas in the x, z-plane and the y, z-plane respectively. For instance the curve $v = 0$ satisfies $2x^3 = 9y^2$, $z = 0$. Along these curves, the surface is perpendicular to the said planes as is shown in our views of Henneberg's surface depicting the parts $|u| \leq 3\pi/10$, $0 \leq v \leq \pi/2$

of Björling's problem for Σ is a minimal surface meeting E perpendicularly at c, and c is a planar geodesic of X as well as a line of curvature.

Let c be given by

$$\begin{aligned} c(t) &= (x(t), 0, z(t)) \\ &= (\cosh(2t) - 1, 0, -\sinh t + \tfrac{1}{3}\sinh(3t)). \end{aligned} \tag{35}$$

From the identities

$$\cosh 2t = 1 + 2\sinh^2 t, \quad \tfrac{1}{3}\sinh(3t) - \sinh t = \tfrac{4}{3}\sinh^3 t$$

we infer that $c(t)$ is a parametrization of *Neil*'s parabola

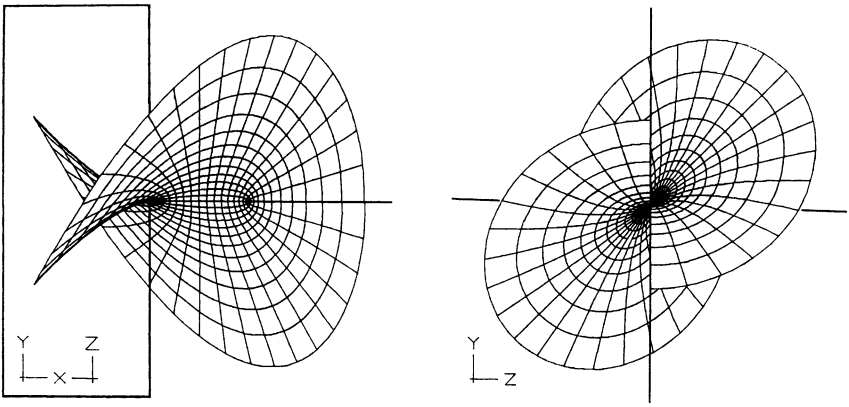

Fig. 23. Parallel projections of the part of Henneberg's surface corresponding to parameter values $|u| \leq 3\pi/10$, $0 \leq v \leq \pi/2$. In particular, one can see that along the two Neil parabolas the surface meets the planes $y = 0$ and $z = 0$ vertically

$$2x^3 = 9z^2 \tag{36}$$

in the plane $\{y = 0\}$. By carrying out Schwarz's construction (cf. formula (1) of Section 3.4), we obtain as solution $X(u, v) = (x(u, v), y(u, v), z(u, v))$ of Björling's problem the *Henneberg surface*

$$\begin{aligned} x &= -1 + \cosh 2u \cos 2v, \\ y &= \sinh u \sin v + \tfrac{1}{3} \sinh 3u \sin 3v, \\ z &= -\sinh u \cos v + \tfrac{1}{3} \sinh 3u \cos 3v. \end{aligned} \tag{37}$$

An isotropic curve $f : \mathbb{C} \to \mathbb{C}^3$ with

$$X(u, v) = \operatorname{Re} f(w), \quad w = u + iv,$$

is given by

$$f(w) = \left(-1 + \cosh 2w, -i \cosh w - \frac{i}{3} \cosh 3w, -\sinh w + \frac{1}{3} \sinh 3w \right). \tag{38}$$

Hence the adjoint surface X^* to X has the form

$$\begin{aligned} x^* &= \sinh 2u \sin 2v, \\ y^* &= -\cosh u \cos v - \tfrac{1}{3} \cosh 3u \cos 3v, \\ z^* &= -\cosh u \sin v + \tfrac{1}{3} \cosh 3u \sin 3v. \end{aligned} \tag{39}$$

The curve $X^*(0, v) = (0, -\frac{4}{3} \cos^3 v, -\frac{4}{3} \sin^3 v)$ lies in the plane $\{x^* = 0\}$ and satisfies

$$y^{*2/3} + z^{*2/3} = (\tfrac{4}{3})^{2/3}, \tag{40}$$

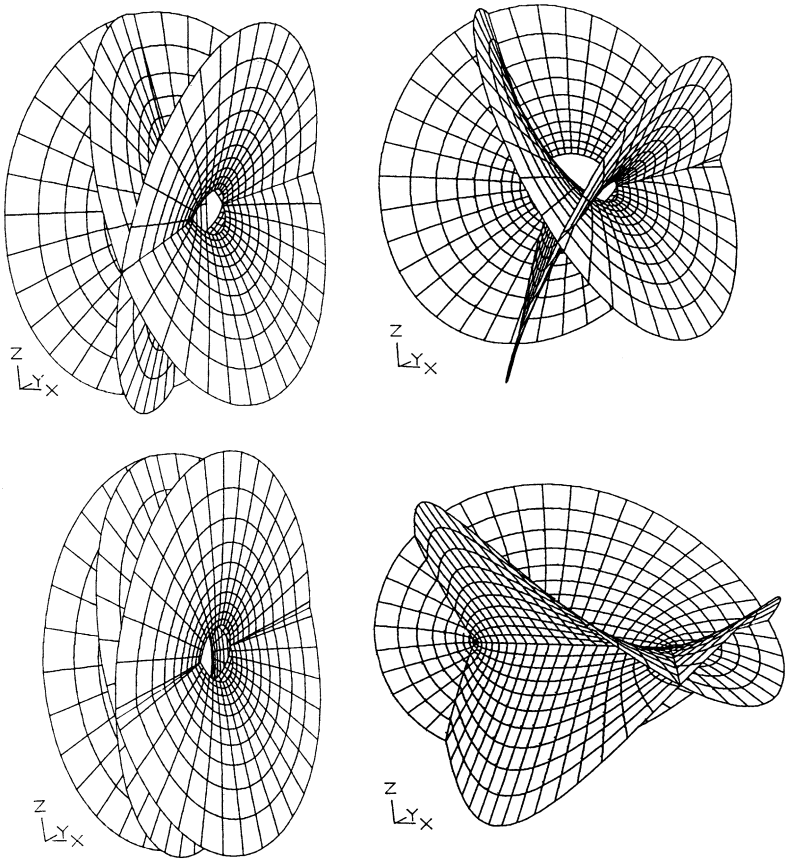

Fig. 24. The parts of Henneberg's surface corresponding to the parameter sets $k\pi/5 \leq |u| \leq (k+1)\pi/5$ for $k = 0, 1, 2, 3$ (counter-clockwise from bottom right) reveal its large scale behavior. Every part of the surface shown in one drawing fits into the hole at the center of the following illustration. In view of the equation $X(-u, v+\pi) = X(u, v)$ each such subset of the surface has two layers glued together and therefore appears to consist of one piece only

that is, the adjoint surface X^* contains an asteroid. This asteroid is a planar geodesic of X^* since $X(0, v) = (-1 + \cos 2v, 0, 0)$ is a straight line and, therefore, a geodesic asymptotic line of X; cf. Section 3.4, Proposition 1. Thus X^* meets the plane $\{x^* = 0\}$ perpendicularly at an asteroid as trace. The straight line $X^*(u, 0) = (0, -\frac{4}{3}\cosh^3 u, 0) = y$-axis is a line of symmetry for X^*.

Remark. Note that in our figures the coordinate function $y^*(u, v)$ in (39) is replaced by $y^* - \frac{4}{3}$. In this way, the origin remains invariant if we bend X into X^* via the associate surfaces to X.

We furthermore note that both $X(u, v)$ and $X^*(u, v)$ are periodic in v with the period 2π.

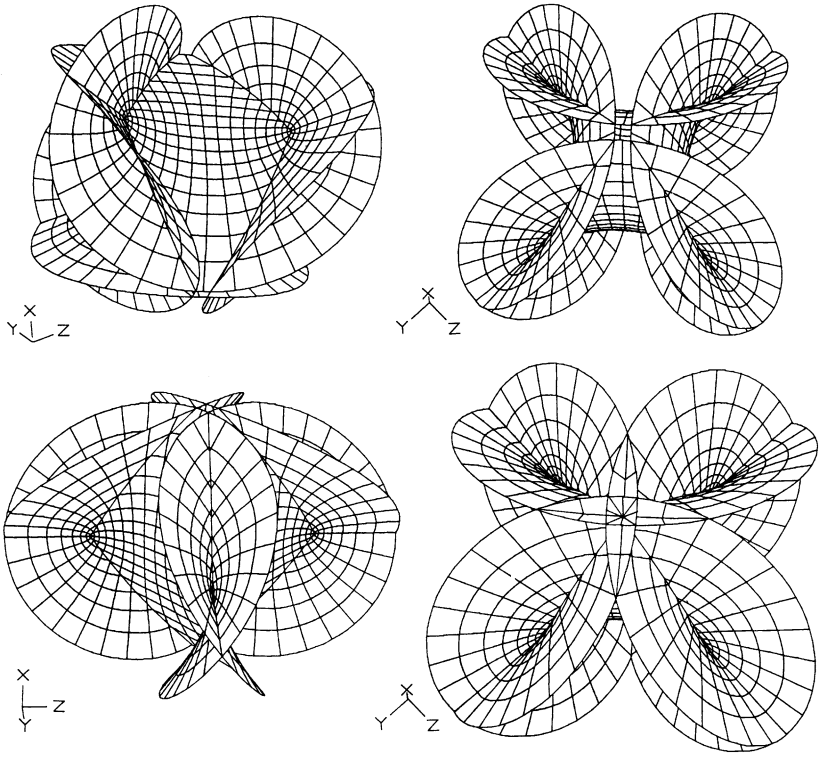

Fig. 25. Some views of parts of the adjoint of Henneberg's surface corresponding to $|u| \leq \pi/5$ and $|u| \leq 9\pi/40$. The adjoint surface encloses a central cavity whose boundary is homeomorphic to the unit sphere and consists of pieces of minimal surfaces. The curve $u = 0$ on the adjoint surface is an asteroid in the y, z-plane connecting the four branch points of the adjoint surface. Along this curve it is orthogonal to the y, z-plane

With the periodicity strip $\{0 \leq v < 2\pi\}$, Henneberg's surface contains four of Neil's parabolas as planar geodesics:

$$
\begin{aligned}
X(u,0) &= \left(-1+\cosh 2u, 0, -\sinh u + \frac{1}{3}\sinh 3u\right),\\
X\left(u,\frac{\pi}{2}\right) &= \left(-1-\cosh 2u, \sinh u - \frac{1}{3}\sinh 3u, 0\right),\\
X(u,\pi) &= \left(-1+\cosh 2u, 0, \sinh u - \frac{1}{3}\sinh 3u\right),\\
X\left(u,\frac{3\pi}{2}\right) &= \left(-1-\cosh 2u, -\sinh u + \frac{1}{3}\sinh 3u, 0\right).
\end{aligned}
\tag{41}
$$

However, only two of these four parabolas are geometrically different. Each of these Neil parabolas is periodically repeated on the surface $X(u, v)$. Hen-

neberg's surface intersects the planes $\{y = 0\}$ and $\{z = 0\}$, respectively, at these Neil parabolas orthogonally.

We also observe that the branch points $w = u + iv$ of X and X^* are given by

$$u = 0, \quad v = \frac{k\pi}{2}, \quad k \in \mathbb{Z}.$$

Moreover, the point set in $\mathbb{R}^3$ represented by $X(u, v)$ is nonorientable. In fact, we easily infer from (39) that

$$X(u, v) = X(-u, v + \pi), \quad X_u(u, v) = -X_u(-u, v + \pi),$$
$$X_v(u, v) = X_v(-u, v + \pi)$$

holds for all $w \in \mathbb{C}$. Let $\omega(t)$, $0 \le t \le 1$, be a smooth path in $\mathbb{C}$, avoiding the branch points $w = \frac{1}{2}ik\pi$, joining some point (u, v) with $(-u, v + \pi)$, say $\omega(t) = (2t-1, \pi(t-\frac{1}{4}))$, $0 \le t \le 1$. Then $\xi(t) := X(\omega(t))$, $0 \le t \le 1$, describes a closed regular loop on Henneberg's surface, but $N(\omega(0)) = -N(\omega(1))$. Thus, if we move around the loop $\xi(t)$ and return to the initial point, the surface normal $N(\omega(0))$ has changed to its opposite. If we slightly thicken the path $\omega(t)$, its image on X will be a Möbius strip (cf. Figs. 27–29). In other words, *Henneberg's surface is a one-sided minimal surface*.

Let us finally mention that the Weierstrass function $\mathfrak{F}(\omega)$ of Henneberg's surface is given by

$$\mathfrak{F}(\omega) = -\frac{i}{2}\left(1 - \frac{1}{\omega^4}\right) \tag{42}$$

if we change the coordinates in $\mathbb{R}^3$ by an orthogonal transformation in such a way that x, y, z become $-z, -y, x$, respectively.

3.5.8 Catalan's Surface

Solving Björling's problem for the strip consisting of the cycloid

$$c(t) = (1 - \cos t, 0, t - \sin t), \quad t \in \mathbb{R} \tag{43}$$

and its principal normal, we obtain *Catalan's surface*

$$X(u, v) = (x(u, v), y(u, v), z(u, v)),$$

given by

$$\begin{aligned} x &= 1 - \cos u \cosh v, \\ y &= 4 \sin \frac{u}{2} \sinh \frac{v}{2}, \\ z &= u - \sin u \cosh v. \end{aligned} \tag{44}$$

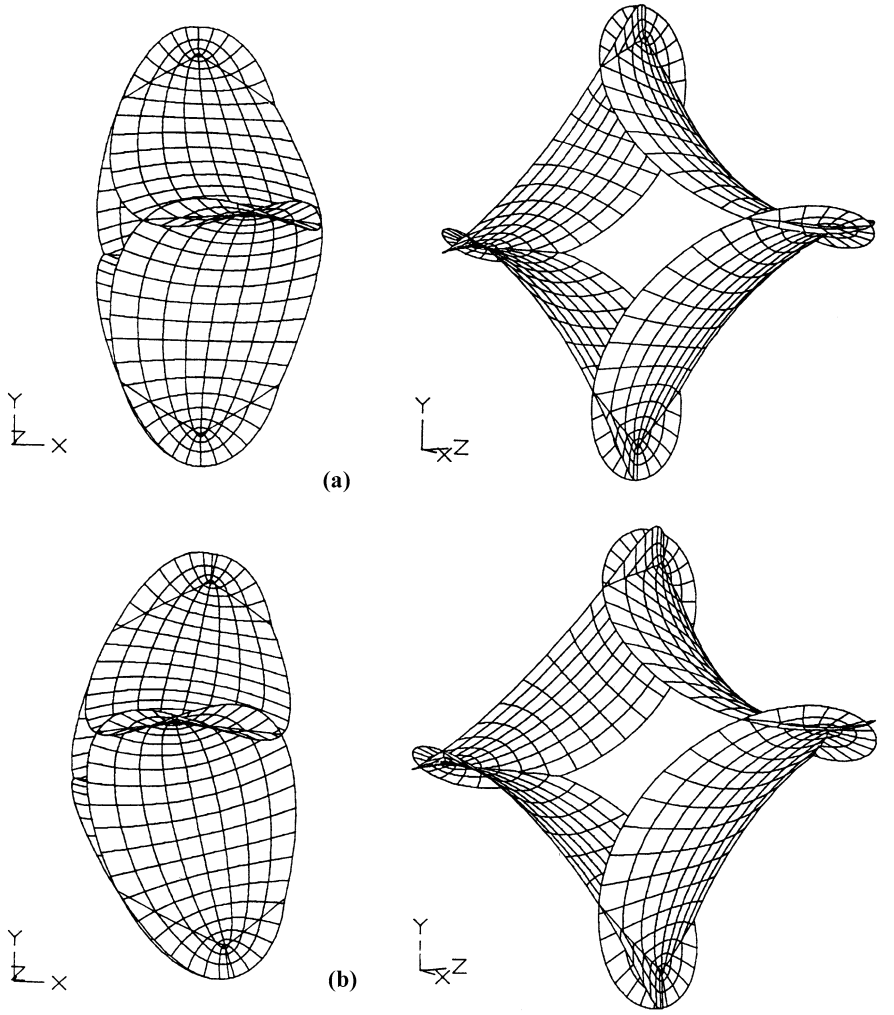

Fig. 26. The bending process for Henneberg's surface into its adjoint surface is so intricate that it is shown here from two different points of view in a long sequence of illustrations. We have arranged for $X^\theta(0) = \text{const}$ for all times θ. The parts of the surfaces depicted here correspond to $|u| \leq \pi/10$; the parameter values θ of the associated surfaces are 90, 75, 60, 45, 30, 20, 10, 0 degrees respectively. The bending process starts with a part of the adjoint surface which has a quadruple symmetry and passes through an asteroid in the y, z-plane connecting the four branch points of the surface, the images of $u = 0, v = 0, \pi/2, \pi, 3\pi/2$. The two boundary curves of this part of Henneberg's adjoint surface alternate between the halfspaces $x > 0$ and $x < 0$. In the bending process from the adjoint surface to Henneberg's surface the branch point opposite the origin moves up to the origin of Henneberg's surface, another branch point. The other two branch points move up to the x, z-plane and simultaneously approach each other until they finally meet on the x-axis. In this process the surface is folded together so that one ends up with the double layer of Henneberg's surface for which half of the surface and two of the four branch points seem to have disappeared

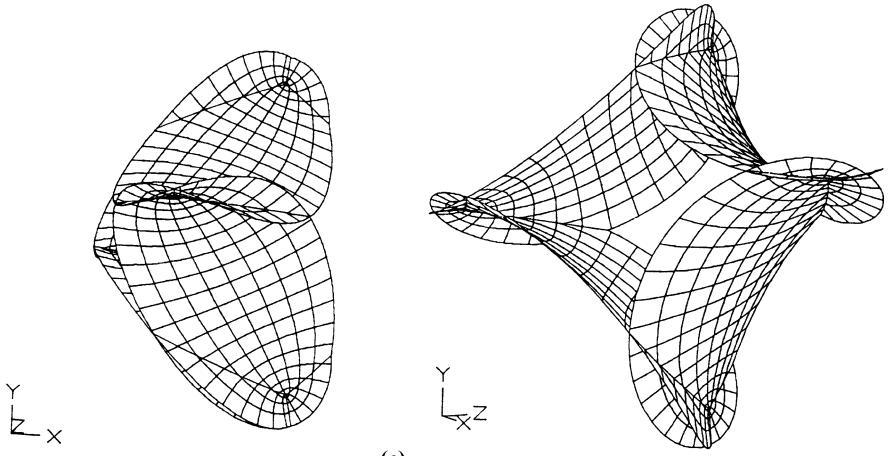

(c)

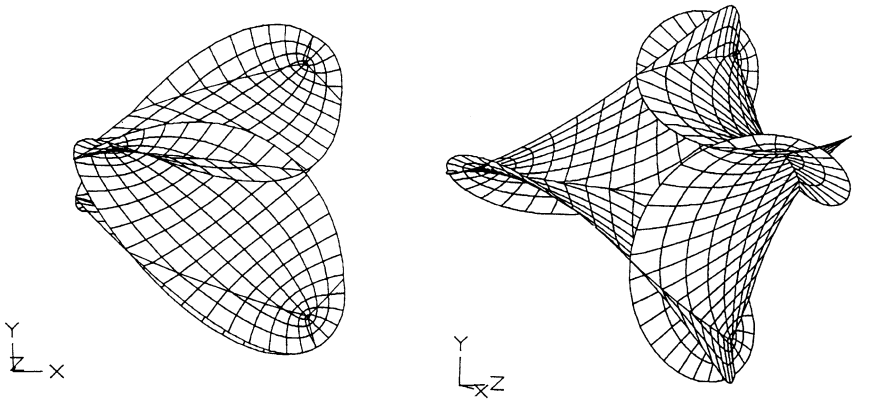

(d)

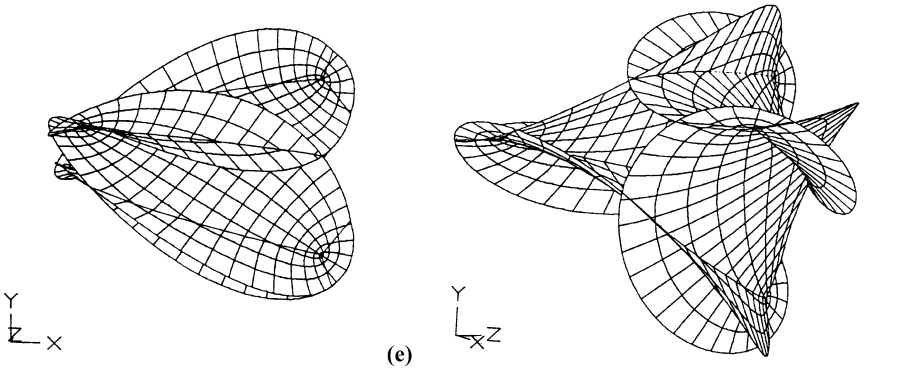

(e)

Fig. 26. c–e.

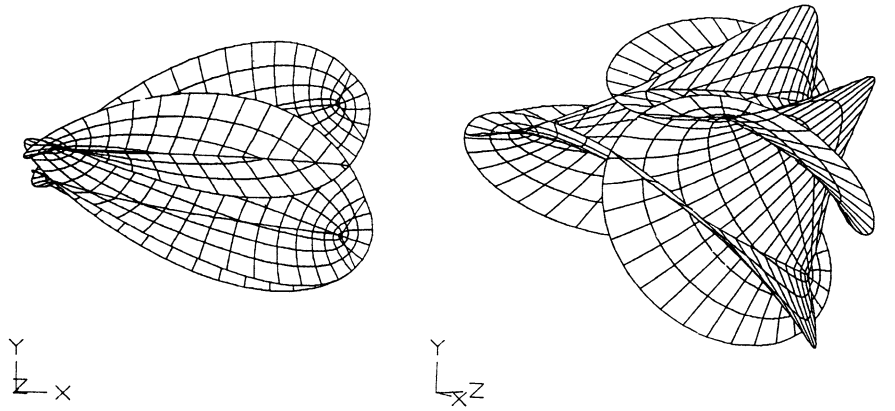

(f)

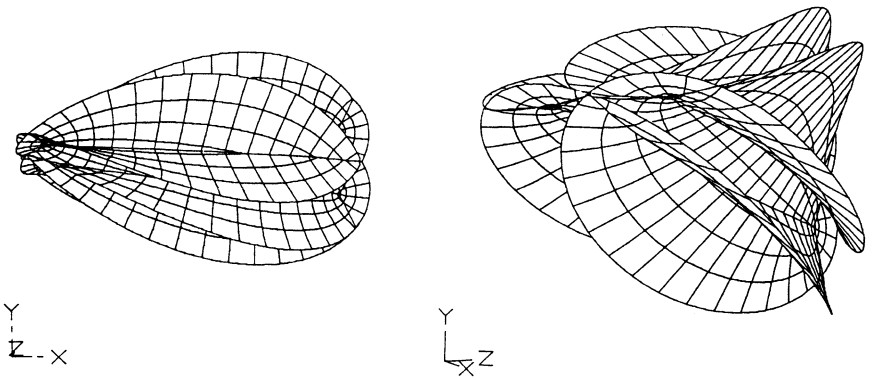

(g)

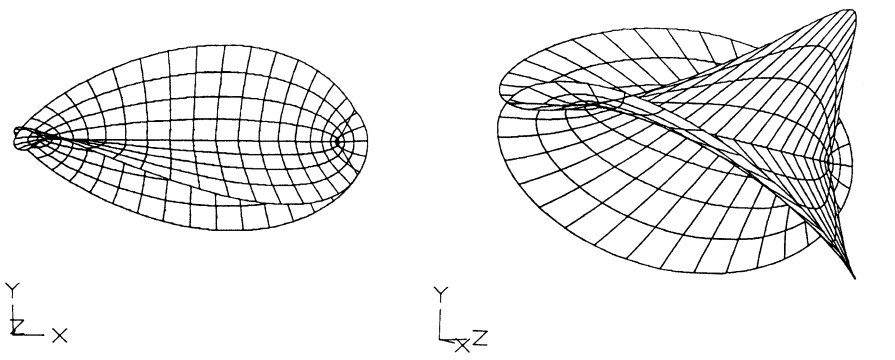

(h)

Fig. 26. f–h.

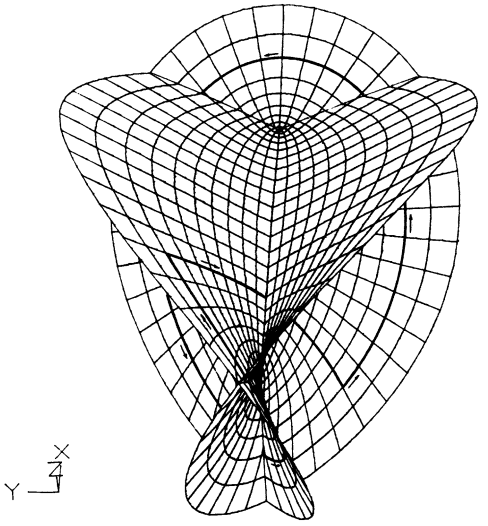

Fig. 27. Henneberg's surface is non-orientable. After a walk on the surface along the emphasized circuit you will find yourself upside down. This results from the equations $X(-u, v+\pi) = X(u, v)$ and $N(-u, v+\pi) = -N(u, v)$ valid on Henneberg's surface

Catalan's surface $X(u, v)$ contains the cycloid $c(u) = X(u, 0)$ as a planar geodesic, and we infer from $X(0, v) = (1 - \cosh v, 0, 0)$ that the x-axis is both an asymptotic line and a line of symmetry for X.

The branch points of X lie on the u-axis and are given by $(u, v) = (2\pi k, 0)$, $k \in \mathbb{Z}$. Their image points $X(u, v)$ are the cusps of the cycloid $c(u) = X(u, 0)$.

Catalan's surface is periodic in the z-direction: The translation in the parameter plane mapping $u + iv$ onto $u + 4\pi + iv$ corresponds to a 4π-shift of the surface along the z-axis.

Catalan's surface also has a number of other symmetries; for example, complex conjugation in the parameter plane (i.e., the map $u + iv$ to $u - iv$) corresponds to a reflection of Catalan's surface across the x, z-plane. Moreover all planes $z = (2k + 1)\pi$, $k \in \mathbb{Z}$, are planes of symmetry of Catalan's surface.

Reflection in the parameter plane across the v-axis (i.e., the map $u + iv$ to $-u + iv$) corresponds to a reflection of the surface across the x-axis. More generally, all lines $y = 0$, $z = 2\pi k$, $k \in \mathbb{Z}$, are lines of symmetry of Catalan's surface.

These properties imply that Catalan's surface is made up of denumerably many copies of the fundamental piece corresponding to

$$0 \leq u \leq 2\pi, \quad 0 \leq v.$$

The part $v = 0$ of the boundary of this fundamental piece lies on the cycloid and is perpendicular to the x, z-plane as the following equation shows:

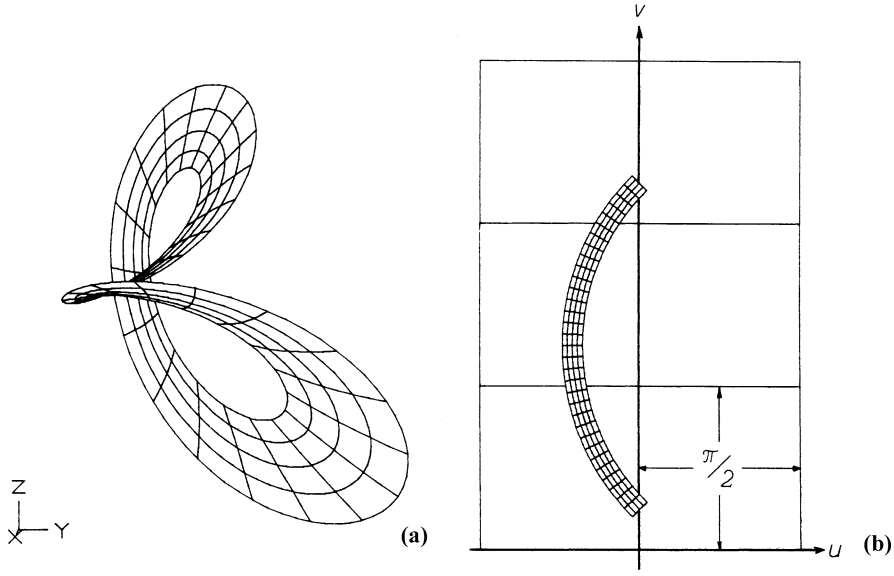

Fig. 28. Henneberg's surface contains a minimal Möbius band with a C^1-smooth boundary curve **(a)**. It corresponds to the quarter of the annulus in the parameter plane shown in **(b)**

$$X_v(u,0) = (0, 2\sin(u/2), 0) \quad \text{for all } u \in \mathbb{R}.$$

The other two boundaries of this fundamental piece, $u = 0$ and $u = 2\pi$ lie on the x-axis and the straight line $y = 0$, $z = 2\pi$ parallel to it respectively. Repeated reflections across the straight lines on the boundary and across the x, z-plane will then build up the complete surface as shown in our illustrations.

Consider now the rolling wheel in the plane $\{y = 0\}$ which is generating the cycloid (43). If we introduce the complex coordinates $\xi = x + iz$ in the x, z-plane, the center of the wheel is described by $\xi = 1 + iu$, and the cycloid is given by $\xi = 1 + iu - e^{iu}$ where u denotes the rotation angle of the rolling wheel which generates the cycloid. Let $R := \{(1 + iu) - (\rho + 1)e^{iu} : \rho > 0\}$ be the ray on the straight line through the centerpoint $1 + iu$ and the point $c(u) := 1 + iu - e^{iu}$ on the cycloid, emanating at $c(u)$ and pointing in direction of $-e^{iu}$.

For fixed $u \in \mathbb{R}$, the projection of $X(u, v)$ onto the plane $\{y = 0\}$ is given by

$$\xi = 1 + iu - e^{iu}\cosh v.$$

Hence the curve $X(u, v), v \in \mathbb{R}$, lies in the plane E that is perpendicular to the x, z-plane and contains the ray R. Using Cartesian coordinates ρ and y in E, we can describe $X(u, \cdot)$ by the formulas

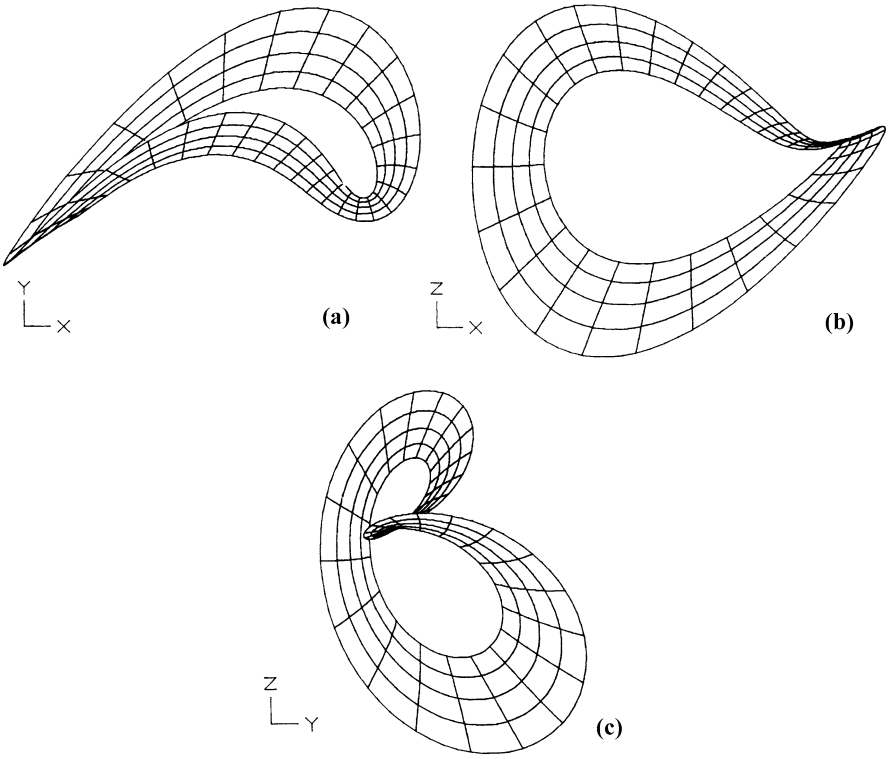

Fig. 29. The projections onto the three coordinate planes convey the shape of this Möbius band. Look at the x, y-projection **(a)** of the Möbius band, then turn it around the x-axis to obtain the x, z-projection **(b)**. Finally rotate it around the z-axis to end up with the y, z-projection **(c)**

$$\begin{aligned} \rho &= \cosh v - 1 = 2\sinh^2 \frac{v}{2}, \\ y &= 4 \sin \frac{u}{2} \sinh \frac{v}{2} \end{aligned} \tag{45}$$

with $v \in \mathbb{R}$. Hence $X(u, \cdot)$ yields a parametrization of the parabola

$$y^2 = a\rho \tag{46}$$

with $a := 8 \sin^2 \frac{u}{2}$ in the plane E. Thus Catalan's surface X is swept out by a one-parameter family of parabolas $\mathcal{P}(u), u \in \mathbb{R}$. The vertex of $\mathcal{P}(u)$ moves on the cycloid $c(u)$, and the plane $E(u)$ of $\mathcal{P}(u)$ intersects the x, z-plane perpendicularly and contains the straight line through $c(u)$ and the center $\xi = 1 + iu$ of the rolling wheel.

From (3) and (44) we infer that

$$X(u, v) = \operatorname{Re} f(w), \quad w = u + iv,$$

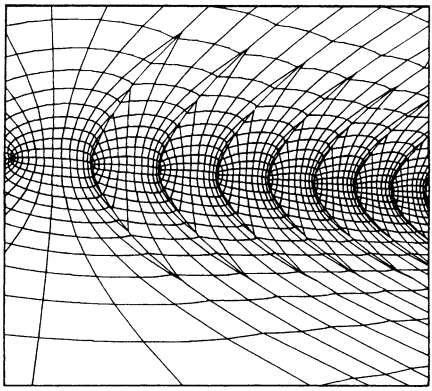

Fig. 30. Catalan's surface as seen from the halfplane $y = 0$, $x > 0$. All points of Catalan's surface remain outside the parabolic cylinder $8(x-2) > y^2$, but the curves $v = (2k+1)\pi$ on Catalan's surface lie on its boundary

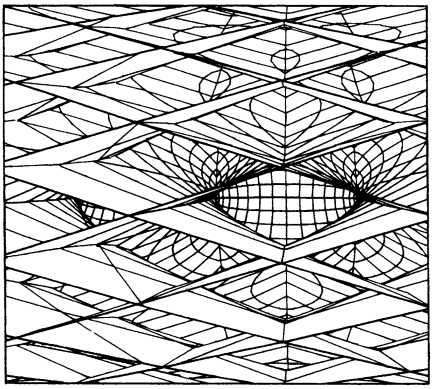

Fig. 31. The view of Catalan's surface from the opposite halfplane $y = 0$, $x < 0$ is quite different. The surface partitions the halfspace $x < 0$ into boxes of rhomboid cross sections

where $f : \mathbb{C} \to \mathbb{C}^3$ is an isotropic curve given by

$$f(w) = \left(1 - \cosh(iw), 4i\cosh\left(\frac{iw}{2}\right), w + i\sinh(iw)\right). \tag{47}$$

This implies that the adjoint surface $X^*(u,v)$ of Catalan's surface has the representation

$$\begin{aligned} x^* &= \sin u \sinh v, \\ y^* &= 4\cos\frac{u}{2}\cosh\frac{v}{2}, \\ z^* &= v - \cos u \sinh v \end{aligned} \tag{48}$$

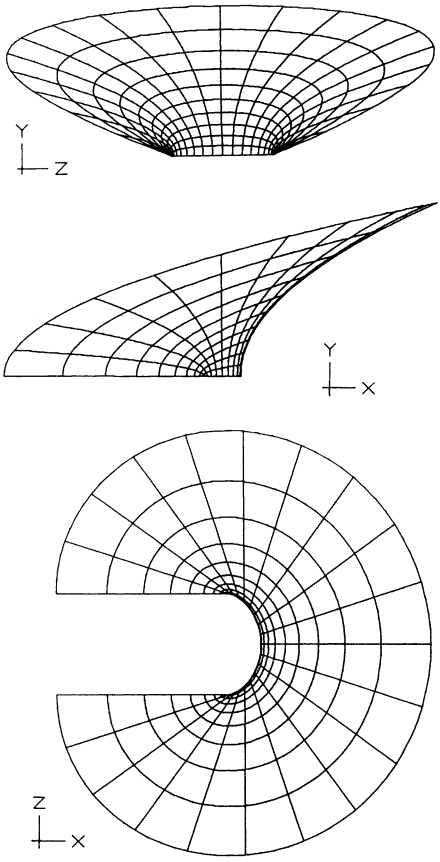

Fig. 32. Catalan's surface is made up of infinitely many copies congruent to its fundamental subset defined by $0 \le u \le 2\pi$, $0 \le v$ and shown here (for $v \le \pi$). Every curve $u =$ constant defines a parabola on the surface having its apex on the cycloid $v = 0$ along which the surface is perpendicular to the x, z-plane. The parabolas $u = 0$ and $u = 2\pi$ degenerate into straight lines, and $z = \pi$ is another plane of symmetry of the surface

with the y-axis as line of symmetry and the y, z-plane as plane of symmetry. The adjoint surface X^* intersects the plane $\{x = 0\}$ perpendicularly along the curve

$$X^*(0, v) = \left(0, 4\cosh\frac{v}{2}, v - \sinh v\right).$$

Points (x, y, z) on Catalan's surface satisfy the following inequality

$$8(x - 2) \le y^2,$$

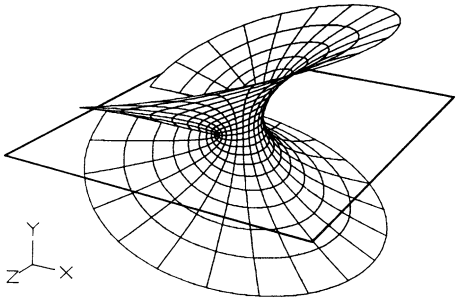

Fig. 33. Reflecting the fundamental piece defined by $0 \leq u \leq 2\pi$, $0 \leq v$ in the x, z-plane yields the part $0 \leq u \leq 2\pi$ of Catalan's surface. According to the reflection principle every minimal surface which is perpendicular to a plane along a part of its boundary can be extended by reflection as a minimal surface (Section 4.8)

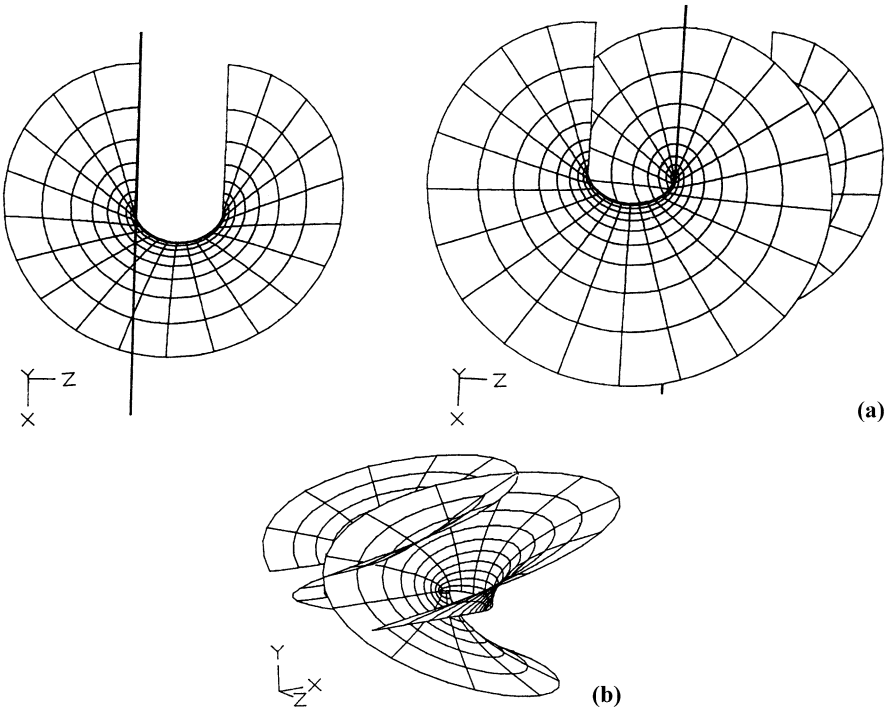

Fig. 34. (a) The part of Catalan's surface obtained by reflecting the fundamental piece $0 \leq u \leq 2\pi$, $v \geq 0$ in the x-axis. **(b)** Repetition of this reflection

i.e., the surface avoids the parabolic cylinder defined by this inequality. This is illustrated in Figs. 30 and 32; note also that the curves $u = (2k + 1)\pi$, $k \in \mathbb{Z}$, lie on the boundary of the cylinder.

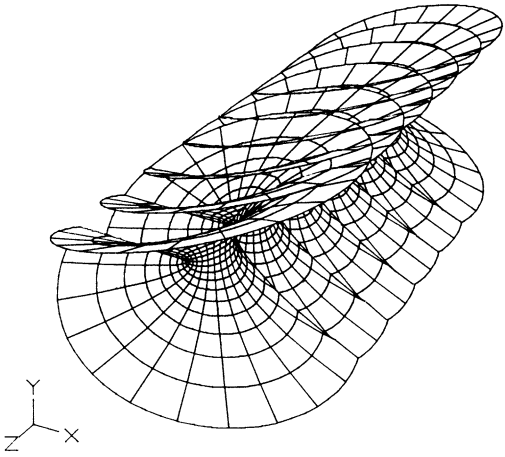

Fig. 35. Starting from the fundamental piece, the complete Catalan surface can be built by repeated reflections across straight lines and the z, x-plane

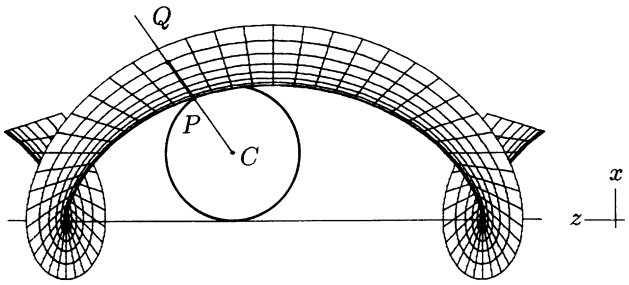

Fig. 36. Construction of Catalan's surface via a Björling problem corresponding to cycloid

The estimate can be obtained by using the following formulas for the trigonometric and hyperbolic functions:

$$\begin{aligned} y^2 &= 16\sin^2(u/2)\sinh^2(v/2) = 4(1-\cos(u))(\cosh(v)-1) \\ &= 4(-1-\cos(u)\cosh(v)+\cosh(v)+\cos(u)), \\ x-2 &= -1-\cos(u)\cosh(v), \\ \cosh(v)\cos(u) &\geq -\cos(u)\cosh(v)+\cos(u) \\ &\geq -\cos(u)\cosh(v)-1 = x-2, \end{aligned}$$

which clearly imply $8(x-2) \leq y^2$.

Finally we note that, except for a suitable orthogonal transformation of the Cartesian coordinates in $\mathbb{R}^3$, the Weierstrass function of Catalan's surface is of the form

$$\mathfrak{F}(\omega) = i\left(\frac{1}{\omega} - \frac{1}{\omega^3}\right).$$

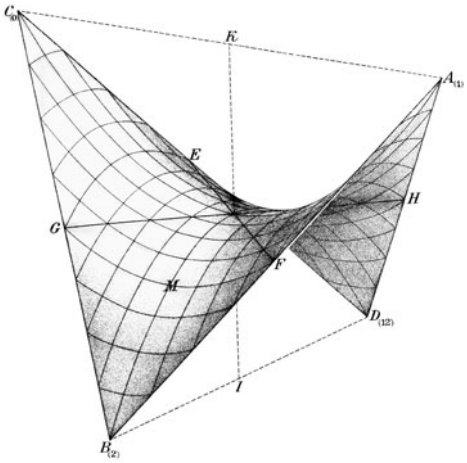

Fig. 37. Schwarz's surface. Lithograph by H.A. Schwarz

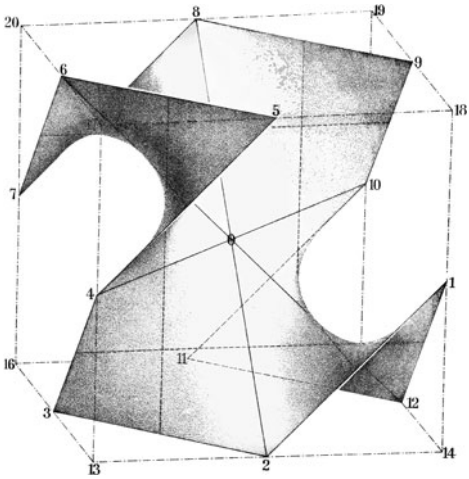

Fig. 38. Extension of Schwarz's surface by reflection. Lithograph by H.A. Schwarz

Remark. In our figures, we have instead of (48) used a translated surface, given by

$$y^* = 4\cos\frac{u}{2}\cosh\frac{v}{2} - 4. \tag{48'}$$

Then the origin is kept fixed if one deforms X into X^*.

3.5.9 Schwarz's Surface

This celebrated surface is a disk-type minimal surface $X : B \to \mathbb{R}^3$ which is bounded by a (nonplanar) quadrilateral Γ, see Fig. 37. By the general

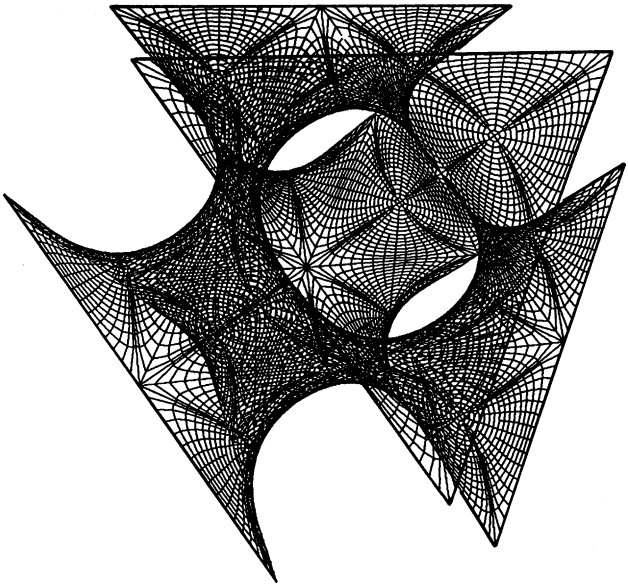

Fig. 39. A part of Schwarz's periodic surface. Courtesy of O. Wohlrab

theory to be developed in the following, there is exactly one such minimal surface which, by the reflection principle, can be continued without limit as a minimal surface if we reflect it at its boundary edges. If the edges are equally long and if the angles at the vertices are $\pi/3$, then we obtain an embedded triply-periodic minimal surface. Its adjoint surface is also triply periodic and embedded. It can be obtained by spanning a symmetric quadrilateral with two angles of $\pi/2$ and two angles of $\pi/3$. Of course, H.A. Schwarz found these two surfaces explicitly (by means of hyperelliptic integrals using the Weierstrass representation formula Section 3.3 (27) with the Weierstrass function

$$\mathfrak{F}(\omega) = \frac{\kappa}{\sqrt{1 - 14\omega^4 + \omega^8}}$$

where κ is a suitable positive constant). As this representation was carefully described by Schwarz himself (see [2], vol. 1) as well as by Bianchi [1] and Nitsche [28,37], we refer the reader to these sources for the study of the classical approach.

3.6 Complete Minimal Surfaces

In this section we want to consider *global minimal* surfaces $\mathcal{X} : M \to \mathbb{R}^3$ in $\mathbb{R}^3$ defined on Riemann surfaces M without boundary.

Let us assume that M is a two-dimensional manifold without boundary which is endowed with a *complex* (or: *conformal*) *structure* c. Such a structure

c is an atlas of charts $\varphi : G \to \mathbb{R}^2$ with the property that the transition map $\varphi \circ \tilde{\varphi}^{-1}$ between any two charts $\varphi : G \to \mathbb{R}^2$ and $\tilde{\varphi} : \tilde{G} \to \mathbb{R}^2$ is a biholomorphic mapping of $\tilde{\varphi}(G \cap \tilde{G})$ onto $\varphi(G \cap \tilde{G})$. A pair (M, c) consisting of a two-manifold M and of a complex structure c is called a *Riemann surface.*

A mapping $\mathfrak{X} : M \to \mathbb{R}^3$ is *harmonic* if, for any chart $\varphi : G \to \mathbb{R}^2$, the mapping $X := \mathfrak{X} \circ \varphi^{-1}$ is harmonic. Since the composition $X \circ \chi$ of a harmonic mapping X with a conformal (i.e., biholomorphic) mapping χ is also harmonic, this definition of harmonicity of $\mathfrak{X}$ is compatible with the complex structure c.

Secondly, we call a nonconstant mapping $\mathfrak{X} : M \to \mathbb{R}^3$ a *minimal surface* with the parameter domain M if, for any chart $\varphi : G \to \mathbb{R}^2$, the mapping $X := \mathfrak{X} \circ \varphi^{-1}$ is a minimal surface in the sense of Section 2.6. That is, for any chart $\{G, \varphi\}$ of the structure c, the map $X(w) = X(u, v)$ defined by $X := \mathfrak{X} \circ \varphi^{-1}$ satisfies

$$\Delta X = 0 \tag{1}$$

and

$$|X_u|^2 = |X_v|^2, \quad \langle X_u, X_v \rangle = 0. \tag{2}$$

Again this definition of a minimal surface is compatible with the conformal structure c of M. This can be seen as follows. The map $\Phi(w) = X_u(u, v) - iX_v(u, v), w = u + iv$, is holomorphic if and only if X is harmonic. Moreover, if $\Phi = (\Phi_1, \Phi_2, \Phi_3)$ is holomorphic, then also

$$\langle \Phi, \Phi \rangle = \Phi_1^2 + \Phi_2^2 + \Phi_3^2$$

is holomorphic, i.e. $\langle X_w, X_w \rangle \, dw^2$ is a holomorphic quadratic differential. Thus, for any harmonic X, the equations (2) are equivalent to the fact that the holomorphic quadratic differential $\langle X_w, X_w \rangle \, dw^2$ vanishes, and we see that the equations (1) and (2) are preserved with respect to biholomorphic changes of the variables $w = u + iv$. Hence the definition of minimality is compatible with the structure c.

A minimal surface $\mathfrak{X} : M \to \mathbb{R}^3$ defined on a Riemann surface M as parameter domain will be called a *global minimal surface*.

A global minimal surface $\mathfrak{X} : M \to \mathbb{R}^3$ is said to be regular if, for any chart $\{G, \varphi\}$ of M, the surface $X = \mathfrak{X} \circ \varphi^{-1}$ is regular. Moreover, $p_0 \in M$ is said to be a *branch point* of $\mathfrak{X}$ if, for some chart $\{G, \varphi\}$ satisfying $p_0 \in G$, the point $w_0 = \varphi(p_0)$ is a branch point of $X = \mathfrak{X} \circ \varphi^{-1}$. It can easily be seen that this definition of a branch point holds for any chart $\{G, \varphi\}$ with $p_0 \in G$ if it holds for a single one, and the order of the branch point is independent of the chart.

The Gauss map $\mathfrak{N} : M \to S^2$ of a global minimal surface $\mathfrak{X} : M \to \mathbb{R}^3$ is defined by means of the charts $\{G, \varphi\}$ of the conformal structure c of M by

$$\mathfrak{N}(\omega) := N(\varphi(\omega))$$

where

$$N = |X_u \wedge X_v|^{-1} X_u \wedge X_v$$

is the surface normal of $X = \mathfrak{X} \circ \varphi^{-1}$. This definition of $\mathcal{N}$ holds in the classical sense if $\mathfrak{X}$ is free of branch points. Otherwise, if p_0 is a branch point of $\mathfrak{X}$ and $w_0 = \varphi(p_0)$, then $N(w_0)$ is defined by $N(w_0) = \lim_{w \to w_0} N(w)$, and correspondingly,

$$\mathcal{N}(p_0) = \lim_{\omega \to p_0} \mathcal{N}(\omega).$$

This definition of $\mathcal{N}$ is compatible with the structure c of M since the transition maps $\varphi \circ \tilde{\varphi}^{-1}$ between charts are biholomorphic and therefore orientation preserving.

Remark. If one admits parameter domains (M, c) with a structure c where the transition maps $\psi := \varphi \circ \tilde{\varphi}^{-1}$ are not necessarily holomorphic but either holomorphic or antiholomorphic (i.e., either ψ or $\bar{\psi}$ is holomorphic), then we include also *nonorientable parameter domains* such as the Klein bottle into the class of admissible parameter domains of minimal surfaces. For instance, the minimal surface $X : \mathbb{C} \to \mathbb{R}^3$ defined by

$$\begin{aligned} X(w) &:= \operatorname{Re}\left[\frac{i}{p(w)}(w^5 - w), -i(w^5 + w), \frac{2}{3}(w^6 + 1)\right] + \left(0, 0, \frac{1}{2}\right), \\ p(w) &:= w^6 + \sqrt{5}\, w^3 - 1, \quad w \in \mathbb{C}, \end{aligned}$$

is a minimal surface of the topological type of the projective plane (see Pinkall [1]). Its inversion in S^2, given by $Z(w) := |X(w)|^{-2} X(w)$, is a Willmore surface, i.e., a critical point of the functional $\int H^2\, dA$ (see Fig. 1).

Again it makes sense to define minimal surfaces $\mathfrak{X} : M \to \mathbb{R}^3$ by means of equations (1) and (2) which are to be satisfied by $X = \mathfrak{X} \circ \varphi^{-1}$ for any chart $\{U, \varphi\}$ of the structure c. In this way we are led to nonorientable minimal surfaces such as the Henneberg surface. However, we can always pass from M to the orientable double-cover $\tilde{M}$ of M, and $\mathfrak{X}$ can be lifted as a minimal surface from M to $\tilde{M}$. Thus nothing is lost if we assume in the sequel that M is orientable.

From now on we want to restrict our attention to regular and orientable global minimal surfaces $\mathfrak{X} : M \to \mathbb{R}^3$. On the parameter domain M of such a manifold we can introduce a Riemannian metric $\langle\!\langle \xi, \eta \rangle\!\rangle$ as pull-back of the Euclidean metric of $\mathbb{R}^3$ to M via the mapping $\mathfrak{X}$. Introducing local coordinates $w = u^1 + iu^2 = \varphi(\omega)$ by means of a chart $\{G, \varphi\}$, the *induced metric* $\langle\!\langle \xi, \eta \rangle\!\rangle$ is given by

$$\langle\!\langle \xi, \eta \rangle\!\rangle = \langle \xi^\alpha X_{u^\alpha}, \eta^\beta X_{u^\beta} \rangle \tag{3}$$

for $\xi = (\xi^1, \xi^2), \eta = (\eta^1, \eta^2)$, where $X = \mathfrak{X} \circ \varphi^{-1}$. In other words, we have

$$\langle\!\langle \xi, \eta \rangle\!\rangle = g_{\alpha\beta}(w) \xi^\alpha \eta^\beta \tag{4}$$

where $g_{\alpha\beta}(w) = \langle X_{u^\alpha}(w), X_{u^\beta}(w) \rangle$.

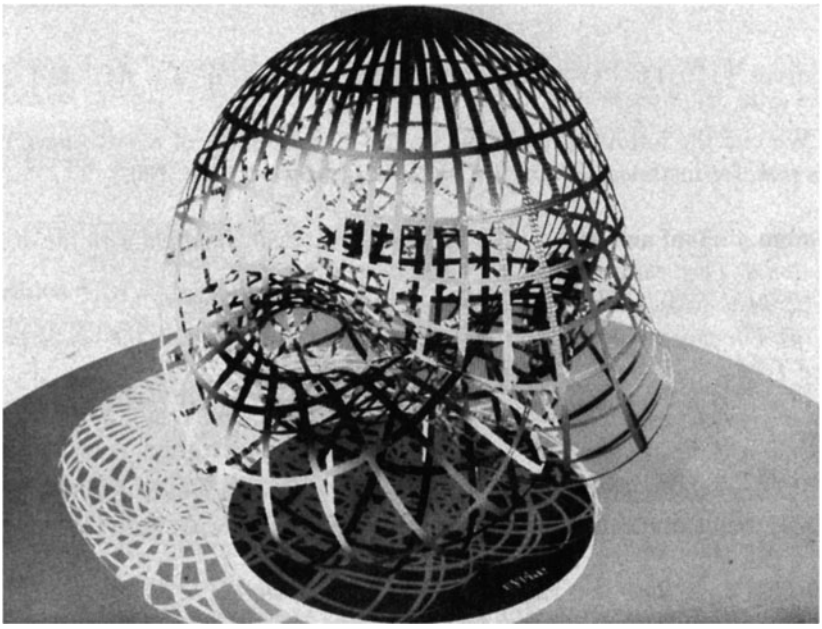

Fig. 1. A photograph of a model of the Wilmore surface $Z : \mathbb{C} \to \mathbb{R}^3$ which is exhibited at the entrance to the library of the Mathematics Research Institute Oberwolfach (Black Forest). Since $Z(\mathbb{C})$ is topologically a projective plane, the surface Z is a realization of a Boy surface (see Hilbert and Cohn-Vossen [1], pp. 276–283). Courtesy of Archive of Mathematisches Forschungsinstitut Oberwolfach

Definition 1. *A regular global minimal surface $\mathcal{X} : M \to \mathbb{R}^3$ is said to be complete if its parameter domain M endowed with the induced Riemannian metric $\langle\langle \cdot, \cdot \rangle\rangle$ of $\mathbb{R}^3$ via $\mathcal{X}$ is a complete Riemannian manifold.*

We recall that a Riemannian manifold M with a metric $\langle\langle \cdot, \cdot \rangle\rangle$ is said to be complete if it is a complete metric space with respect to its distance function $d(p, q)$. Here the distance $d(p, q)$ of any two points p, q of M is defined as infimum of the lengths

$$l(\gamma) = \int_0^1 \|\dot{\gamma}(t)\| \, dt$$

of curves $\gamma : [0, 1] \to M$ connecting p, q, i.e., $p = \gamma(0)$, $q = \gamma(1)$, and $\|\dot{\gamma}\| = \langle\langle \dot{\gamma}, \dot{\gamma} \rangle\rangle^{1/2}$.

We cite the following criterion for the completeness of Riemannian manifolds (see, for instance, Gromoll, Klingenberg, and Meyer [1], p. 166):

Theorem of Hopf and Rinow. *Let M be a Riemannian manifold with the distance function d. Then the following statements are equivalent*:

(i) *M is complete, i.e. (M, d) is a complete metric space.*

(ii) *For any $p \in M$, the exponential map $\exp_p$ is defined on the whole tangent space T_pM.*

(iii) *If G is a bounded subset of the metric space (M, d), then its closure $\bar{G}$ is compact.*

In order to formulate another condition for completeness that will be particularly useful for the discussion of global minimal surfaces, we need the following

Definition 2. *A* **divergent path** *on a Riemannian manifold M is a continuous curve $\gamma : [0, 1] \to M$ such that, for any compact subset K of M, there is a number $t_0(K)$ such that $\gamma(t)$ is contained in the complement $M \setminus K$ for all $t > t_0(K)$.*

In other words: A divergent path on M is a ray that ultimately leaves every compact subset of M.

Proposition 1. *A Riemannian manifold M is complete if and only if every divergent C^1-path $\gamma : [0, 1) \to M$ has infinite length.*

Proof. (i) If M is complete and $\gamma : [0, 1) \to M$ is an arbitrary C^1-path of finite length, then $\gamma([0, 1))$ is bounded. Consequently, the closure of $\gamma([0, 1))$ is compact by the Hopf–Rinow theorem, and therefore γ is not divergent.

(ii) Conversely, if M is not complete, then we can find a geodesic $\gamma : [0, 1) \to M$ having $[0, 1)$ as its maximal domain of definition (to the right). The curve γ is divergent since otherwise $\lim_{t\to 1-0} \gamma(t)$ would exist and $\gamma(t)$ could be extended beyond $t = 1$. Since γ is a geodesic, its speed $\|\dot{\gamma}(t)\|$ is constant for all $t \in [0, 1)$ and therefore the length $l(\gamma) = \int_0^1 \|\dot{\gamma}(t)\|\, dt$ of γ is finite. □

Let us now consider a global minimal surface $\mathfrak{X} : M \to \mathbb{R}^3$ which is not necessarily regular. Then $\mathfrak{X}$ may have isolated singularities on M, branch points, and its parameter domain M can be viewed as a generalized Riemannian 2-manifold with isolated singular points whose metric tensor $(g_{\alpha\beta}(w))$ is defined as before by $g_{\alpha\beta}(w) = \langle X_{u^\alpha}(w), X_{u^\beta}(w)\rangle$, $X = \mathfrak{X} \circ \varphi^{-1}$, for any chart $\{G, \varphi\}$ of the complex structure c of M. The only difference is now that $(g_{\alpha\beta}(w))$ will vanish at points $w = w_0$ corresponding to branch points of $\mathfrak{X}$. Thus the notion of the length of a curve in M retains its meaning, and the same holds for the notions distance function, closed set, compact set in M, as well as for the notion divergent path on M. This leads us to

Definition 3. *A* **divergent path** *on a global minimal surface $\mathfrak{X} : M \to \mathbb{R}^3$ is a continuous curve $\Gamma : [0, 1) \to \mathbb{R}^3$ of the form $\Gamma = \mathfrak{X} \circ \gamma$ where $\gamma : [0, 1) \to M$ is a divergent path on the generalized Riemannian manifold M endowed with the metric of $\mathbb{R}^3$ via the mapping $\mathfrak{X}$.*

Furthermore, Proposition 1 suggests the following

Definition 4. *A global minimal surface $\mathfrak{X} : M \to \mathbb{R}^3$ is called* **complete** *if the length of every divergent C^1-path Γ on $\mathfrak{X}$ is infinite.*

Note that a regular minimal surface $\mathfrak{X} : M \to \mathbb{R}^3$ is complete in the sense of Definition 4 if it is complete in the sense of Definition 1. Thus Definition 4 can be viewed as a legitimate extension of our preceding definition of a complete global minimal surface. *In the sequel we shall drop the epithet global if we speak of a minimal surface* $\mathfrak{X} : M \to \mathbb{R}^3$ *with a Riemann surface* M *as a parameter domain.*

If one wants to consider minimal surfaces in the large, one has to deal with surfaces $\tilde{\mathfrak{X}} : \tilde{M} \to \mathbb{R}^3$ which are defined on Riemann surfaces $\tilde{M}$. However, in certain situations the investigation can be simplified by passing from $\tilde{M}$ to its universal covering M which is a simply connected manifold of the same dimension as $\tilde{M}$. Any minimal surface $\tilde{\mathfrak{X}} : \tilde{M} \to \mathbb{R}^3$ can be lifted from $\tilde{M}$ to M as a minimal surface $\mathfrak{X} : M \to \mathbb{R}^3$, and we shall see that $\mathfrak{X}$ is complete if and only if $\tilde{\mathfrak{X}}$ is complete.

Recall that the universal covering of $\tilde{M}$ is, precisely speaking, a mapping $\pi : M \to \tilde{M}$ of a simply connected two-dimensional manifold M with the property that every point p of $\tilde{M}$ has a neighborhood U such that $\pi^{-1}(U)$ is the disjoint union of open sets S_i in M, called the sheets of the covering above U, each of which is mapped homeomorphically by π onto U.[3]

If $\tilde{M}$ is a Riemann surface with the conformal structure $\tilde{c}$, then π^{-1} induces a conformal structure c on M such that $\pi : (M, c) \to (\tilde{M}, \tilde{c})$ becomes a holomorphic mapping of the Riemann surface (M, c) onto the Riemann surface $(\tilde{M}, \tilde{c})$. Consequently, if $\tilde{\mathfrak{X}} : \tilde{M} \to \mathbb{R}^3$ is a minimal surface with $\tilde{M}$ as parameter domain, and if $\pi : M \to \tilde{M}$ is the universal covering of $\tilde{M}$, then $\mathfrak{X} := \tilde{\mathfrak{X}} \circ \pi$ defines a mapping $\mathfrak{X} : M \to \mathbb{R}^3$ which is again a minimal surface. We call this map the *universal covering of the minimal surface* $\tilde{\mathfrak{X}}$. Note that $\mathfrak{X}$ is regular if and only if $\tilde{\mathfrak{X}}$ is regular, and the images of the Gauss maps $\mathfrak{N}$ and $\tilde{\mathfrak{N}}$ of $\mathfrak{X}$ and $\tilde{\mathfrak{X}}$ coincide.

Proposition 2. *A minimal surface* $\tilde{\mathfrak{X}} : \tilde{M} \to \mathbb{R}^3$ *is complete if and only if its universal covering* $\mathfrak{X} : M \to \mathbb{R}^3$ *is complete.*

Proof. If $\tilde{\mathfrak{X}}$ is regular, the result is an immediate consequence of statement (ii) of the Hopf–Rinow theorem since the projection $\pi : M \to \tilde{M}$ is a local isometry.

To prove the result in general, we have to use Definition 4.

Suppose first that $\mathfrak{X}$ is complete. We consider an arbitrary divergent path $\tilde{\Gamma}$ on $\tilde{\mathfrak{X}}$. Lifting $\tilde{\Gamma}$ to the covering surface $\mathfrak{X}$, we obtain a divergent path Γ on $\mathfrak{X}$ which must have infinite length as $\mathfrak{X}$ is complete. Since $\pi : M \to \tilde{M}$ is a local isometry, it follows that $\tilde{\Gamma}$ has infinite length, and we conclude that $\tilde{\mathfrak{X}}$ is complete.

Conversely, let now $\tilde{\mathfrak{X}}$ be complete. Consider an arbitrary divergent path Γ on $\mathfrak{X}$ given by $\Gamma = \mathfrak{X} \circ \gamma, \gamma : [0, 1) \to M$. We have to show that the length of Γ is infinite. We look at the paths $\tilde{\gamma} := \pi \circ \gamma$ on $\tilde{M}$ and $\tilde{\Gamma} := \tilde{\mathfrak{X}} \circ \tilde{\gamma} = \mathfrak{X} \circ \gamma = \Gamma$

[3] Concerning the universal covering we refer the reader to Weyl [4], Springer [1], Greenberg [1].

on $\tilde{\mathfrak{X}}$, respectively. If $\tilde{\gamma}$ is divergent, then the completeness of $\tilde{\mathfrak{X}}$ implies that $\tilde{\gamma}$ has infinite length whence also γ has infinite length since π is locally an isometry.

On the other hand, if $\tilde{\gamma}$ is not divergent, then there is a compact subset K of $\tilde{M}$ and a sequence of parameter values t_n in $[0,1)$ converging to 1 such that $\tilde{\gamma}(t_n)$ belongs to K for all n. Passing to a subsequence we may assume that the points $\tilde{\gamma}(t_n)$ converge to a point $p_* \in \tilde{M}$. Then we choose a chart $\varphi : G \to \mathbb{R}^2$ around p_* such that $\varphi(p_*) = 0$, and that $\pi^{-1}(G)$ is the disjoint union of open sheets S_i. Since the branch points are isolated, there is an $\varepsilon > 0$ such that $\Omega_\varepsilon := B_\varepsilon(0) \setminus \bar{B}_{\varepsilon/2}(0)$ is contained in $\varphi(G)$ and that the metric of M is positive definite on $\varphi^{-1}(\bar{\Omega}_\varepsilon)$. Since the points $\tilde{\gamma}(t_n)$ converge to p_*, almost all of them belong to the compact set $\varphi^{-1}(\bar{B}_{\varepsilon/2}(0))$. Therefore and since γ is divergent, the points $\gamma(t_n)$ are distributed over infinitely many sheets S_i. From this fact we infer that the path $\varphi \circ \tilde{\gamma}$ has to cross Ω_ε an infinite number of times, implying that the length of $\tilde{\gamma}$ is infinite. Therefore also the length of γ is infinite.

Thus $\mathfrak{X}$ is shown to be complete if $\tilde{\mathfrak{X}}$ is complete. □

Let us note a simple but basic result on parameter domains M of global minimal surfaces $\mathfrak{X} : M \to \mathbb{R}^3$ satisfying $\partial M = \emptyset$.

Proposition 3. *The parameter domain M of a global minimal surface $\mathfrak{X} : M \to \mathbb{R}^3$ cannot be compact, i.e. there are no compact minimal surfaces.*

Proof. If M were compact, each of the components $\mathfrak{X}^j(p)$ of $\mathfrak{X}(p)$ would assume its maximum in some point $p_j \in M$, and since the functions $\mathfrak{X}^j(p)$ are harmonic on M, the maximum principle would imply that $\mathfrak{X}^j(p) \equiv \text{const}$ on M for $j = 1, 2, 3$. Since $\mathfrak{X}(p)$ is supposed to be nonconstant, this is a contradiction. □

By the uniformization theorem, a simply connected Riemann surface is either of the conformal type of the sphere S^2, or of the complex plane $\mathbb{C}$, or of the unit disk $B = \{w\colon |w| < 1\}$. Because of Proposition 3 the first case is excluded, and we obtain

Proposition 4. *If the parameter domain M of a global minimal surface $\mathfrak{X} : M \to \mathbb{R}^3$ is simply connected, then M is conformally equivalent to the complex plane or to the unit disk.*

A minimal surface $\mathfrak{X} : M \to \mathbb{R}^3$ is said to be of *parabolic type* if $M \sim \mathbb{C}$, and of *hyperbolic type* if $M \sim B$. If M is not simply connected, we may pass to the universal covering $\hat{\mathfrak{X}} : \hat{M} \to \mathbb{R}^3$ whose parameter domain $\hat{M}$ is simply connected, and we call $\mathfrak{X}$ to be of parabolic or hyperbolic type if its universal covering $\hat{\mathfrak{X}}$ is of parabolic or hyperbolic type respectively.

3.7 Omissions of the Gauss Map of Complete Minimal Surfaces

A minimal surface which is a graph over $\mathbb{R}^2$ is a complete minimal surface whose Gauss map omits a whole hemisphere of S^2, and Bernstein's theorem states that such a surface must necessarily be a plane. More generally one may ask how large the set of omissions of the Gauss map for an arbitrary nonplanar and complete minimal surface in $\mathbb{R}^3$ can be. In order to get a feeling for what can be true we first consider some special cases and a few examples before we state the main result of this section.

Again we shall throughout consider global minimal surfaces $\mathcal{X} : M \to \mathbb{R}^3$ whose parameter domains M are Riemann surfaces without boundary, i.e.

$$\partial M = \emptyset. \tag{1}$$

A first information is provided by the following result.

Proposition 1. *The Gauss map of a minimal surface $\mathcal{X} : M \to \mathbb{R}^3$ of parabolic type misses at most two points unless $\mathcal{X}(M)$ is contained in a plane.*

Proof. If $\mathcal{X}$ is of parabolic type, then the corresponding universal covering $\hat{\mathcal{X}} : \hat{M} \to \mathbb{R}^3$ is defined on a parameter domain $\hat{M}$ that is conformally equivalent to the complex plane $\mathbb{C}$. Since the spherical images of $\mathcal{X}$ and $\hat{\mathcal{X}}$ are the same, it suffices to prove the following result:

Lemma 1. *The Gauss map of a minimal surface $X : \mathbb{C} \to \mathbb{R}^3$ misses at most two points if $X(\mathbb{C})$ is not contained in a plane.*

Proof. We represent X by a Weierstrass representation formula

$$X(w) = X(0) + \operatorname{Re}\left(\int_0^w \frac{1}{2}\mu(1-\nu^2)\, d\zeta, \int_0^w \frac{i}{2}\mu(1+\nu^2)\, d\zeta, \int_0^w \mu\nu\, d\zeta \right) \tag{2}$$

where $\mu(\zeta)$ is holomorphic, $\nu(\zeta)$ is meromorphic, $\mu(\zeta) \not\equiv 0, \nu(\zeta) \not\equiv 0$, and $\mu\nu^2$ is holomorphic on $\mathbb{C}$. As we have seen in Section 3.3, the meromorphic mapping ν is just the Gauss map N of X followed by the stereographic projection $\sigma : S^2 \to \bar{\mathbb{C}}$ of the Riemann sphere into the complex plane, i.e., $\nu = \sigma \circ N$. As Picard's theorem implies that ν misses at most two values of $\bar{\mathbb{C}} = \mathbb{C} \cup \{\infty\}$, the assertion of the lemma follows from the representation $N = \sigma^{-1} \circ \nu$. □

Now we shall use formula (2) to construct some examples. Let Ω be the complex plane $\mathbb{C}$ or the unit disk B, and suppose that μ and $\mu\nu^2$ are holomorphic and nowhere vanishing on Ω. Then formula (2) defines a regular minimal surface $X : \Omega \to \mathbb{R}^3$ which has the line element

$$ds = \lambda |dw|, \quad \lambda = \tfrac{1}{2}|\mu|(1+|\nu|^2) \tag{3}$$

(see Section 3.3, (10)). Hence we can compare the line element ds on Ω with the ordinary Euclidean line element $|dw|$. Moreover, compact sets in (Ω, ds) correspond to compact sets in the domain Ω equipped with the Euclidean metric $|dw|$, and divergent paths in (Ω, ds) correspond to divergent paths in $(\Omega, |dw|)$, and vice versa. Recall that by definition the surface $\mathcal{X}$ (or, equivalently, the manifold (Ω, ds)) is complete if every divergent path $\gamma : [0, 1) \to \Omega$ has infinite length, that is, if

$$\int_\gamma \lambda |dw| = \frac{1}{2} \int_\gamma |\mu|(1 + |\nu|^2)|dw| = \infty. \tag{4}$$

Then we obtain the following

Examples.

1 If $\mu(w) = w^2$ and $\nu(w) = p(w)/w$ where $p(w)$ is a polynomial of degree not less than two satisfying $p(0) \neq 0$, then μ and $\mu\nu^2$ are holomorphic, and ν maps $\mathbb{C}$ onto $\mathbb{C}$. Moreover, there is a number $\delta > 0$ such that $|\lambda(z)| \geq \delta$ for all $z \in \mathbb{C}$ whence

$$\int_\gamma \lambda |dw| \geq \delta \int_\gamma |dw|$$

for any path $\gamma : [0, 1) \to \mathbb{C}$. By the preceding observations we infer that formula (2) defines a complete regular minimal surface $X : \mathbb{C} \to \mathbb{R}^3$ the Gauss map of which omits no points of S^2.

2 If we choose $\mu(w) = c$ and $\nu(w) = p(w)$ for some constant $c \neq 0$ and some polynomial $p(w)$ of degree at least one, then ν maps $\mathbb{C}$ onto $\mathbb{C}$, and a similar reasoning as in 1 shows that (2) defines a complete regular minimal surface $X : \mathbb{C} \to \mathbb{R}^3$ whose Gauss map omits exactly one point, the north pole of S^2. In particular, if we choose $\mu(w) = \frac{1}{2}$ and $\nu(w) = w$, formula (2) yields Enneper's surface.

3 If we take $\mu(w) = 1, \nu(w) = e^w$, and $\Omega = \mathbb{C}$, then $\nu(w)$ omits exactly the value zero, and we infer that (2) defines a complete regular minimal surface $X : \mathbb{C} \to \mathbb{R}^3$ whose Gauss map omits exactly two points of S^2, the north pole and the south pole. The same holds true for the catenoid (after a suitable rotation).

4 Now we want to construct minimal surfaces $X : \Omega \to \mathbb{R}^3$ whose Gauss map omits a finite number of points. In fact, we want to prescribe a finite set $E = \{a_1, a_2, \ldots, a_{n+1}\}$ on S^2 which is to be omitted by the Gauss map of X. Without loss of generality we can assume that a_{n+1} is the north pole of S^2 as a_{n+1} can be moved into this position by a suitable rotation of $\mathbb{R}^3$. Let $w_1, w_2, \ldots, w_n, \infty$ be the images of $a_1, a_2, \ldots, a_n, a_{n+1}$ under the stereographic projection σ of S^2 onto $\mathbb{C}$. Then we choose

$$\Omega := \mathbb{C} \setminus \{w_1, w_2, \ldots, w_n\}, \quad \mu(w) := \prod_{k=1}^{n} (w - w_k)^{-1}, \quad \nu(w) := w.$$

Since Ω is not simply connected, the surface $X : \Omega \to \mathbb{R}^3$ defined by (1) is multiple-valued as its values depend on the paths of integration. However, the universal covering $\hat{X} : \hat{\Omega} \to \mathbb{R}^3$ of X will be single-valued and the Gauss maps of X and $\hat{X}$ omit the same set of points E. Moreover, $\hat{X}$ is complete exactly when X is complete, and $\hat{X}$ is regular since X is a regular surface. *Thus we can construct a regular minimal surface $\hat{X} : \hat{\Omega} \to \mathbb{R}^3$ of parabolic or hyperbolic type whose spherical image is $S^2 \setminus E$, where $E = \{a_1, \ldots, a_{n+1}\}$ is an arbitrarily prescribed set of points on S^2.*

Are the surfaces $\hat{X}$ constructed in this way complete surfaces? As we shall see, this is true if and only if $n \leq 4$, i.e., if and only if the exceptional set E contains at most four points.

To this end we consider a curve $\gamma : [0, 1) \to \Omega$ in the parameter domain of X and the corresponding curve $\Gamma = X \circ \gamma$ on the minimal surface X. In order to show that X is complete we have to prove that the length

$$L(\Gamma) = \int_\Gamma ds = \int_\gamma \lambda(w)|dw| = \frac{1}{2} \int_\gamma |\mu|(1 + |\nu|^2)|dw|$$

of Γ is infinite if Γ is a divergent curve on X. Because of (4) we then have to show that

$$L(\Gamma) = \frac{1}{2} \int_\gamma (1 + |w|^2) \prod_{k=1}^{n} |w - w_k|^{-1} |dw| \tag{5}$$

is infinite if $\Gamma = X \circ \gamma$ is a divergent path on X.

For any $R > 0$ there is a number $\varepsilon = \varepsilon(R) > 0$ such that

$$\frac{1}{2}(1 + |w|^2) \prod_{k=1}^{n} |w - w_k|^{-1} \geq \varepsilon \quad \text{for all } w \in B_R(0). \tag{6}$$

Hence, if $\gamma(t) \in \Omega \cap B_R(0)$ for all $t \in [0, 1)$, we obtain

$$L(\Gamma) \geq \varepsilon l(\gamma)$$

where $l(\gamma) := \int_\gamma |dw|$ denotes the Euclidean length of γ. We then conclude that a divergent path $\Gamma = X \circ \gamma$ can have finite length $L(\Gamma)$ only if $l(\gamma) < \infty$; but this assumption would imply that $\gamma(t)$ converges to some point $w_0 \in \mathbb{C}$ as $t \to 1 - 0$, and since Γ is divergent, we obtain that $w_0 \notin \Omega$. We then arrive at $w_0 \in \sigma(E \setminus \{a_{n+1}\}) = \{w_1, \ldots, w_n\}$, and therefore $L(\Gamma) = \infty$ on account of (4). Thus we see that a divergent path $\Gamma = X \circ \gamma$ has infinite length if $\gamma([0, 1))$ is contained in a bounded set of $\mathbb{C}$.

Suppose now that $\Gamma = X \circ \gamma$ is a divergent path such that γ is not contained in a bounded set of $\mathbb{C}$. Then either $\lim_{t \to 1-0} |\gamma(t)| = \infty$ or there are

two sequences $\{t_j\}, \{t'_j\}$ of points $t_j, t'_j \in [0,1)$ such that $\lim_{j\to\infty} |\gamma(t_j)| = \infty$, whereas the sequence of points $\gamma(t'_j)$ remains bounded. In the first case, the integral (4) diverges for $n \leq 3$ while it converges if $n \geq 4$. In the second case we find that $L(\Gamma) = \infty$ since γ must cross some annulus $A := \{w \in \mathbb{C}\colon R' < |w| < R\}$ infinitely often, and we have a bound of the kind (6) on A.

Let us resume the main result of this example.

Proposition 2. *For any set E consisting of four or less points of S^2 there exists a regular, complete minimal surface $X : \Omega \to \mathbb{R}^3$ of parabolic or hyperbolic type whose Gauss map omits exactly the points of E.*

The preceding construction suggests that in general the Gauss map of a complete regular minimal surface cannot omit more than four points. Although the construction given in [4] is not conclusive as there might be other choices of μ and ν leading to a complete minimal surface with the desired omission property, the result is nevertheless true and will now be stated as the main result of this section.

Theorem 1. *If $\mathcal{X} : M \to \mathbb{R}^3$ is a complete regular minimal surface such that $\mathcal{X}(M)$ is not a plane, then the Gauss map of $\mathcal{X}$ can omit at most four points.*

This result is due to Fujimoto [3]. The proof given below was found by Mo and Osserman [1] (cf. also Osserman [24]). Weaker results were earlier obtained by Osserman, Ahlfors-Osserman, and Xavier.

Before we prove Fujimoto's theorem we shall derive another result that was conjectured by Nirenberg and proved by Osserman [1]. Although it is weaker than Theorem 1, it already provides a considerable sharpening of Bernstein's theorem stated in Section 2.4.

Theorem 2. *Let $\mathcal{X} : M \to \mathbb{R}^3$ be a regular complete minimal surface such that $\mathcal{X}(M)$ is not a plane. Then the image of the Gauss map of $\mathcal{X}$ is dense in S^2.*

We remark that in this theorem the assumption of regularity can be replaced by the weaker requirement that $\mathcal{X}$ has only finitely many branch points provided that M is assumed to be simply connected. However, the result does not remain true if we admit arbitrary minimal surfaces as we can see from the following example.

[5] *There exist complete nonplanar minimal surfaces the spherical images of which lie in an arbitrarily small neighborhood of the south pole of S^2.* This can be seen as follows. We set $\nu(w) = \varepsilon w$ for some $\varepsilon > 0$, and choose a holomorphic function $\mu : B \to \mathbb{C}$ of the unit disk such that

$$\int_\gamma |\mu(w)||dw| = \int_0^1 |\mu(\gamma(t))||\dot{\gamma}(t)|\, dt = \infty$$

holds for every divergent path $\gamma : [0, 1) \to B$. Defining $X : B \to \mathbb{R}^3$ by formula (2) we obtain a complete minimal surface whose spherical image is contained in an arbitrarily small neighborhood of the south pole provided that $\varepsilon > 0$ is sufficiently small. For the construction of such functions $\mu(w)$ we refer to Osserman's thesis [25] where it is shown that the images of the functions μ are precisely those Riemann surfaces of class A which are of hyperbolic type. In the last section of his thesis, Osserman gave a number of examples for such surfaces which, consequently, lead to implicit examples of functions μ described above.

An explicit example, pointed out by Osserman, is provided by $\mu := J' \circ F$ where J is the elliptic modular function and F a conformal map of the unit disk B onto the upper halfplane. In particular, μ maps B onto a hyperbolic Riemann surface of class A with no boundary points at finite distance.

Note that Bernstein's theorem is an immediate corollary of Theorem 2, as a nonparametric minimal surface $\mathcal{X}(x, y) = (x, y, z(x, y))$ defined for all $(x, y) \in M = \mathbb{R}^2$ is a complete regular minimal surface. Since the Gauss map of $\mathcal{X}$ maps $\mathbb{R}^2$ into a hemisphere of S^2, the set $\mathcal{X}(M)$ has to be a plane, and then a straightforward computation yields that $z(x, y)$ is an affine function, i.e.,

$$z(x, y) = ax + by + c$$

for suitable constants $a, b, c \in \mathbb{R}$.

The *proof of Theorem 2* will be based on the following

Lemma 2. *If $f : B \to \mathbb{C}$ is a holomorphic function with at most finitely many zeros, then there is a divergent path $\gamma : [0, 1) \to B$ of class C^∞ such that*

$$\int_\gamma |f(w)||dw| < \infty.$$

Proof. If $f(w) \neq 0$, then the holomorphic mapping $F : B \to \mathbb{C}$ defined by

$$F(w) := \int_0^w f(\zeta)\, d\zeta$$

is invertible in a neighborhood of the origin in B. Let $G(z)$ be the local inverse of F around $z = 0$ which is defined on some disk $B_R(0)$, and be

$$G(z) = a_1 z + a_2 z^2 + \cdots$$

the Taylor expansion of G. We can assume R to be its radius of convergence; it could be infinite as, for instance, it is the case for $f(w) \equiv 1$. Let us introduce the set I of all $\rho \in (0, R]$ such that $G(B_\rho(0)) \subset B$ and that the mapping

$$G : B_\rho(0) \to \Omega_\rho := G(B_\rho(0))$$

is bijective. By Liouville's theorem the number

$$r := \sup I$$

is finite since G is nonconstant.

We claim that there is a point $z_0 \in \partial B_r(0)$ such that

$$\lim_{t\to 1-0} |G(tz_0)| = 1$$

which would then imply that the path

$$\gamma(t) := G(tz_0), \quad 0 \le t < 1,$$

is divergent in B, but

$$\int_\gamma |f(w)||dw| = \int_\gamma |F'(w)||dw| = \int_{F(\gamma)} |dz| = |z_0| = r < \infty$$

and the assertion of the lemma were proved.

If we could not find some $z_0 \in \partial B_r(0)$ as claimed, then for any $z_0 \in \partial B_r(0)$ we could select a sequence $\{t_n\}$ of numbers $t_n \in (0,1)$ such that $t_n \to 1-0$ and that $G(t_n z_0)$ converges to some point $w_0 \in B$. Since $F'(w_0) \neq 0$, there is a neighborhood $\mathcal{V}$ of w_0 where F is invertible. Let $\hat{G}$ be the inverse of $F|_{\mathcal{V}}$. Since

$$F(w_0) = \lim_{n\to\infty} F(G(t_n z_0)) = \lim_{n\to\infty} t_n z_0 = z_0,$$

the intersection $F(\mathcal{V}\,) \cap B_r(0)$ is nonempty, and $\hat{G}$ must be an extension of G to some neighborhood of z_0. By a compactness argument we infer that G admits a holomorphic extension to some disk $B_{\rho'}(0)$ such that $r < \rho' < R$ and $G(B_{\rho'}(0)) \subset B$. By the principle of unique continuation we infer that G is bijective on $B_{\rho'}(0)$ since $F(G(z)) = z$ for $z \in B_\rho(0)$ if $0 < \rho < r$. However, the existence of such a ρ' would contradict the definition of r. Thus the lemma is proved if $f(w) \neq 0$ on B.

If $f(w)$ has finitely many zeros $w_1, \ldots, w_n \in B$ of order $\nu_1, \ldots, \nu_n$, then the function

$$\tilde{f}(w) := f(w) \prod_{k=1}^{n} \left(\frac{1 - \bar{w}_k w}{w - w_k} \right)^{\nu_k}$$

does not vanish on B. For any $a \in B$, the transformation $w \mapsto \frac{w-a}{1-\bar{a}w}$ provides a conformal mapping of B onto itself whence $|\tilde{f}(w)| \ge |f(w)|$ on B. The preceding argument implies that there is a divergent path $\gamma : [0,1) \to B$ such that $\int_\gamma |\tilde{f}(w)||dw| < \infty$ whence $\int_\gamma |f(w)||dw| < \infty$, and the lemma is proved in the general case. □

Now we turn to the

Proof of Theorem 2. Passing to the universal covering of $\mathfrak{X}$, we may assume that M is equal to $\mathbb{C}$ or to $B = \{w\colon |w| < 1\}$.

If $\mathfrak{X}$ is of parabolic type (i.e., $M = \mathbb{C}$), and if the spherical image of $\mathfrak{X}$ is not dense in S^2, then Proposition 1 yields that $\mathfrak{X}(\mathbb{C})$ is contained in an affine plane of $\mathbb{R}^3$, and since $\mathfrak{X}$ is complete, the set $\mathfrak{X}(\mathbb{C})$ must be the whole plane.

Suppose now that $\mathfrak{X}$ is of hyperbolic type (i.e., $M = B$), and that the spherical image of $\mathfrak{X}$ is not dense in S^2. Then the Gauss map of $\mathfrak{X}$ misses an open set which can be assumed to be a neighborhood of the north pole. Representing $\mathfrak{X}(w) = X(w)$ by formula (2) we then infer that the function $\nu(w)$ is a bounded holomorphic function on B, and the branch points of X are precisely the zeros of the holomorphic function μ. We have assumed that there are no such zeros, but we could admit finitely many. By Lemma 2 there is a divergent path γ in B such that $\int_\gamma |\mu||dw| < \infty$. On the other hand, the length $L(\Gamma)$ of $\Gamma := X \circ \gamma$ is given by

$$L(\Gamma) = \int_\Gamma ds = \frac{1}{2}\int_\gamma |\mu|(1 + |\nu|^2)|dw|$$

whence

$$L(\Gamma) \leq \text{const} \int_\gamma |\mu||dw| < \infty.$$

But this result is a contradiction to the completeness of the minimal surface X which requires that any divergent path on X is of infinite length. □

Now we shall outline the

Proof of Theorem 1. Suppose that $\mathfrak{X} : M \to \mathbb{R}^3$ is a complete regular minimal surface whose Gauss map omits at least five points $a_1, \ldots, a_5 \in S^2$. We can assume that a_5 is the north pole. Then we pass to the universal covering X of $\mathfrak{X}$ which we can assume to be defined on a simply connected domain of $\mathbb{C}$. On account of Proposition 1, the surface X must be of hyperbolic type, and thus we can suppose that its parameter domain is the unit disk $B = \{w \in \mathbb{C}\colon |w| < 1\}$. In other words, we are given a complete regular minimal surface $X : B \to \mathbb{R}^3$ which is represented on B by formula (1) where $\nu(w)$ is meromorphic, $\mu(w)$ and $\mu\nu^2$ are holomorphic, and $\mu(w) \not\equiv 0$, $\nu(w) \not\equiv 0$ on B. The meromorphic function ν is just the Gauss map of X followed by the stereographic projection $\sigma : S^2 \to \bar{\mathbb{C}}$. Consequently $\nu(w)$ omits the four points $w_k := \sigma(a_k)$, $1 \leq k \leq 4$, and the value $\infty = \sigma(a_5)$, i.e., ν is holomorphic. Since X is regular, we have $\mu(w) \neq 0$ for all $w \in B$.

Now we want to proceed in a similar way as in the proof of Lemma 2. We define a mapping $F : B \to \mathbb{C}$ by

$$F(w) := \int_0^w f(\zeta)\, d\zeta \tag{7}$$

where f has the properties stated in Lemma 2; a specific choice will be made later on. Let $G(z)$ be the inverse of F in a neighborhood of the origin, and

let r be defined as in the proof of Lemma 2. Then we have $F(G(z)) = z$ for all $z \in B_r(0)$, and there is a point $z_0 \in \partial B_r(0)$ such that $|G(tz_0)| \to 1$ as $t \to 1-0$, and that G cannot be extended to a neighborhood of z_0 as a holomorphic function.

Let us introduce the curves γ^*, γ, and Γ by setting $\gamma^*(t) := tz_0$, $0 \le t \le 1$, $\gamma := G \circ \gamma^*$, and $\Gamma := X \circ \gamma$. Then the length

$$L(\Gamma) = \frac{1}{2}\int_\gamma |\mu|(1+|\nu|^2)|dw|$$

of Γ can be expressed in the form

$$L(\Gamma) = \frac{1}{2}\int_{\gamma^*} |\mu \circ G|(1+|\nu \circ G|^2)\left|\frac{dw}{dz}\right||dz| \tag{8}$$

where

$$\frac{dw}{dz}(z) = \frac{1}{\frac{dz}{dw}(w)} = \frac{1}{f(w)}, \quad w = G(z).$$

Now we choose the function f in the form

$$f(w) := \tfrac{1}{2}\mu(w)\varphi(w) \tag{9}$$

where $\varphi(w)$ is to be determined later. From (7) we then infer that

$$L(\Gamma) = \int_{\gamma^*} \frac{1+|\nu(G(z))|^2}{|\varphi(G(z))|}|dz|. \tag{10}$$

We now want to choose φ in such a way that $L(\Gamma)$ becomes finite, and since Γ is by construction a divergent path on X (see the proof of Lemma 2), this would yield a contradiction to the completeness of $X : B \to \mathbb{R}^3$.

Note that $h := \nu \circ G$ is holomorphic in $B_r(0)$ and omits at least the four values w_1, w_2, w_3, w_4. Then, for any choice of the numbers ε and ε' satisfying $0 < \varepsilon < 1$ and $0 < \varepsilon' < \frac{\varepsilon}{4}$, there is a real number b depending only on $\varepsilon, \varepsilon'$ and the points w_j such that

$$\{1+|h(z)|^2\}^{(1/2)(3-\varepsilon)} \prod_{j=1}^{4} |h(z)-w_j|^{\varepsilon'-1}|h'(z)| \le \frac{2br}{r^2-|z|^2} \tag{11}$$

holds true for all $z \in B_r(0)$.

For the moment we shall dispense with the proof of this inequality, and we proceed with the proof of the theorem by showing that $L(\Gamma) < \infty$ for a suitable choice of φ. Choose some $\varepsilon \in (0,1)$ and set $p := 2/(3-\varepsilon)$; then we have $\frac{2}{3} < p < 1$. Now we try to choose φ in such a way that

$$(\varphi \circ G)(z) = \{h'(z)\}^{-p} \prod_{j=1}^{4} [h(z)-w_j]^{p(1-\varepsilon')} \tag{12}$$

is satisfied. On account of (11), this would imply the inequality

$$\frac{1+|\nu(G(z))|^2}{|\varphi(G(z))|} \le \left(\frac{2br}{r^2-|z|^2}\right)^p = \frac{\kappa}{(r^2-|z|^2)^p} \quad \text{for } |z|<r \tag{13}$$

where $\kappa := (2br)^p$, and $\frac{2}{3} < p < 1$. Then (10) and (13) would yield the desired estimate $L(\Gamma) < \infty$.

However, we have defined G as the inverse of

$$F(w) = \frac{1}{2}\int_0^w \mu(\zeta)\varphi(\zeta)\,d\zeta.$$

Thus G is defined in terms of φ, and we cannot by rights use (12) for defining φ. To remove this difficulty, we transform in (12) everything from z to w using the relations $w = G(z)$, $h(z) = \nu(G(z)) = \nu(w)$ and $h'(z) = \nu'(w)\frac{dw}{dz} = \nu'(w)/\frac{dz}{dw}$. Then (12) can be expressed in the form

$$\left(\frac{dz}{dw}\right)^{1-p} = \frac{1}{2}\mu(w)\prod_{j=1}^{4}[\nu(w)-w_j]^{p(1-\varepsilon')}\{\nu'(w)\}^{-p},$$

that is,

$$f(w) = \left\{\frac{1}{2}\mu(w)\right\}^{1/(1-p)}\prod_{j=1}^{4}[\nu(w)-w_j]^{p(1-\varepsilon')/(1-p)}\{\nu'(w)\}^{-p/(1-p)}. \tag{14}$$

On the right-hand side of (14) we only have given quantities that do not involve φ, and therefore we can use (14) to define $f(w)$ for $w \in B$ provided that $\nu'(w) \neq 0$ in B. Then $F(w)$ will be defined by (6), and G is the inverse of F. We now derive from (14) that (12) holds whence we obtain (13) and then $L(\Gamma) < \infty$.

We still have to consider the case where $\nu'(w)$ vanishes on a nonempty set Σ in B. Since X is nonplanar we have $\nu(w) \not\equiv \text{const}$, whence $\nu'(w) \not\equiv 0$. Thus Σ is either a finite set, or it consists of a sequence of points tending to the boundary of B. If we now define $f(w)$ for $w \in B \setminus \Sigma$ by (14), and then $F(w)$ by (6), we might obtain a multivalued function which, however, can be lifted to a single-valued function $\hat{F}$ on the universal covering surface $\hat{B}$ of $B \setminus \Sigma$. The surface $\hat{B}$ is conformally equivalent to the unit disk, and the reasoning of the proof of Lemma 2 leads again to a largest disk $B_r(0)$ where the inverse $\hat{G}$ of $\hat{F}$ is defined, and to a boundary point $z_0 \in \partial B_r(0)$ which is a singular point for $\hat{G}$. Now we define a mapping $G : B_r(0) \to B \setminus \Sigma$ by $G := \pi \circ \hat{G}$ where $\pi : \hat{B} \to B \setminus \Sigma$ is the canonical projection of the universal covering $\hat{B}$ onto $B \setminus \Sigma$. Defining γ^*, γ, and Γ as before we see that $L(\Gamma) < \infty$. To obtain a contradiction we have to verify that Γ is a divergent path on X. If this were not true, we could find a sequence of points $z_n = t_n z_0$ on γ^* with $t_n \to 1-0$ such that their images $w_n = G(z_n)$ on γ converge to an interior point w_0

of B. Then w_0 cannot be contained in $B \setminus \Sigma$ on account of the reasoning of Lemma 2, and therefore w_0 must be an element of Σ, i.e., $\nu'(w_0) = 0$. Thus we have the power series expansion

$$\nu'(w) = \alpha(w - w_0)^m + \cdots$$

for some $\alpha \neq 0$ and some integer $m \geq 1$ whence

$$\{\nu'(w)\}^{p/(1-p)} = \beta(w - w_0)^{mp/(1-p)} + \cdots \quad \text{as } w \to w_0$$

where we have set $p := 2/(3-\varepsilon)$ for some fixed $\varepsilon \in (0, 1)$. Note that $p/(1-p) = 2/(1-\varepsilon) > 2$.

Case (i). Suppose that $\gamma(t) \to w_0$ as $t \to 1-0$. Then we arrive at the relations

$$r = \int_{\gamma^*} |dz| = \int_{\gamma} |f(w)||dw| \geq c \int_{\gamma} |w - w_0|^{-2}|dw|$$

with a positive constant $c > 0$. Since

$$\int_{\gamma} |w - w_0|^{-2}|dw| = \infty$$

we have found a contradiction.

Case (ii). If $\gamma(t)$ does not tend to w_0 as $t \to 1-0$, there is another accumulation point of $\gamma(t)$ in $B \setminus \Sigma$, and the reasoning of the proof of Lemma 2 leads to a contradiction.

Thus Γ is divergent but $L(\Gamma) < \infty$, and this contradicts the completeness of X.

It remains for us to verify the estimate (11). Let Ω be the domain

$$\mathbb{C} \setminus \{w_1, w_2, w_3, w_4\}.$$

Its universal covering is conformally equivalent to the unit disk B, and the standard Poincaré metric is pulled back to a conformally equivalent metric $ds = \rho(w)|dw|$ on Ω whose Gauss curvature is equal to -1. For $\rho(w)$ we have the asymptotic expansions

$$\rho(w) \sim \frac{C_j}{|w - w_j| \log |w - w_j|} \quad \text{as } w \to w_j, \quad 1 \leq j \leq 4 \tag{15}$$

and

$$\rho(w) \sim \frac{C_0}{|w| \log |w|} \quad \text{as } w \to \infty = w_5 \tag{16}$$

where C_0 and C_j are constants different from zero (see R. Nevanlinna [1], pp. 259–260 and 250).

Now consider the function

$$\psi(w) := (1+|w|^2)^{(3-\varepsilon)/2}\rho(w)^{-1}\prod_{j=1}^{4}|w-w_j|^{\varepsilon'-1}, \quad w\in\Omega, \tag{17}$$

which is positive and continuous on Ω. By (15) and (16) we have $\psi(w)\to 0$ as $w\to w_j$, $j=1,\dots,5$. Hence $\psi(w)$ has a positive maximum on Ω, the value b of which depends only on ε,ε', and $w_1,\dots,w_4$, and we therefore obtain

$$\psi(w)\le b \quad \text{for all } w\in\Omega. \tag{18}$$

Now we consider an arbitrary holomorphic function $h(z)$ in $B_r(0)$ which omits the points $w_1,\dots,w_4$, say, the function $h=\nu\circ G$ that we considered before. We lift h to a conformal mapping H from $B_r(0)$ to B and apply the Schwarz–Pick lemma to $H\circ\tau$ where τ denotes a conformal rescaling mapping which maps B onto $B_r(0)$. This lemma states that holomorphic mappings of the unit disk B into itself decrease the noneuclidean length of an arc (cf. Ahlfors [6], p. 3, Carathéodory [5], vol. 2, pp. 14–20) which implies that

$$\rho(h(z))|h'(z)|\le\frac{2r}{r^2-|z|^2} \quad \text{for } |z|<r. \tag{19}$$

From (17) and the two inequalities (18), (19) we infer the desired estimate (11). □

A detailed exposition of Fujimoto's work, in particular on the value distribution of the Gauss map of minimal surfaces, can be found in Fujimoto [5,8].

3.8 Scholia

1 Historical Remarks and References to the Literature

In Sections 3.1–3.6 we had a glimpse at the theory of minimal surfaces developed during the 19th century. The principal tools were methods of complex analysis, conformal mappings, the Gauss map and related differential geometric ideas, symmetry arguments and geometric intuition. Hence it is no surprise that this part of the theory of minimal surfaces has always been a preferred playground of differential geometers. During the last years this classical field has experienced a remarkable revival which is to no small extent the merit of computer graphics nowadays available. By the pioneering work of David Hoffman this amazing tool has become a useful working aid and a source of inspiration.[4] In former times it was rather difficult to visualize minimal surfaces in the large and, in fact, the classical treatises do not show many figures.

[4] See Callahan, Hoffman, and Hoffman [1], Hoffman [1–5], and Hoffman and Meeks [1,2,5,8,9,11].

This absence of figures cannot only be explained by the dislike of some of the great French mathematicians for the old custom of supporting geometric reasoning by figures.[5] An exception from the rule was H.A. Schwarz who put much effort in the construction of permanent models of minimal surfaces (see also the figures at the end of vol. 1 of his *Abhandlungen* [2]). Also the work of Neovius (cf. in particular [5]) contains beautiful illustrations. In recent years crystallographers and chemists have discovered the use of minimal surfaces for the description of complicated crystalline structures, and, in addition to the use of computer graphics, they have developed various means of visualizing these surfaces by models.

A brief survey of the history of minimal surfaces until the time of Riemann's death can be found in the introduction to Riemann's paper [2]. It is missing in the reprint included in Riemann's *Gesammelten mathematischen Werken* [2] since the editor H. Weber had decided to omit it as it was written by Riemann's student Hattendorf.

Hattendorf begins his survey with the derivation of the minimal surface equation by Lagrange (1760/61), and he mentions that Lagrange found no other solution than the plane. Then he states the contributions of Meusnier (1776): The minimal surface equation is equivalent to $H = 0$ and has the catenoid and the helicoid as solutions. Moreover, he mentions the integration of the minimal surface equation by Monge (1784) and Legendre (1787) as well as a basic discovery by Dupin (1813): The asymptotic lines of a minimal surface are perpendicular to each other and enclose angles of 45 degrees with the lines of curvature.

The representation formulas of Monge and Legendre were, as Hattendorf remarks, not well suited for deriving other specific minimal surfaces besides the helicoid and the catenoid found by Meusnier. New surfaces were first derived by Scherk (in his prize-essay for the Jablonowski Society at Leipzig, 1831) by a kind of separation of variables. A similar approach was followed by Catalan (1858), and Hattendorf also mentions that, in two papers from 1842 and 1843, Catalan showed that the helicoid is the only ruled minimal surface (apart from the plane). Then Hattendorf discusses the solution of Björling's problem by Björling (*Grunert's Archive*, vol. 4, 1843) and later by Bonnet (*Comptes Rendus* 1853, 1855, 1856; *Liouville's Journal* 1860). He mentions that Bonnet investigated asymptotic lines, lines of curvature and geodesic lines on minimal surfaces and that he looked for those surfaces of zero mean curvature which satisfy certain geometric conditions. For instance, the surface might be generated by a curve via a screw motion, it might have plane lines of curvature, or it might pass through given lines. Of this latter problem, Bonnet

[5] Lagrange wrote in the preface to his *Mécanique analytique* (second edition, vol. 1, 1811): On ne trouvera point de Figures dans cet Ouvrage. Les méthodes que j'y expose ne demandent ni constructions, ni raisonnemens géométriques ou mécaniques, mais seulement des opérations algébriques, assujéties à une marche regulière et uniforme. Ceux qui aiment l'Analyse, verront avec plaisir la Mécanique en devenir une nouvelle branche, et me sauront gré d'en avoir étendu ainsi le domaine.

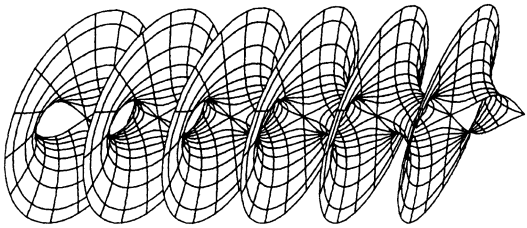

Fig. 1. Riemann's periodic minimal surface: an example with a translational symmetry. Courtesy of K. Polthier and M. Wohlgemuth

treated the problem of finding minimal surfaces containing a given strip or passing through two intersecting straight lines; the last question was also investigated by Serret (1855). Hattendorf closes his report with the remark that nothing more is known on minimal surfaces with given boundaries, and he states that Bonnet stopped at that point where the true problem begins, namely, the investigation of the limit and discontinuity properties. And then: *Diese Untersuchung gehört ihrem Wesen nach in die von Riemann geschaffene Theorie der Funktionen von complexen Variablen.*

A new period in the theory of minimal surfaces began in 1865 with the solution of Plateau's problem by H.A. Schwarz in the case that the boundary curve is a regular quadrilateral, and, in 1867, for the general quadrilateral (see Schwarz [2], vol. 1, pp. 1–91). These papers are based on the representation formulas for minimal surfaces derived in Section 3.3. Weierstrass had lectured on these formulas at the Mathematical Seminar of Berlin University as early as 1861, and he reported them to the Berlin Academy in 1866 (see Weierstrass [2–4]). Somewhat different representation formulas were stated by Enneper [1] in 1864 who used the lines of curvature as parameter lines $u = \text{const}$ and $v = \text{const}$ on a minimal surface. Other representation formulas were introduced by Weingarten (1863), Riemann (1866), Peterson (1866) and Beltrami (1868).[6]

Riemann's posthumous paper [2], published in 1867, treated minimal surfaces passing through one or several straight lines. In particular, it dealt with the following special boundaries: (i) Two infinitely long, skew straight lines. (ii) Three straight lines, two of which lie in a plane E and intersect; the third lies in a plane E' parallel to E. (iii) Three intersecting straight lines. (iv) A quadrilateral. (v) Two arbitrary circles which lie in parallel planes.

Already in 1866, Weierstrass [1] reported in a lecture to the Academy that he was able to solve Plateau's problem for an arbitrary [unknotted] polygonal boundary, but the details appeared only about thirty years later (cf. Weierstrass [4]).

The whole development can be studied in the first volume of Schwarz's *Abhandlungen* published in 1890 and exclusively dedicated to the study of

[6] For references, see R.v. Lilienthal: *Besondere Flächen*. Encyklopädie der Mathematischen Wissenschaften III.3, pp. 307–333, in particular pp. 310–315.

minimal surfaces. In several later supplements and annotations to his papers and to the whole volume Schwarz gives a very clear picture of what was known in his time. Particularly interesting is his report *Miscellen aus dem Gebiete der Minimalflächen* (see [2], pp. 168–189 and 325–333).

A comprehensive presentation of the whole field can be found in Darboux's *Leçons* [1]. (Especially relevant to the field of minimal surfaces are vols. 1 and 3.)

A brief but very readable description of the Schwarz–Riemann–Weierstrass approach to the solution of Plateau's problem for polygonal boundaries is given in chapters 14 and 15 of Bianchi's treatise [1]. The main topic of chapter 15 is the construction of Schwarz's minimal surface spanning a quadrilateral and a discussion of its properties and of its adjoint surface.

The knowledge available at the turn of this century is surveyed in Lilienthal's encyclopedia article [1].

An extensive presentation from the modern point of view can be found in Nitsche's treatise [28] (see also [37]); it is at the same time a rich source of bibliographic and historical references.

During the years 1900–1925 not much progress was made in the theory of parametric minimal surfaces apart from work of Neovius on periodic minimal surfaces which, however, is largely an extension of his earlier work carried out in the nineteenth century. The essential though indirect contributions of that period to the theory of minimal surfaces were the development of a powerful measure and integration theory by Lebesgue, of the direct methods by Hilbert, Lebesgue, Courant, Tonelli, and the foundation of functional analysis by Hilbert, F. Riesz, E. Schmidt, Fréchet, Hahn, and Banach. Moreover, the basic techniques of the theory of elliptic equations, regularity theorems and a priori estimates, were created by Korn, S. Bernstein, Lyapunov, Müntz and Lichtenstein in those years. The noteworthy results of S. Bernstein concern nonparametric minimal surfaces. Between 1925 and 1950 the theory of minimal surfaces sprang to new life; the following two chapters will give an impression of the achievements in that period. From then on boundary value problems for minimal surfaces have stood in the center of interest. In the sixties, DeGiorgi, Fleming, Federer, and Reifenberg developed the powerful tool of geometric measure theory which since then has become more and more important for the study of minimal surfaces.

For some time the Weierstrass–Schwarz theory of minimal surfaces moved into the background, and mainly the pioneering work of Osserman on complete minimal surfaces showed its usefulness and importance; in this respect we also mention the interesting contributions by Leichtweiß, Nitsche and Voss from that period, the main results of which are presented in Osserman's survey [10] which had a great influence on the subsequent development. We also refer to chapter 8 of Nitsche's *Vorlesungen* [28].

Thereafter, the interest in this area seemed more or less exhausted despite some interesting contributions by Gackstatter and the exciting discoveries of new triply periodic minimal surfaces by the physicist Alan Schoen (about

1970); their existence, however, seemed not to be sufficiently rigorously established. At the beginning of the 1880ties, the theory of complete and of periodic minimal surfaces gathered new speed. This is particularly the merit of Costa, D. Hoffman and Meeks who disproved a longstanding conjecture according to which the only complete embedded minimal surfaces in $\mathbb{R}^3$ of *finite topological type* are the *plane*, the *catenoid*, and the *helicoid*. This conjecture turned out to be false as there is a complete minimal surface $\mathfrak{X} : M \to \mathbb{R}^3$ defined on the square torus $\mathbb{C}/\mathbb{Z}^2$ with three points removed. This surface was discovered by Costa [1,2]. Its representation formula (7) in Section 3.3 uses the functions $\mu = \wp$ and $\nu = a/\wp'$ where $\wp$ is the Weierstrass p-function, $\wp'$ its derivative, and a denotes some constant $\neq 0$. Costa showed that $\mathfrak{X}$ is a complete surface of genus one with three ends; Hoffman and Meeks proved that it is an embedded surface. Later on, many more similar surfaces were found, so that today a fascinating new theory is developing. We shall collect a few results in the next subsection. A second major achievement is the verification of A. Schoen's examples of triply periodic minimal surfaces by Karcher, see Section 3.5. However, many more beautiful and fascinating new examples of embedded minimal surfaces have recently been discovered, and the subject is still growing fast. Another 200–300 pages (or more) would be needed to do it justice. Thus we have to content ourselves with mentioning a few survey papers and some comprehensive presentations.

At an early stage, the development was documented in the lecture notes of Barbosa and Colares [1]. In his paper [1], Karcher showed how more embedded minimal surfaces can be derived from some of the Scherk examples, and in [2] he established the existence of Alan Schoen's triply periodic minimal surfaces. The reader should begin by studying Karcher's lecture notes [3] where he outlines devices to construct interesting examples of increasing topological complexity. Then we refer to the works of D. Hoffman and Meeks cited in our bibliography. Particularly, we mention Hoffman [1–5], Hoffman and Meeks [11], Meeks [6,7], Hoffman and Wohlgemuth [1], Wohlgemuth [1], and Polthier [1,2].

Lately crystallographers have showed much interest in triply periodic minimal surfaces, and they have very much stimulated recent developments. We especially refer the reader to the works of Sten Andersson, Blum, Bovin, Eberson, Ericsson, Fischer, Hyde, Koch, Larsson, Lidin, Nesper, Ninham, and v. Schnering—cited in our bibliography—where many beautiful surfaces are depicted.

The following collection of results is mainly drawn from the papers of Osserman, Karcher, Hoffman and Meeks quoted above.

2 Complete Minimal Surfaces of Finite Total Curvature and of Finite Topology

The first basic results on complete minimal surfaces of finite total curvature are due to Osserman; an excellent presentation is given in §9 of Osserman's survey [10].

Theorem 1. *Let M be a complete, orientable Riemannian two-manifold whose Gauss curvature K satisfies $K \leq 0$ and $\int_M |K|\, dA < \infty$. Then there exist a compact Riemannian two-manifold $\tilde{M}$ and a finite number of points $p_1, \ldots, p_k$ in $\tilde{M}$ such that M and $\tilde{M}' := \tilde{M} \setminus \{p_1, \ldots, p_k\}$ are isometric. In other words, there is a length preserving diffeomorphism from M onto $\tilde{M}'$.*

As a consequence of this result we obtain

Theorem 2. *A complete regular minimal surface $\mathfrak{X} : M \to \mathbb{R}^3$ of finite total curvature $\int_M |K|\, dA$ defined on an orientable parameter manifold M is conformally equivalent to a compact Riemann surface $\mathfrak{R}$ that has been punctured in a finite number of points.*

That means:

(K1) *Complete orientable minimal surfaces without branch points and of finite total curvature can be assumed to be parametrized on parameter domains $M = \mathfrak{R} \setminus \{p_1, \ldots, p_k\}$ which are compact Riemann surfaces $\mathfrak{R}$ with k points removed $(k \geq 1)$.*

Definition 1. *A two-manifold is said to have finite topology if it is homeomorphic to a compact two-manifold from which finitely many points are removed. Correspondingly, a surface $\mathfrak{X} : M \to \mathbb{R}^3$ is said to be of finite topology if its parameter manifold M has finite topology.*

Then property (K1) states that a complete minimal surface of finite total curvature has necessarily finite topology. However, the converse is not true as one can see from the helicoid. This minimal surface has the complete plane $\mathbb{C}$ as parameter domain which is conformally equivalent to the once punctured sphere. As the helicoid is periodic and not flat, its total curvature is infinite. (Note, however, that this example is somewhat artificial because of its periodicity, and a suitable, more stringent definition of finite topology dividing out the periodicities would remove the helicoid from the list of examples.) Meeks and Rosenberg [1,3] proved that the only complete, embedded, simply connected and periodic minimal surface is the helicoid.

Until recently, the plane, the catenoid, and the helicoid were the only known examples of complete embedded minimal surfaces with a finite topology. The first new example depicted in Fig. 20 (see also the frontispiece) is the Costa surface whose embeddedness was proved by Hoffman and Meeks. It is conformally a torus punctured in three points. More complicated examples of higher genus were discovered by D. Hoffman and Meeks. A sample is depicted in Plate II.

Let $\mathfrak{R}$ be a compact Riemann surface (without boundary), and $p_1, \ldots, p_k$ a finite number of points in $\mathfrak{R}$. We consider a regular minimal surface $\mathfrak{X} : M \to \mathbb{R}^3$ of finite topology, defined on $M := \mathfrak{R} \setminus \{p_1, p_2, \ldots, p_k\}$.

The image $E_j := \mathfrak{X}(B_j')$ of a punctured disk neighborhood $B_j' = B_j \setminus \{p_j\}$ of p_j is called an *end* of the surface $\mathfrak{X}$.

What can one say about the behavior of $\mathcal{X}$ at its ends? Some answers should be obtainable from information about the behavior of the Gauss map $\mathcal{N} : M \to S^2 \subset \mathbb{R}^3$ of $\mathcal{X}$ at the ends E_j, that is, from the meromorphic function $\nu := \sigma \circ \mathcal{N}$ obtained by composing $\mathcal{N}$ with the stereographic projection $\sigma : S^2 \to \bar{\mathbb{C}}$. Let η be the holomorphic 1-form on M associated with $\mathcal{X}$ which in local coordinates w is given by $\eta(w) = \mu(w)dw$ (here $\mu(w)$ is the function from the representation formula (7) in Section 3.3). Then we have the following basic information (see Osserman [5,10]):

Theorem 3. *Let $\mathcal{X} : M \to \mathbb{R}^3$ be a complete regular minimal surface of finite total curvature $\int_M K\, dA$; for the sake of brevity we call such a mapping a* (K1)*-surface. Then we have*:

(K2) *The meromorphic function $\nu : M \to \bar{\mathbb{C}}$ extends to a meromorphic function on $\mathcal{R}$ and the holomorphic* 1*-form η on M extends to a meromorphic* 1*-form on $\mathcal{R}$.*

(K3) *The number $m := \frac{1}{4\pi}\int_M K\, dA$ is an integer satisfying $m \le -(\boldsymbol{g} + k - 1)$ where $\boldsymbol{g}$ is the genus of M and k is the number of puncturing points in $\mathcal{R}$.*

(K4) *The mapping $\mathcal{X} : M \to \mathbb{R}^3$ is proper (i.e., pre-images of compact sets in $\mathbb{R}^3$ are compact sets in M).*

Further properties of (K1)-surfaces $\mathcal{X} : M \to \mathbb{R}^3$

(K5) *Set $S_j(R) := \{Q \in \mathbb{R}^3 : RQ \in E_j \text{ and } Q \in S^2\}$. Then $S_j(R)$ converges smoothly as $R \to \infty$ to a great circle on S^2 covered an integral number of times, say, d_j times. Moreover, we have*

$$\int_M K\, dA = 4\pi\left\{1 - \boldsymbol{g} - k - \sum_{j=1}^{k}(d_j - 1)\right\}, \quad \boldsymbol{g} = \text{genus}(M)$$

(see Jorge and Meeks [1], Gackstatter).

(K6) *Denote by $n(\mathcal{X}) := \sum_{j=1}^{k} d_j$ the total spinning of $\mathcal{X}$; clearly, $n(\mathcal{X}) \ge k$. Then we have*: $n(\mathcal{X}) = k \Leftrightarrow \int_M K\, dA = -4\pi(\boldsymbol{g} + k - 1) \Leftrightarrow$ *all of the ends of $\mathcal{X}$ are embedded (that is, for each $j = 1, \ldots, k$, the map $\mathcal{X}$ embeds some punctured neighborhood of p_j)* (see Jorge and Meeks [1]).

(K7) *Let E_j be an embedded end corresponding to the puncture p_j. The Gauss map $\mathcal{N} : M \to S^2$ can be extended continuously from M to $\mathcal{R}$* (see (K2)). *Assume that $\mathcal{N}(p_j) = (0, 0, 1)$. Then outside of a compact set, the end E_j has the asymptotic behavior*

$$z(x, y) = \alpha \log r + \beta + r^{-2}(\gamma_1 x + \gamma_2 y) + O(r^{-2})$$

as $r = \sqrt{x^2 + y^2} \to \infty$ (see R. Schoen [3]).

We call the end E_j *flat* or *planar* if $\alpha = 0$; for $\alpha \neq 0$ we speak of a *catenoid end*. This means that, far out, all (K1)-surfaces look at their embedded ends either like planes or like half catenoids.

(K8) *If* $\mathcal{X} : M \to \mathbb{R}^3$ *is an embedded* (K1)*-surface of genus* $\boldsymbol{g}$ *with* k *ends, then we have*:

(i) *If* $\boldsymbol{g} = 0$, *then* $k \neq 3, 4, 5$ (*Jorge and Meeks* [1]). *In fact,* $\boldsymbol{g} = 0$ *implies that* $\mathcal{X}$ *is a plane* ($k = 1$) *or a catenoid* ($k = 2$) (*Lopez and Ros* [1]).

(ii) *If* $k = 1$, *then* $\mathcal{X}(M)$ *is a plane* (*see, e.g. Hoffman and Meeks* [8]).

(iii) *If* $k = 2$, *then* $\mathcal{X}(M)$ *is a catenoid* (*R. Schoen* [3]).

Property (ii) *follows from the strong halfspace theorem stated below.*

(K9) *The plane has total curvature* 0, *the catenoid* -4π; *all other embedded* (K1)*-surfaces have a total curvature of less than or equal to* -12π (Hoffman and Meeks [8]).

(K10) *The Costa surface* $\mathcal{X}$ *is an embedded* (K1)*-surface of genus* 1 *with three ends and total curvature* -12π. *One end is flat, the other two are catenoid ends. The function* $\nu = \sigma \circ \mathcal{N}$ *is of the form* $\nu = a/\wp'$ *where* $\wp$ *is the Weierstrass p-function and* a *is a constant. The Costa surface contains two straight lines intersecting perpendicularly; moreover, it can be decomposed into eight congruent pieces, each of which lies in a different octant and each of which is a graph* (Hoffman and Meeks [1]). *Generalizing the Costa example, Hoffman and Meeks were able to show that, for any genus* $\boldsymbol{g} \geq 1$, *there is an embedded* (K1)*-surface with one flat end and two catenoid ends. The total curvature* $\int_M K\, dA$ *of this surface is* $-4\pi(\boldsymbol{g}+2)$. *In fact, each of these examples belongs to a* 1*-parameter family of embedded minimal surfaces* (Hoffman [4], Hoffman and Meeks [7]).

A sample of a Hoffman–Meeks surface is depicted in Plate II.

We mention that the underlying Riemann surface $\mathcal{R}$ is the $(\boldsymbol{g}+1)$-fold covering of the sphere given by $\zeta^{\boldsymbol{g}+1} = w^{\boldsymbol{g}}(w^2 - 1)$ punctured at $w = \pm 1$ and $w = \infty$.

(K11) Callahan, Hoffman, and Meeks [3] constructed *examples of embedded* (K1)*-surfaces with four ends, two of which are flat, the others catenoidal.* Following a suggestion of Karcher, Wohlgemuth and Boix constructed many more examples of increasing complexity.

3 Complete Properly Immersed Minimal Surfaces

A very useful result proved by means of the maximum principle is the following

Halfspace Theorem (Hoffman and Meeks [4,10]**).** *A complete, properly immersed minimal surface* $\mathcal{X} : M \to \mathbb{R}^3$ *cannot be contained in a half space, except for a plane.*

(An immersed minimal surface is a surface without branch points, and properly means that the pre-image of any compact set on $\mathcal{X}(M)$ is a compact subset of M.)

Note that the assumption of properness cannot be omitted as Jorge and Xavier [1] exhibited examples of complete minimal surfaces $\mathcal{X} : M \to \mathbb{R}^3$ contained between two parallel planes; see also Rosenberg and Toubiana [1].

A strengthening of the previous result is the **strong halfspace theorem** (Hoffman and Meeks [4,10]): *Two complete, properly immersed minimal surfaces $\mathcal{X} : M \to \mathbb{R}^3$ must intersect if they are not parallel planes.*

4 Construction of Minimal Surfaces

The material of this subsection is essentially drawn from Karcher's excellent lecture notes [3] to which the reader is referred for details. We adjust our notation from Chapter 3 to that of Karcher [3] so that we can immediately use Karcher's formulas. A very detailed presentation of the following material and of related topics is given in the encyclopaedia article by D. Hoffman and H. Karcher [1]; see [EMS].

Let us recall the representation formula (7) of Section 3.3 for a minimal surface $X : \Omega \to \mathbb{R}^3$ by means of a holomorphic function $\mu(w)$ and a meromorphic function $\nu(w)$ on Ω:

$$X(w) = X(w_0) + \operatorname{Re} \int_{w_0}^{w} \psi'(\zeta)\, d\zeta \tag{1}$$

where ψ is defined by

$$\psi' = \left(\frac{1}{2}\mu(1-\nu^2), \frac{i}{2}\mu(1+\nu^2), \mu\nu \right). \tag{2}$$

If we introduce the two meromorphic functions g and h by

$$g := \nu, \quad h' := \mu\nu, \tag{3}$$

we have

$$dh = \mu\nu\, d\zeta,$$

and we can write (2) as

$$d\psi = \left(\frac{1}{2}\left(\frac{1}{g} - g\right), \frac{i}{2}\left(\frac{1}{g} + g\right), 1 \right) dh. \tag{4}$$

Clearly, the functions ψ and h are multiple-valued while the 1-forms $d\psi$ and dh are single-valued on Ω, and mutatis mutandis Ω can be replaced by a domain on a Riemann surface.

The Gauss map $N : \Omega \to S^2$ associated with X is given by

$$N = \frac{1}{|g|^2+1}(2\operatorname{Re} g, 2\operatorname{Im} g, |g|^2 - 1). \tag{5}$$

The line element ds of $X : \Omega \to \mathbb{R}^3$ can be written as

$$ds = \frac{1}{2}\left(|g| + \frac{1}{|g|}\right)|dh| \tag{6}$$

and the Gauss curvature K has now the form

$$K = -16\left(|g| + \frac{1}{|g|}\right)^{-4}\left|\frac{dg}{g}\right|^2 |dh|^{-2}. \tag{7}$$

For $w = u + iv$ and for a tangent vector $W \in T_w\Omega = \mathbb{C}$, the second fundamental form $\mathrm{II}(W, W)$ can be written as

$$\mathrm{II}(W, W) = \operatorname{Re}\left\{\frac{dg}{g}(W) \cdot dh(W)\right\}. \tag{8}$$

Moreover, *W describes an asymptotic direction exactly if $\frac{dg}{g}(W)\cdot dh(W) \in i\mathbb{R}$, and W is a principal curvature direction if and only if $\frac{dg}{g}(W) \cdot dh(W) \in \mathbb{R}$.*

The **reflection principles** yield: *If a straight line or a planar geodesic lies on a complete minimal surface, then the* $180°$*-rotation around the straight line or the reflection at the plane of the planar geodesic respectively is a congruence of the minimal surface.*

This observation has the following useful *application*: If there is a line $\gamma : I \to \Omega$ such that the stereographic projection $g \circ \gamma : I \to \mathbb{C}$ of its Gauss image is contained in the stereographic projection of a meridian or of the equator of S^2, and if also $h' \circ \gamma$ is contained in the stereographic projection of a meridian of S^2, then analytic reflection at γ does not change the values of $|g| + \frac{1}{|g|}$ and of $|h'|$, nor does it change the Euclidean metric $|dw|$. Therefore this reflection is a Riemannian isometry for the metric (6) and, consequently, the curve γ defines a geodesic $c := X \circ \gamma$ on the minimal surface. Moreover, $g \circ \gamma$ corresponds either to a meridian of S^2 or to its equator.

The following constructions will be based on Osserman's results described in Subsection 2 of these Scholia. The guiding idea is to describe meromorphic Weierstrass data g and h on Riemann surfaces M which are punctured Riemann surfaces $\mathcal{R}$, i.e., $M = \mathcal{R} \setminus \{p_1, p_2, \ldots, p_k\}$.

A translational symmetry of the minimal surface generated by integrating its Weierstrass data around a homotopically nontrivial loop on M is called a **period of the Weierstrass data**. Integration of the Weierstrass data leads to a single-valued minimal surface $X(w) = \operatorname{Re}\psi(w)$ if all periods $P = (P_1, P_2, P_3)$ vanish or, more generally, if the components of all periods are purely imaginary (i.e., $P \in i\mathbb{R}^3$).

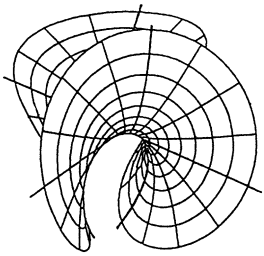

Fig. 2. (A1) Enneper's surface: $g(w) = w$. Courtesy of K. Polthier

Proposition 1. *If a line of symmetry L passes through a puncture, then we can consider closed curves around the puncture p which are symmetric with respect to L. The integrated curve on the minimal surface then consists of two congruent parts which are symmetric either with respect to a reflection plane E or with respect to the axis A of a $180°$-rotation. The period P is the difference vector between the two pieces of the curve; thus it is perpendicular either to E or to A.*

This observation can sometimes be used to show without computation that some punctures cause no periods, for instance, if two nonparallel symmetry planes pass through the punctures.

A very useful tool for proving embeddedness of surfaces is the following theorem presented at the end of Section 3.3:

Theorem of R. Krust. *If an embedded minimal surface $X : B \to \mathbb{R}^3$ can be written as a graph over a convex domain of a plane, then the corresponding adjoint surface $X^* : B \to \mathbb{R}^3$ is also a graph.*

Now we turn to the discussion of specific examples.

A. Minimal Surfaces Parametrized on Punctured Spheres

(A1) *Enneper's surface*. Here we have

$$g(w) = w, \quad dh = w\,dw, \quad w \in \mathbb{C},$$
$$\psi(w) = \tfrac{1}{2}\big(w - \tfrac{1}{3}w^3, i\big(w + \tfrac{1}{3}w^3\big), w^2\big).$$

Reflections in straight lines through 0 are Riemannian isometries for the corresponding metric

$$ds = \frac{1}{2}\left(|w| + \frac{1}{|w|}\right)|w||dw|.$$

All these radial lines are therefore geodesics, and rotation about the origin is an isometry group. Moreover, $\mathbb{R}$ and $i\mathbb{R}$ are planar symmetry lines, and the $45°$-meridians are straight lines on Enneper's surface. The Riemannian

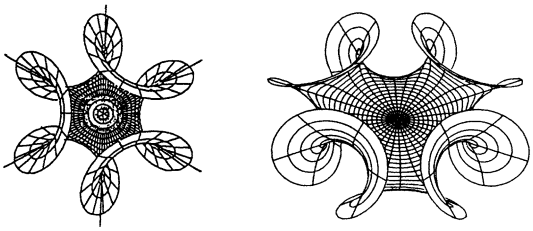

Fig. 3. (A2) Higher order Enneper surfaces. **(a)** $g(w) = w^2$. With courtesy of K. Polthier. **(b)** $g(w) = w^3$. Courtesy of J. Hahn and K. Polthier

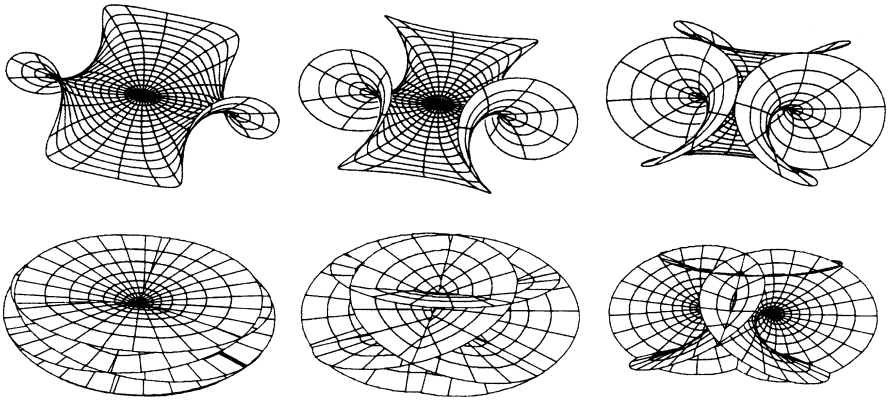

Fig. 4. A view of increasing parts of a higher order Enneper surface ($g(w) = w^2$) from an increasing distance. Courtesy of J. Hahn and K. Polthier

metric ds is complete on $M := \mathbb{C} \cong S^2 \setminus \{\text{north pole}\}$ and nondegenerate, i.e., Enneper's surface is a regular minimal surface. Moreover, all associate surfaces of Enneper's surface are congruent. Circles $\gamma(\varphi) = \mathrm{Re}^{i\varphi}$ of sufficiently large radius R are mapped to curves $c(\varphi) = \mathrm{Re}\,\psi(\gamma(\varphi))$ which wind three times about the z-axis. Therefore the end of Enneper's surface is not embedded, but $d = 3$.

(A2) *Higher order Enneper surfaces* are defined by

$$g(w) = w^n, \quad dh = w^n dw, \quad w \in \mathbb{C}, \quad n = 1, 2, 3, \ldots,$$

and they allow the same reasoning. However, we have more symmetry lines, and the end winds $(2n + 1)$-times about the z-axis ($d = 2n + 1$).

Interesting deformations can be obtained in the form

$$g(w) = w^n + tp(w), \quad dh = g(w)dw, \quad w \in \mathbb{C},$$

where $t \in \mathbb{R}$, and $p(w)$ is a polynomial of degree $\leq n - 1$. These surfaces are regular and have the same behavior at their ends as the corresponding higher order Enneper surfaces given by $t = 0$.

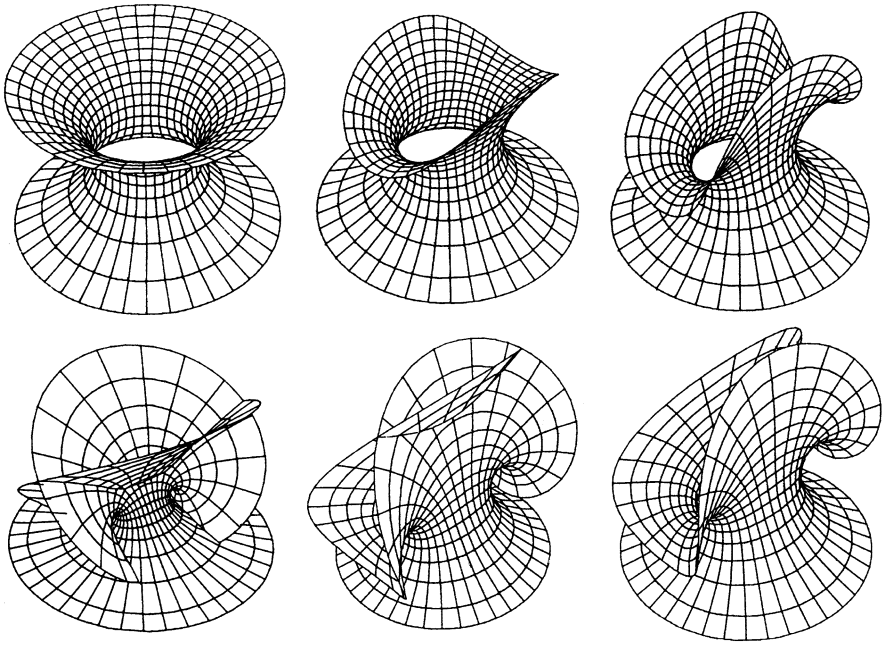

Fig. 5. Deformation of a catenoidal end into an Enneper end. Courtesy of K. Polthier and M. Wohlgemuth

The simplest minimal immersions of higher genus such as the *Chen–Gackstatter surface* (see (B2)) can be obtained from Weierstrass data which have the same behavior at their end as an Enneper surface.

(A3) *The catenoid* is given by

$$g(w) = w, \quad dh = \frac{dw}{w},$$

$w \in \mathbb{C} \setminus \{0\} \cong S^2 \setminus \{p_1, p_2\}, p_1 =$ north pole, $p_2 =$ south pole. Integration of the Weierstrass data once around 0 adds the period $P = (0, 0, 2\pi i)$ to ψ. Hence the catenoid is defined on $\mathbb{C} \setminus \{0\}$ whereas its adjoint, the helicoid, lives on the universal cover of $S^2 \setminus \{p_1, p_2\}$, and its symmetry group is a screw motion.

(A4) *examples with one planar end* can be obtained by the data

$$g(w) = w^{n+1}, \quad dh = w^{n-1}\, dw$$

for $w \in \mathbb{C} \setminus \{0\} \cong$ twice punctured sphere $= M$. Hence we have

$$\psi(w) = \left(\frac{1}{2}\left(-\frac{1}{w} - \frac{w^{2n+1}}{2n+1}\right), \frac{i}{2}\left(-\frac{1}{w} + \frac{w^{2n+1}}{2n+1}\right), \frac{w^n}{n}\right)$$

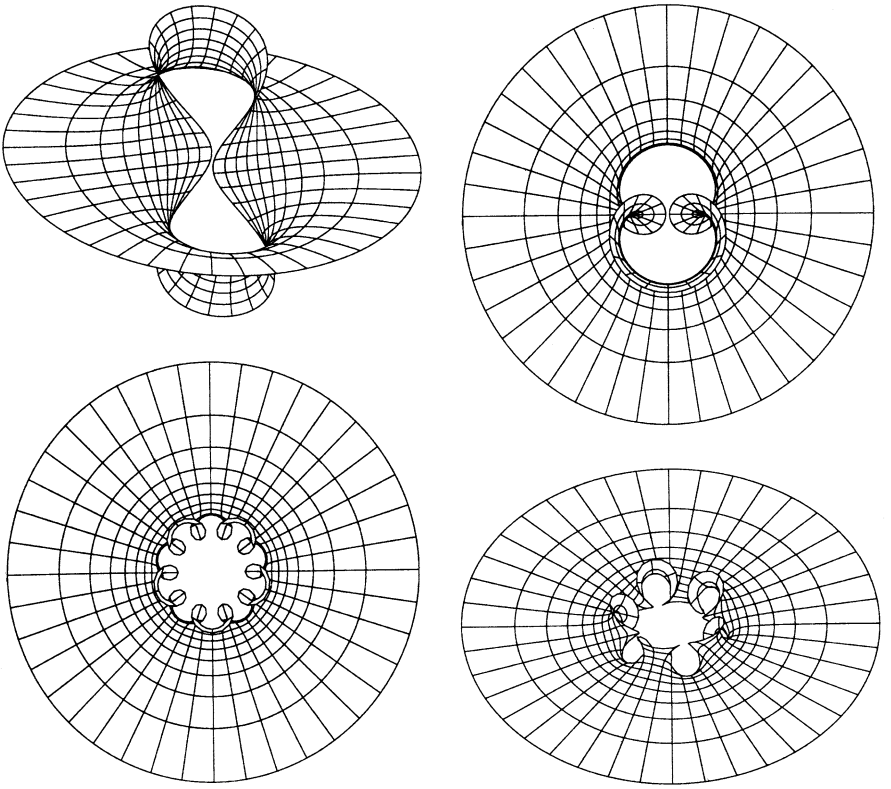

Fig. 6. Minimal surfaces with one planar end. Courtesy of K. Polthier

and

$$ds = (|w|^{2n} + |w|^{-2})|dw|.$$

This metric is complete on M. Reflections in all meridians define Riemannian isometries. The end at $w = \infty$ winds $(2n+1)$-times around the z-axis just as in the case of the higher order Enneper surfaces. The end at $w = 0$ is embedded and turns out to be a flat end which is asymptotic to the x, y-plane.

(A5) *Scherk's saddle tower* (*Scherk's fifth surface*) is given by the Weierstrass data

$$g(w) = w, \quad dh = \frac{1}{w^2 + w^{-2}} \frac{dw}{w}, \quad w \in M,$$

where $M = \bar{\mathbb{C}} \setminus \{\pm 1, \pm i\}$ is conformally the four times punctured sphere. The line element of Scherk's fifth surface $X = \operatorname{Re} \psi$ is given by

$$ds = \frac{|w| + |w|^{-1}}{|w^2 + w^{-2}|} \left| \frac{dw}{w} \right|.$$

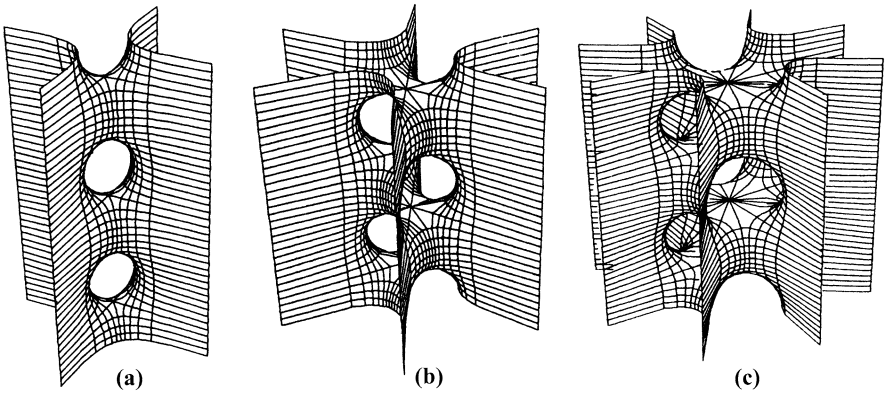

Fig. 7. Saddle towers, **(a)** Scherk's saddle tower (A5): $g(w) = w$. This surface is also called Scherk's fifth surface. It can be described by the equation $\sin z = \sinh x \sinh y$. **(b)**, **(c)** Higher order saddle towers (A6): **(b)** $g(w) = w^2$, **(c)** $g(w) = w^3$. Parts **(a), (b)** with courtesy of K. Polthier and part **(c)** with courtesy of J. Hahn and K. Polthier

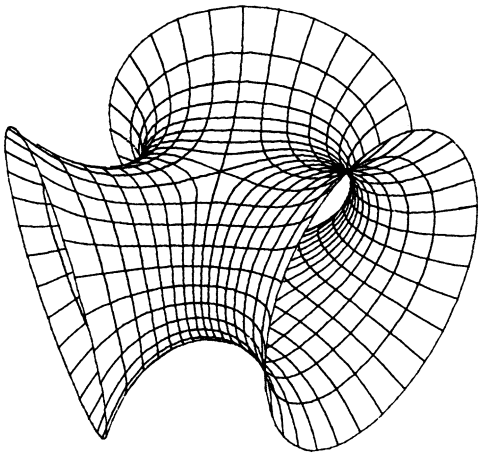

Fig. 8. The Jorge–Meeks 3-noid ($g(w) = w^2$). It can be viewed as limit of saddle towers. Courtesy of J. Hahn and K. Polthier

The corresponding metric is complete. The unit circle S^1 in $\mathbb{C}$, the axes $\mathbb{R}$, $i\mathbb{R}$ and the 45°-meridians allow Riemannian reflections. In particular we have a horizontal symmetry line (corresponding to S^1) through all four punctures whence all periods are vertical (and equal up to sign). Hence, on the open unit disk B, the mapping $X : B \to \mathbb{R}^3$ defines a regular minimal surface bounded by four horizontal symmetry lines which lie in only two parallel planes. Extension by reflection in these planes yields a complete minimal surface with one vertical period, and this surface is embedded if the fundamental piece is embedded. In fact, it turns out to be a graph. By Krust's theorem, the adjoint

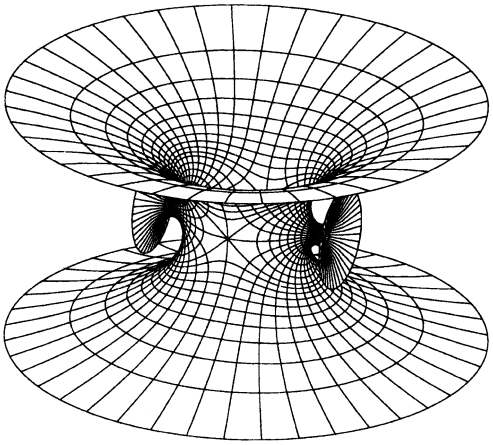

Fig. 9. A 4-noid with two orthogonal symmetry planes through each puncture. Courtesy of K. Polthier and M. Wohlgemuth

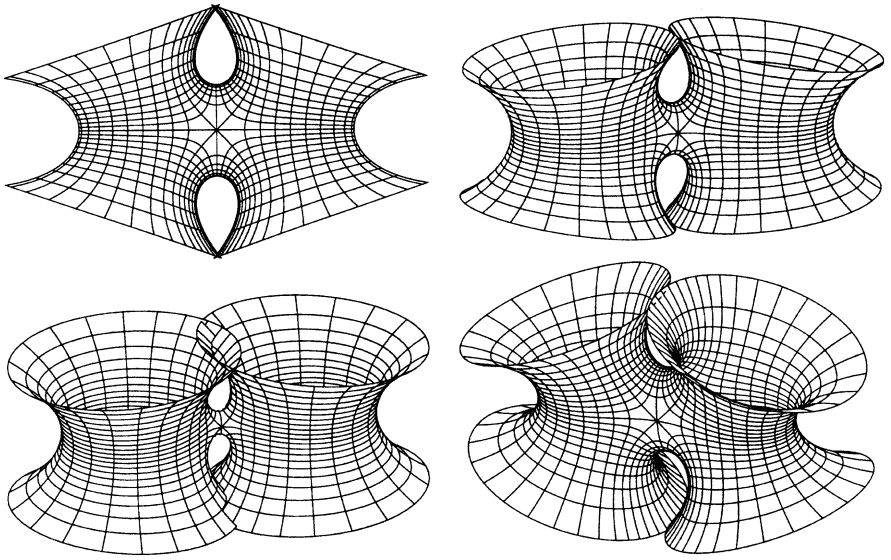

Fig. 10. Several 4-noids. Courtesy of K. Polthier

surface is also embedded; it is *Scherk's doubly periodic minimal surface.* Its Weierstrass data are

$$g(w) = w, \quad dh = \frac{i}{w^2 + w^{-2}} \frac{dw}{w},$$

(A6) *Higher order saddle towers* (Karcher) are defined by the Weierstrass data

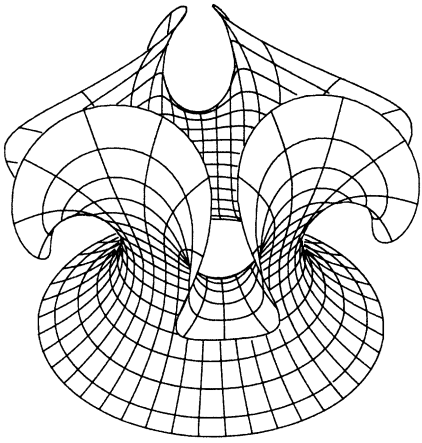

Fig. 11. An Enneper catenoid (corresponding to $g(w) = w^{-1} + w^3$). Courtesy of J. Hahn and K. Polthier

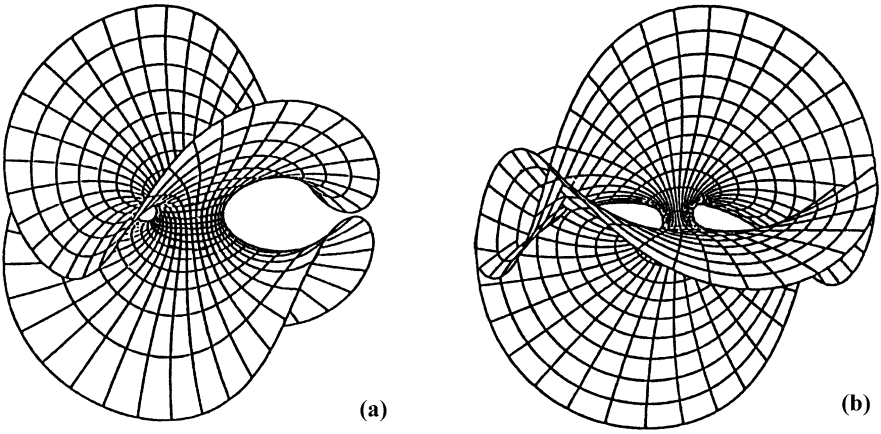

Fig. 12. Doubled Enneper surfaces. **(a)** without symmetry planes (rotated ends), **(b)** with symmetry planes. Courtesy of K. Polthier

$$g(w) = w^{n-1}, \quad dh = \frac{1}{w^n + w^{-n}} \frac{dw}{w}$$

which are defined on $M = \bar{\mathbb{C}} \setminus \{\varepsilon_1, \varepsilon_2, \ldots, \varepsilon_{2n}\}$ where ε_j are the $(2n)$-th roots of 1; M is conformally the $2n$-times punctured sphere.

(A7) *Less symmetric saddle towers* are obtained from

$$g(w) = w^{n-1}, \quad dh = (w^n + w^{-n} - 2\cos n\varphi)^{-1} \frac{dw}{w}$$

$w \in M$, where M is $\bar{\mathbb{C}}$ punctured at $w = e^{\pm i\varphi} e^{2\pi i l/n}$, $l = 0, 1, \ldots, n-1$, and φ is a real parameter restricted by $0 < \varphi \leq \frac{\pi}{2n}$.

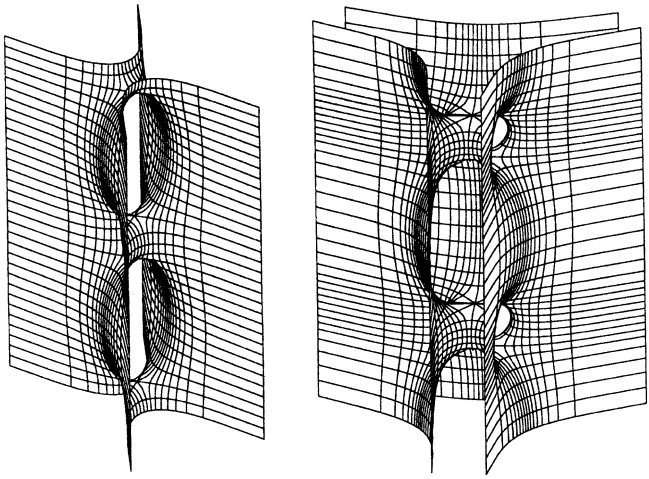

Fig. 13. (A7) Less symmetric saddle towers. Courtesy of K. Polthier

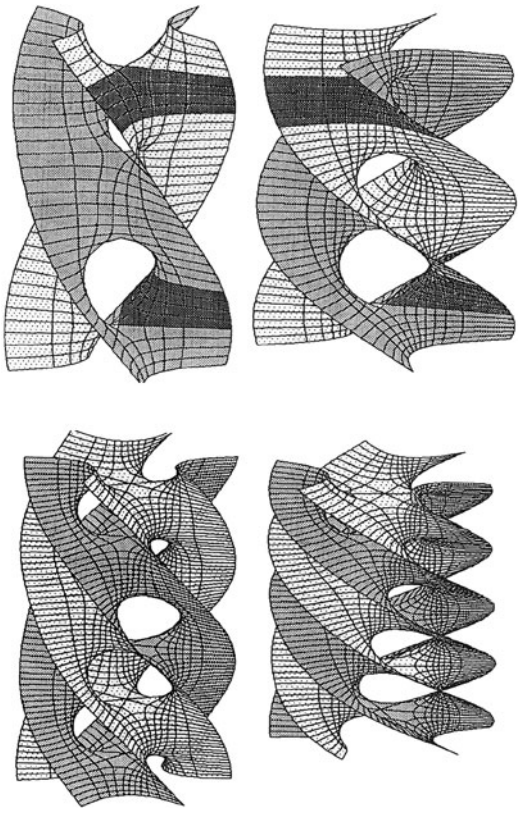

Fig. 14. Helicoidal saddle towers: Deformed Scherk surfaces constructed by Karcher. Courtesy of H. Karcher

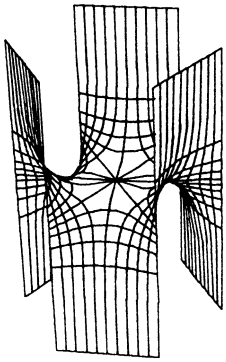

Fig. 15. The Jenkins–Serrin theorem for the hexagon ($n = 3$). Courtesy of J. Hahn and K. Polthier

If $\varphi \to 0$, then the punctures move pairwise together to become double poles of dh, and their images lie on vertical symmetry planes. Hence the punctures have no periods, and their ends turn out to be embedded catenoidal ends. In fact, the surfaces with $\varphi = 0$ are the *n-noids of Jorge–Meeks* which are not embedded.

We remark that the saddle towers as well as the n-noids allow deformations which are again complete minimal surfaces. For more details, see Karcher [1, 3], and also Figs. 7–14.

Moreover, the construction of *embedded saddle towers* can be obtained from a result by Jenkins and Serrin [2] by passing to the adjoint of the *Jenkins–Serrin surface* and by applying the reflection principle and Krust's theorem; see Karcher [3].

Theorem of Jenkins and Serrin. *Let Ω be a convex $2n$-gon with all edges of the same length and alternatingly marked $\infty, -\infty, \infty, -\infty, \ldots$. Then there is a uniquely determined nonparametric minimal surface $z = u(x, y)$, $x, y \in \Omega$, over Ω which converges to ∞ or $-\infty$ respectively as it approaches the marked edges of Ω. The graph of u is a minimal surface bounded by the vertical lines over the vertices of $\partial\Omega$ which has finite total curvature.*

B. Minimal Surfaces Parametrized on Punctured Tori

While the examples (A) were constructed by Weierstrass data which are rational functions on the punctured sphere, we shall now use meromorphic maps $T^2 \to \bar{\mathbb{C}}$ on the torus T^2, that is, doubly periodic functions (or: elliptic functions). Karcher [3] effectively operates with a doubly periodic function $\gamma : T^2 \to \bar{\mathbb{C}}$ which, by reflection, is built from a biholomorphic map $\gamma : B \to D$ of a rectangle B with the corners a, b, c, d onto the quarter circle D with the vertices $0, 1, i$. The mapping γ is obtained by Riemann's mapping theorem. Using the 3-point-condition $\gamma(a) = i, \gamma(b) = 0, \gamma(c) = 1$, we define an angle

$\alpha \in (0, \frac{\pi}{2})$ by $\gamma(d) = e^{i\alpha}$; this angle is called the *conformal parameter* of γ. One obtains

$$\left(\frac{\gamma'}{\gamma}\right)^2 = \kappa(\gamma^2 + \gamma^{-2} - 2\cos\alpha)$$

where κ is a positive constant. As γ turns out to be a degree-two elliptic function, there is a close connection to the geometric p-function. In fact, we have

$$\gamma^2 = \frac{-\tan\alpha - \cot\alpha}{p - \frac{1}{p} + \tan\alpha - \cot\alpha}$$

and

$$p'\gamma = \kappa^* p \quad (\kappa^* = \text{positive constant}).$$

Note that, in section B, the geometric p-function is not the usual Weierstrass $\wp$-function, but the one that has been modified linearly such that it has a double zero in the middle, and that the product of the two finite branch values is -1. Another useful elliptic function f is defined as extension by reflection of the biholomorphic mapping from a rectangle B to the quarter disk D such that b, c, d are mapped into $0, 1, i$ respectively whereas a goes to $i\tan\frac{\alpha}{2}$. The functions γ, p and f are linked by

$$f\gamma = \frac{p}{\cos\alpha - p\sin\alpha}.$$

(B1) *A fence of catenoids* (*Hoffman–Karcher*). One can construct a periodic surface with a translational symmetry as depicted in Fig. 16. Dividing out the symmetry, we obtain a torus with two embedded catenoidal ends. The stereographic projection g of the Gauss map of this surface turns out to be γ whereas f determines dh:

$$g = \gamma, \quad dh = f\,dw.$$

The symmetries of f and γ yield that reflections in the expected symmetry lines are Riemannian isometries for the metric

$$ds = \left(|\gamma| + \frac{1}{|\gamma|}\right)|f||dw|$$

of the fence.

(B2) *The Chen–Gackstatter surface* was the first minimal surface without periods or branch points defined on a punctured torus that was discovered. It has one puncture and therefore one end. Thus it is the direct relative of Enneper's surface, only that it possesses a handle (see Fig. 17). The Weierstrass data are given as

$$g = r\gamma, \quad dh = p'\,dw$$

where the parameter $r \in \mathbb{R}^+$ has to be chosen in such a way that the periods vanish. The removal of the periods is one of the difficulties in this and other examples.

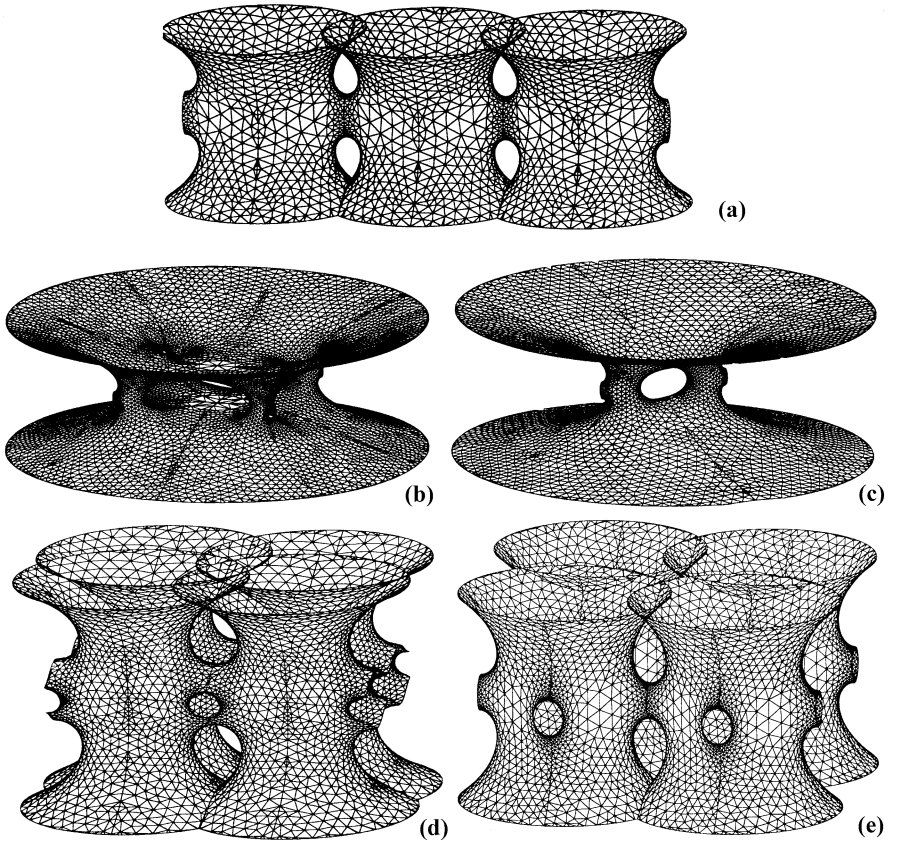

Fig. 16. Construction of higher genus minimal surfaces by growing handles out of a catenoid. **(a)** A fence of catenoids (B1), **(b)–(e)** More catenoids with handles. Courtesy of E. Boix, J. Hoffman, and M. Wohlgemuth

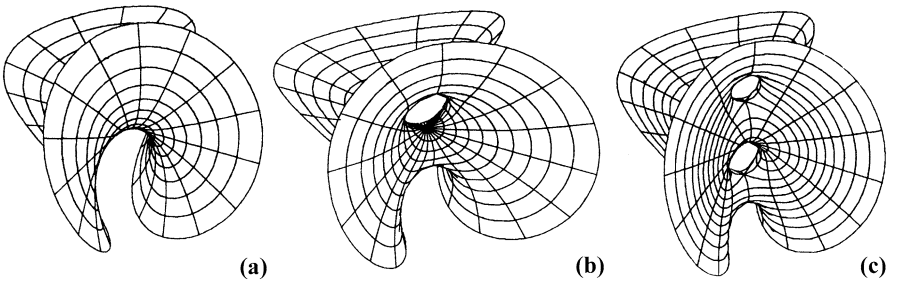

Fig. 17. (a) Enneper's surface (A1): no handle. Courtesy of K. Polthier. **(b)** Chen–Gackstatter surface (B2): one handle. Courtesy of J. Hahn and K. Polthier. **(c)** Chen–Gackstatter surface with two handles. Courtesy of K. Polthier and M. Wohlgemuth

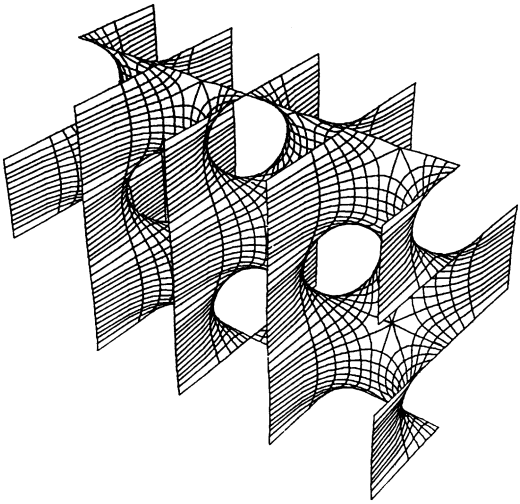

Fig. 18. A fence of Scherk towers—a doubly periodic toroidal surface (B3). Courtesy of K. Polthier

(B3) *Doubly periodic examples* are depicted in Figs. 18 and 19.

(B4) *Riemann's minimal surface* is a simply periodic embedded minimal surface defined on a twice punctured rectangular torus and with one period. Its two ends are flat. A careful discussion can be found in Nitsche's treatise [28]. The corresponding Weierstrass data are

$$g = p, \quad dh = dw = \frac{dp}{p'}.$$

In fact, there is a 1-parameter family of Riemann examples, two for each rectangular torus. The adjoint surface of a Riemann example is another Riemann example which is not congruent to the first, except in the special case of a square torus.

(B5) *Costa's surface* is an embedding of the three times punctured square torus (i.e., without periods). In Karcher's description [3], its Weierstrass data are

$$g = rp' = r\frac{p}{\gamma},$$

$$dh = \gamma\, dw = \frac{\gamma}{\gamma'}\, d\gamma = \frac{2}{1-p^2}\, dp.$$

Again, the parameter $r \in \mathbb{R}^+$ is used to remove all periods.

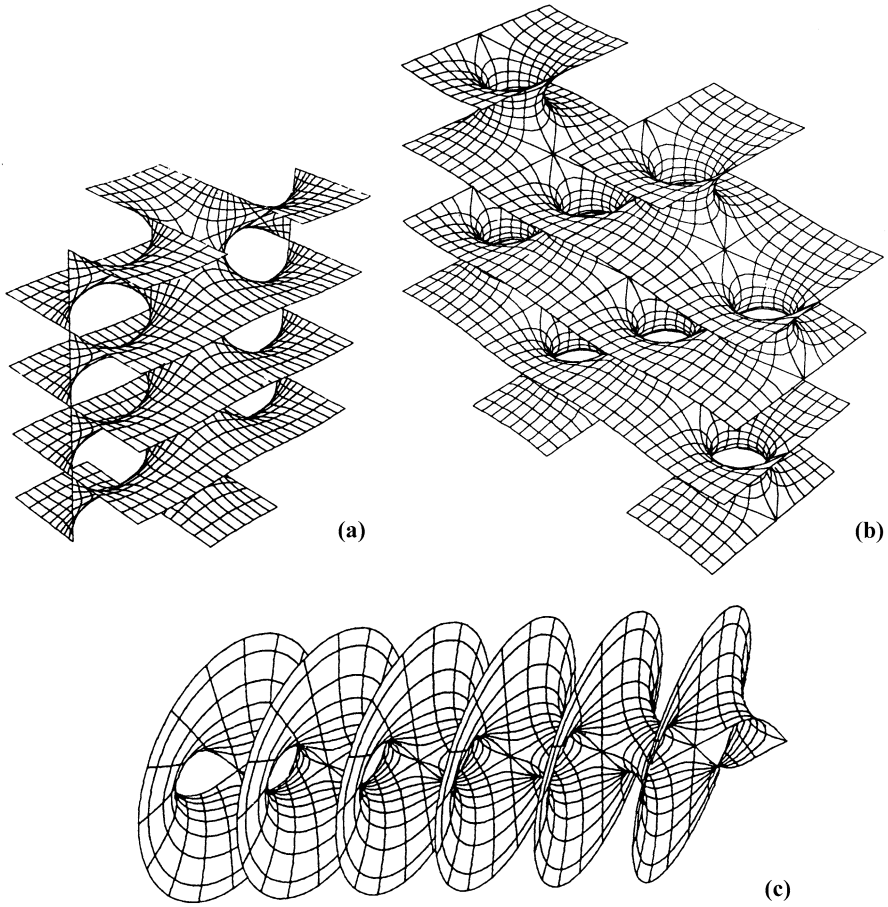

Fig. 19. (a) and **(b)** A conjugate pair of embedded doubly periodic minimal surfaces (B3). Part **(a)** with courtesy of K. Polthier and M. Wohlgemuth and part **(b)** with courtesy of K. Polthier. **(c)** Riemann's periodic minimal surface (B4) can be viewed as a limit of **(b)** under deformation. Courtesy of K. Polthier and M. Wohlgemuth

5 Triply Periodic Minimal Surfaces

Five surfaces of this type were already known to H.A. Schwarz (see [2], vol. 1, pp. 1–125, 136–147; cf. also Figs. 21–27 of this section, Figs. 37–39 of Section 3.5, and Plates II–VII). They were obtained by spanning a disk-type minimal surface $X : B \to \mathbb{R}^3$ into a polygon Γ and then reflecting this surface at the edges of Γ. In 1891, A. Schoenflies (see [1,2]) proved that in this way exactly six different periodic minimal surfaces can be obtained from (skew) quadrilaterals, whereas Schwarz had erroneously claimed that there existed exactly five surfaces of this type (see [2], vol. 1, pp. 221–222). All of these

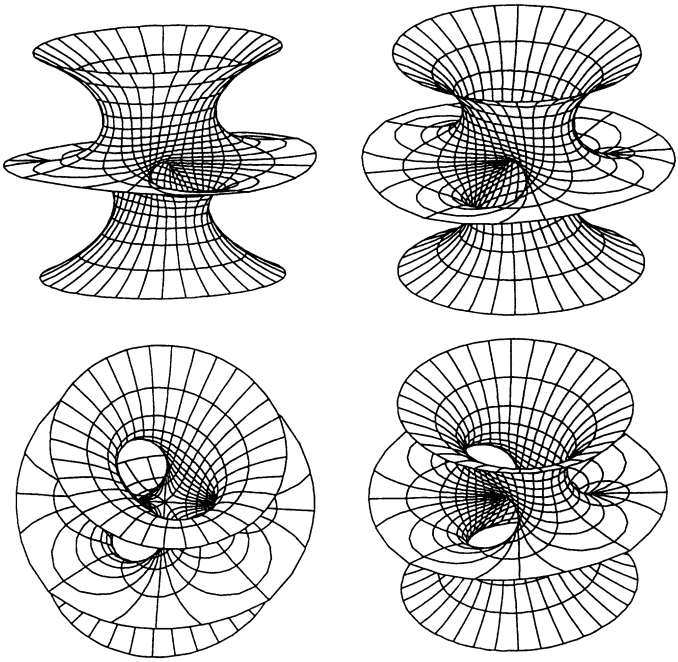

Fig. 20. The Costa surface (B5). Courtesy of K. Polthier

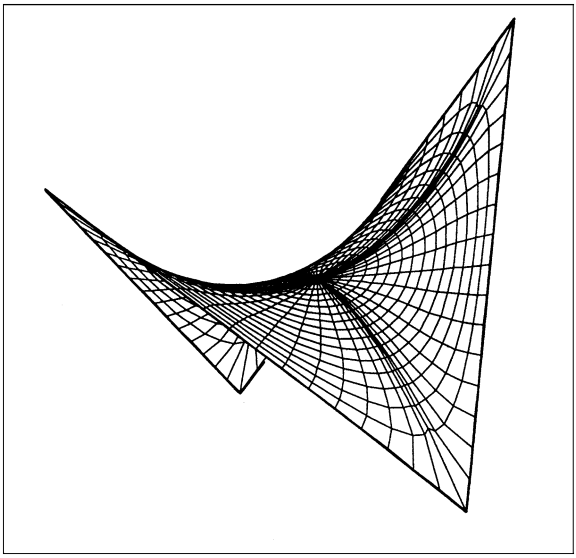

Fig. 21. Schwarz's surface. Courtesy of O. Wohlrab

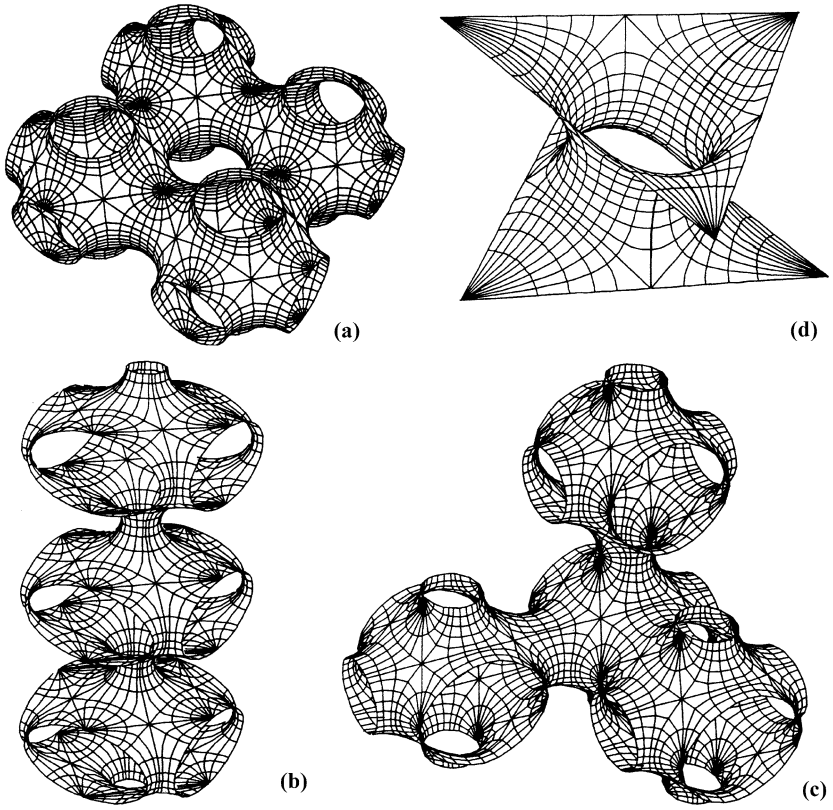

Fig. 22. (a) Schwarz's P-surface and **(b)**, **(c)** deformations thereof. **(d)** This annulus bounded by two triangles is part of the adjoint of the Schwarzian P-surface if the ratio of edge length to height is $2\sqrt{3}$. Courtesy of K. Polthier

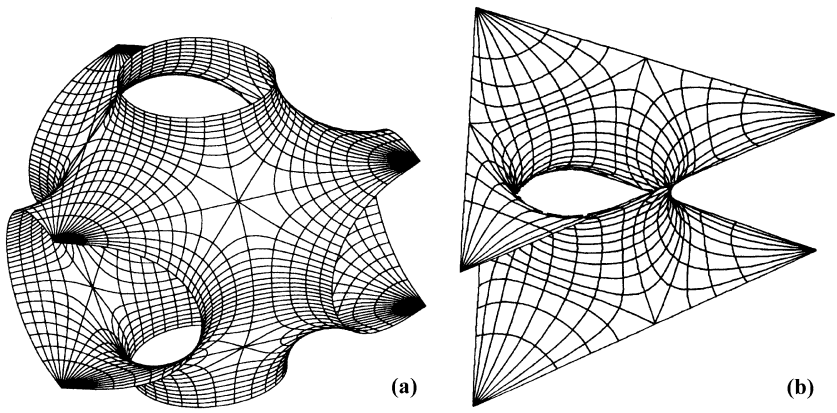

Fig. 23. (a) A part of Schwarz's H-surface. **(b)** An annulus-type minimal surface bounded by two triangles which is part of the H-surface. Courtesy of K. Polthier

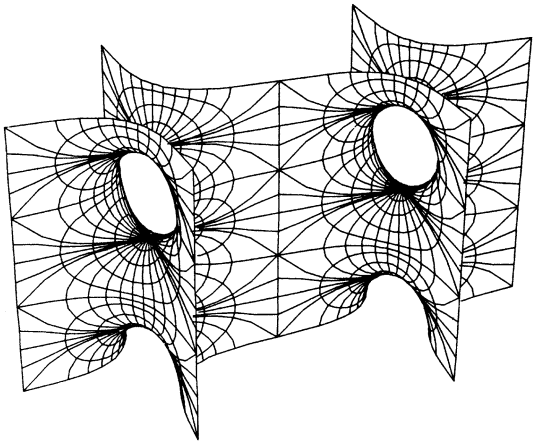

Fig. 24. Schwarz's *CLP*-surface. Courtesy of K. Polthier

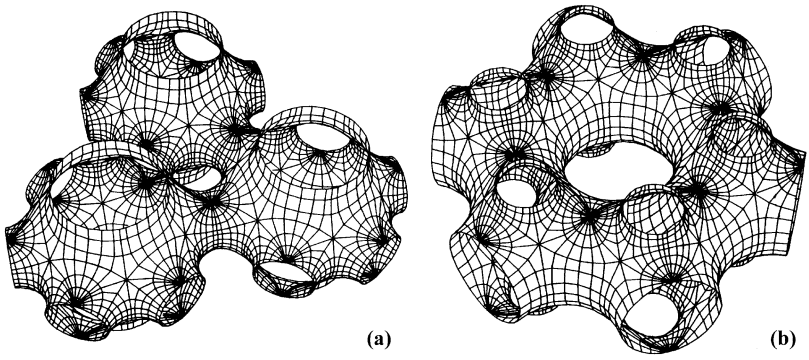

Fig. 25. Alan Schoen's H'–T-surface: **(a)** in a trigonal cell, **(b)** in the dual hexagonal cell. Courtesy of K. Polthier

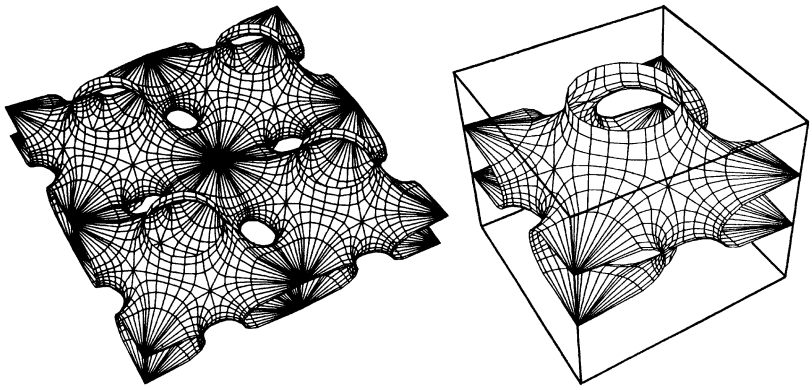

Fig. 26. Alan Schoen's S'–S''-surface. This part solves a free boundary problem with regard to the faces of a cube. Courtesy of K. Polthier

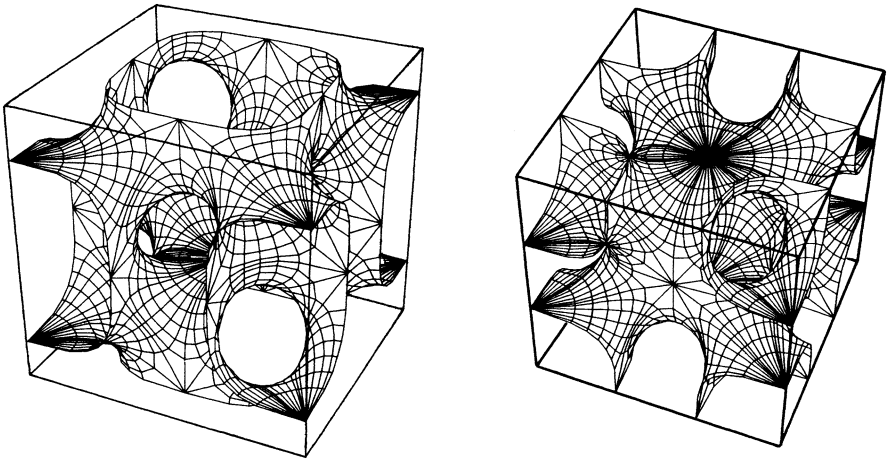

Fig. 27. Two views of A. Schoen's *I–Wp*-surface. Both parts sit in a cube and meet its faces at a right angle. Courtesy of K. Polthier

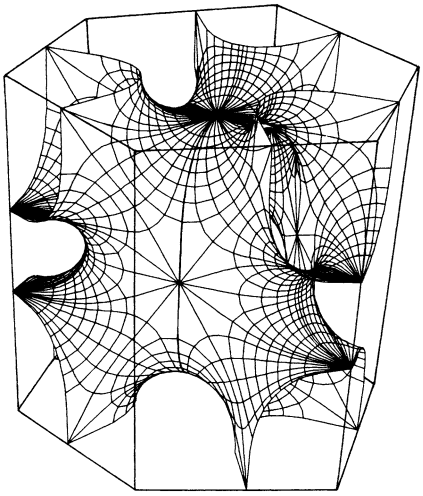

Fig. 28. An analogue to A. Schoen's *I–Wp*-surface found by Karcher; it sits in a hexagonal cell and meets the faces of this cell perpendicularly. Courtesy of K. Polthier

periodic minimal surfaces were described in detail by Steßmann [1]; one of them was discovered by Neovius.

Clearly one can try to obtain other triply periodic minimal surfaces by spanning pieces of minimal surfaces as stationary points of the area functional into a general Schwarzian chain $\langle \Gamma_1, \ldots, \Gamma_k, S_1, \ldots, S_l \rangle$ and then reflecting them at the edges Γ_j and the planar faces S_j. In this way, Neovius, Nicoletti, Marty, Tenius, Stenius and Wernick generated more triply periodic minimal

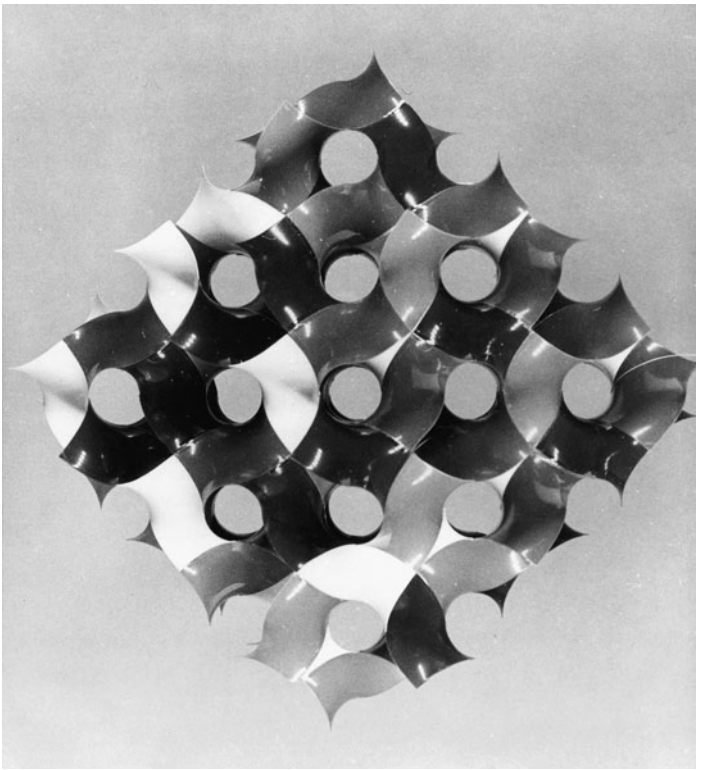

Fig. 29. Alan Schoen's gyroid, an associate to Schwarz's surface, is an embedded triply periodic minimal surface. Courtesy of A. Schoen

surfaces. We refer to Nitsche's treatise [28], § 818, pp. 664–665 for pertinent references. After Steßmann's paper, the subject was at rest for more than 30 years until the physicist and crystallographer Alan Schoen [1,2] revived it. He discovered many new triply periodic minimal surfaces, and he built marvelous models of enormous size which stunned everyone who had a chance to see them (a few are depicted in Hildebrandt and Tromba [1]). However, Schoen's reports were a bit sketchy and thus, among mathematicians, there remained some doubts whether all details could be filled in, whereas Schoen's work became very popular among crystallographers and chemists. Schoen's remarkable geometric intuition proved to be correct; H. Karcher established the existence of all of Schoen's surfaces, and he found *triply periodic constant mean curvature companions* to them (see Karcher [2] and also [3]). By solving conjugate Plateau problems, Karcher and his students found many more triply periodic embedded minimal surfaces and even whole families of them. The strategy for finding such examples is lucidly described in Section 4 of Karcher's lecture notes [3].

6 Structure of Embedded Minimal Disks

In a series of papers (cf. bibliography), T.H. Colding and W.P. Minicozzi investigated the structure of embedded minimal disks, i.e. of minimal surfaces $X : \overline{B} \to \mathbb{R}^3$ defined on closed disks $\overline{B} \subset \mathbb{R}^2$ being embeddings. (In particular such surfaces are free of branch points.) One of their main results states that every embedded minimal disk can either be modeled by a minimal graph or by a piece of the helicoid depending on whether the supremum of the Gauss curvature is small or not. Together with a Heinz-type curvature estimate which is also due to Colding & Minicozzi, Meeks and Rosenberg [GTMS] proved that the plane and the helicoid are the only complete, properly embedded, simply-connected minimal surfaces in $\mathbb{R}^3$.

7 Complete Minimal Surfaces and the Plateau Problem

One might think that a complete minimal surface "extends" to infinity, i.e. cannot be contained in a compact set. The question whether or not this is true had been raised by E. Calabi in the 1960ies, and in 1996 N. Nadirashvili [1] found a surprising answer: He constructed a complete minimal surface in $\mathbb{R}^3$ which is contained in a ball. Even more surprising is a result obtained by Martín and Nadirashvili [1] in 2007: *There exists a minimal surface* $X : B \to \mathbb{R}^3$ *on the unit disk of* $\mathbb{R}^2$ *which is complete and possesses a continuous extension to* $\overline{B}$ *such that* $X|_{\partial B} : \partial B \to \mathbb{R}^3$ *provides a nonrectifiable Jordan curve* Γ *of dimension* 1. Such curves Γ are not rare: *For any Jordan curve* Γ_0 *in* $\mathbb{R}^3$ *and any* $\epsilon > 0$ *one can find a Jordan curve* Γ *such that the Hausdorff distance of* Γ *and* Γ_0 *satisfies* $\delta^H(\Gamma, \Gamma_0) < \epsilon$*, and that* Γ *is the boundary of a complete minimal surface* $X : B \to \mathbb{R}^3$ *in the sense described above.* (Concerning the Plateau problem we refer to Sections 4.1–4.5 and 4.12.) We note that these surfaces have infinite area, and they cannot be embedded on account of work by Colding and Minicozzi.

Color Plates

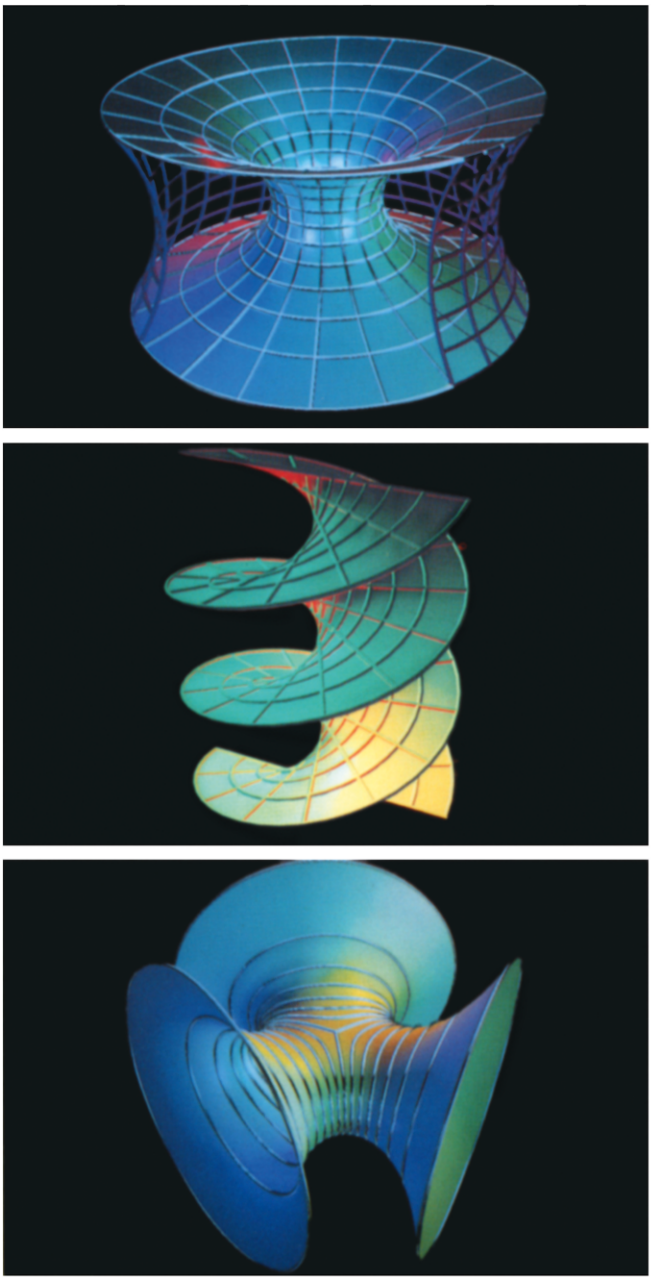

Plate I. (a) Stable and unstable catenoid, **(b)** helicoid and double helix, **(c)** Jorge–Meeks surface. Courtesy of K. Polthier

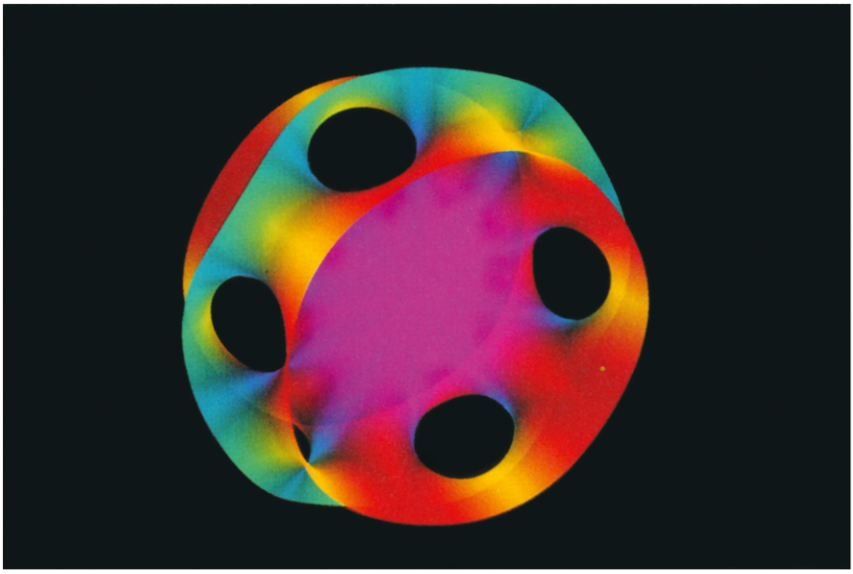

(a)

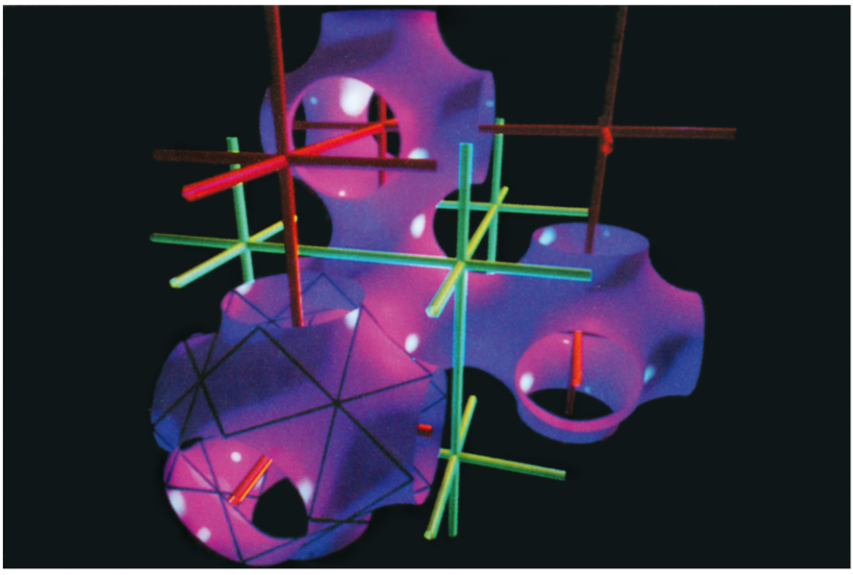

(b)

Plate II. (a) A Hoffman–Meeks surface, **(b)** part of Schwarz's *P*-surface. Courtesy of D. Hoffman and K. Polthier

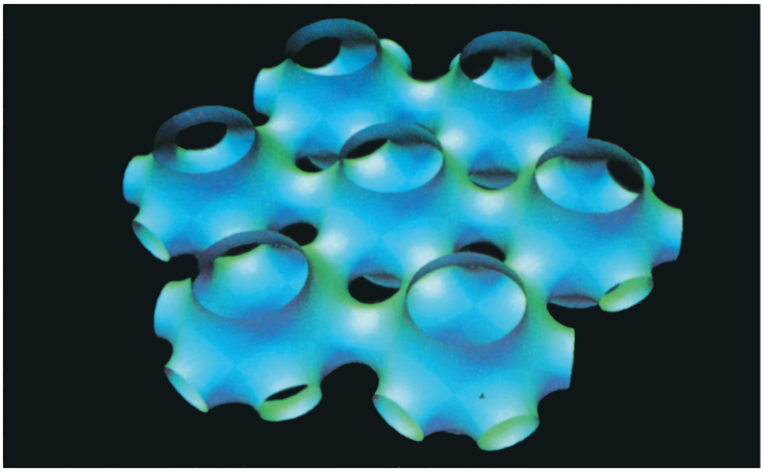

(a)

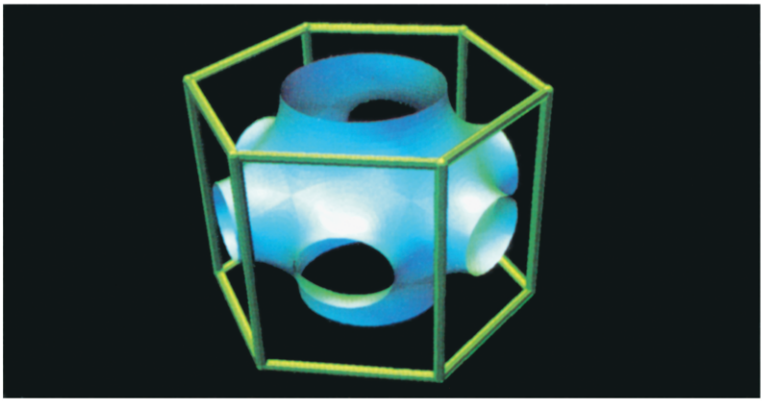

(b)

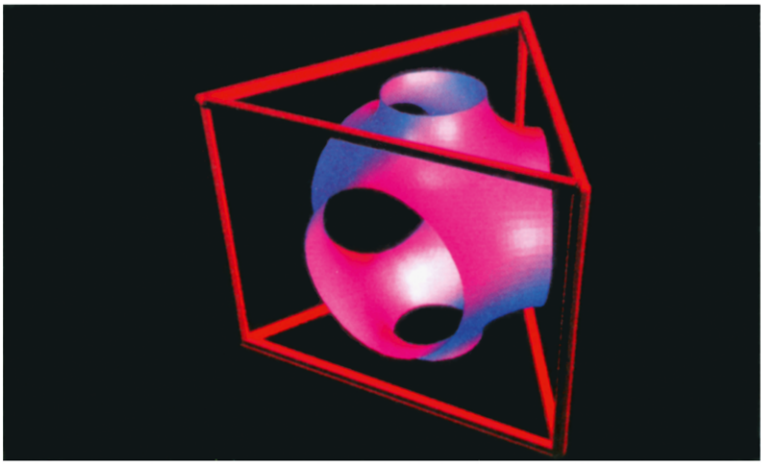

(c)

Plate III. A. Schoen's H'–T-surface. **(a)** One layer of the dual lattice, **(b)** hexagonal fundamental cell, **(c)** trigonal fundamental cell. Courtesy of K. Polthier

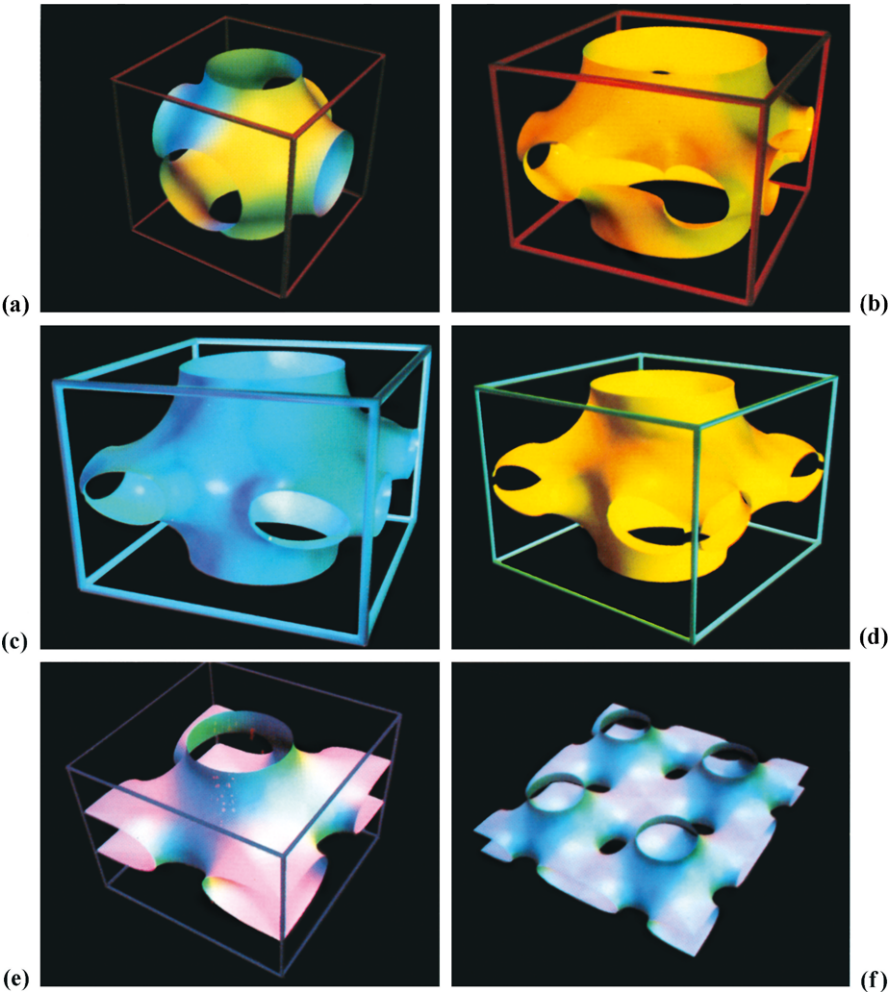

Plate IV. (a)–(e) The Karcher process of handle growing demonstrated by the transition from Schwarz's P-surface to Schoen's S'–S''-surface, **(f)** Schoen's S'–S''-surface. Courtesy of K. Polthier

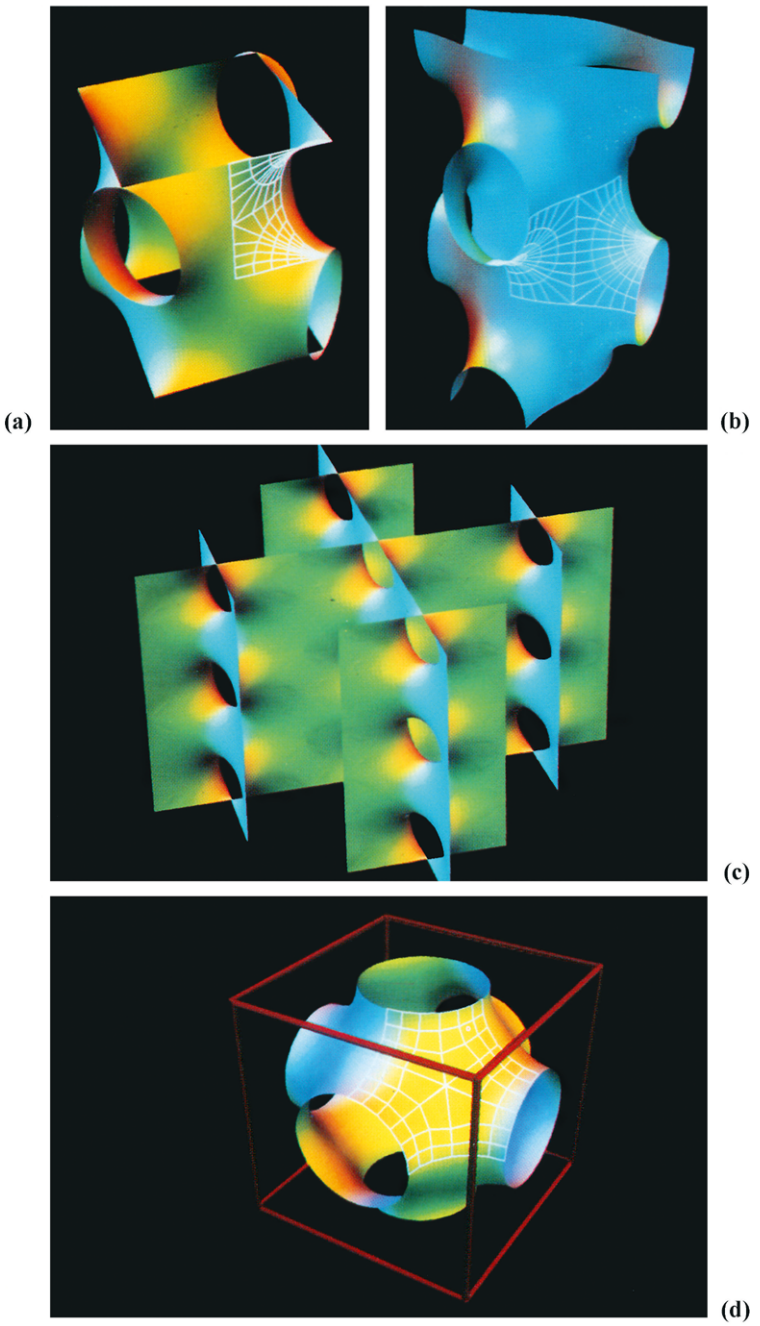

Plate V. (a)–(c) Schwarz's *CLP*-surface, **(d)** Schwarz's *P*-surface. Courtesy of K. Polthier

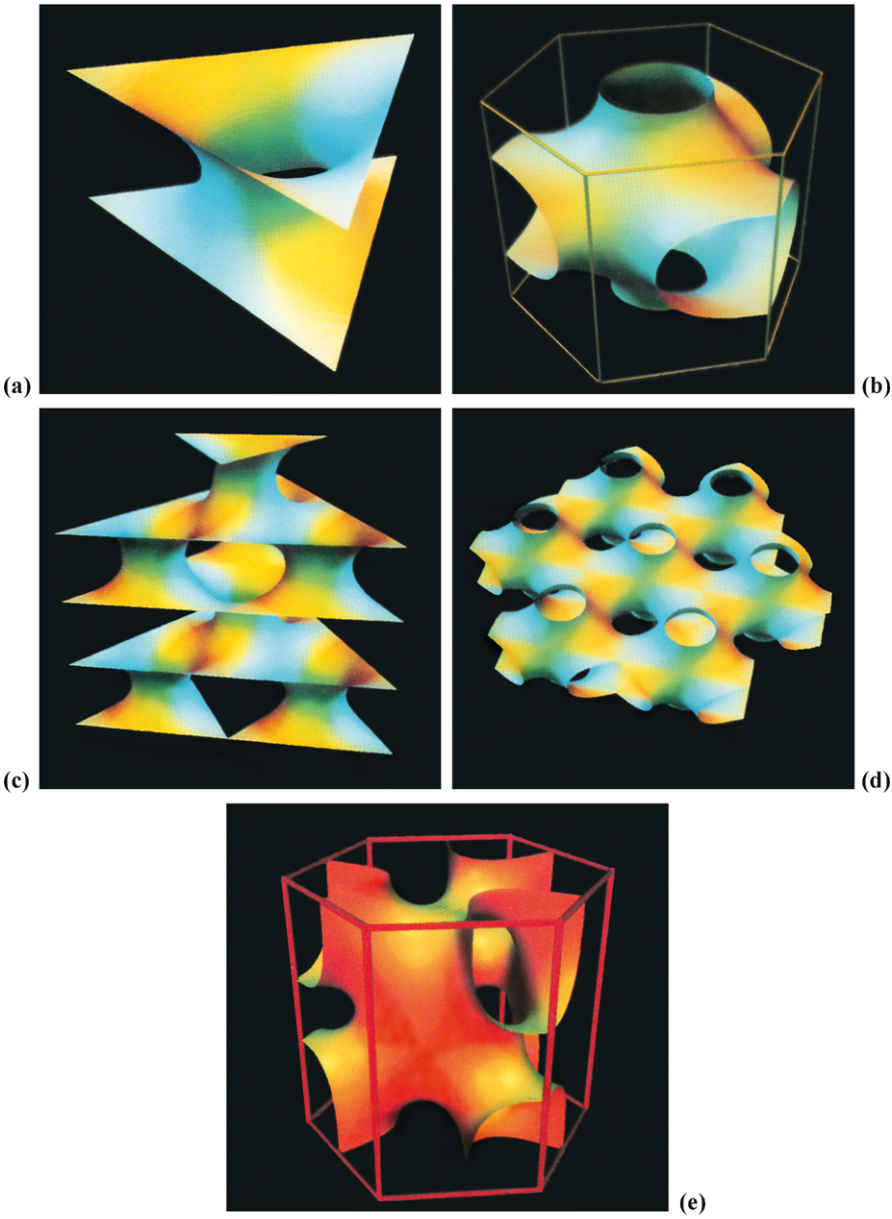

Plate VI. **(a)–(d)** Schwarz's H-surface, **(e)** Karcher's T–WP-surface. Courtesy of K. Polthier

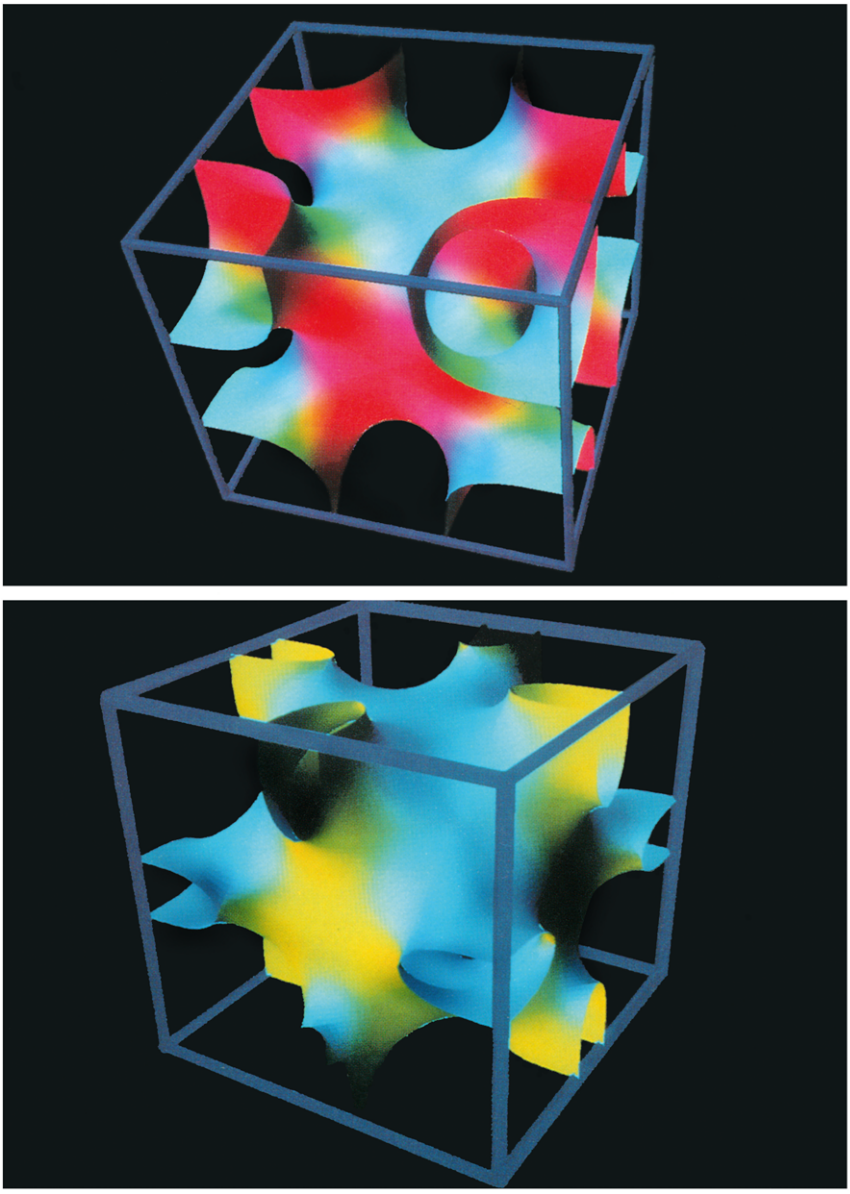

Plate VII. Fundamental cells. **(a)** A. Schoen's I–WP-surface, **(b)** Neovius surface. Courtesy of K. Polthier

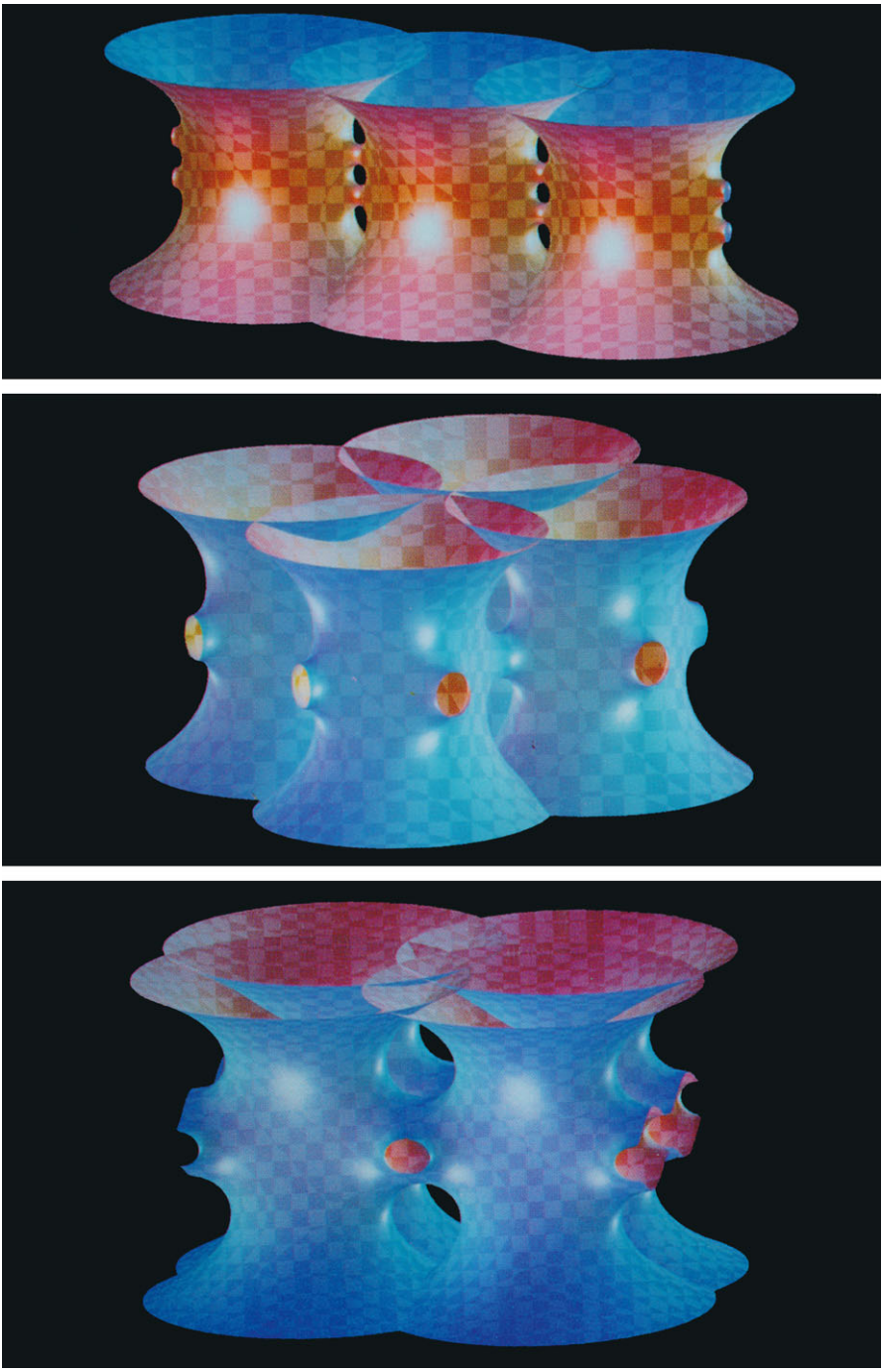

Plate VIII. Fences of catenoids. Courtesy of E. Boix, J. Hoffman, and M. Wohlgemuth